Mucosal cell responses to *Clostridium difficile* toxins

NIVETTE K. MULLAN, BSc

Thesis submitted to the University of Nottingham

for the degree of Doctor of Philosophy

July 2011

ABSTRACT

Colonic inflammation in *C. difficile* infection is mediated by released toxins A and B. I have investigated responses to *C. difficile* toxin A and B by primary human colonic myofibroblasts, which represent a distinct subpopulation of mucosal cells that are normally located below the intestinal epithelium and epithelial cell lines, Caco-2 and HT29. Myofibroblasts, isolated from normal human colonic mucosal specimens, Caco-2 and HT29 cells incubated with purified toxin A or B displayed a dose dependent response. Myofibroblast morphology changed to a stellate shaped cell, with processes that were immunoreactive for alpha smooth muscle actin. Most of the myofibroblasts remained viable, with persistent stellate morphology, despite exposure to high concentrations (up to 10 μg/ml) of toxin A for 72 h. In contrast, a majority of the toxin B exposed myofibroblasts lost their processes prior to cell death over 24-72 h. Investigating toxin A+B on myofibroblasts, at low concentrations, toxin A provided protection against toxin B-induced cell death. Most of the intestinal epithelial, HT29 cells remained viable despite exposure to high concentrations of either toxin (up to 10 μg/ml). By contrast, a significant loss in cell viability was observed in Caco-2 cells exposed to either toxin. Within 4 h, myofibroblast and epithelial cell types exposed to either toxin A or B lost expression of the non-glucosylated form of Rac1, but total intracellular RhoA remained unchanged in myofibroblasts and Caco-2 cells. A time-dependent reduction in RhoA expression was seen in HT29 in response to toxin A or B. Active RhoA expression was lost within 4 h in myofibroblasts exposed to either toxin. Despite pre-exposure to high concentrations of toxin A for 3 h, colonic myofibroblasts were able to recover their morphology and proliferative capacity during prolonged culture in medium. This was also shown when pre-exposure to toxin A was extended to 48 h. However, toxin B-pre-exposed myofibroblasts were not able to recover. In conclusion, primary human colonic mucosal myofibroblasts are resistant to toxin A (but not toxin B)-induced cell death. Responses by colonic myofibroblasts may play an important role in mucosal protection, repair, and regeneration in colitis due to *C. difficile* infection. Investigation into the apparent resilience of HT29 cells has highlighted the importance of cell specific substrate specificity by *C. difficile* toxins.

PUBLICATIONS

Papers

N Mullan, K R Hughes, Y R Mahida (In press) 2011

Primary human colonic myofibroblasts are resistant to *C. difficile* toxin A (but not toxin B)-induced cell death (Copy of manuscript can be found in Appendix 2)

Poster Presentations

'Caco-2 cells are more sensitive to toxin A induced cell death than HT29 cells'

British Society of Gastroenterology, 23- 26 March 2009, Glasgow.

Cell specific sensitivity of Caco-2 cells to *C.difficile* toxin A

Digestive Disease Week, 30 May- 4 June 2009, Chicago, IL.

ACKNOWLEDGEMENTS

Where do I start! So many have supported and cajoled me through this PhD. Perhaps I should start with the funding body but whilst they supported the financial side of my studies another source of financial support has made my dream of becoming a doctor, a reality. I would therefore thank my fiancé, Richard; my rock, whose love and humour has lightened the many hours of studying.

To my son, Ben, I am so proud of you and have missed spending time with you – no more studying – I have had enough – I want to play now.

And now, I would like to thank my supervisor, Prof Y. R. Mahida whose guidance and support have never faltered, not once.

I would like to say a big thank you to my friend and colleague Karen McCartney. I don't know how much we have spent on Costa Coffee or the extra inches gained from eating Victoria sponge but your love and friendship has made it all worth it.

To Jacky and Anuska, thanks for all your help. No more feeding my cells!

And finally, my thanks to the Medical Research Council and the School of Clinical Sciences who jointly funded this project.

Table of Contents

LIST OF FIGURES

CHAPTER 1

1 Introduction

1.1 *Clostridium difficile* Infection - the clinical significance

C. difficile infection (CDI) leads to a spectrum of disease ranging from the asymptomatic carrier, mild diarrhoea, colitis, pseudomembranous colitis (PMC) and fulminant colitis (Borriello 1998).

The asymptomatic carrier state is often the end result for many patients; however these patients may act as silent reservoirs perpetuating contamination within the hospital environment (Lawrence, Puzniak et al. 2007). Treatment of asymptomatic carriers has not been found to eradicate the carrier state and will therefore not reduce the spread of nocosomial transmission (Kelly and LaMont 1998).

Accounting for 20% of all antibiotic associated cases of diarrhoea, most patients do not progress to pseudomembranous colitis and fulminant colitis. With a speedy diagnosis and cessation of contributing antibiotic therapy, diarrhoea is self limiting (Hookman and Barkin 2009). Some individuals will develop colitis without pseudomembrane formation and may present with a fever, malaise, abdominal pain, nausea and watery diarrhea (Schroeder 2005). Endoscopic examination may reveal patchy non-specific redness without pseudomembranes (Kawamoto, Horton et al. 1999).

The presence of pseudomembrane plagues (raised yellow plaques ranging from 2mm to 10mm in diameter) on the colorectal mucosa (Kawamoto, Horton et al. 1999) signal full-blown *C. difficile* colitis and a more serious

disease. Approximately 3% of patients will develop fulminant colitis from *C. difficile infection* (Hookman and Barkin 2009). Patients with fulminant colitis may present with severe diarrhoea and abdominal pain, high fevers and marked peripheral leukocytosis (Bennett, Allen et al. 1984; Schroeder 2005). PMC can be complicated by dehydration, shock, septicaemia, toxic megacolon and peritonitis (Borriello 1998) and can result in death.

1.1.1 Acquisition

Clostridium difficile infection generally occurs as a result of ingesting the heat resistant spores released by the bacterium, the vegetative cells are unable to survive in an aerobic environment (Larson, Price et al. 1978). Transmission can occur by fecal-oral; person to person or; fomite/instrument to patient routes (McFee and Abdelsayed 2009). On ingestion the spores migrate to the colon and mature into vegetative cells. Whilst *C. difficile* is found the gut of 3-5% of the population (Bartlett 2002), the gut flora of the healthy individual is able to control the over-growth of *C. difficile* preventing colonisation and subsequent clinical manifestation (Bartlett, Chang et al. 1978).

The acquisition of *Clostridium difficile* is linked primarily to hospitalisation (Bartlett 2002; Dallal, Harbrecht et al. 2002), the rate of which rises from 13% in stays of up to 2 weeks to 50% in those staying longer than four weeks (Clabots, Johnson et al. 1992). Although the risk of acquiring a *Clostridium difficle* infection in the community is low current figures suggest that community CDI rates in the United States have been reported as 7.7 cases per 100,000 person years (Hirschhorn, Trnka et al. 1994). Of those cases

35% received no antibiotics within 42 days of detected infection (ibid, 1994) More recent investigations completed by the Centers for Disease Control report similar rates of infection but increased disease severity (Chernak 2005). What remains apparent is that community associated CDI without previous direct or indirect contact with a hospital environment is rare when compared with hospital acquired attrition (Rupnik, Wilcox et al. 2009). The hypervirulent strain B1/Nap1/027 has been reported in community acquired cases however community presence has been strongly correlated with its presence in local healthcare facilities (ibid, 2009).

Other potential community sources of CDI include soil, water, pets, animals used for food, meat and vegetables (al Saif and Brazier 1996). At this stage there is no evidence to suggest that food contaminated with *C. difficile* has resulted in clinical disease in humans (Rupnik, Wilcox et al. 2009), however should the dramatic increase in infection rates be attributed to the presence of more virulent strains or could it be an unknown vehicle for transmission contributing to the increase.

1.1.2 Risk factors

The disruption of the gut flora by antibiotic therapy and advanced age are the commonest pre-disposing factors to *Clostridium difficile* infection but a number of other factors can be related to whether a person remains asymptomatic, develops fulminant colitis and PMC or experience recurrent bouts of infection.

Immune-suppression using chemotherapeutic or immunosuppressant agents (Anand and Glatt 1993; Blot, Escande et al. 2003; Svenungsson, Burman et al. 2003), patients having undergone gastrointestinal surgery or manipulation (Zerey, Paton et al. 2007) and patients with IBD (Issa, Vijayapal et al. 2007) are at greater risk of CDI, see Table 1-1. In addition, an association between the use of proton-pump inhibitors and H_2 receptor antagonists to suppress acid production has also been reported. Further studies are required to establish any causal relationship but a potential mechanism could be the survival of vegetative forms in the gastric content caused by the increased pH (Jump, Pultz et al. 2007; Leonard, Marshall et al. 2007).

Table 1-1 Populations at increased risk of *C. difficile* infection

Adapted from (Hookman and Barkin 2009)

Patients who take the following drugs:

- Antibiotics
- Proton Pump Inhibitors (Dial, Delaney et al. 2005; Yearsley, Gilby et al. 2006)
- Valacyclovir (De Andres, Ferreiro et al. 2004)

Patient characteristics

- IBD (Issa, Vijayapal et al. 2007)
- Serious underlying illnesses / co-morbidities
- Gastrointestinal surgery / manipulations (Zerey, Paton et al. 2007)
- Advanced age
- Immune-compromising conditions (post transplantation) (Munoz, Giannella et al. 2007)
- Peri-partum (Rouphael, O'Donnell et al. 2008)

Environment

- Prolonged stay in health care settings (Clabots, Johnson et al. 1992)

Laboratory factors

- Hypoalbuminemia (Dansinger, Johnson et al. 1996)
- Low levels of anti toxin A and B antibodies

1.1.3 Diagnosis

The suspicion of *Clostridium difficile* infection is often based on foul smelling diarrhoea, this is however not sufficient for an accurate diagnosis but can be used to the isolate suspected cases (Bartlett and Gerding 2008). The traditional gold standard for diagnosis of *C. difficile* infection is a cytotoxin assay that detects cell cytotoxicity of toxin B and in some cases toxin A and the subsequent neutralisation of the cytotoxic effect using anti toxin antibodies (Fekety 1997; Bartlett 2006). As an alternative, cytotoxigenic culture detects strains capable of producing toxin rather than actual toxin production are used but care should be taken as capacity to produce the toxin does not confirm that it actual produces it (Monaghan, Boswell et al. 2008). Several commercial kits are available with variable accuracy, a recent systematic review of six toxin detections kits found that positive predictive value (PPV) was unacceptably low and as the PPV reduces as the prevalence of CDI decreases (Planche, Aghaizu et al. 2008). New molecular methods identifying genes encoding the toxins may provide a rapid and sensitive alternative but face the similar limitations discussed for the cytotoxigenic culture (Rupnik, Wilcox et al. 2009). Any test that fails to test the activity of the toxins produced will have limited accuracy and will need to be compared against patient records and clinical treatment outcomes for confirmation of accuracy.

1.1.4 Treatment

Clostridium difficile is resistant to a wide range of antibiotics allowing the bacterium to colonize and infect in the presence of antibiotics (Pituch, vavn

Belkum et al. 2003). Individuals remain resistant to *C. difficile* if their normal gut flora is not disrupted by antibiotics. The introduction of antibiotic therapy gradually destroys the gut flora and the bacteria colonise, releases toxins and cause clinical manifestation. The treatment of CDI has not changed dramatically since 1981 when oral Vancomycin was found to be highly effective (Silva, Batts et al. 1981). The replacement of Clindamycin, with Metronidazole has been effective in treating Clindamycin-resistant strains (Teasley, Gerding et al. 1983). The management of recurrent CDI is a major challenge and whilst patients with multiple recurrences typically respond to Metronidazole or Vancomycin, the diarrhoea returns when treatment is stopped (Rupnik, Wilcox et al. 2009). Strategies for multiple recurrent infections include prolonged tapering of antibiotic treatment, pulse dosage (giving antibiotic treatment every other day or every three days) in the hope that the inhibitory levels will keep the bacteria under control whilst allowing the gut flora to establish (ibid, 2009). Recent research has found that the most effective treatment in recurrent infections is the replenishment of the normal bacterial flora by faecal transplant (Aas, Gessert et al. 2003). An effective treatment for severe complicated CDI has not been found, and if after management with intravenous fluids, vasopressors, oral and intravenous antibiotic use then removal of the colon may be the only life-saving option remaining (Lamontagne, Labbe et al. 2007).

1.2 Epidemiology

In the United Kingdom, the Health Protection Agency has been monitoring the increasing incidence of *C. difficile* infection since the early 1990's (Djuretic, Wall et al. 1996; HPA 2006). Whilst reporting was initially voluntary,

mandatory reporting was introduced in January 2004 for all cases in persons aged 65 years and over. Whilst it has be speculated that the 26.2% increase in cases of infection between 2004 and 2006 (HPA 2007) can be linked to more stringent monitoring it is generally accepted that the marked increase can only be explained in part by the mandatory reporting. Since April 2007 this mandatory reporting was extended to NHS Trusts reporting cases of CDI in patients aged 2 years and over (HPA 2007).

More recent figures of infection rates in the UK have shown a marked decrease in the number of cases in England after years of steady increases. This marked decrease has been championed by the Department of Health's target to reduce *C. difficile* infections by 30% by 2011. In June 2009, data published by the Health Protection Agency confirmed the early achievement of this target (HPA 2010). Despite this apparent success the Department of Health reports a wide variation between the best and worst performers in reducing rates of infection and some 30,000 cases are still recorded annually (HPA 2010).

During the year following the introduction of enhanced surveillance for CDI there were over 55,000 reports of CDI, representing a baseline quarterly average of approximately 14,000 reports. For the most recent quarter, July-September 2010 just under 6,000 reports of CDI were recorded, corresponding to a 58% reduction on the baseline year's quarterly average. This is a decrease of 1.5% on the previous quarter (HPA 2010).

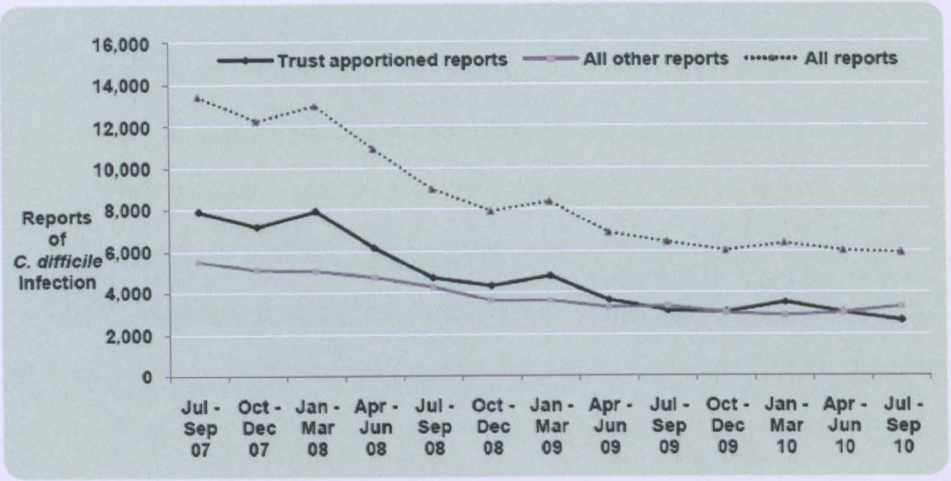

Figure 1-1 Counts of all *Clostridium difficile* infection reports. July - September 2007 to July September 2010. Taken from (HPA 2010)

In contrast to the 1.5% decrease in all reports since April-June 2010 a 9.5% increase in cases reported from April-June 2010 to July-September 2010 (2,988 to 3,272, respectively) is reported in non-trust (not hospital linked) figures. By comparison there was a 12.5% decrease in Trust patients (in-patient, day-patients, emergency assessment patients who have had a specimen taken and the specimen was taken 4 or more days after admission) reports of CDI over the same period (2,995 to 2,622). The decrease in the number of Trust reports was also observed during the second and third quarters of 2009 and 2008. Despite the seasonal spikes observed the overall trend appears to be flattening.

The trend observed in the number of CDI reports is also seen in the rates of infection with the population rate of infection for all CDI reports increasing very slightly in the present quarter (July-September 2010) compared to the last quarter. However, the rate for all CDI reports has remained between 4.7 reports/10,000 population and 5.5 reports/10,000 population since April-June 2009 (HPA 2010).

Although a decrease in the number of reported cases is being observed in the United Kingdom, the number of *Clostridium difficile* infections is on the rise across Canada, America and other areas of Europe (Monaghan, Boswell et al. 2008). In the United States, it is estimated that there are ~500,000 cases of

CDI per year in hospitals and care facilities (Rupnik, Wilcox et al. 2009). This is a marked increase on the 150,000 cases reported in 2000 and the 300,000 cases in 2006. Of these cases, it is estimated that 15,000-20,000 patients die from CDI in the US each year (ibid, 2009). In Europe, few countries have the necessary systems to monitor CDI and the rates of death linked to *C. difficile* and in some countries even the facilities to test for CDI are poor (ibid, 2009). What is evident is the incidence of CDI in on the increase across Europe; Spain reported a threefold increase in CDI between 1997-2005 (Soler, Nogareda et al. 2008) and Germany reported an increase between 2002 and 2006 (Burckhardt, Friedrich et al. 2008).

In addition, a dramatic increase in the number of cases of severe CDI was being reported and molecular analysis of *C. difficile* isolates from a number of healthcare facilities across North America during 2005 led to the identification of the strain responsible for the increase in infection rates, B1/NAP1/027 (Loo, Poirier et al. 2005; McDonald, Killgore et al. 2005). This strain has now been isolated in hospitals all over America, in all provinces of Canada and in most European countries (Loo, Poirier et al. 2005; McDonald, Killgore et al. 2005; Muto, Pokrywka et al. 2005; Pepin, Saheb et al. 2005; Hubert, Loo et al. 2007; Kuijper, Barbut et al. 2008). The increased infection rates and severity are not all attributed to this strain as in some countries, other strains have also been linked to increasing rates of infection and or disease severity (Borgmann, Kist et al. 2008; Goorhuis, Bakker et al. 2008; Rupnik, Widmer et al. 2008).

1.3 Prevention and Control

Reducing the incidence of *Clostridium difficile* infections is a significant challenge and three main strategies are used to meet this challenge; prudent use of antimicrobials; prevention of cross infection, and; active surveillance/reporting.

1.3.1 Prudent use of antimicrobials

The principle risk factor for CDI is the use of antimicrobial therapy and some drugs gave been identified as having a higher propensity to cause disease than others, see Table 1-2.

Table 1-2 Risk of *Clostridium difficile* for different antibiotics.

Adapted from (Monaghan, Boswell et al. 2008)

Low Risk	Medium Risk	High Risk
Aminoglycosides	Co-amoxiclav	Second/third generation cephalosporins
Vancomycin	Macrolides	Clindamycin
Trimethroprim	Amoxicillin/ampicillin	Fluoroquinolones
Tetracyclins		
Piptazobactam		
Benzylpenicillin		

It is expected that over time this will change, the appearance of fluoroquinolone resistant strains have changed the previously low risk choice

to that of medium risk choice when compared with cephalsporins (Monaghan, Boswell et al. 2008). It is now accepted that prudent antimicrobial use is an essential control measure, particularly within high risk health care areas, see Table 1-3.

Table 1-3 Reported success in the control of *C. difficile* infection by restriction of high risk broad spectrum antibiotics

Adapted from (Monaghan, Boswell et al. 2008)

Setting	Antibiotics reduced	Antibiotics increased
Elderly care	Cephalosporins	Benzylpenicillin, trimethoprin, gentamycin
Elderly care	Co-amoxiclav	Benzylpenicillin, amoxicillin, trimethropin
Elderly care	Cefotaxime	Ciprofloxacin
Medicine surgery	Ceftriaxone, oral cephalosporins	Levofloxacin
Elderly care	Cefotaxime	Piptazobactum
Medicine, elderly care	Ceftriaxone, cefuroxime	Moxifloxicin, piptazobactam
Hospital wide	Clindamycin	Various

1.3.2 Prevention of cross-infection

The infection prevention and control measures for patients with CDI are well established. Disease is spread via the faecal-oral route and the biggest challenge in the healthcare setting is the heat-resistant spores produced by the bacteria which remain viable on surfaces for extended periods of time

(Jump, Pultz et al. 2007). Patients suspected of CDI should be isolated as soon as possible into a room with an en-suite bathroom preferably, or a patient designated commode (Monaghan, Boswell et al. 2008). If an outbreak is suspected then patients should be grouped into specific areas and designated nurses assigned (Schroeder 2005). The failure to rapidly isolate symptomatic patients was one of the main contributory factors in the outbreaks at Stoke Mandeville Hospital, UK (CHAI 2006). Enhanced environmental and equipment cleaning is essential and care taken to ensure disinfectants being used possess some sporicidal activity, as most commonly used disinfectants are ineffective against *C. difficile* spores (Monaghan, Boswell et al. 2008). Vaporised hydrogen peroxide is suggested for environmental disinfection but this cannot be completed with staff or patients in the room (ibid, 2008). For those staff treating patients with CDI protective clothing should be worn and a rigorous hand washing routine with soap and water after treating each patient (Gerding, Muto et al. 2008).

1.3.3 Surveillance

Surveillance should be conducted at a local, regional and national level to ensure timely feedback to clinicians and other healthcare professionals (Schroeder 2005; Monaghan, Boswell et al. 2008). Although this is routinely completed in the United Kingdom, other countries have poorly defined surveillance systems meaning potential outbreaks are not effectively monitored and early interventions not employed. In the UK, our effective surveillance has resulted in current treatment practices being reviewed and modified to meet changing the epidemiology.

1.4 Mucosal Immunity

1.4.1 The intestine

The intestine with its large surface area is the subject of constant antigenic challenge and therefore in a high state of activity (MacDonald 2003). These challenges can come from a plethora of origins but can be categorised into three broad groups, food; normal bacterial flora and; pathogens. The main function of the gut is the digestion of nutrients from food and the absorption of water and electrolytes.

The intestine can be split into two regions, the small intestine comprising the duodenum, jejunum and the proximal ileum and the large intestine comprising distal ileum and colon. Each area can be characterised by their specific histology and function, see Table -1-4.

Table -1-4 Differences in the large and small intestine

The main differences are outlined below; however a number of histological differences are also present including the absence of Taeniae coli, Haustra and presence of Plicae in the small intestine with the opposite being observed in the large intestine.

Small intestine	Large intestine
Three sections	Two sections
Long 4.5 to 6 metres	Shorter 1.5 metres
Digestion completed	No role in digestion
Secretes hormones	No hormone secretion
Absorbs the digested nutrients	Absorbs water
Villi present	No villi
Peyers Patches present	No Peyers Patches

Lining the huge surface area of the gut is a single layer of epithelial cells which are replaced every 2-5 days from pluripotent stem cells in the base of the crypts (Bach, Renehan et al. 2000). Six different lineages have been identified and each cell is joined to its neighbouring cell by desmosomes, adherens and tight junctions (Maldonado-Contreras and McCormick). The role of this single cell layer in sensing and promoting a host immune response and its ability to distinguish between self and non-self, food, commensals and pathogens is vital. The single layer of epithelial cells is attached to the basement membrane and immediately subjacent to this are the colonic sub-epithelial myofibroblasts. Together with interstitial fibroblasts the myofibroblasts form a network of interconnected cells throughout the lamina propria (Adegboyega, Mifflin et al. 2002). The closeness of these cells to the epithelium has lead to research considering the role of myofibroblasts in the regulation of epithelial cell function and extracellular matrix metabolism (Powell, Mifflin et al. 1999). It may also be that myofibroblasts are among the first cells to interact with pathogens and their products, presenting them to T-lymphocytes (Saada, Pinchuk et al. 2006).

The many facets of the mucosal defence mechanism can be split between those of innate immunity and those of adaptive immunity and by working in synergy we have mucosal immunity.

1.4.2 Innate Immunity - mucus and epithelial barrier

The obvious starting point is the barrier function provided by the single layer of cells lining that separates the intestinal lumen (mucosal) from the sub-epithelial lamina propria or basolateral domain (serosal) where the mucosal

immune cells reside (Maldonado-Contreras and McCormick). However, this layer of epithelial cells are also protected, a mucus layer covers the cells restricting contact by microorganisms. This mucus layer is produced by goblet cells located in both the crypt and villus epithelium throughout the intestinal tract and is made up of mucin glycoproteins and trefoil peptides, of which MUC2 and TFF3 predominate (ibid, 2010). The absence or thinning of this mucus barrier has been reported in patients with Irritable Bowel Syndrome (IBS) and Crohns disease (CrD) and highlights the importance of this in the protection of the epithelium (Fyderek, Strus et al. 2009).

1.4.2.1 Immunoglobulin A

The epithelial cell also has its own protective mechanism in the form of immunoglobulin A (IgA), the most abundant immunoglobulin found in the gut (Maldonado-Contreras and McCormick). Within the cell IgA can deactivate bacterial lipoproteins and IgA secreted into the lumen by undifferentiated crypt enterocytes (Mostov 1994) bind to the mucus layer, prevent infiltration and neutralize bacteria (Apodaca, Bomsel et al. 1991).

1.4.2.2 Antimicrobial Peptides

Another important group of secreted proteins are the antimicrobial peptides (AMPs) which disrupt the microbial cell membrane (Ganz 1999). Secreted by the Paneth cells, three primary AMP's are expressed in the gut: defensins, lyzozymes and cathelicidins. Of these, defensins are the predominant AMP and two different types have been identified, α and β defensins, based on their molecular structure (Maldonado-Contreras and McCormick).

1.4.2.2.1 Alpha-defensins

Alpha-defensins are mainly expressed by neutrophils and natural killer cells (NK) but have also been found in Paneth cells within the small intestine (Ouellette and Selsted 1996). Interestingly this AMP has also been reported in the distal colon suggesting this protein does not undergo degradation or proteolysis on its journey through the GI tract (Mastroianni and Ouellette 2009). Defects in α-defensin expression have been linked to chronic inflammation and in an extensive study by Salzman and colleagues comparing the intestinal microbiota in homozygous and heterozygous strains of transgenic mice encoding α-defensin 5 (DEFA5), a significant increase in Firmicutes and a decrease in Bacteroides was found in mice over expressing DEFA-5 (Salzman, Hung et al.). This suggests α-defensins, specifically DEFA5 plays a fundamental role in microbiota composition (ibid, 2010).

1.4.2.2.2 Beta-defensins

Beta-defensins are produced by epithelial (Fehlbaum, Rao et al. 2000) and non-epithelial cells (Garcia, Krause et al. 2001) and are found at the epithelial surface throughout the gastrointestinal tract. As with α-defensins, this group also play a role in controlling the microbial population and are linked to the host response towards bacteria and fungi (Maldonado-Contreras and McCormick). HBD1 is effective in eradicating *E-coli* and *S. typhimurium* (Zhao, Wang et al. 1996). HBD2 and HBD3 have antimicrobial activity against Gram-negative bacteria, several Gram-positive bacteria and some yeast (Jia, Schutte et al. 2001). Using histamine and prostaglandin D2, β defensins also trigger the activation and degranulation of mast cells (Bensch, Raida et al. 1995). Linking the increased levels of histamine to CrD and ulcerative colitis

it is possible that the activation and degranulation of mast cells is responsible (Raithel, Matek et al. 1995).

1.4.2.3 Lysozymes

Lysozymes are another AMP produced by Paneth cells which provide protection against Gram-positive infections by catalyzing the hydrolysis of murein on the bacterial cell wall (Fleming, 1922 cited by (Maldonado-Contreras and McCormick). The human cathelicidin, LL37 expressed by epithelial cells is also involved in microbial homeostasis (Hase, Eckmann et al. 2002).

1.4.3 Adaptive Immunity

This first line of defense maintains boundaries and homeostasis, however many microbes have evolved mechanisms to counter this barrier and gain access to the basolateral epithelial domain where the immune cells reside (MacDonald 2003). The intimate relationship between the mucosa, particularly the epithelial cell layer; the inductor and effector sites of adaptive immunity are pivotal to the organized immune response seen in the gastrointestinal tract (Maldonado-Contreras and McCormick).

1.4.3.1 Peyers Patches and Microfold (M) cells

One of the major histological differences in the small and large intestine is the presence of Peyers Patches (PP), known as the inductive site of the mucosal immune response (MacDonald 2003). This organized lymphoid tissue can only

be found in the mucosa of the small bowel and is overlaid with specialized epithelium, microfold cells (M cells) (Neutra, Phillips et al. 1987). The follicles of the PP are covered with a layer of cubiodal epithelium containing few goblet cells and the most prominent feature of the PP is the follicle centre (Owen and Jones 1974). The follicle centre contains centrocytes and centroblasts surrounded by small lymphocytes which join together with plasma cells, dendritic cells, small B cells (centrocyte-like cells) and macrophages to form the mixed cell dome which infiltrate the overlying epithelium (Spencer, Finn et al. 1986). B cells are not found in the villus or crypt epithelium. The lymphoid tissues are capable of sampling antigens in the luminal space (Neutra, Phillips et al. 1987) and also acting as an entry point for many pathogens (Wolf, Rubin et al. 1981; Neutra, Pringault et al. 1996). Although the transcytotic function of M cells has been established, it is not clear whether the cells present the antigen directly to B and T cells or whether it uses the Major Histocompatibility Complex (MHC)-II to present antigen peptides (Neutra, Phillips et al. 1987). Sampling the luminal content, the microfold cell take antigens and microorganisms from the lumen into the underlying gut associated lymphoid tissue (GALT). The invaginated basolateral surface provides a large intra-epithelial pocket where T and B lymphocytes and macrophages reside and the translocation of bacteria across the M cell triggers IgA release and the proliferation of B lymphocytes (Corr, Gahan et al. 2008). The adaptive secretory IgA response is mostly generated in the PP, the products of which migrating to the lamina propria (Craig and Cebra 1971; Guy-Grand, Griscelli et al. 1974). PP are the major route for lymphocyte recirculation (Gowans and Knight 1964). Naïve T cells enter the PP and bind to L-selectin (Boursier, Farstad et al. 2002), if these cells subsequently become activated in the PP they lose the L-selectin and the co-

expression of α4β7 integrin and L-selectin by CD54RO+ cells signal that the T cells are on their way to the lamina propria via the blood (Farstad, Norstein et al. 1997).

1.4.3.2 Induction, Activation and effector sites for B and T cells

The B cells (Pierce and Gowans 1975) and T cells (Guy-Grand, Griscelli et al. 1978) leave the PP following induction and travel from the follicles of the PP through lymphatic's and pass via the mesenteric lymph nodes and the thoracic duct to recirculate in the peripheral blood and then travel to the effector site, the mucosal lamina propria. The effector site of the intestinal mucosal immune system is made up of lymphocytes and plasma cells of the lamina propria and the epithelium (MacDonald 2003). Interspersed between the epithelial cells of the intestinal villi and colonic crypts are the intraepithelial lymphocytes (IEL's).

1.4.3.3 Intraepithelial lymphocytes

The IEL's are a highly unusual population of T cells with many features distinct from T cells populations of the lamina propria and systemic lymphoid tissues (MacDonald 2003). This heterogeneous collection of T cell populations consist predominantly of CD8+ cells expressing α/β or γ/δ with fewer CD4+ cells and even fewer CD3+ cells (Lefrancois 1991). Whilst systemic T cells express CD8+ as a heterodimer consisting of two (CD8α and CD8β) polypeptide chains, most of the γ/δ and many of the α/β express a homodimer of CD8αα (ibid, 1991).

The expression of these specific molecules on the cell surface, which bind to respective ligands on the intestinal epithelium, promote adhesion and trafficking. The IEL's located in the intestinal epithelium express the integrin $\alpha 4\beta 7$, as well as other binding molecules and this particular integrin recognizes the ligand E-cadherin, expressed by epithelial cells (Cepek, Shaw et al. 1994; Blikslager and Roberts 1997). Adhesion of the IEL has also been shown to be associated with the extracellular matrix (ECM), with IEL's binding to collagen type I and IV (Roberts, Brolin et al. 1999). Colonic IEL's have been shown to express L-selectin and it is postulated that the localized expression may be regulated by the MMP, sheddase (Seibold, Seibold-Schmid et al. 1998). The homing and activation receptor, L-selectin, binds to a carbohydrate domain of MAdCAM-1 and is subsequently transported to the mucosal region (ibid, 1998). Another molecule expressed by IEL's, LFA-1 binds to Intercellular Adhesion Molecule-1 (ICAM-1), may also play an important role in cell localization (Smart, Calabrese et al. 1991). These surface molecules allow cells to enter the gut associated lymphoid tissue (GALT) and more specifically the Peyers patches and other antigen priming sites (Mahida 2001).

More recently, research has established chemokine receptors on the cell surface of IEL's suggesting they may play a role in chemotaxis to mucosa and surface epithelium (Ebert 1995). Indeed IEL's have been reported to migrate towards IL-8, macrophage inflammatory protein -1 (MIP-1) and monocyte chemoattractant protein (MCP) and an increased migratory activity has been observed in response to TNF-α (Roberts, Bilenker et al. 1997).

Essential to the growth and development of T cells, cytokines are also needed for their functional activity and whilst a number of cytokines have been associated with IEL's most of their roles are still to be elucidated (Mahida 2001). To further complicate this, it has been suggested that intestinal location, which may reflect different IEL populations, may also reflect the cytokines expressed (Beagley, Fujihashi et al. 1995). Of particular interest, IEL proliferation and survival of the activated form have been observed in response to IL-15 and given that IL-15 is produced by intestinal epithelial cells (IEC), it may conceivable that IEC are capable of local IEL stimulation (Reinecker, MacDermott et al. 1996). This has been supported by the down regulation of isolated IEL's by IEC membrane fractions irrespective of E-cadherin, TGF-β, CD1 or MHC Class I or II (Yamamoto, Fujihashi et al. 1998). It is also reported that bacteria and their by-products are capable of IEL activation and cytokine production (Beagley, Fujihashi et al. 1993; Sperber, Silverstein et al. 1995).

IEL's are in a unique state of activation and upon activation they rapidly upregulate Fas-ligand and CD66a (bilary glycoprotein) (Chott, Gerdes et al. 1997). It is suggested that the upregulation of Fas may provide inhibitory signals to IEL's once activated (Morales, Christ et al. 1999). Co-stimulation of the intraepithelial lymphocyte by CD28 has been studied and debated in great detail, however its role remains unclear (Mahida 2001). Another molecule, BY-55 has also been reported to play a similar co-stimulatory role in IEL activation and it has been demonstrated to be present on all IEL's as well as a subset of NK cells and CD8+ CD28 negative peripheral blood T cells (Anumanthan, Bensussan et al. 1998). The investigation of cytolytic activity in IEL's have provided mixed results, with suggestions that IEL immediately

possess cytolytic activity, ex-vivo (Lundqvist, Melgar et al. 1996), but others report no activity (Russell, Nagler-Anderson et al. 1993). Investigating in-situ cells has revealed that IEL's are at rest and do not display the cytolytic phenotype until activated (Chott, Gerdes et al. 1997).

The function of this population of T cells remains unclear and despite being exposed to a plethora of antigenic stimulants they appear restricted in their T cell receptor usage being in a unique state of activation. It is postulated that the role of this population in mucosal immunity is in immuno-survelliance and activity in immuno-regulation (Mahida 2001).

The lamina propria (LP) is home to mainly IgA secreting plasma cells, induced in the PP's and transported to the LP as described previously, and CD4+ T cells (Mahida 2001). The secreting dimeric IgA binds to the polymeric Ig receptor expressed on the intestinal epithelial cell and the entire complex is endocytosed (Stokes, Soothill et al. 1975). Once inside the cell the complex is transported to the apical surface where proteolysis removes the receptor and the IgA is released into the intestinal lumen where it can bind to luminal antigens and prevent epithelial cell penetration ('immune exclusion') (ibid, 1975). Antigens that manage to penetrate the epithelial cell layer can be transported back to the lumen or neutralized intracellularly by being bound to IgA ('immune elimination') (Mazanec, Coudret et al. 1995).

The lamina propria T cells are of the αβ TCR, CD4+ subset, having similar characteristics to activated memory cells (Mahida 2001). In comparison to systemic lymphocytes, the T cells of the lamina propria are slow to proliferate and crosslink surface CD3 molecules following stimulation, however they do

produce a vast array of cytokines which may increase IgA secretion by plasma cells (ibid, 2001).

The M cell however represents are very small percentage of the total surface area and bacteria have devised methods of penetrating this surface (Maldonado-Contreras and McCormick). A number of structures connect the epithelial cell to its neighbor, the most of apical of which is the tight junction complex (TJC). The TJC is the target of a number of bacterial products including the enterotoxin of *Clostridium perfingens* (Sonoda, Furuse et al. 1999), the cytotoxic necrotizing factor 1 from *E. coli* (Oswald, Sugai et al. 1994) and toxins A and B from *Clostridium difficile* (Nusrat, Giry et al. 1995; Nusrat, von Eichel-Streiber et al. 2001).

Upon penetration of this barrier the pathogen or pathogen associated molecular pattern (PAMP) will be recognized by specialized receptors (Maldonado-Contreras and McCormick). The extracellular Toll-like receptors (TLR's) of which at least 11 TLR homologs have been identified (Kawai and Akira 2006) and intracellular Nod-like receptors (NLR's) recognize conserved microbial elements such as flagellin, lipopolysaccharide (LPS), formylated peptides and peptidoglycan (Maldonado-Contreras and McCormick). The identification of a specific microbe results in the recruitment of an adaptor protein which brings about a signaling cascade that controls the expression of nuclear factor kappa-β (NF-κβ), mitogen activated protein kinases (MAPK) or caspase-dependent signaling pathways (ibid, 2010). The activation of these specialized receptors also triggers the expression of interleukin (IL)-6, TNF-α and IL-1β (Kawai and Akira 2006). The TLR's have the remarkable ability of recognizing self from non self and therefore are able to induce the production

of inflammatory cytokines, chemotactic factors and antimicrobial factors in response to specific cues (Takeda, Kaisho et al. 2003). The location of each TLR on the extracellular surface determines ligand specificity and accessibility, for example TLR 4, the most studied receptor is located at the apical pole of differentiated intestinal epithelial cells (Maldonado-Contreras and McCormick). In-vitro challenge of epithelial cells with LPS has been shown to cause TLR4 redistribution (Cario, Brown et al. 2002) and although its role as a basolaterally placed TLR4 receptor is not known, the TLR4 receptor has been found on the basolateral domain during active ulcerative colitis (Cario and Podolsky 2000).

The intracellular recognition of PAMP's is orchestrated by NLR's and the best known are NOD1 and NOD2 which recognize different structural motifs from peptidoglycan, a protein which makes up the cell wall (Maldonado-Contreras and McCormick). NOD1 is ubiquitously expressed by epithelial cells and NOD2 is only expressed by monocytes, macrophages, dendritic cells and intestinal Paneth cells (ibid, 2010). The activated NOD1/NOD2 recruits an adaptor protein Rip2 which results in the signaling to NF-κβ and Mitogen activated protein kinase (MAPK) pathways (Girardin, Tournebize et al. 2001; Pauleau and Murray 2003). NOD2 also known as a CARD receptor 15 (CARD15) is highly expressed in Paneth cells and stimulation leads to the activation of NF-κβ and α-defensin production (Hisamatsu, Suzuki et al. 2003). A significant reduction in HD5 and HD6 has been linked to CrD (Wehkamp, Salzman et al. 2005) and chronic inflammation in IBS (Arijs, De Hertogh et al. 2009), have been linked to a mutation of NOD2. In fact, Cho et al have reported that mutations in NOD2 alter the mucosal host microbial interactions through the modulation of α-defensins (Cho 2008) and others have revealed the

importance of NOD2 in homeostasis of the gut microbiota (Petnicki-Ocwieja, Hrncir et al. 2009). Therefore functional NOD2 not only restricts chronic inflammation but also by using a feedback mechanism, NOD2 together with other commensals maintains the balance in the intestine (Maldonado-Contreras and McCormick).

The interplay of innate and adaptive mechanisms maintains the delicate balance between responsiveness to pathogens and tolerance to a vast array of harmless antigens.

1.5 Clostridium *spp.*

The genus Clostridium was originally described by Prazmowski in 1880 and included gram positive rods that were obligate anaerobes metabolically and produced heat resistant spores that swell inside the cell. Bergey expanded on this definition in 1923 and in 1986 Cato describe in Bergey's Manual of Systematic Bacteriology, Volume 2 the inclusion criteria for the genus Clostridium, the species must be an anaerobic or micro-aerophillic spore-forming rods that do not sporulate in the presence of air and do not complete dissimilatory sulphate reduction (Sneath, Mair et al. 1986). The genus Clostridium contains approximately 100 species and in 1994 the heterogeneity of the species was confirmed by 16S rRNA gene sequencing. As a result five new genera and eleven new species have been proposed (Collins, Lawson et al. 1994), none of which have been linked to human disease (Winn, Allen et al. 1997).

Criteria essential for inclusion in the genus are principally morphological and some flexibility has been observed when considering the inclusion of a species, with morphological differences significantly dependent on culture age and medium used. Likewise, the early requirement that clostridia be gram-positive was challenged as some species are only gram positive when viewed as very young cultures, and in other species only gram-negative cells are ever seen (De Vos P. 2009).

This flexibility has also been observed in the degree of anaerobiosis required for inclusion in the genus Clostridium. Some species are strict anaerobes (*Clostridium Noyvi* Type A and *C. heamolytium*), conversely others species are aero-tolerant growing aerobically with the addition of 5-10% CO_2 (*Clostridium tertium, Clostridium histolyticum* and *Clostridium carnis*) (Winn, Allen et al. 1997).

The single requirement of spore formation has grouped together species of wide diversity, both phenotypically and genetically into one genus. Most species have straight or curved rods but spirals are described in two species and in one species the cells are round to oval. The cells can vary in length and width and have blunt rounded or pointed ends. The species may produce motile or non-motile spores that may or may not swell the cell and they may be terminal, central or subterminal (De Vos P. 2009).

The first criteria used for classification to species and identification within the genus Clostridium is metabolic activity. Sub groups within the genus are based on biochemical substrate utilisation producing a mixture of organic acids and alcohols from carbohydrates (e.g. *Clostridium butyricum*, *C.*

acetobutylicum) or peptones (*Clostridium pasteurisnum*). Clostridia are ubiquitous and species have been identified from soil (Sanada and Nishida 1965; Warnick, Methe et al. 2002), marine and freshwater sediment (Segner, Schmidt et al. 1971; Finne and Matches 1974), human faeces (Drasar, Goddard et al. 1976) and the intestinal tracts of mammal (Savage 1977), poultry (Mead and Impey 1970), and humans (Hall and O'Toole 1935).

Nine species of Clostridium have been reported to cause human disease and the clinically significant species produce a variety of toxins (HPA 2008). The four most frequently isolated in the United Kingdom being, *C. perfringens* - responsible for food poisoning from poorly prepared meat and poultry; *C. septicum* – responsible for gas gangrene; *C. tertium*; and *C. difficile* (HPA 2008) - the most identified bacterial agent to cause diarrhoea, second only to *C. perfringens* (Borriello 1995). The remaining species, *C. novyii* Type A, *C. sordelli, C. tetani, C. histolyticum, C. botulinum* whilst causing human disease are rarely isolated in the UK (HPA 2008).

1.5.1 Clostridial toxins

Three classes of clostridial toxins have been established; 1) neurotoxins; 2) binary toxins; and 3) 'large clostridial cytotoxins', so called due to their high molecular weights (Mr>200,000 Da) (Just and Gerhard 2004).

The neurotoxins (produced by *C. tetanus* and *C. botulinum*) target the neuronal cells and inhibit the release of neurotransmitters (Montecucco and Schiavo 1995). With a distinctive heavy chain and light chain structure held together by a di-sulphide bond, the heavy chain is responsible for host

targeting. When bound to surface proteins of the host the toxin is endocytosed wherein the light chain can cleave endocytotic vesicles; enter the cytoplasm and protealytically degrade the target protein resulting in inhibition of neurotransmitters.

The binary toxins secreted by *C. perfringens, C. botulinum* and others consist of two separate and independent proteins, labeled components A and B, that work synergistically to intoxicate the host cell, exerting a potent biological effect. Component A is described as enzymatic, whilst Component B is responsible for binding. Working together component A docks onto the extracellular binding component B and the A/B complex is translocated into the cytosol by acidified endosomes. Once inside the cell component A acting as an ADP-ribosyltranferase catalyses the transfer of an ADP-ribosyl group from nicotinamide adenine dinucleotide (NAD^+) onto monomeric actin; inhibiting the polymerisation of actin filaments causing cytoskeletal disorganisation and ultimately cell death (Barth, Aktories et al. 2004).

The final group to be described are the large clostridial toxins. As mentioned previously these toxins are named such due to their large molecular weight. With an A-B modular structure, the catalytic N-terminal can be found in the A domain and is responsible for the biological activity. The C-terminal receptor binding region and the central translocation region make up the B domain. This group includes toxin A and B from *C. difficile*, the α-toxin of *C. noyvil* and the lethal toxins of *C. sordellii*. The toxins bind to surface receptors on host cells and are internalised into endosomes by receptor mediated endocytosis. Upon endosomal activation catalytic domain is released into the cytoplasm

leading to inactivation of key molecular switches; cell rounding and death (Just and Gerhard 2004).

1.6 *Clostridium difficile* - history and discovery

Clostridium difficile, a spore forming Gram positive anaerobic bacillus was first isolated in 1935 under the name '*Bacillus difficulus*' from healthy infant faeces (Hall and O'Toole 1935). With infrequent reports of isolation and a lack of evidence supporting this organism as a pathogen it was initially labelled a commensal bacterium. By the early 1970's Pseudomembranous colitis (PMC) was a prevalent disease, thought to be caused by *Staphylococcus aureus.* Disproving this theory in 1974, Tedesco et al reported a link between the disease and the use of the antibiotic Clindamycin (Tedesco, Barton et al. 1974).

In 1978, *Clostridium difficile* was identified as the primary causative agent of PMC following the discovery of toxigenic activity in the stool filtrates isolated from patients undergoing antibiotic therapy that could be neutralised by *C. sordellii* anti-toxin (Chang, Gorbach et al. 1978). Subsequent isolation of *C. difficile* from patient stool filtrates were found to exhibit the same characteristic cytotoxicity observed previously, confirming the role of *C. difficile* in pseudomembranous colitis disease (Bartlett, Moon et al. 1978; George, Symonds et al. 1978; Larson, Price et al. 1978; Rolfe and Finegold 1979; Willey and Bartlett 1979).

Initially, the cytotoxicity observed was thought to be caused by a singular 'cytotoxin' produced by *C. difficile* (Rolfe and Finegold 1979; Taylor and

Bartlett 1979) however further purification of the cytotoxin revealed a second distinct cytotoxic activity, which was clearly implicated in the pathological changes being ascribed to *C. difficile* disease (Taylor, Thorne et al. 1981). Initially designated D1 and D2 (Banno, Kobayashi et al. 1984), the toxins were later renamed to toxin A (enterotoxin) and toxin B (cytotoxin) based on the elution profiles from anion-exchange resins (Sullivan, Pellett et al. 1982).

In 1988, researchers identified a third toxin (48kDa), with similar mechanism of action to the *C. botulinum* C2 toxin and the *C. perfringens* iota toxin. The new toxin named after the strain CD196, was termed CDT (CD196- ADP-ribosyltransferase toxin) (Popoff, Rubin et al. 1988). Early findings reported the toxin as non-cytotoxic when tested in isolation on cultured cells and despite being linked with the hypervirulent NAP01/027 strain responsible for outbreaks across America and Northern Europe, research still suggests that that the toxin CDT is not capable of facilitating the biological response seen with toxins A and B but may play an adjunct role in *C. difficile* associated disease (Geric, Carman et al. 2006).

Some thirty years have elapsed since *C. difficile* was identified as the cause of PMC, it is currently believed to be responsible for almost all cases of PMC (Monaghan, Boswell et al. 2008) and 150 PCR ribotypes and 24 toxinotypes have been characterised (Kuijper, Coignard et al. 2006) and the number of *C. difficile* infections has increased with antibiotic resistant and hyper-virulent strains causing endemic infections worldwide (Johnson, Samore et al. 1999; Loo, Poirier et al. 2005; McDonald, Killgore et al. 2005; Muto, Pokrywka et al. 2005).

1.7 Major virulence factors

The major virulence factors in the pathogenesis of *Clostridium difficile* are the two high molecular weight enterotoxins, toxin A (TcdA) and toxin B (TcdB) (Borriello, Davies et al. 1990) secreted from the bacterium. In addition a number of other attributes of the bacteria assist in the pathogenesis either by facilitating colonization; including the ability of fimbriae to associate with the mucosal lining and capsule formation, and; the production of hydrolytic enzymes that contribute to tissue damage (Borriello 1998).

Among the largest clostridial toxins, Toxin A (308kDa) and Toxin B (270kDa) are glucosyltransferases that inactivate Rho, Rac and Cdc42, modulating numerous physiological events in the cell (Just, Selzer et al. 1995; Just, Wilm et al. 1995). The toxins are encoded on the chromosomal pathogenicity region and are expressed efficiently during late log and stationary phases of growth in response to a variety of environmental stimuli. The precise environmental signals that modulate toxin expression remain unclear. In vitro studies indicate that toxin expression may be enhanced by stress, including antibiotics, and catabolic repression (Dupuy and Sonenshein 1998). Given the role of antibiotic therapy in PMC early studies focused on the effects of various antimicrobials on toxin production. It was found that sub-inhibitory levels of penicillin and vancomycin increased toxin production in cultures of *C. difficile* (Onderdonk, Lowe et al. 1979; Adams, Riggs et al. 2007). Whilst evidence suggests that antibiotic therapy is a stressor, inducing toxin expression, other factors may also contribute. Limiting biotin, a water-soluble B-complex vitamin, in culture media has been reported to reduce growth of *C. difficile* but enhance toxin production when grown in the presence of 0.05nM biotin.

(Yamakawa, Karasawa et al. 1996). In contrast, limiting amino acids did not enhance toxin production (Yamakawa, Kamiya et al. 1994). Research has also proposed links between toxin production and purine biosynthesis. Despite these findings, other studies have argued against stress and catabolic repression as a mechanism of regulating toxin production (Karlsson, Burman et al. 1999; Maegawa, Karasawa et al. 2002) and further research is needed to clarify our understanding about the factors that facilitate and regulate toxin production.

The toxins have provided one of the quickest areas to understanding the clinical disease with a number of studies establishing the role of these toxins in the pathogenesis of *Clostridium difficile* associated disease (CDAD).

Early research established the presence of a cytotoxin in over 90% of patients suffering from *C. difficile* infection and the clinical manifestation, pseudomembranous colitis (Bartlett, Onderdonk et al. 1977; Bartlett, Chang et al. 1978; Keighley, Burdon et al. 1978). At this point in time scientists were of the opinion that *C. difficile* produced just one toxin (Taylor and Bartlett 1979). In 1981, Taylor and colleagues purified the cytotoxin further and revealed a second distinct cytotoxic activity which could also be linked to *C. difficile* disease (Taylor, Thorne et al. 1981). In that same year, Burdon and colleagues demonstrated that the toxins caused clinical disease by showing a direct relationship between toxin levels and development of pseudomembranous colitis and duration of diarrhoea (Burdon, George et al. 1981).

Direct evidence of the role of toxin A has been shown in animal studies, with the hallmarks of PMC; fluid accumulation, inflammation and cell damage reported (Libby, Jortner et al. 1982; Czuprynski, Johnson et al. 1983; Lonnroth and Lange 1983; Arnon, Mills et al. 1984). Toxin A given intragastrically caused hemorrhage, fluid accumulation in the intestine, diarrhoea and death in hamsters (Lyerly, Saum et al. 1985). Kurtz *et al* have shown that *C. difficile* toxins can be neutralized with an anionic high molecular weight polymer, protecting 80% of experimental hamsters exposed to the organism (Kurtz, Cannon et al. 2001). In addition, levels of immunoglobulin G against toxin A correlate directly with protection from disease following colonisation, indicating that the antibody response to this toxin is sufficient for protection from CDAD. (Kyne, Warny et al. 2001).

The role of TcdB in disease is not as well understood. Early research using crude supernatant containing both toxins suggested that the toxins worked synergistically to elicit disease (Lyerly, Saum et al. 1985). The isolation of numerous TcdA- TcdB+ strains capable of causing disease and in some cases extensive Pseudomembranous colitis and death challenged this belief (Alfa, Kabani et al. 2000) and these strains have been useful in characterising the role of TcdB in disease and confirming its cytotoxic presence. (Kato, Kato et al. 1998; Limaye, Turgeon et al. 2000; Sambol, Merrigan et al. 2000; Kuijper, de Weerdt et al. 2001; Pituch, van den Braak et al. 2001; Komatsu, Kato et al. 2003; Rupnik, Kato et al. 2003; Drudy, Harnedy et al. 2007). Alfa and colleagues characterized a TcdA- strain and demonstrated that whilst the strain was TcdA- TcdB+ was capable of eliciting the full clinical spectrum of disease, when investigated on intestinal tissue the strain was unable to alter tight junctions, a response indicative of TcdA (Alfa, Kabani et al. 2000).

With the acceptance of TcdB as a potent cytotoxin consideration of earlier research demonstrating that monoclonal antibodies to TcdA were able to block disease progression in mice treated with both toxins questions the role of toxin A as a facilitator of toxin B cytotoxic effect (Corthier, Muller et al. 1991).

In 1988, a new ADP-ribosyltransferase was identified in *C. difficile* strain (CD196) and was found to covalently modify cell actin (Popoff, Rubin et al. 1988). This binary toxin (CDT) has now been identified in about 6-12.5% of clinical *C. difficile* isolates taken in the United States and Europe (Stubbs, Rupnik et al. 2000). The structure and function of CDT are similar to those found in other binary toxins (Gulke, Pfeifer et al. 2001). The binary toxin is encoded by two chromosomal genes (*cdtA and cdtB*), separate from the chromosomal pathogenicity locus. The *cdtB* gene arbitrates cell surface binding and translocation, whilst *cdtA* ribosylates adenosine phosphate resulting in the disruption of actin filament and cell death (Barth, Aktories et al. 2004). The pathogenic role of CDT in *Clostridium difficile* associated diseases is not clear but it is a suspected virulence factor in strains that carry the toxin (Gulke, Pfeifer et al. 2001).

1.7.1 Other toxins

A small number of clinical isolates have also been found to produce binary toxins that display ADP-ribosyltransferase activity (Perelle, Gibert et al. 1997; Stubbs, Rupnik et al. 2000). CD196, a strain isolated from a patient with pseudomembranous colitis, was shown to produce a ≈43 kDa protein capable of modifying the actin cytoskeleton via ADP-ribosyltransferase activity (Popoff,

Rubin et al. 1988). Early findings established the toxin not to be cytotoxic and was subsequently identified to be a two-component ADP-ribosyltranferase toxin encoded by the genes *cdtA* and *cdtB* (Perelle, Gibert et al. 1997). The more recent isolation of NAP1/027 (Bartlett 2002; McDonald, Killgore et al. 2005), this epidemic strain expresses all three toxins (Warny, Pepin et al. 2005) and whilst the increased virulence is suggested to be attributable to a gene deletion in the TcdC regulatory region of the pathogenicity locus (Stabler, Dawson et al. 2008) the role of CDT still needs to be characterized.

In addition to TcdA, TcdB and CDT, strains of *C. difficile* that contain variant toxin genes that produce hybrid toxins have been identified. The most characterised of which is produced by *C. difficile* strain 1470 (von Eichel-Streiber, Meyer zu Heringdorf et al. 1995; Chaves-Olarte, Low et al. 1999). TcdB-1470 is a hybrid toxin that is closely related to the non-hybrid toxin, TcdB, showing 99% homology in the C-terminus and middle domain. This hybrid toxin has the ability to modify Ras, Rac, Rap and Ra1 and is believed to be a unique hybrid between TcsL and TcdB (Chaves-Olarte, Low et al. 1999).

1.8 Genetics of toxin A and toxin B

1.8.1 Pathogenicity Locus (PaLoc)

The genes encoding TcdA and TcdB have been identified, sequenced and are found in a single open reading frame located within a ≈19kb pathogenicity locus (Barroso, Wang et al. 1990; Dove, Wang et al. 1990), see Figure 1-2. The two toxins are closely situated with a 1,350 nucleotide intervening sequence. The toxin genes show similar sequence and functional homology

with low G+C content, comparable with the overall *C. difficile* genome. In addition to *tcdA* and *tcdB*, three other open reading frames are located on the pathogenicity locus and are believed to be involved in regulation of toxin production or release of the toxins from the cell (Hammond and Johnson 1995).

The gene, *tcdC* can be found downstream and unlike the other genes located on the pathogenicity locus, it is transcribed in the opposite direction. TcdC is highly expressed in the early exponential phase of bacterial growth but later declines in the stationary phase (Hundsberger, Braun et al. 1997). The decrease in TcdC expression corresponds with an increase in toxin A and B secretion suggesting that TcdC may function as a negative regulator of toxin production (Hundsberger, Braun et al. 1997). *tcdR* (formerly *tcdD)* is encoded upstream of TcdB and expressed at the same time as TcdA and TcdB. TcdR (formerly TcdD) shows homology with TetR and BotR positive regulators of tetanus and botulinum toxin production. It has also been reported that TcdR can auto-regulate its own expression in response to environmental conditions such as growth phase and local surroundings. Thus TcdR may serve as a major positive regulator of toxin synthesis in *C. difficile* (Hundsberger, Braun et al. 1997; Mani and Dupuy 2001; Mani, Lyras et al. 2002).

The gene encoding TcdE is located between TcdA and TcdB and shows homology with holin proteins and has been speculated to facilitate the release of TcdA and TcdB through the permeabilization of the *C. difficile* cell wall (Tan, Wee et al. 2001). It can therefore be postulated that toxin expression appears to be dependent on decreases in TcdC, enhanced expression of TcdR and TcdE mediated release from the cell.

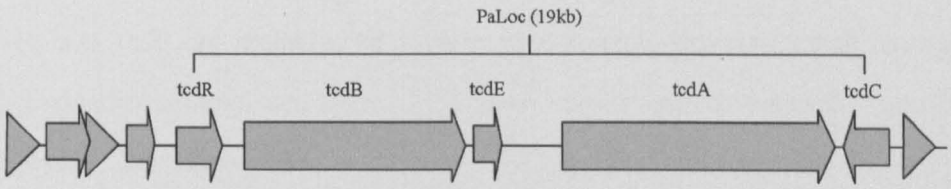

Figure 1-2 Pathogenicity Locus (PaLoc)

Contains five genes *tcdB* and *tcdA* encode for the major virulence factors Toxin A and B. *tcdR*, formerly *tcdD* is involved in positive transcriptional regulation and *tcdC* encodes a negative regulator. *tcdE* codes a protein similar to phage holins. Adapted from (Rupnik, Wilcox et al. 2009).

It has been proposed that the two toxin genes may have arisen from a gene duplication event (von Eichel-Streiber, Laufenberg-Feldmann et al. 1992). Supporting this idea, both toxins use a highly conserved N-terminal domain with 74% homology to modify identical substrates (von Eichel-Streiber, Laufenberg-Feldmann et al. 1992). The major areas of homology between toxin A and B fall within the enzymatic and receptor binding domains of the two toxins (von Eichel-Streiber, Laufenberg-Feldmann et al. 1990). The C-terminal domains show a number of short homologous regions termed combined repetitive oligopeptides (CROPS) (von Eichel-Streiber, Laufenberg-Feldmann et al. 1992). Both toxins encode five groups of CROPs ranging in size from 21-50 residues and can be repeated throughout the C terminus of the protein, four of the CROPs in toxin B show homology to four of the CROPS in toxin A but the CROPs found in toxin B display more divergence and appear less frequent than those found in toxin A. Whilst the CROPs appear to play a role in initial target cell interaction and receptor binding the need for these repeats in cell binding remains unclear (Voth and Ballard 2005).

1.8.2 Functional domains of toxin A and B

TcdA and TcdB are predicted to have three domains, enzymatic, translocation and receptor binding, see Figure 1-3. Each domain serves a specific function during cellular intoxication.

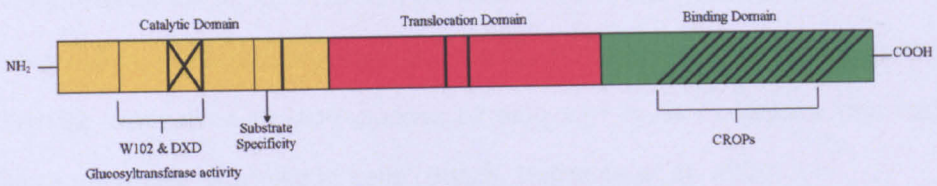

Figure 1-3 Three domain structure of toxin A and B

Diagrammatic representation of *C. difficile* toxin A and B protein structure. Both toxins are single chain proteins with three functional domains. Adapted from (Voth and Ballard 2005).

1.8.2.1 The enzymatic domain

The enzymatic domain of TcdB contains a 546-residue region responsible for glucosylation activities (Hofmann, Busch et al. 1997). This region has been shown to effectively glucosylate substrates in vitro but lacks any cytotoxic activity. Recent research conducted by Rupnik and co-workers has shown that a fragment of the enzymatic domain was in fact cytotoxic when microinjected into cells (Rupnik, Pabst et al. 2005). Spyres and colleagues report any deletion in the enzymatic region of the PaLoc results in a complete loss of enzymatic activity and micro-injection of TcdB mutants are capable of inhibiting wild-type TcdB enzymatic activity (Spyres, Qa'Dan et al. 2001; Spyres, Daniel et al. 2003). Challenging these findings, another group reportedly reduced the enzymatically active portion substantially whilst retaining the ability of the region to glucosylate Rho Rac and Cdc42 in vitro (Wagenknecht-Wiesner, Weidmann et al. 1997). Using chimeric hybrids

between TcdB and TcsL, the substrate recognition region of TcdB has been reduced to residues 364 to 516 (Hofmann, Busch et al. 1998). In addition to finding this site Busch and colleagues also found that glucosyltransferase activity is dependent on a DXD motif in the enzymatic domain and mutations in this vital motif lead to the production of toxins unable to modify GTPases via glucosylation in vitro (Busch, Hofmann et al. 1998). Another critical region involved in TcdB glucosylation is Trp102, Busch and colleagues report that Trp102 is involved in UDP-glucose binding and mutants lacking this residue were no longer cytotoxic to cells (Busch, Hofmann et al. 2000).

1.8.2.2 The receptor binding domain

Making up approximately one third of the toxin the receptor binding domain contains up to 38 repeating CROP modules. The hemagglutinating activity of TcdA may be explained by the high degree of repetition within these CROP modules (Wren 1991). It has also been suggested that the CROP region of toxin A contains isolate-specific repeats and deletions demonstrating that this region may have originated from multiple duplication and recombination events (Rupnik, Avesani et al. 1998). The CROP sequences vary in length but all contain a consensus triad YYF and an overall hydrophilic stretch indicative of a solvent exposed area of the protein (Wren, Russell et al. 1991).

Supporting the role of the C-terminal as the binding domain, specific monoclonal antibodies capable of neutralizing the enterotoxic activity of toxin A were found to bind to two epitobes in this region (Frey and Wilkins 1992) and recombinant protein produced from the C terminal region neutralized the effect of TcdA by competitive inhibition of receptor binding (Sauerborn, Leukel

et al. 1997). The same fragment was also found to immunize mice against toxin A (Ward, Douce et al. 1999). More recently Frisch and colleagues have shown that the entire C terminal receptor domain is required for both receptor binding the endocytosis of the holotoxin (Frisch, Gerhard et al. 2003).

Toxins A and B also share a high degree of similarity to the other large clostridial toxins. Toxin B shows the most homology with the cytotoxin TscL, produced by *Clostridium sordellii* which glucosylates Ras, Rac, Rap and Ral (Chang, Gorbach et al. 1978). The main differences in these proteins are found in the N-termini and are responsible for the difference in substrate specificity (Hofmann, Busch et al. 1998). Toxin A is thought to be most similar to the enterotoxin TcsH, produced by *C. sordellii (Chang, Gorbach et al. 1978).* The close homology between these large clostridial toxins is further demonstrated by antiserum to toxin A recognising TcsH; and antiserum to toxin B recognising TscL; and vice versa (Martinez and Wilkins 1988). Showing the least homology, Tcnα, produced by *C. novyi* also glycosylates Rho, Rac and Cdc42 and differs only in the co-substrate used (Voth and Ballard 2005).

1.8.3 Toxinotypes of *C. difficile* isolates

Variations in the PaLoc sequence determine which toxinotype the isolate belongs to. In non-toxigenic TcdA negative TcdB positive strains the PaLoc region is replaced by a 115bp of non-coding sequence (Rupnik, Avesani et al. 1998). Rupnik established a typing system to distinguish the various toxinotypes and there are at 22 toxinotypes of *C. difficile* established, twenty one are pathogenic and one non-pathogenic (toxinotype XI). Toxinotypes I-

VII, IX, XII-XV, and XVIII-XXII produce toxins A and B. Toxinotype VIII, X, XVI and XVII only produce toxin B (Rupnik, Avesani et al. 1998; Rupnik, Kato et al. 2003).

Research investigating the role of TcdA and TcdB in the pathogenesis of *Clostridium difficile* associated disease (CDAD) has been completed using the reference strain VPI10463, however several genetic variants of these toxins have been isolated from clinical samples. Some of which are hybrids occurring as a result of genetic exchange between large clostridial toxin producing Clostridia. More commonly subtle sequence variations, deletion and duplication within the pathogenicity locus account for the various toxinotypes. This typing has proved very useful in categorising new strains based on major virulence factors. Serotyping has also been established to distinguish between different strains of *C. difficile*. Currently 14 different serotype groups have been recorded.

1.8.3.1 TcdA-negative strains in disease

Although TcdA is thought to play an important role in *Clostridium difficile* associated disease, an increasing number of TcdA-negative, TcdB-positive strains have been reported in clinical isolates (al-Barrak, Embil et al. 1999; Brazier, Stubbs et al. 1999; Alfa, Kabani et al. 2000; Wilcox and Fawley 2001; Barbut, Lalande et al. 2002; Johnson, Sambol et al. 2003; Komatsu, Kato et al. 2003; Pituch, vavn Belkum et al. 2003). The TcdA-negative strains produce TcdB but contain deletions in *tcdA* gene and encode shortened forms of the protein (Rupnik, Avesani et al. 1998; Soehn, Wagenknecht-Wiesner et al. 1998; Rupnik, Kato et al. 2003). Over 20 toxinotypes of *C. difficile* have

been identified, nine of which contain deletions in the 3' end of the *tcdA* gene (Rupnik, Avesani et al. 1998; Rupnik, Kato et al. 2003). Absence of the CROP region not only reduces cytopathic activity but also prevents the recognition of TcdA-negative strains by most detection systems as they use the presence of toxin A to confirm *C. difficile* infection (Voth and Ballard 2005).

TcdA-negative, TcdB-positive strains have been isolated in a variety of different patients, spanning from the elderly to children (Johnson, Kent et al. 2001; Rupnik, Kato et al. 2003). Early reports suggest TcdA-negative, TcdB-positive strains occurred at a low frequency (Sambol, Merrigan et al. 2000; Pituch, van den Braak et al. 2001; Geric, Rupnik et al. 2004), however a study of individuals suffering severe disease reported over 55% of stool specimens analysed were TcdA-negative, TcdB-positive strains (Samra, Talmor et al. 2002). The reported increase in TcdA-negative, TcdB-positive strains over recent years may also reflect our increased understanding of *C. difficile* epidemiology and the typing systems put in place over the same period.

The ability of TcdA-negative, TcdB-positive strains to cause disease has caused some confusion. Early research argued that TcdB was ineffective unless TcdA was administered first suggesting that TcdB not only lacked the ability to cause disease but also needed TcdA to gain access to target cells (Lyerly, Saum et al. 1985). This finding was supported by limited evidence to suggest that TcdB had any impact on the cells in the gastrointestinal tract (Riegler, Sedivy et al. 1995; Fiorentini, Fabbri et al. 1998; Savidge, Pan et al. 2003).

Interestingly, the clinical presentation is remarkably similar between TcdA-negative (TcdB-positive) and TcdA-positive strains (Johnson, Kent et al. 2001). The identification of more TcdA- strains from clinical isolates of *C. difficile* may highlight a more prominent role of TcdB in CDAD. In fact Savidge et al reported that TcdB functions as a potent enterotoxin (Savidge, Pan et al. 2003). TcdB interactions with other *C. difficile* factors may explain why the toxin is cytopathic in the absence of TcdA.

It has also been suggested that the increasing number of TcdA-negative, TcdB-positive strains may also highlight a selection event within the host. Most of the *tcdA* deletions occur in the CROP region and given the repeat sequences, this area would be susceptible to deletion by recombination. It has been suggested therefore that the disease is in fact initiated by a TcdA strain but there is selection for strains that have lost their ability to produce toxin (Voth and Ballard 2005). This idea has been refuted by Sambol and co-workers who argue that TcdA-negative, TcdB-positive isolates are able to cause disease in hamster models (Sambol, Merrigan et al. 2000; Sambol, Tang et al. 2001). Until recently, the absence of an isogenic strain lacking TcdA or select deletions in *tcdA* this argument could not be resolved. In a recent publication Kuehne and fellow workers report *C. difficile* isogenic mutants capable producing toxin A or toxin B can cause fulminant disease and the construction of a double-mutant strain completely attenuated disease (Kuehne, Cartman et al.). These findings re-establish the importance of both toxins when studying the pathogenesis of *Clostridium difficile* associated disease (CDAD).

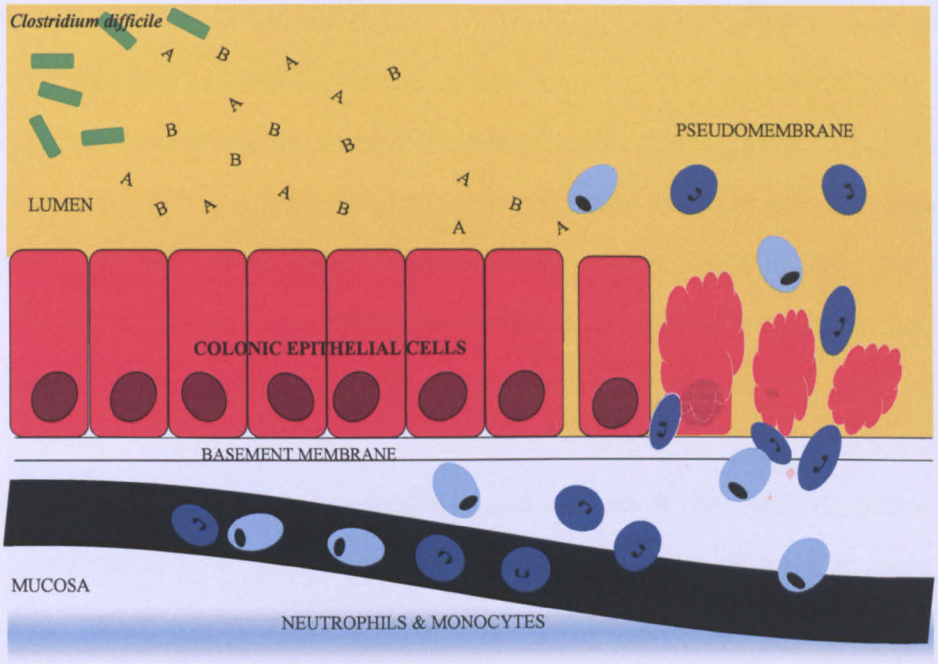

Figure 1-4 Pathogenesis of *Clostridium difficile* associated disease

Ingested spores are transported down the intestinal tract and the spores mature into vegetative cells and release toxin A and toxin B into the lumen. Toxins bind to surface receptors located on colonic epithelial cells and upon internalisation the toxins inactivate key intracellular signals. The epithelial cells round and undergo apoptosis, tight junctions open. The simultaneous release of TNF-α and pro-inflammatory interleukins increase vascular permeability and neutrophils and monocytes are recruited to the site of injury. Production of hydrolytic enzymes leads to tissue degradation and pseudomembrane formation. Illustration adapted from UK *Clostridium difficile*.

1.9 Pathophysiological response

1.9.1 Cell death – apoptosis

Cell death is the most obvious impact of TcdA and TcdB on cell physiology but our understanding of the mechanisms that precede this are still being elucidated.

Cell rounding caused by the inactivation of Rho, Rac and Cdc42; the subsequent cytoskeletal rearrangement; cell rounding; and basement membrane detachment have been suggested as temporally distinct events to

cell death (Voth and Ballard 2005). This is supported by research conducted by Qa'Dan and colleagues indicating cell rounding and cell death may be temporally distinct events in toxin B exposed cells as cell rounding was visible in less than 2 hours and cell death did not occur until at least 24 hours. (Qa'Dan, Ramsey et al. 2002). The mechanism of cell death in cells exposed to TcdA and TcdB is apoptosis and a number of studies have been conducted providing evidence to suggest that inactivation of Rho causes cell death (Fiorentini, Fabbri et al. 1998). Inactivation of Rho in an endothelial cell line resulted in the activation of caspase-3 and caspase-9 (Hippenstiel, Schmeck et al. 2002). In a similar study, Brito and colleagues report that toxin A induced the apoptotic pathway in T84 cells via the release of caspase-3, -6, -8, -9 and Bid activation (Brito, Fujji et al. 2002). Further delineating the apoptosis-signalling cascade induced by toxin A in T84 cells, Carneiro and colleagues found that toxin A induced caspases 6, 8 and 9 prior to caspase 3 activation and induced Bid cleavage using a caspase independent mechanism. (Carneiro, Fujii et al. 2006)

Purporting toxin A to induce apoptosis independently of Rho protein inactivation, He Hagen et al reported the intoxication of cells with toxin A results in an accumulation of toxin at the mitochondria prior to any detectable glucosylation of Rho proteins (He, Hagen et al. 2000). It may be therefore toxin A causes apoptosis by disrupting the mitochondria and promoting proapoptotic events.

In contrast and implicating in-activation of Rho proteins and caspase dependent apoptosis Qa'Dan and co-workers demonstrated that the intoxication of HeLa cells with toxin B resulted in caspase-3 dependent

apoptosis with a simultaneous loss of host cell vimentin and apoptosis induced by substrate inactivation (Qa'Dan, Ramsey et al. 2002). In a recent study, Nottrott and colleagues report cultured human adenocarcinoma cells (HT29) undergo TcdA induced apoptosis following the glucosylation of Rho GTPases leading to the activation of cathespins and caspase-3 (Nottrott, Schoentaube et al. 2007). This paper also reported that whilst TcdA induced mitochondrial damage and cytochrome c release, p53 was not activated.

Intoxication of cells with TcdA and TcdB at relatively low concentrations has been shown to induce distinct morphological alterations (Donta, Sullivan et al. 1982). TcdB has been identified as a more potent cytotoxin (Chaves-Olarte, Weidmann et al. 1997; Riegler, Sedivy et al. 1997), able to intoxicate a variety of cell lines, and depending on cell type exert a cell specific effect ranging from 4-fold to 200-fold increase in cytotoxic activity than TcdA (Donta, Sullivan et al. 1982). Supporting the cell-specific effect mouse teratocarcinoma cells were more sensitive than Chinese Hamster Ovary (CHO) cells when exposed to TcdA and it was proposed that increased expression of TcdA specific carbohydrate receptors may be responsible (Tucker, 1990 #96). Research conducted by Chaves-Olarte and co-workers sought to establish why TcdA and TcdB displayed different cytotoxic potency despite intoxicating target cells by the same mechanism. Using Don and T84 cells, two main differences were identified, with differing enzymatic activities highlighted as the main determinant and receptor binding difference contributed less (Chaves-Olarte, Weidmann et al. 1997).

The substrate targets Rho, Rac and Cdc42 also regulate other cellular events outside of the actin cytoskeleton (Prepens, Just et al. 1996; Schmidt,

Rumenapp et al. 1996; Caron and Hall 1998; Brito, Fujji et al. 2002; Hippenstiel, Schmeck et al. 2002). Given the temporal differences between cell rounding and cell death reported by Qa'Dan and colleagues and the many other pathways linked to the small GTPases it would be pertinent to conclude that other events downstream of actin condensation may also contribute to cell death.

1.9.2 Increased epithelial cell permeability

The first and most obvious impact on cell physiology is loss of structural integrity caused by the disruption of the actin cytoskeleton in cells exposed to toxins A and B. Chang et al reported alterations in cell surface projections and rearranged microvilli (Chang, Lin et al. 1979) and in a later paper reported that toxin A altered the ultrastructure of CHO cells, with clear actinomorphic changes and marginalization of the nucleus seen using electron microscopy (Fiorentini, Malorni et al. 1990). Similar observations were viewed in TcdB exposed cells (Feltis, Wiesner et al. 2000). Exposure of cultured human intestinal epithelial (T84) cell monolayers to TcdA and TcdB reduced transepithelial resistance and increased epithelial cell permeability, with flux studies identifying that the permeability failing occurred at the intercellular tight junction (Hecht, Pothoulakis et al. 1988; Hecht, Koutsouris et al. 1992). The disruption of epithelial tight junctions of the epithelium is considered to be directly attributable to the toxins (Feltis, Wiesner et al. 2000). Supporting these early studies, Johal and co-workers investigated barrier function of cultured human intestinal epithelial cells (T84) in response to varying concentrations of TcdA and demonstrated that after pre-exposure to >10 ng/ml a complete and irreversible loss of epithelial resistance was observed,

exposure to lower concentrations resulted in loss of resistance followed by recovery, enhanced by recombinant isoforms of TGF-β (Johal, Solomon et al. 2004). Transforming growth factor (TGF)-β has previously been shown to regulate paracellular permeability of epithelial cells via their effects on tight junctions (McKay and Baird 1999).

The loss of structural integrity is however expected since Rho, Rac and Cdc42 each regulate structural processes dependent on actin polymerization and this was supported by Nusrat and colleagues who presented strong evidence that the Rho protein regulates tight junctions and the organization of actin microfilament in polarized T84 colonic cell monolayers (Nusrat, Giry et al. 1995).

This disruption is likely due to the inactivation of Rho proteins, small GTPases known to be important in tight junction maintenance (Nusrat, Giry et al. 1995). A reduction in epithelial monolayer resistance in <3 hrs following toxin A intoxication was report by Johal and colleagues (Johal, Solomon et al. 2004), by contrast Hecht et al, reported. Loss of resistance appeared to occur prior to loss of confluence suggesting that cell to cell contact was disrupted before contraction of the cell. Toxin B has also been found to disrupt epithelial integrity through the decline in F-actin and disruption of the perijunctional actomyosin ring (Hecht, Koutsouris et al. 1992).

Further definition has been provided by Nusrat and co-workers who demonstrated the loss of apical and basal F-actin, is associated with loss of intact occludin and ZO- in the tight junction membrane (Nusrat, von Eichel-

Streiber et al. 2001). Collectively these studies suggest that the loss of epithelial barrier integrity may be due to direct interactions with the cell.

1.9.3 Inflammatory Response

Many of the symptoms described in patients with *C. difficile* disease can be ascribed to inflammatory events and TcdA and TcdB would appear to be, given the wealth of evidence, implicated as likely modulators of these events.

TcdA and TcdB are capable of imitating the physiological events occurring in *Clostridium difficile* disease and pseudomembranous colitis (Savidge, Pan et al. 2003). The inflammatory response seen in PMC can be triggered in rabbit or rat ileal loop models by toxin A (Lima, Lyerly et al. 1988). The pathologies observe in PMC have been attributed to inflammation caused by increased epithelial permeability (Feltis, Wiesner et al. 2000), production of cytokines and chemokines (Castagliuolo, Keates et al. 1998; He, Sougioultzis et al. 2002), neutrophil infiltration (Kelly, Becker et al. 1994), activation of submucosal neurons (Neunlist, Barouk et al. 2003), construction of reactive oxygen intermediates (He, Sougioultzis et al. 2002), mast cell activation (Wershil, Castagliuolo et al. 1998), substance P production (Pothoulakis, Castagliuolo et al. 1994) and direct damage to the intestinal mucosa (Mantyh, Pappas et al. 1996).

The contribution of other toxin activities in causing inflammation remains a target for research. Whilst PMC associated inflammation can be induced with toxin alone, isogenic strains lacking both toxins have been suggested as a possible route of future research. In addition, direct links between

inactivation of Rho proteins and the induction of inflammation have not been reported and therefore consideration should be directed toward other toxin activities contributing to inflammation.

Early studies found that the rat intestinal response to TcdA could be attenuated by a substance P antagonist (Mantyh, Pappas et al. 1996). Substance P is an 11-amino acid polypeptide associated with sensory neurons that line the submucosal regions of the intestinal epithelium and has been shown to be involved in inflammatory diarrhea (Pothoulakis, Castagliuolo et al. 1994). Treatment of rat ileal loops with TcdA has resulted in an increase in substance P production (Mantyh, Maggio et al. 1996). Amplifying the inflammatory response substance P has been shown to activate lamina propria macrophages to release tumour necrosis factor – alpha (TNFα) (Castagliuolo, Keates et al. 1998). As a result of this substance P mechanism, neutrophil recruitment and inflammation is increased.

Later research has shown that removal of neural endopeptidase, an important protein in substance P synthesis, amplifies the inflammatory response (Kirkwood, Bunnett et al. 2001). Together these studies highlight the contributions of neuronal signalling to inflammatory pseudomembranous colitis.

Toxin A has been shown to stimulate cytokine production. TcdA triggers interleukin-8 (IL-8) secretion and the production of reactive oxygen intermediates by human colonocytes (Mahida, Makh et al. 1996; He, Sougioultzis et al. 2002). Jefferson and colleagues have demonstrated that IL-8 activation is dependent on TcdA entering the cell and activating nuclear

factor kappa beta (NK-κβ) and activating protein-1 (AP-1) (Jefferson, Smith et al. 1999). Along the same theme, Castagluiolo found that interleukin-11 (IL-11) inhibits TcdA related damage by blocking the release of TNF-α and macrophage inflammatory-protein 2 (MIP-2) (Castagliuolo, Kelly et al. 1997). Causing further inflammation, macrophages have been shown to release intestinal secretory factor following exposure to TcdA (Rocha, Soares et al. 1998).

In addition to the many direct interactions of TcdA, it has also been suggested that products of these initial interactions may also exacerbate the inflammatory response. This is true in neutrophils; responding neutrophils release reactive oxygen metabolites (Qiu, Pothoulakis et al. 1999). TcdA also induces responses in macrophages and mast cells furthering the inflammatory response through the release of TNFα (Calderon, Torres-Lopez et al. 1998). Mast cell deficient mice have reduced neutrophil recruitment and exhibit reduced levels of fluid accumulation following TcdA intoxication (Wershil, Castagliuolo et al. 1998).

Whilst early research into mast cell activation by TcdA and TcdB was conducted on rat basophilic leukaemia cells and murine peritoneal mast cells (Calderon, Torres-Lopez et al. 1998), a recent study used a novel model system to investigate mast cell-mediated processes. Using human mast cells (HMC-1), Meyer and colleagues demonstrated the activation of human mast cells by TcdA and TcdB resulted in degranulation and IL-8 release (Meyer, Neetz et al. 2007).

1.9.4 Toxin cell surface receptors

Receptor binding is the first step in cell entry. Understood to be non-proteinaceous the receptor for toxin A displays the disaccharide Galβ1-4GlcNac. This disaccharide is found on blood antigens I, X and Y on a variety of cells and these antigens have been shown to act as receptors for toxin A (Tucker and Wilkins 1991). Recent analyses of the C-terminal crystal structure of TcdA have provided insights into the interaction of the toxins with carbohydrate receptor structures (Ho, Greco et al. 2005) and our knowledge extended with the construction of a high resolution co-crystal structure (Greco, Ho et al. 2006).

Animal studies have identified many species susceptible to TcdA but receptors are not identical and in one particular study the receptor Galα-1-3Galβ1-4 GlcNac is reported to bind TcdA but it does not appear to be present in human cells (Krivan, Clark et al. 1986). Supporting these studies, treatment of cells or tissues with galactosidase reduces binding of toxin A (Krivan, Clark et al. 1986; Clark, Krivan et al. 1987; Smith, Cooke et al. 1997; Cooke and Borriello 1998). The receptor for toxin B whilst undefined is ubiquitous with TcdB capable of intoxicating a broad range of cell types.

1.9.5 Receptor-mediated endocytosis and membrane translocation

As mentioned previously, Toxin A & B enter the cell by receptor mediated endocytosis and require an acidified endosome for translocation into the cytosol (Florin and Thelestam 1983; Fiorentini, Malorni et al. 1990). In support, it has been demonstrated that lysomotropic inhibitors such as

bafilomycin A and ammonium chloride can directly inhibit cytotoxic effects of large clostridial toxins (Florin and Thelestam 1983). In addition, preventing lysosome fusion with the endosome weakens toxin B activity (Florin and Thelestam 1986).

It would appear that a low pH is essential for conformational changes within the toxin, leading to the exposure of the hydrophobic domain and subsequent insertion into the target membrane (Qa'Dan, Spyres et al. 2000). This idea was supported by Barth and colleagues, who observed the formation of channels in the lipid bilayers by toxin B through an acid pH-dependent process (Barth, Pfeifer et al. 2001).

With the toxin packaged inside the acidified endosome, researchers found that following proteolytic cleavage only the N-terminal domain exits the endosome and gains access to the substrates (Pfeifer, Schirmer et al. 2003) and the cleavage of TcdB occurs after residue 543 (Rupnik, Pabst et al. 2005). These finding are supported by the rapid cytotoxicity demonstrated when microinjection of the N-terminal fragment was compared with the cytotoxicity of the microinjected holotoxin into the host cell (Rupnik, Pabst et al. 2005). Once internalized the N-terminal fragment targets intracellular proteins - small GTPases.

1.10 Small GTPases and the Ras Super-family

Before delineating specific protein interactions and subsequent modification discussion will begin small GTPases; the Ras Super family and highlight the cellular importance of these proteins.

Found in all eukaryotic organisms, small GTPases are small monomeric guanine triphosphate (GTP) binding proteins with molecular masses ranging from 20-25kDa. These monomers act as molecular switches, facilitating intracellular signalling and controlling a variety of cellular functions. Members share approximately 30% amino acid homology across the super-family and this identity is derived from the highly conserved domains needed for guanine diphosphate (GDP), GTP and GTPase activity.

The members of this super family of small GTPases can be divided into five distinct sub-families: Ras; Rho/Rac; Rab; Arf/Sar1 and Ran. Each sub-family shares in the order ≥40% amino acid homology and conserved motifs identify specific classes of downstream effectors.

The molecular switch has two states; the inactive – GDP-bound, and; the active – GTP bound. The process of GDP/GTP cycling is illustrated in Figure 1-5. Intracellular signalling occurs only when the small GTPase is in its active form (Schmidt and Hall 2002). In response to extra-cellular signals, the dissociation of GDP inhibitors from the GDP-bound protein is carried out and the monomer localises to the cell membrane where guanine nucleotide exchange factors (GEF's) catalyze the removal of GDP and GTP binds (Schmidt and Hall 2002). The inherent hydrolysis of GTP by the activated Rho and enhanced by GTPase activating proteins (GAP's) removes the γ-phosphate group thereby returning the complex to the inactive GDP-bound state (Bernards and Settleman 2004).

The GDP dissociation inhibitors provide extra regulation by blocking nucleotide exchange and maintain GDP-bound form in its inactive state. This prevents any association with the membrane and interactions with guanine exchange factors (Fukumoto, Kaibuchi et al. 1990; Mizuno, Kaibuchi et al. 1991; Bishop and Hall 2000).

1.10.1 The Rho Family

Rho proteins, small GTPases present in three isoforms (A, B, and C) are found in mammalian cells. These proteins are primary regulators of the actin cytoskeleton found ubiquitously in eukaryotic cells (Bishop and Hall 2000). As discussed previously, following expression, the small GTPase Rho is subject to posttranscriptional modification that aids localization to the cytoplasmic side of the plasma membrane where exchange of GTP and GDP occur (Adamson, Marshall et al. 1992; Marshall 1993; Schmidt and Hall 2002). The mechanisms of regulation in Rac and Cdc42 are relatively identical to the mechanism discussed for Rho (Etienne-Manneville and Hall 2002).

Rho plays a major role in regulation and localisation of stress fibre at focal adhesion sites, cell motility and the formation of perijunctonal rings at the apical side of epithelial cells (Ridley 2001). Rho interacts with and activates a diverse range of effector proteins including Rho-kinase (Fujisawa, Madaule et al. 1998), citron K (Madaule, Eda et al. 1998) and phosphotidylinositol 4-phosphate 5 kinase (Chong, Traynor-Kaplan et al. 1994). Rac and Cdc42 are specifically involved with lamellipodium and filopodium formation and are essential to cellular movement and sensing the external environment (Wennerberg and Der 2004).

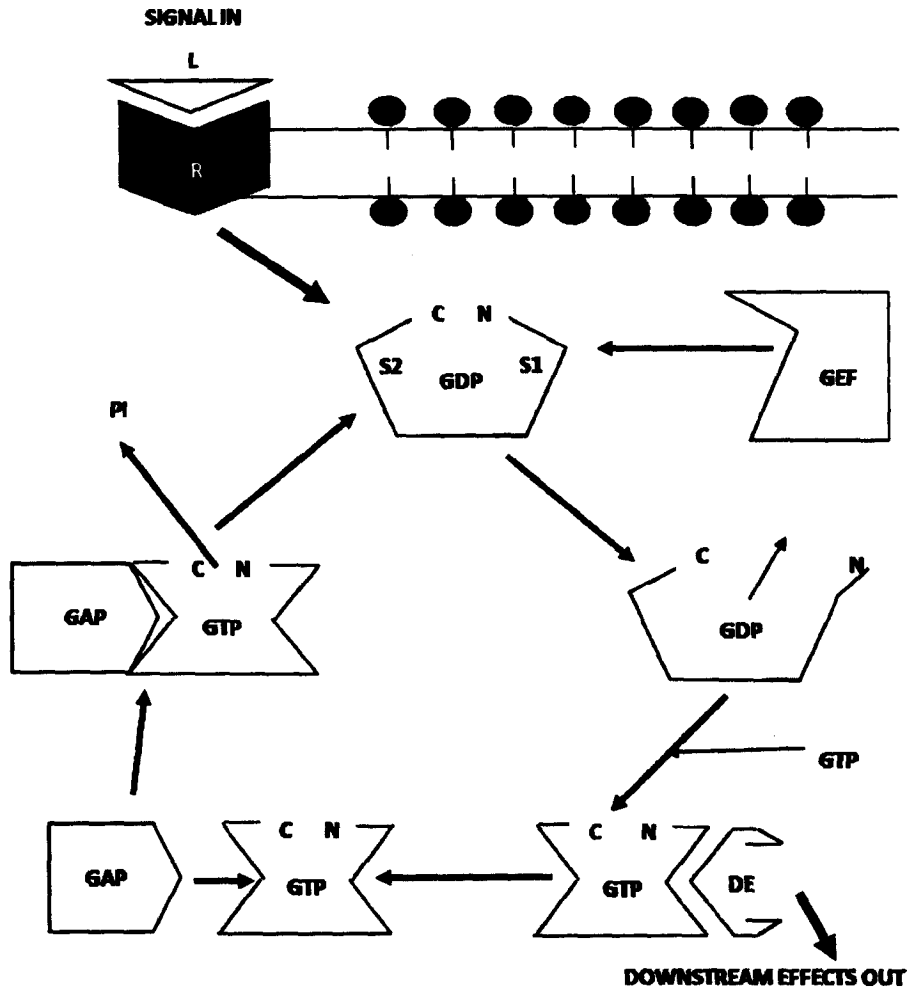

Figure 1-5 Monomeric G-protein - Transduction of cell signalling

The ligand (L) binds to its receptor (R) initiating the activation of membrane bound G protein. The G protein has two domains; Switch 1 (S1) and Switch 2 (S2), (C) and (N) represent the C-terminal and N-terminal, respectively. In its non-activated GDP-bound state S1 and S2 are off. The interaction of S1 with guanine exchange factor (GEF) facilitates the removal of GDP allowing GTP to bind. The bound GTP induces conformational changes in the G protein which allows interaction with downstream effectors (DE) initiating a cascade of downstream events. Stimulation continues until GTP is hydrolysed to GDP by the endogenous GTPase activity of G protein. The rate of endogenous hydrolysis is increased by interaction of GAP (GTPase-activating protein) with S2. The G-protein is reduced to it inactive state once more. Adapted from (Mims C A 2000)

Early studies into the effects of TcdB on cell structure indicated cells underwent marked changes in the organization of their actin cytoskeleton (Thelestam and Bronnegard 1980; Wedel, Toselli et al. 1983; Mitchell, Laughon et al. 1987). This effect has since become the hallmark of the intoxication of cells by TcdA and TcdB and is believed to preface cell death in a variety of cell types. The Rho proteins are known regulators of the cytoskeleton.

Supporting these early observations, Just and co-workers found that the small GTPase Rho was no longer subject to ADP-ribosylation by *C. botulinum* C3 co-enzyme, indicating that toxin B altered Rho within the cell (Sekine, Fujiwara et al. 1989; Just, Fritz et al. 1994). Over-expression of Rho protected cells from TcdB induced rounding, further linking this protein as a target of TcdB. TcdA was subsequently found to exercise a comparable effect on Rho (Just, Selzer et al. 1995).

With Rho identified as the putative target of TcdA and TcdB, it was demonstrated by Just et al that TcdB glucosylated RhoA via the transfer of a sugar moiety to Thr-37 of the GTPase using UDP-glucose as the co-substrate (Just, Fritz et al. 1994; Just, Selzer et al. 1995) (see Figure 1-7). This seminal study also reported TcdB glucosylated two further GTPases, Rac and Cdc42 (Just, Selzer et al. 1995). This group also observed TcdA modify RhoA with the same mechanism previously observed in TcdB (Just, Selzer et al. 1995; Just, Wilm et al. 1995). The modification of Rac and Cdc42 however, resulted from the addition of the sugar moiety to Thr-35 and not Thr-37 (see

Figure 1-7) (Just, Selzer et al. 1995; Just, Selzer et al. 1995; Just, Wilm et al. 1995). In line with these observations, cells with reduced levels of UDP-glucose have been reported to be less sensitive to the toxins (Chaves-Olarte, Florin et al. 1996).

TcdA and TcdB target isoforms of Rho, Rac and Cdc42, leading to actin condensation, rounding of cells, and membrane swelling and eventual apoptosis of the target cell. These toxins exert their activities on a wide range of cell types; however TcdB has been shown to exhibit a higher rate of enzymatic activity than TcdA, proving more cytopathic in some cell types (Chaves-Olarte, Weidmann et al. 1997). Another group have reported that UDP glucose hydrolysis by TcdB occurs at a rate ≈5 fold greater than that by TcdA (Ciesla and Bobak 1998). TcdA and TcdB appear to promote neutrophil migration whilst at the same time inactivate the primary cellular proteins needed to facilitate this process (Pothoulakis, Sullivan et al. 1988; Souza, Melo-Filho et al. 1997).

Supporting earlier observations, the elucidation of crystal structures clarifying the RhoA/GDP and RhoA/GTP complex has provided vital information regarding the effects of glucosylation on these small GTPases and enabled a number of predictions to be cast (Wei, Zhang et al. 1997; Ihara, Muraguchi et al. 1998). Examination of the structure suggested glucosylation prevented Thr-37 forming a complex with the γ phosphate on the bound GTP molecule. These findings support research shown previously, in particular the ability of TcdA and TcdB to glucosylate both the GDP-bound and GTP bound forms of Rho, with easier modification of GDP bound Rho (Just, Selzer et al. 1995). The group also observed TcdA modifying RhoA with the same mechanism as

TcdB (Just, Selzer et al. 1995; Just, Selzer et al. 1995; Just, Wilm et al. 1995). In line with these observations, cells with reduced levels of UDP-glucose are less sensitive to the toxins (Chaves-Olarte, Florin et al. 1996). Collectively these studies defined TcdA and TcdB as glucosyltransferases – glucosylating Thr-37 in Rho and Thr-35 in Rac and Cdc42, preventing binding of GTP and subsequently blocking activation.

The inactivation of Rho by TcdA and TcdB may result in any of the following steps being blocked; membrane localisation; guanine exchange factor interactions; or contact with downstream signalling proteins.

As mentioned earlier, TcdA and TcdB are unable to elicit their cytotoxic effects extracellularly and therefore must be internalised into the host cell. Entry into the host cell is via receptor mediated endocytosis and requires an acidic endosome for access to the cytosol (Florin and Thelestam 1986; Henriques, Florin et al. 1987; Mitchell, Laughon et al. 1987). Frisch and colleagues later demonstrated that the complete receptor-binding domain is necessary for binding-induced endocytosis (Frisch, Gerhard et al. 2003).

1.11 The cell cycle

In its simplest form the cell cycle can be described as a process by which cells copy their content and then divide into two identical cells. However this description fails to capture the complex series of events and chemical signals that are needed for the cell to grow, replicate its DNA and divide. A number of mechanisms monitor the progression to ensure errors are corrected or bring about cell death if errors remain. The malfunctioning of this regulatory

function caused by genetic mutations is seen in cancer, where the genetic mutations result in uncontrolled cell proliferation (Bury and Cross 2003).

1.11.1 The cell cycle phases

The eukaryote cell cycle progresses through four distinct phases, G1, S, G2 and M, see Figure 1-6

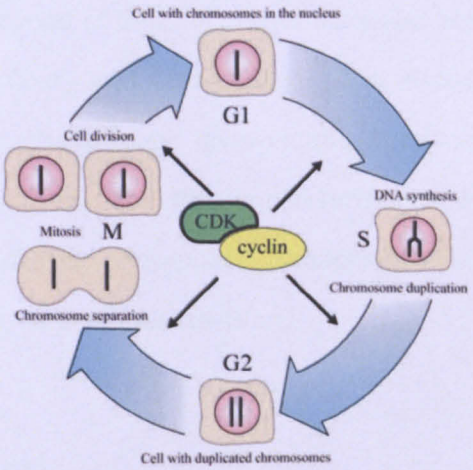

Figure 1-6 The Cell Cycle

In the first phase (G1) the cell grows. When it has reached a certain size it enters the phase of DNA-synthesis (S) where the chromosomes are duplicated. During the next phase (G2) the cell prepares itself for division. During mitosis (M) the chromosomes are separated and segregated to the daughter cells, which thereby get exactly the same chromosome set up. The cells are then back in G1 and the cell cycle is completed. Image taken from (Anon 2001)

G1 or gap phase represents a critical period where the cell cycle can proceed with cell growth or decide the cell will enter G0 (quiescence). Cell metabolism is at its highest level to prepare for the synthesis of DNA (Bury and Cross 2003). The period of time a cell takes to progress through G1 is particularly variable and is the main determinant of the overall length of the cell cycle. The rapidly proliferating cells of intestinal epithelium spend around 11 hours of their total 24 hour cycle in the G1 phase (Bury and Cross 2003).

In S (synthesis) phase DNA replication occurs and usually takes around 8 hours, however any damage to the DNA will extend this time (Howard 1953).

During G2 or gap 2 phase, the cell will complete the DNA replication process by packaging the chromosomes and sister chromatids. The cell continues to grow and essentials proteins are synthesized for mitosis.

Taking the shortest period of time, M phase makes up only 5 % of time taken to complete a cycle (Bury and Cross 2003). The M phase can be split into mitosis, referring to the nuclear division and cytokinesis the subsequent formation of the daughter cells. Mitosis can further be split into five stages; prophase, prometaphase, metaphase, anaphase and telophase, each completing specific roles in nuclear division.

1.11.2 Cell cycle control

The cell cycle relies on signals from growth factors and other external stimuli and in the absence of suitable stimuli, cells in G0 will not re-enter the cell cycle and daughter cells produced after cell division will enter G0 and not undergo further division (Bury and Cross 2003). Once stimulated the cell cycle is completed in full, even if the initiating stimuli is removed. The ability of the cell to ignore external stimuli after initiation ensures the cell will not leave the cycle early, avoiding unfavourable outcomes (Blagosklonny and Pardee 2002).

The timepoint at which a cell becomes committed to division independent of further stimulation occurs 2-3 hour before the G1/S transition and it is termed the 'restriction point' (Pardee 1974). The 'restriction point' determines that fate of daughter cells resulting from mitosis and the mechanism controlling the balance between cell differentiation and proliferation (ibid, 1974). Once the cell has successfully passed this point a combination of intrinsic links and checkpoint pathways operate at key timepoints to halt progress until particular conditions have been achieved.

The second checkpoint 'replication checkpoint' operates during S-phase to ensure mitosis is halted until DNA replication is complete (Samuel, Weber et al. 2002). These specific checkpoint pathways monitor intracellular conditions and by recruiting three families of molecules; the cyclin dependent kinases (CDKs) and their regulators, the cyclins and the cyclin dependent inhibitors (CKIs) key transitions between phases in the cell cycle occur (Bury and Cross 2003).

Four CDK molecules are known to effect cell cycle progression in humans; CDK 1, 2, 4 and 6 and different cyclins are responsible for activation and similarly are inhibited by different families of CDK inhibitors (ibid, 2003), see Table 1-5.

Table 1-5 Cyclin dependent kinases (CDKs) their activating cyclins and inhibitory cyclin dependent kinases (CKIs)

Adapted from (Bury and Cross 2003)

CDK	Activating cyclin (s)	Inhibitory CDKI family
CDK 1	Cyclin-B	
CDK 2	Cyclin-A, Cyclin-E	Cip/Kip
CDK 4	Cyclin-D	Cip/Kip, INK4
CDK 6	Cyclin-D	Cip/Kip

Whilst CDK's are present throughout the cell cycle, they are unable to exert an effect until bound to their regulatory subunit, the cyclin. As with CDKs there are four different cyclins known to influence cell cycle control, cyclins –A, -B, -D and –E and as shown in Table 1-5, binding between cyclins and CDK's is type specific. It is also necessary for this signal to be inhibited and this is achieved using cyclin dependent kinase inhibitors (CDKI's). These inhibitors can be split into two main classes based on their structure and function and unlike the invariant nature of the CDK and cyclin, CDKI's are cell and tissue specific (Pardee 1974).

The INK4 ('Inhibitor of CDK 4') family of proteins comprises p15, p16, p18 and p19 and three proteins are found in the Cip/Kip ('CDK interacting protein' or 'kinases inhibitory protein') family, p21, p57 and p27 (Roussel 1999). As the name suggests, INK4 proteins compete with cyclin D for the regulatory subunit CDK4 and serve to negatively regulate cell cycle progression (ibid, 1999). In fact, active CDK4/cyclin-D is required for progression past the restriction point and entry into the cell cycle. The Cip/Kip proteins are linked

to a diverse range of pathways including the involvement of p21 in cell cycle arrest when DNA is damaged via the p53 pathway and p27 is increased in response to a anti-mitotic signals and TGFβ (Yue and Mulder 2001).

The homeostatic balance of cyclins and CDKI's is dependent upon accurate transcription and timely proteolytic degradation (Clarke 2002). The correct functioning of these two processes ensures the smooth functioning and the avoidance of 'mixed messages' throughout cell cycle progression.

CDK 1 is responsible for the initiating mitosis and CDK 2, 4 and 6 are involved in the progression of the cell through the restriction point in G1 and initiation of S phase(Bury and Cross 2003).

1.11.3 The role of Rho GTPases in cell cycle progression

As discussed previously the cell cycle moves through four successive phases. The transition from one phase to the next is controlled by cyclin- Cdk (cyclin dependent kinase) complexes which ensure timely and accurate progression by phosphorylating a set of substrates which includes members of the retinoblastoma (RB) proteins (Coleman, Marshall et al. 2004). GTPases are essential at all points in the cell cycle affecting key components via numerous mechanisms (ibid, 2004).

Rho GTPases have been shown to influence the cell cycle at two specific phases: G1 progression and; the organisation of the microtubule and actin cytoskeletons during M phase (Jaffe and Hall 2005).

1.11.3.1 G1 progression

G1 progression is ultimately controlled by the cellular levels of two types of cyclin-CDK complex, cyclin D/Cdk6 and cyclin E/Cdk2 and subsequently inhibited by binding to one of the Cip/Kip ('CDK interacting proteins' or 'kinases inhibitory protein') p21, p27 and p57(Bury and Cross 2003). The cyclin D/Cdk4 complex can be inhibited by binding to the INK4A ('Inhibitor of CDK4'), p15, p16, p18 and p19 and Cip/Kip, p21, p27 and p57 (ibid, 2003).

The largest body of research investigating the role of Rho GTPases on cell cycle progression has focused on the progression through G1. Whilst it is evident that inhibition of Rho, Rac or Cdc42 blocks G1 progression and microinjection of active Rho A, Rac1 or Cdc42 into quiescent cells induced G1-S phase progression (Olson, Ashworth et al. 1995), the mechanism appears to be cell-type dependent and establishing the pathways leading to this end have been difficult (Jaffe and Hall 2005). As mentioned earlier the cellular levels of cyclins and CDK inhibitors are key to G1 progression and the best understood pathway is the transcription of cyclin-D1 by the Ras/ERK (extracellular signal-regulated kinases) pathway (Coleman, Marshall et al. 2004). Cyclin-D1 is usually the first cyclin to be expressed and levels increase during G1 (Klein, Campbell et al. 2008). To achieve the correct levels of cyclin-D at mid G1 sustained ERK/MAPK activation is needed and therefore additional signals from adhesion to the ECM are essential (Assoian and Schwartz 2001). It is thought that many of the Rho GTPase effects on G1 progression are linked to the adhesion/anchorage dependent proliferation. Indeed, epithelial cell proliferation requires signals from integrins but is also strongly influenced by the cell-cell adhesion protein, E-cadherin (Fournier, Campbell et al. 2008).

It has been shown that whilst both Rac and ERK signaling induce cyclin D1, the timing of cyclin D1 gene expression is different (Klein, Campbell et al. 2008). The Rac signal results in an early G1 phase expression of cyclin D1, however the ERK signaling resulted in mid G1 phase induction (Welsh, Roovers et al. 2001). Very little is known of the interplay between ERK and Rac activation of cyclin D1 as research has focused on different cell types or used different methods (Klein, Campbell et al. 2008).

Active RhoA was found to be necessary for sustained ERK/MAPK activation (Welsh, Roovers et al. 2001) and ERK activity can regulate cip/kip family of cdk inhibitors (Yang, Klein et al. 2008). Inhibition of ERK activity blocks S-phase entry and increases p21 levels, however knocking down p21 using siRNA did not result in cell cycle progression (Klein, Campbell et al. 2008). Rho has also been shown to regulate Cdk2 inhibitors by attenuating high levels of p21 triggered by Ras (Jaffe and Hall 2005). At high levels, p21 and p27 inhibit cyclin E resulting in cell cycle arrest (Weber, Hu et al. 1997; Olson, Paterson et al. 1998). RhoA induced p21 transcription is mediated by cell type dependent signaling pathways (Roovers and Assoian 2003). Rac has also been linked to the induction of cyclin-D1 (Klein, Yung et al. 2007), however in fibroblasts Rac-dependent induction of cyclin D1 is not seen unless Rho signaling is inactive (Welsh, Roovers et al. 2001). Rho inhibition blocks stress fiber formation and in cells without a need for intracellular tension the Rac-dependent gene expression of cyclin D1 is detectable (Fournier, Campbell et al. 2008). Rac-dependent expression of cyclin D1 early in G1 is not sufficient to support Rb phosphorylation and S phase entry and joint Rac/ERK

expression of cyclin D1 throughout G1 is required (Coleman, Marshall et al. 2004).

1.11.3.2 Mitosis and cytokinesis

During mitosis the spindle positioning is arranged following interaction of Cdc42 with Par6 (Gotta, Abraham et al. 2001). The conformational change in Par6 by Cdc42 led to activation of aPKC (atypical protein kinase C) (ibid, 2001). Inactivation of Cdc42 has also been linked to mitotic arrest (Yasuda, Oceguera-Yanez et al. 2004).

The assembly of a cleavage furrow and an actin/myosin contractile ring marks the beginning of cell division and the end of mitosis and Rho plays a crucial role in the formation of these structures via at least three known effector proteins; ROCK, Citron kinase and mDia (Glotzer 2004).

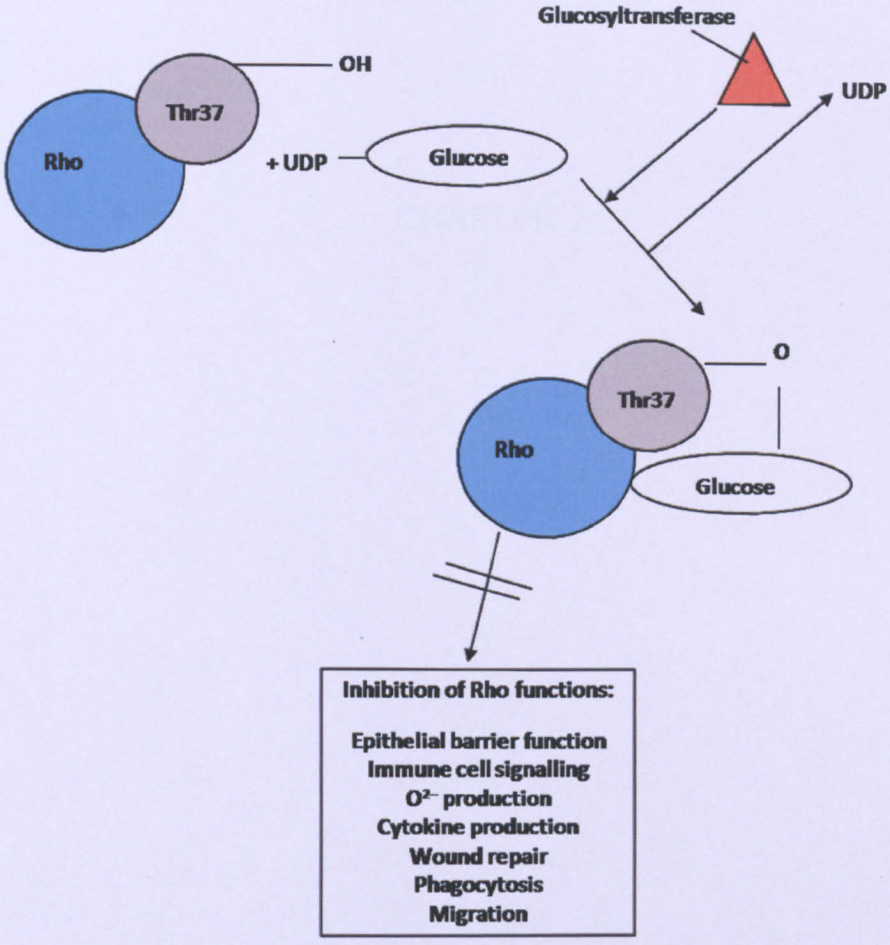

Figure 1-7 Glucosylation and downstream effects

Rho GTPases are glucosylated at Thr37 (e.g. RhoA) or at Thr35 (e.g. Rac, Cdc42). Glucosylation blocks the active conformation of Rho GTPases and inhibits downstream signalling events controlled by the GTPases. Adapted from (Nottrott, Schoentaube et al. 2007)

CHAPTER 2

2 Materials and methods

2.1 Toxin A purification

2.1.1 Introduction

The unique structure and activity of *C. difficile* toxin A has made possible the efficient purification of this protein. A number of purification protocols have been formulated (Sullivan, Pellett et al. 1982; Kamiya, Reed et al. 1989; Meng, Kamiya et al. 1993) and are widely used. These protocols utilize the temperature dependent specific binding of toxin A to Galα1-3Galβ1-4GlcNAc carbohydrate residues found on the bovine thyroglobulin molecule. Toxin A was found to bind to this residue at low temperatures (4°C) and dissociate at high temperatures (37°C). Exploiting this temperature dependent binding and utilizing a thermal affinity chromatographic procedure toxin A was separated from toxin B and other contaminants. Further purification used the negative charge of the toxin A molecule and employed two sequential anion exchange chromatography steps to remove traces of toxin B and any other remaining contaminants.

2.2 Bacterial Culture

2.2.1 Bacterial strains

C. difficile, VPI 10463 (Toxinotype 0), a widely used reference strain was chosen for this study as it expresses the genes *tcdA* and *tcdB* and produces active forms of toxin A and toxin B proteins.

2.2.2 Recovery of viable bacteria

Clostridium difficile spores were retrieved from long-term storage in cooked meat broth (Oxoid). 50 µl of broth supernatant was mixed with the same volume of 70 % ethanol and left for 1 hour to ensure vegetative bacteria were destroyed. 20 µl of the resultant solution was streaked asceptically onto blood agar plates (Oxoid) and incubated anaerobically for 4 days at 37°C.

2.2.3 Bacterial growth and harvesting

C. difficile colonies grown on blood agar plates were transferred to universals containing 10 ml of brain heart infusion (BHI) broth (see Solutions – Appendix 1), and incubated anaerobically at 37°C for two days. The purity of the culture was checked by inoculation of an aliquot of the bacterial suspension onto a blood agar plate and streaking to single colonies. After the preparation of five, one litre spouted flasks with visking dialysis tubing (pore size <12,400 MW) suspended in 1 litre of BHI broth as shown in Figure 2-1, Phosphate buffered saline (PBS) (Sigma) was dialysed into the sterile tubing and the flasks autoclaved at 121°C for 20 minutes. To straighten out any creases in the tubing, sterile PBS was inoculated asceptically and the flasks left overnight to equilibrate. 5 ml of the bacterial harvest was pipetted into the dialysis tubing and the flasks incubated anaerobically at 37°C for 3-4 days.

The contents of the dialysis tubing were centrifuged at 4,000 rpm for 30 minutes and the bacterial pellet removed. The remaining supernatant was syringe filtered using a 0.2 µm filter and stored at 4°C.

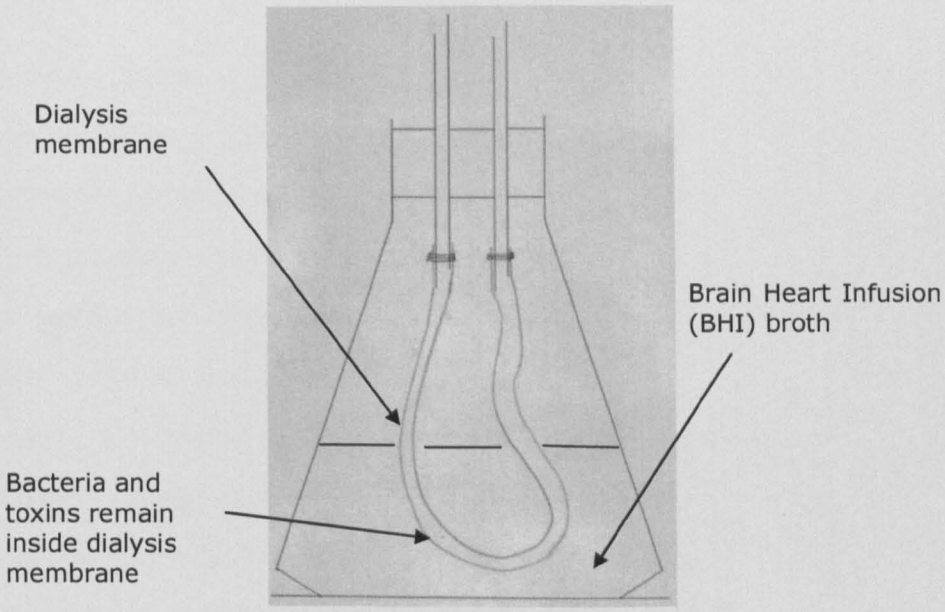

Figure 2-1 Schematic diagram of flask assembly

Clostridium difficile bacterial suspension is inoculated aseptically into the dialysis membrane and following 3-4 days of anaerobic incubation, the bacteria and toxins are retained in the dialysis tubing.

2.3 Protein purification chromatography

2.3.1 Bovine thyroglobulin affinity chromatography column

2.3.1.1 Column preparation

A bovine affinity gel was prepared by dissolving 1250 mg of bovine thyroglobulin (Sigma) in 250 ml of 0.1 M morpholinepropane-sulphonic acid buffer pH 7.0 (Sigma) before allowing it to bind with 50 mls of Affi-Gel 15 beads (Bio-Rad Laboratories) by overnight rotation at 4°C. The remaining active sites on the beads were blocked by treatment with 100 µl of 0.1 M ethanolamine (Sigma) for 30 minutes at 4°C before the gel was poured into a 50 ml column (Amersham Biosciences).

Previously stored in sodium azide solution at 4°C, the thyroglobulin column was washed with 100-200ml of Tris buffer solution (TBS), (see solutions – Appendix 1). The filtered supernatant of cultured *C. difficile* was then applied to thyroglobulin column overnight at 4°C. Any unbound supernatant was washed from the column with TBS at 4°C. The column was then transferred to 37°C and allowed to warm for an hour. Warm (37°C) TBS was then run through the column to elute the bound toxin A. A 40 ml fraction was collected, syringe filtered and stored at 4°C. The column was then washed with 100 mls of acidic buffer followed by 100 mls of basic buffer (see solutions – Appendix 1 for both) at 37°C. The three step cleaning process removes any protein and / or contaminants from the column prior to storage. The column was then returned to 4°C and washed with TBS. Finally, the column was stored in 0.02% sodium azide/TBS solution.

Crude toxin A eluted from the thyroglobulin column was dialysed overnight at 4°C, in 20 mM TBS to remove excess salt.

2.3.2 Anion-exchange chromatography

Anion exchange chromatography uses the positively charged beads inside the column to bind the negatively charged protein of choice. This ionic interaction is broken and the protein is eluted using a NaCl gradient, see Figure 2-2.

Using AKTA Purifier P900 (GE Healthcare) two sequential anion exchange chromatography runs were completed using ready prepared DEAE Q-

Sepharose (Amersham Biosciences, Uppsala, Sweden) and Mono Q columns (Amersham Biosciences).

2.3.2.1 DEAE-Sepharose anion exchange chromatography

The supernatant was syringe filtered using a 0.2 µm filter and degassed using helium. The sample was then injected into the superloop and passed through the DEAE (diethylaminoethyl, a weak anionic exchanger) Sepharose-FF column. Toxin A binds to the coated beads and all other proteins and contaminants pass through into the waste. Unbound proteins are washed out of the column and a 0-1.0 M salt gradient is subsequently passed through the column to elute toxin A, which was collected in fractions. A representative graph profiling the elution of toxin A is shown in Figure 2-3. A dot blot of fractions was completed to confirm the presence of toxin A, details of which can be in Figure 2-4. Toxin A positive fractions were pooled and dialysed against 20 mM TBS overnight at 4°C.

2.3.2.2 Mono-Q anion exchange chromatography

The pooled DEAE fractions (B13-D1) as identified in Figure 2-3 were syringe filtered using a 0.2 µm filter; degassed using helium and injected into the superloop and this time passed through a Mono-Q (quaternary amine, a strong anionic exchanger) column. Fractions were collected after the elution using 0-1M NaCl gradient. Figure 2-5 illustrates a representative graph profiling the elution of toxin A from the Mono-Q column, a single peaked graph was representative of pure toxin A. A dot blot of fractions was completed to confirm the presence of toxin A in A9-B2, see Figure 2-6.

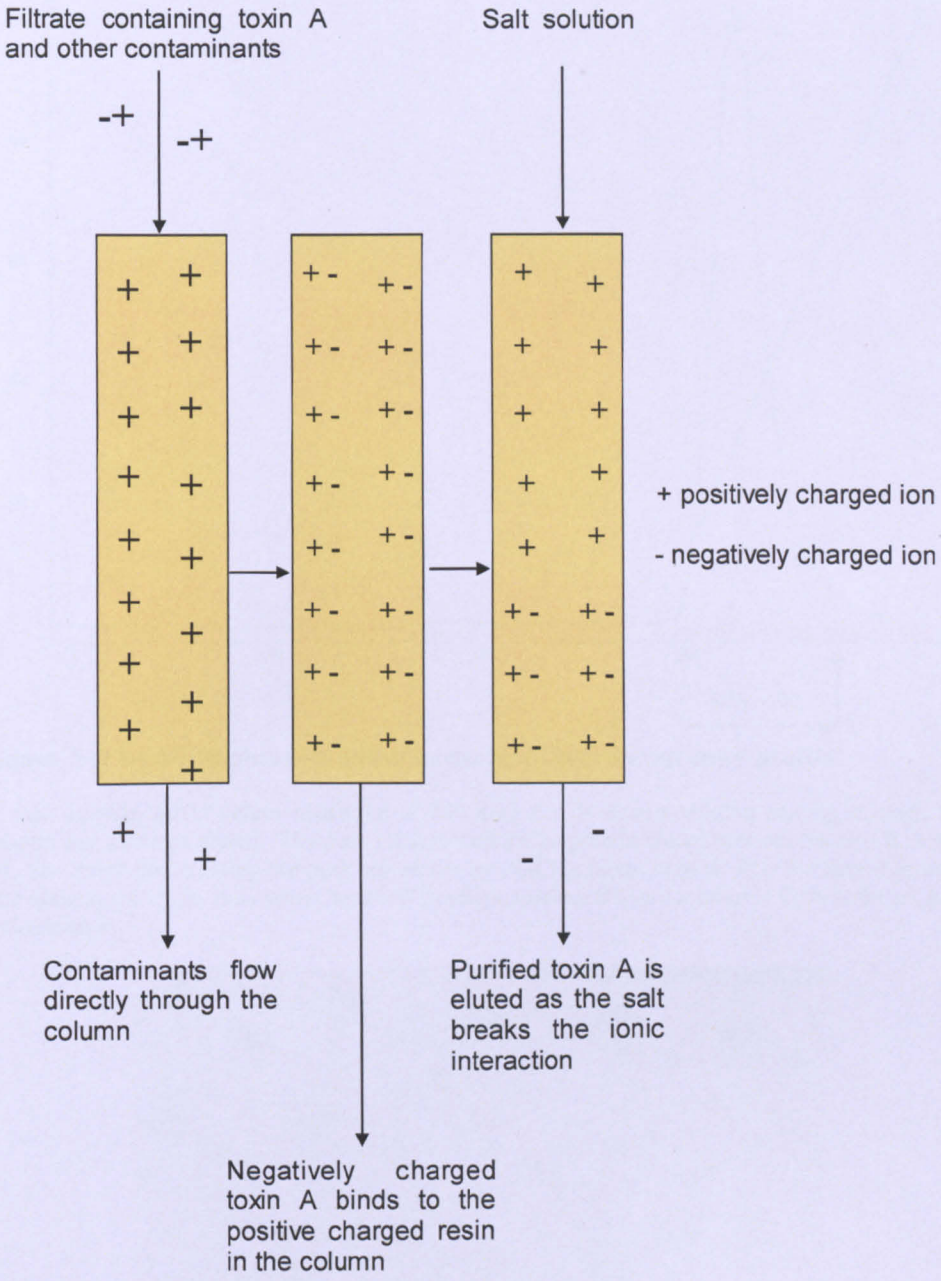

Figure 2-2 Ion Exchange Chromatography

Ion Exchange Chromatography relies on charge-charge interactions, negatively charged toxin A binds to the positively charged resin in the column. The ionic interaction is broken using a NaCl gradient and the toxin A is eluted.

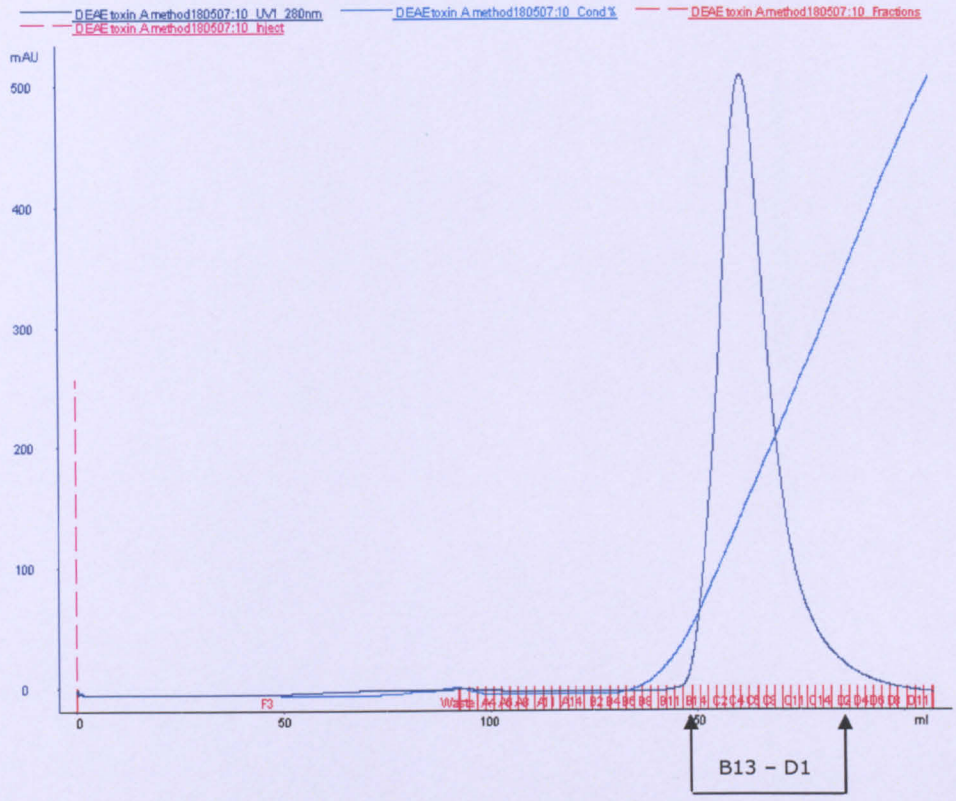

Figure 2-3 DEAE-Sepharose anion exchange chromatography profile

X axis displays mAU values measured at 280 nm; Y axis details volume passing through the column and fractions eluted. The peak represents purified protein eluted between fraction B13 and D1. The linear line crossing the peak represents the NaCl gradient used to elute the bound protein. The toxin A started to elute when the NaCl gradient reached 6% and measured 22% at the peak of concentration.

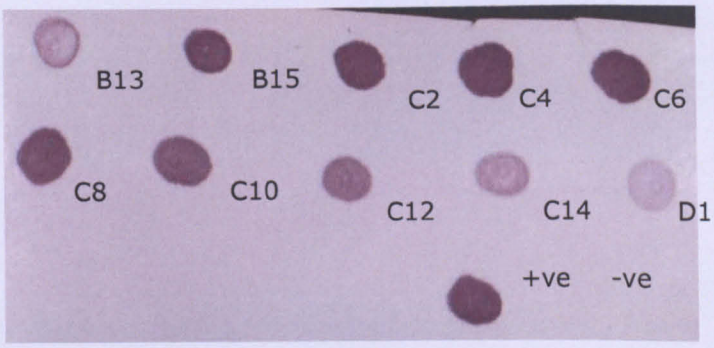

Figure 2-4 Dot blot of DEAE-Sepharose eluted fractions

Using fractions B13-D1, a positive control of previously purified toxin A and a negative control (BHI) broth. All fractions were confirmed to be toxin A when compared with positive control. The representative membrane shows an increase in immune-reactivity correlating with the peak shown in the profile Figure 2-3

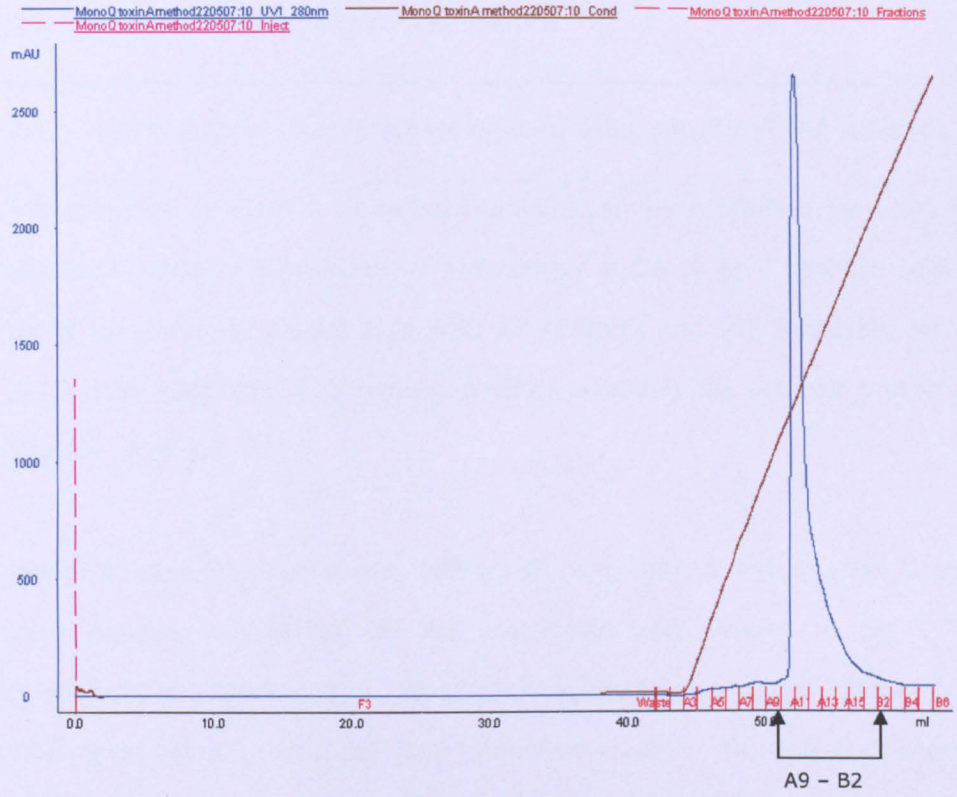

Figure 2-5 Mono-Q anion-exchange chromatography profile

X axis displays mAU values measured at 280 nm; Y axis details volume passing through the column and fractions eluted. The peak represents purified protein eluted between fraction A9 and B2. The linear line crossing the peak represents the NaCl gradient used to elute the bound protein. The toxin A started to elute when the NaCl gradient reached 14% and measured 22% at the peak of concentration.

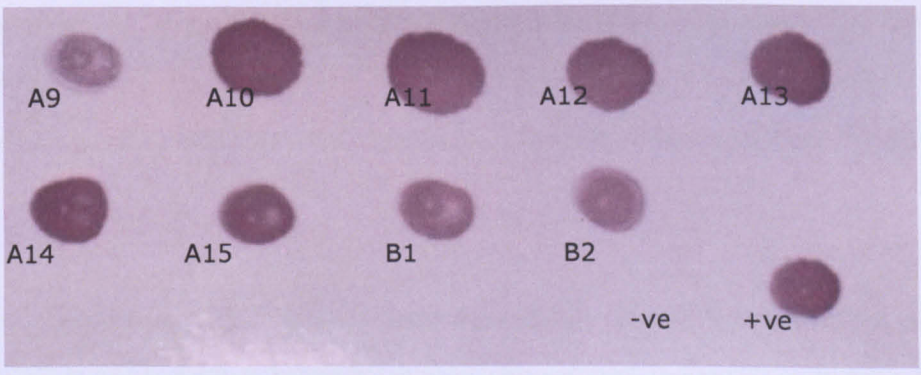

Figure 2-6 Dot blot of Mono-Q eluted fractions

Using fractions A9-B2, a positive control sample of previously purified toxin A and a negative control (BHI). All fractions were confirmed to be toxin A when compared with positive control The representative membrane shows an increase in immune-reactivity correlating with the peak shown in the profile Figure 2-5

2.4 Characterisation of purified toxin A

2.4.1 Dot blot (immunoperoxidase system) using specific PCG-4 antibody

The presence of toxin A in eluted fractions can be confirmed by using the specific binding of mouse PCG-4 monoclonal antibody to *C. difficile* toxin A using Vectastain Universal Elite ABC kit (Vector) and VIP Substrate kit for peroxidase (Vector). A schematic diagram outlining the dot blot protocol is shown in Figure 2-7.

Using nitrocellulose membrane (GE Healthcare) with a +ve charge, 5 µl of each fraction was placed on the membrane and allowed to dry. The membrane was covered with TBS blocking buffer (see solutions – Appendix 1) and placed on a rocking platform overnight at 4°C. Toxin A (-ve charge) binds to the membrane and the milk protein in the blocking buffer blocks all other areas.

The membrane was washed thoroughly using TBS wash buffer (see solutions – Appendix 1). PCG-4 (125 µg/ml) antibody was diluted 1:20 with TBS wash buffer, poured over the membrane and incubated on a rocking platform at room temperature for 1 hour. The PCG-4 antibody binds specifically to toxin A.

The membrane was washed with TBS wash buffer and covered with biotinylated secondary antibody (containing blocking serum and biotinylated affinity purified anti-mouse immunoglobulin) and incubated on a rocking platform at room temperature for 30 minutes. The biotinylated secondary antibody binds to the PCG-4.

The preformed avidin/biotinylated horseradish peroxidase macromolecular complex was prepared and left to incubate for 30 minutes before use. After washing the membrane to remove the biotinylated secondary antibody the pre-prepared avidin/biotin complex was poured over the membrane and left to incubate on the rocking platform at room temperature for 30 minutes.

The membrane was washed once more. The horseradish peroxidase is visualized using peroxidase substrate, when prepared the peroxidase substrate was poured over the membrane. As soon as the colour developed the membrane was rinsed with water to end the reaction. When dry the membrane was scanned for future reference.

2.4.2 Determination of protein concentration

Early purification of toxins used the Nanodrop to determine protein concentration, however later purification run employed the Bradford Assay to determine total protein concentration.

2.4.2.1 Using the Nanodrop

In brief, the Nanodrop was blanked with nuclease free water, 1 µl of each fraction was analysed for protein concentration at 280 nm. Values are reported as concentration in mg/ml.

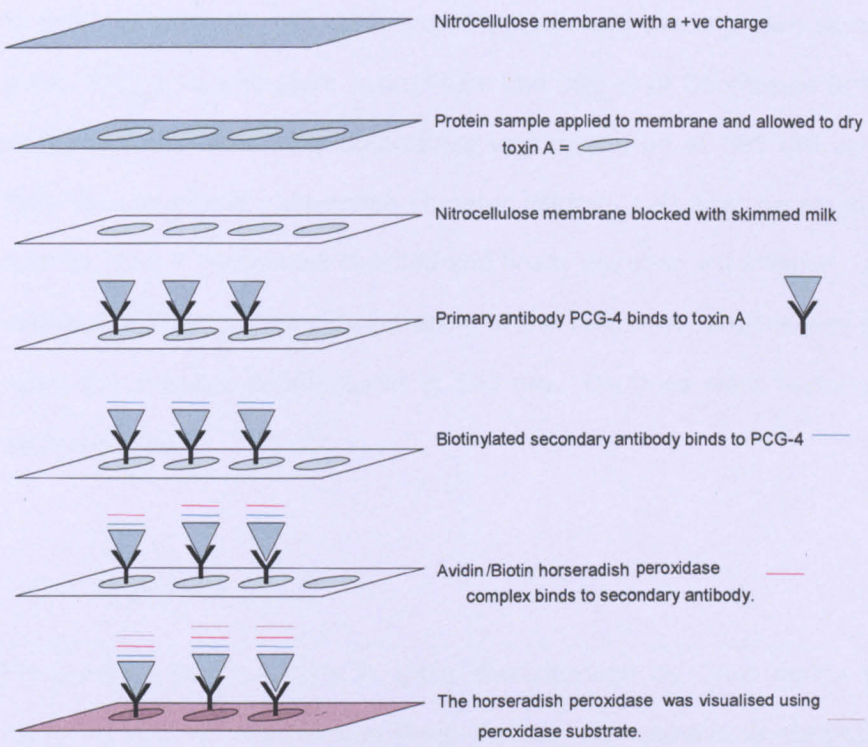

Figure 2-7 Schematic diagram of dot blot for toxin A

Specific binding of primary antibody PCG-4 to *Clostridium difficile* toxin A and the subsequent secondary antibody avidin/biotin complex (Vectastain Universal ABC Kit, Vector) visualized using peroxidase substrate (VIP Substrate Kit, Vector).

2.4.2.2 Using Bradford Assay

The Bradford Assay is a standard colormetric assay that can, when used with a selection of known standards and standard curve prepared, calculate the concentration of protein in a solution. The assay is based on the observation that the absorbance maximum for an acidic solution of Coomassie Brilliant Blue G-250 (Sigma) shifts from 465 nm to 595 nm when binding to protein occurs. Both hydrophobic and ionic interactions stabilize the anionic form of the dye, causing a visible color change.

In brief, 10 µl of 25, 125, 250 and 500 µg/ml and the unknown samples were placed into a 96 well plate in duplicate and 300 µl of Coomassie Brilliant Blue added to each well. The absorbance was measured at 595 nm using Bench Mark Plus microplate spectrophotometer (Biorad, UK).and the standard curve plotted. The R^2 value was checked and linear equation established. Using this equation - total protein concentration of the unknown samples was calculated using the absorbance measured at 595 nm. Dilutions were factored and the mean reported.

2.4.3 Cytotoxicity Assay

Fractions of purified toxin A were characterised by their ability to induce rounding in Vero cells [African Green Monkey (Cercopithecus aethiops) kidney cells]. Vero cells were obtained from American Type Culture Collection (ATCC) (Cat No. CCL-81) and used at passage 20-25. Using the method outlined in (Donta, Sullivan et al. 1982), a series of 10 fold dilutions in supplemented DMEM was applied to a confluent cell monolayer. The cells were visualized after 24 hours and the toxin titre determined, defined as the concentration of toxin able to induce 50% cell rounding (Donta, Sullivan et al. 1982). Cell culture methods start from page 84.

2.4.4 Polyacrylamide gel electrophoresis

2.4.4.1 The gel

The homogeneity of the purified product was identified by native polyacrylamide gel electrophoresis (PAGE).

A resolving gel was prepared (see solutions in Appendix 1) and poured into the assembled apparatus (BioRad), a comb inserted, layered with water and left for 30 minutes to polymerise. When set, the gel was placed into electrophoresis apparatus (BioRad) and the reservoirs filled with 1 x running buffer (25 mM Trisma, 0.192 M glycine in dH_2O). Each 10 ul sample was prepared by the addition of 10 ul of loading buffer (0.01% bromophenol blue in glycerol). A high molecular weight protein marker was also prepared and 10ul of this marker and samples were added to each well. A constant voltage of 100 V was applied for 100 minutes.

2.4.4.2 Coomassie Staining

The gel was removed from the apparatus and stained by soaking in Coomassie staining solution (0.25 g Coomassie brilliant blue (Sigma), 90 ml methanol, 10 ml acetic acid) for 1 hour.

The gel was then destained by repeated washes with destaining solution: (10 % methanol & 10 % acetic acid in 500 mls distilled water) until the solution ran clear and the background staining was minimised. The gel was stored in distilled water until the image was scanned.

2.4.4.3 Silver Staining

The gel was removed from the apparatus and using a silver staining kit (BioRad) the gel was immersed into the fixative (40% methanol/10% acetic acid v/v for 30 minutes). Whilst fixing the oxidizer and silver reagent were

made up using 5 ml of the oxidizer (10-fold solution containing potassium dichromate and nitric acid) and silver reagent (10 fold solution containing silver nitrate) stock solutions and 45 ml of dH_2O and left at room temperature. In addition the developer (powder containing sodium carbonate and paraformaldehyde, 32 g dissolved in 1 L distilled water) was also prepared. The fixed gel was completely immersed in the oxidizer for 5 minutes followed by 3 water washes to remove yellow colouring from the gel and then immersed in the silver reagent for 20 minutes. The gel was rinsed and enough developer poured to immerse the gel for 30 seconds or until a smoky brown precipitate was visible. The developer was removed and replaced repeatedly until the desired intensity of banding was achieved and then the reaction was stopped by immersing the gel in a 5% acetic v/v solution for 15 minutes. The gel was then scanned.

2.4.5 Purified toxin A - Storage

Toxin A was labelled with the eluted fraction reference and stored in 100 µl aliquots at -80°C.

2.5 Cell Culture

2.5.1 Mammalian cell lines

Vero cells (African Green Monkey (*Cercopithecus aethiops*) kidney cells), HT29 cells (human intestinal epithelial cells) and Caco-2 cells (human intestinal epithelial cells) were obtained from ATCC (Cat No. CCL-81; HTB-38 and HTB-

37) respectively. Vero cells were used at passage 20-25, HT29 cells at passage 145-150 and Caco-2 cells at passage 80-85.

2.5.2 Primary human intestinal Myofibroblasts

2.5.2.1 Isolation from intestinal tissue

Fresh, histologically normal colonic mucosal were obtained (after informed consent) from patients undergoing resection of the large bowel, median age of tissue donors was 69 yrs (range 47-87 yrs; 6 female; 8 male). Ethical committee approval was provided by Nottingham Research Ethics Committee (REC Q1020310). Intestinal myofibroblasts were isolated and established in pure culture as previously described (Mahida, Beltinger et al. 1997). The myofibroblasts used in these experiments were isolated by Mrs J. Webb and immunohistochemistry performed by K. R. Hughes. The tissue was initially cleaned by washing three times in 20 ml Hanks Buffered Saline Solution (HBSS) w/o Mg+ & Ca+ (Gibco) and surface epithelial cells were detached from mucosal samples by three sequential treatments with 1 mmol Ethylenediaminetetraacetic acid (EDTA), with intermediate wash cycles using cold HBSS w/o Mg+ Ca+ (Gibco). The remaining tissue was washed five times with HBSS with Mg+ & Ca+ and plated into culture dishes in Roswell Park Memorial Institute media (RPMI) supplemented with 10% FCS. Myofibroblasts migrate via the basement membrane pores of the mucosal samples denuded of epithelial cells to form colonies in the culture dish (Mahida, Beltinger et al. 1997). The tissue was removed and the media changed to DMEM (Sigma) supplemented with 10% fetal calf serum (FCS) and 1% non-essential amino acids (NEAA), (Gibco). The cells proliferate to

establish a monolayer in the culture dish and are then trypsinised with 0.1% trypsin and transferred to a normal cell culture flask. The isolated myofibroblasts can be maintained over many passages and for this research they have been studied at passages 3 – 7. To confirm the myofibroblast phenotype, immunohistochemical staining of cells fixed onto glass coverslips confirmed the presence of smooth muscle actin and vimentin and the absence of desmin, see Figure 1-2-8.

2.5.2.2 Culture Medium

All cells were cultured in Dulbecco Modified Eagle Medium – DMEM (Gibco) supplemented with 10% fetal calf serum (FCS), 200 mM L-Glutamine and antibiotics; penicillin (100 ng/ml), streptomycin (100 ng/ml) and gentamycin (50 ng/ml) (PSG). In addition to the above additions, Caco-2 cell medium was also supplemented with holotransferin (Sigma) and Myofibroblast medium supplemented with 1% non essential amino acids (NEAA).

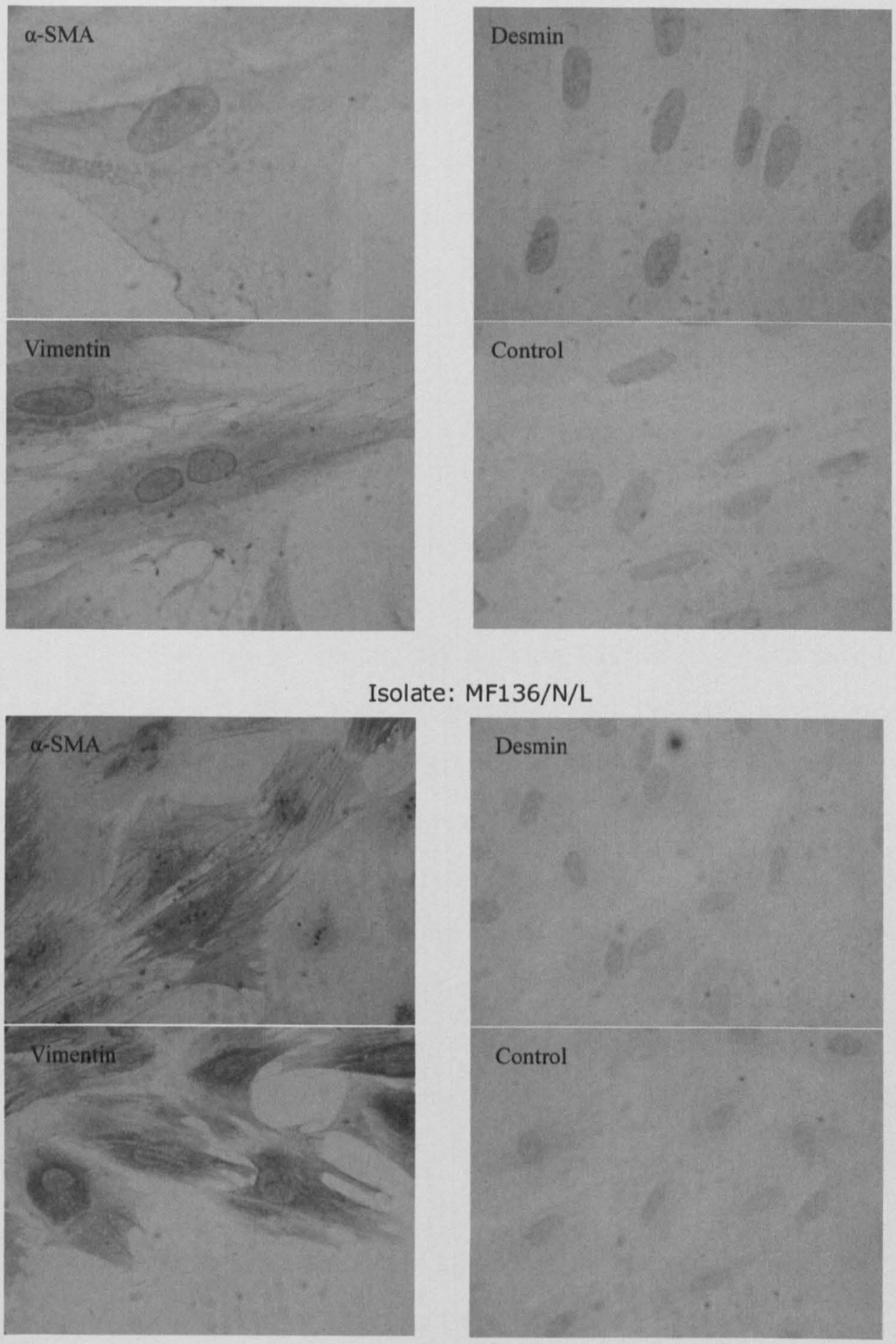

Figure 1-2-8 Immuno-histochemical staining of intestinal myofibroblasts

Intestinal myofibroblast characterisation of two isolates indicate the presence of alpha-smooth muscle actin and vimentin and the absence of desmin, performed by K. R. Hughes.

2.5.2.3 Resurrection of cells

Cells were removed from nitrogen storage, thawed rapidly in a 37°C waterbath. Cells were then transferred into a 75 cm^2 flask (Nunc) containing 15 ml of supplemented DMEM (Gibco) before incubation at 37°C, 5% CO_2. 24 hours later the media in the flask was replaced and cells re-incubated at 37°C, 5% CO_2 until confluent.

2.5.2.4 Cell passage

Upon confluence, the used media was discarded from Caco-2, HT29 and Vero cells and the cells washed with 2 ml 0.25 % trypsin (x10 Trypsin (Gibco) and versine (0.02% EDTA in PBS pH7.2)), before incubation in the presence of 3 ml trypsin at 37°C, 5% CO_2 for 10 minutes. Detached cells were removed from the flask and together with 7 ml of new media pelleted by centrifugation at 1000 rpm for 5 minutes and the resultant supernatant discarded. The cell pellet was then resuspended in 15 ml of new media and 5 ml aliquots seeded into three 75 cm^2 flasks containing 10 ml of fresh media. Cells were incubated at 37°C, 5% CO_2 until confluent. Myofibroblast cell passage used a less concentrated solution of trypsin (0.1 %) and the cells were not centrifuged, the 3 ml of trypsin containing the cells was transferred into new flasks containing 19 mls of warmed media. Vero cells were split 1:2 – 1:7; Caco-2 cells split 1:2 – 1:4; HT29 cells spilt 1:2 – 1:5; and myofibroblasts split 1:2 - 1:3. A confluent 75 cm^2 flask of Caco-2, HT29 and Vero cells held approx 4×10^7, 4×10^7, 7×10^6 and 1×10^6 cells, respectively.

2.5.2.5 Cell freezing

Confluent cells were trypsinised as previously described and resuspended in 7 ml of fresh, warm DMEM. The cells were pelleted by centrifugation at 1000 rpm for 5 minutes and the supernatant discarded. The pellet was resuspended in the residual media and 1 ml of freezing media (100 µl Dimethyl Sulphoxide (DMSO, Sigma) in 900 µl FCS (Gibco). The cells were frozen immediately at -80°C overnight before transfer to long-term nitrogen storage.

2.5.2.6 Culture in 24-well plates

Confluent cells in a 75 cm^2 flasks were trypsinised as previously described and a cell count conducted. Cells were subsequently resuspended in 25 ml of fresh media to achieve 1 x 10^4 cells/ml and 1000 µl of the cell suspension aliquoted into each well of a 24-well plate (Costar, UK). Plates were incubated at 37°C, 5 % CO_2 until confluent.

2.5.2.7 Culture in 96-well plates

Confluent cells in a 75 cm^2 flasks were trypsinised as previously described and a cell count conducted. Cells were subsequently resuspended in 10 ml of, fresh media to achieve 1 x 10^4 cells/ml and 100 µl of the cell suspension was aliquoted into each well of a 96-well plate (Costar, UK). Plates were incubated at 37°C, 5 % CO_2 until confluent. NB Vero cells were seeded at 1 x 10^5

2.5.2.8 Culture in 6-well plates

Cells confluent in a 75 cm^2 flasks was trypsinised as previously described and resuspended in 25 ml of fresh media. 4 ml of the cell suspension was aliquoted into each well of a 6-well plate (Costar, UK). Plates were incubated at 37°C, 5 % CO_2 until confluent.

2.6 Morphological assessment

Phase contrast microscopy was used to investigate morphological changes in response to toxin exposure and micrographs taken using a Kodak 206 camera attached to the microscope.

2.7 Cell viability

Cell viability was established using a selection of methods that assessed chemical properties and physical characteristics.

2.7.1 MTT (3-[4,5-Dimethylthiazol-2-yl]-2,5-diphenyltetrazolium bromide) assay

3-[4,5-Dimethylthiazol-2-yl]-2,5-diphenyltetrolium bromide, MTT (Sigma) is a water soluble tetrazolium salt, yellow in colour used in a colorimetric assay to establish cell viability (Mosmann 1983). By dissolving the MTT, dehydrogenase enzymes produced in metabolizing cells convert the soluble tetrazolium salt to insoluble purple formazan crystals that can be solubilised using acid/SDS (5% SDS in 0.01 M HCl) and the absorbance of the converted

dye can then be read spectrophotometrically at 570 nm (recommended wavelength is 550-600 nm) (Mosmann 1983).

Stock solution was prepared using MTT powder and distilled water to a concentration of 5 mg/ml. The solution was syringe filtered through a 0.2 µm filter and stored at 2-8 °C or frozen for use at a later date.

The stock solution was diluted 1:10 using specific cell culture medium and following the removal of the media covering the cells to be assessed, 500 µl of the MTT/DMEM solution was added to each well and incubated at 37°C, 5% CO_2 for 4 hours. After which, 500 µl of acid SDS lysis buffer was added to each well and returned to the incubator overnight.

Transferring the content of each well into a 1 ml eppendorf the cell debris was removed by centrifugation at 130,000 rpm for 10 minutes. 100 µl of each eppendorf was transferred into a 96-well plate and the absorbance of the converted dye was measured spectrophotometrically at 570 nm using a Bench Mark Plus microplate spectrophotometer (Biorad, UK).

2.7.2 Trypan blue exclusion assay

The trypan blue exclusion assay is simple method used to establish the number of viable and non viable cells in a given sample. By mixing the sample with an equal volume of trypan blue dye viable cells excluding the dye and non-viable cells stained blue (due to a breakdown in their cell membranes and increased permeability) can be counted and the percentage of viable cells calculated.

Cells were harvested by trypsinisation using 0.25% trypsin (Sigma) and 20 µl of the cell suspension mixed with an equal volume (20 µl) of 0.08 % trypan blue solution (Sigma). 20 µl of the trypan blue stained cell suspension was transferred to the edge of the haemocytometer and allowed to spread evenly by capillary action.

Using the 10 x objective of the light microscope the 16 square grid was focused on (total area 1 mm^3) and the total number of unstained (viable) cells and blue (dead) cells counted separately in four (0.1 mm^3) squares. Calculating the average cells in 0.1 mm^3, the total number of cells is equal to the average cell number in 0.1 mm^3 multiplied by the dilution factor and the total volume in one square (10^{-4} cm^3). Cell viability was calculated using the following equation and reported as percentage cell viability.

$$\% \text{ cell viability} = \frac{\text{total viable cells (unstained)}}{\text{Total cells (stained + unstained)}} \times 100$$

2.7.3 DNA and Cell Cycle Analysis using Propidium Iodide and flow cytometry

The propidium iodide (PI) flow cytometric assay (Nicoletti, Migliorati et al. 1991) was used to investigate DNA/cell fragmentation and cell cycle progression. Propidium iodide, a fluorogenic compound, binds stoichiometrically to nucleic acids and the fluorescence emitted, measured by Fluorescence Activated Cell Sorting (FACS), is directly proportional to the DNA content of the cell. All eukaryotic cells progress through a cycle of DNA

replication and nuclear/cell division separated by two gap phases (G_1 and G_2) and by using the data compiled from PI cytometric assay and the Cylchred, cell cycle analysis program based on algorithms by (Ormerod, Payne et al. 1987; Watson, Chambers et al. 1987) written by Terry Hoy, analysis of cell cycle progression and DNA fragmentation completed.

2.7.3.1 Fixing cells

Cells were harvested by trypsinisation using 0.25% trypsin (Caco-2 and HT29 cells) or 0.1% trypsin (primary human colonic myofibroblasts). The cells (including non-adherent cells removed with the culture media) were pelleted by centrifugation at 1000 rpm for five minutes. The pellet was re-suspended in 1 ml PBS and pelleted by centrifugation at 1000 rpm for five minutes. This washing process was carried out twice. The remaining pellet was resuspended in 1 ml of ice cold 70% v/v ethanol and placed on ice. Samples were stored at -20 °C and all timepoints stained and analysed together.

2.7.3.2 Propidium Iodide staining

FACS tubes containing suspended cells in ethanol were pelleted by centrifugation at 1000 rpm for 5 minutes and the pellet resuspended in 1 ml of PBA [Phosphate buffered solution with 0.1% BSA (Bovine Serum Albumin, Sigma) and sodium azide] and pelleted by centrifugation twice. The pellet was finally resuspended in 500 µl of PBA; 5 µl of RNase solution (DNase Free, Sigma) added to remove any contaminating RNA and 25 µl of Propidium iodide solution (Sigma) placed in each tube. The cells were then incubated for 20 minutes at 37 °C and placed on ice prior to analysis by flow cytometry.

2.7.3.3 Flow Cytometry

Using the BD Coulter 500, fluorescence emitted and side scatter of PI stained cells (488 nm excitation) was measured using the red fluorescent channel (>600 nm) and 20,000 events collected. The data was plotted side scatter verses fluorescence. Using WinMDi 2.9, the data was converted into a scatter plot and a region drawn on the plot to identify single cells and remove cell debris. The gated region was subsequently used to produce a histogram.

2.7.3.4 Analysis of WinMDI histograms using Cylchred

Raw data files (histograms) prepared using WinMDI were entered into entered into Terry Hoy's cell cycle analysis program, Cylchred [written by Terry Hoy based on mathematical algorithms (Ormerod, Payne et al. 1987; Watson, Chambers et al. 1987), downloaded from http://archive.uwcm.ac.uk/uwcm/hg/hoy/software.html]. Each histogram was analyzed and the software provided total number of events and sub G1 events. In addition, the software provided a percentage value for events in each phase of cell cycle following the subtraction of events in the sub-G1 region.

The % of sub G1 events was calculated using the following equation:

(100 / total events) x events in sub G1

2.8 Western Blot analysis using Sodium Dodecyl Sulphate - Poly-acrylamide gel electrophoresis (SDS-PAGE)

The SDS-PAGE is used to separate proteins based on their size and electrophorectic mobility and in this study the technique has been used to investigate the presence of intracellular proteins and confirm the homogeneity of purified toxin B. The latter of which will be discussed in Chapter 4. The SDS-PAGE gel contains two distinct sections; the resolving gel; and the stacking gel. The components of the stacking gel remain constant, however the percentage resolving gel is dependent on the molecular weight of the protein of interest. The intracellular proteins of interest are between 20-25 kDa and the loading control β-actin 49 kDa and therefore a 10% resolving gel was chosen. Details of component chemicals and solutions needed to prepare the gels are provided in Appendix 1.

2.8.1 The Gel

A 10% resolving gel was prepared and poured into the assembled apparatus (BioRad). A thin layer of iso-propanol was placed onto the resolving gel and left for 30 minutes to polymerise. The isopropanol was removed by washing with dH_2O and any excess moisture was removed with a small piece of blotting paper. The stacking gel was prepared and poured onto the resolving gel layer and a comb inserted. The gel was left for 30 minutes to polymerise. When

set, the gel was placed into electrophoresis apparatus (BioRad) and the reservoirs filled with running buffer.

2.8.2 Whole cell lysate - Sample Preparation

Control and toxin treated cell lysates were prepared by removing the medium, washing the cells with warmed PBS and lysing the cells with Cellytic (Sigma); 25 µl placed into each well and using a cell scraper the content of each well was removed and centrifuged for five minutes at 10,000 rpm to remove cell debris. The lysate was stored at -20°C. The samples were defrosted and concentrated using Amicon Ultra 0.5 ml centrifugal filter devices (Millipore) and the total protein concentration ascertained using the Bradford Assay. Samples were diluted with ice cold PBS to give maximum identical total protein concentration. The diluted cell lysates were then mixed 1:1 with Laemelli sample buffer (4% SDS, 20% glycerol, 10% 2-mercaptoethanol, 0.004% bromphenol blue and 0.125 M Tris HCl, pH approx. 6.8) and placed in a block heated to 100 °C for five minutes. When cool, 17 µl of the sample was loaded into a well and 5 µl of a full range molecular rainbow marker was loaded into the spare well. A constant voltage of 100 V was applied for 100 minutes.

2.8.3 Transfer for Western Blot

After 100 minutes the gel was removed and prepared for transfer onto PVDF (Polyvinylidene Diflouride) membrane by soaking in 25 mls of transfer buffer. The PVDF membrane was activated by immersion in 100% methanol for 15

seconds, followed by a 2 minute dH_20 wash and a 5 minute immersion in transfer buffer (see Appendix 1). The gel and membrane were sandwiched together, covered with transfer buffer and a variable voltage not exceeding 0.2 amps (100 V) applied for 50 minutes.

2.8.4 Membrane processing

After the proteins are transferred onto the PVDF membrane all remaining protein interaction sites were blocked by incubating the membrane in blocking buffer (2g skimmed milk powder dissolved in TBS wash buffer, see Appendix 1) for one hour at room temperature for whole cell lysate membranes and overnight at 4°C for β-actin loading control membranes. The blocking buffer was removed and the membranes incubated with their respective primary antibodies; 1 hour at room temperature for toxin B membranes and β-actin loading control membranes and overnight at 4°C for whole cell lysate membranes specifically Rho A and Rac-1 primary antibodies.

The membrane was washed with wash buffer and covered with biotinylated secondary antibody (containing blocking serum and biotinylated affinity purified anti-mouse immunoglobulin) and incubated on a rocking platform at room temperature for 30 minutes. The biotinylated secondary antibody binds to the primary antibody.

The preformed avidin/biotinylated horseradish peroxidase macromolecular complex was prepared and left to incubate for 30 minutes before use. The biotinylated secondary antibody was removed, the membrane washed and the

pre-prepared avidin/biotin complex poured over the membrane and left to incubate on the rocking platform at room temperature for 30 minutes.

The membrane was washed and the horseradish peroxidase visualized using peroxidase substrate. The peroxidase substrate was poured over the membrane and as soon as the colour developed the membrane was rinsed with water to end the reaction. When dry the membrane was scanned.

2.9 Statistical analysis

Statistical analysis and graphical presentation was performed on GraphPad Prism v.4 (GraphPad Software, Canada) using one way analysis of variance (ANOVA) and the students t-test. Statistical significance was reported when $p=<0.05$.

CHAPTER 3

3 Caco-2 cells are more sensitive to toxin A induced cell death than HT29

3.1 Introduction

Intestinal epithelial cells are believed to be the first host cells that interact with luminal *C. difficile* toxins. Responses by the epithelial cells (e.g. loss of barrier function due to cell death) may determine the severity of mucosal inflammation that develops. Currently, there is little information regarding differences between epithelial cell types in their responses to *C. difficile* toxins. It has been reported that areas of mucosa and underlying lamina propria from individuals with *C. difficile* associated disease can appear normal despite adjacent areas of ulceration and pseudo-membrane formation. Investigation of epithelial response may go some way to explain why individuals colonized with toxigenic *C. difficile* remain asymptomatic and others develop fulminant colitis.

C. difficile toxin A exerts a dramatic effect on mammalian cell physiology, altering cell signalling events and ultra-structural maintenance. The first and most obvious impact on cell physiology in cells exposed to toxins A and B is the 'cytopathic response'; loss of structural integrity caused by actin reorganisation (Fiorentini, Malorni et al. 1990); opening of tight junctions, and; cell rounding. Exposure of cultured human intestinal epithelial cell monolayer's to TcdA and TcdB reduced trans-epithelial resistance and increased epithelial cell permeability, with flux studies identifying that the permeability failing occurred at the intercellular tight junction (Hecht, Pothoulakis et al. 1988; Hecht, Koutsouris et al. 1992). Alterations in cell surface projections and rearranged microvilli are observed in toxin A treated cells (Chang, Lin et al. 1979) and clear

actinomorphic changes can be seen using electron microscopy (Fiorentini, Malorni et al. 1990).

These structural and functional alterations are believed to be due to toxin induced modifications of the Rho proteins, more specifically the mono-glucosylation of Rho, Rac and Cdc42 using UDP-glucose as a co-substrate. Nusrat and colleagues found that inactivation of Rho by toxin A led to loss of organisation in the perijunctional F-actin ring in T84 colonic cell monolayers, resulting in the reduction of TER and an influx of solutes into the epithelium (Nusrat, Giry et al. 1995). The substrate targets Rho, Rac and Cdc42 also regulate other cellular events outside of the actin cytoskeleton (Prepens, Just et al. 1996; Schmidt, Rumenapp et al. 1996; Caron and Hall 1998; Brito, Fujji et al. 2002; Hippenstiel, Schmeck et al. 2002).

Following the dramatic change in morphology, the second impact of *C. difficile* toxins on the host cell is the 'cytotoxic response', cell death. Cell death following toxin A intoxication occurs via apoptosis but our understanding of the mechanisms that precede this are still being unraveled. Some consider cell death as dependent on Rho inactivation with inactivation of Rho in an endothelial cell line resulting in the activation of caspase-3 and caspase-9 (Hippenstiel, Schmeck et al. 2002). Whilst others argue that apoptosis is independent of Rho glucosylation with toxin A inducing the apoptotic pathway in T84 cells via the release of caspase-3, -6, -8, -9 and Bid activation (Brito, Fujji et al. 2002) and others reporting an accumulation of toxin A at the mitochondria prior to any detectable glucosylation of Rho proteins (He, Hagen et al. 2000). Similarly Carneiro and colleagues found that toxin A exposed T84 cells induced caspases 6, 8 and 9 prior to caspase 3 activation and induced Bid cleavage using a

caspase independent mechanism (Carneiro, Fujii et al. 2006). In non-transformed human colonic NCM460 cells exposed to toxin A, apoptosis involved p38 activation of p53. The subsequent induction of p21 resulted in cytochrome c release and caspase-3 activation (Kim, Kokkotou et al. 2005).

To confuse the issue further; others claim that both Rho inactivation and caspase independent signalling facilitate apoptosis in cells exposed to *C. difficile* toxin A. It may be that the pathway to apoptosis is also cell specific.

Supporting the cell-specific effect mouse teratocarcinoma cells were more sensitive than CHO cells when exposed to TcdA and it was proposed that increased expression of TcdA specific carbohydrate receptors may be responsible (Tucker, Carrig et al. 1990). Research conducted by Chaves-Olarte and co-workers sought to establish why TcdA and TcdB displayed different cytotoxic potency despite intoxicating target cells by the same mechanism. Using Don and T84 cells, two main differences were identified, with differing enzymatic activities highlighted as the main determinant and receptor binding difference contributing less (Chaves-Olarte, Weidmann et al. 1997).

A cell specific response to *C. difficile* toxins have been mentioned previously by others however direct comparison of both toxins on multiple cell types is poorly documented. We have previously studied the response of several intestinal cell types together with primary tissue biopsies and whilst not primary objectives of this study a differential response was evident with significant differences in toxin A induced cell death. This study concluded that epithelial cell death occurred via apoptosis as a result

of detachment from the basement membrane. Cells adherent to each other survived longer, than single cells, despite basement membrane detachment (Mahida, Makh et al. 1996). Also of relevance, we reported a dose dependent link to histological severity. Intestinal epithelial cells incubated with toxin A express differential levels of TGF-β and IL8 depending on the incubated toxin A concentration (Mahida, Makh et al. 1996).

The aim of this work is to compare responses to *C. difficile* toxin A by Caco-2 and HT29 human intestinal epithelial cells.

3.2 Purification of toxin A

Toxin A was purified by application of cultured *C. difficile* (VPI 10463) supernatant samples to a bovine thyroglobulin affinity column. Toxin A-containing fractions, which demonstrated cytotoxicity in Vero cells and dot blot positive, were subsequently subjected to two sequential anion exchange chromatographic steps as detailed in Chapter 1, 2.1.

Using the fractions of purified toxin A a number of assessments were carried out to ascertain purity, concentration and cytotoxicity prior to use.

3.2.1 Protein Concentration

The protein concentration of the final purified toxin A fractions (Batch 16) was calculated to be within the range of 0.04 – 1.70 mg/ml (Figure 3-1).

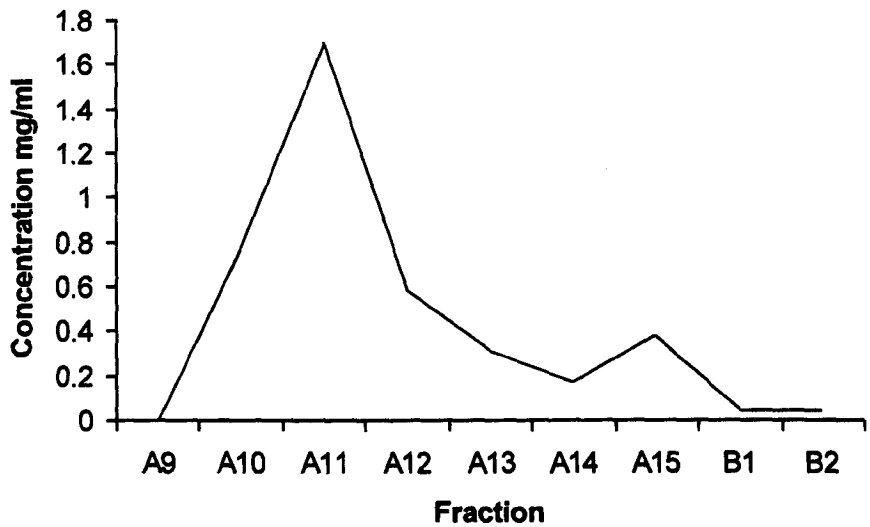

Figure 3-1 Concentration of purified toxin A fractions

The X axis displays codes for fractions eluted from the Mono-Q column from Batch 16. Toxin concentration peaked at fraction A11. The Y axis shows concentration of measured sample (mg/ml) when measured using Nanodrop at A_{280}

3.2.2 Native Polyacrylamide gel electrophoresis (PAGE)

To check the purity of the purified toxin A and to estimate its molecular weight under non-denaturing conditions a Native PAGE gel using a 5% resolving gel was performed with fractions, A10, A11, A12, A13 and A14 eluted from Mono-Q column (see Figure 2-3); concentration 0.77 mg/ml; 1.70 mg/ml; 0.58 mg/ml; 0.31 mg/ml; and 0.17 mg/ml, respectively. A high weight molecular weight protein mixture (Amersham Biosciences) was used as a marker.

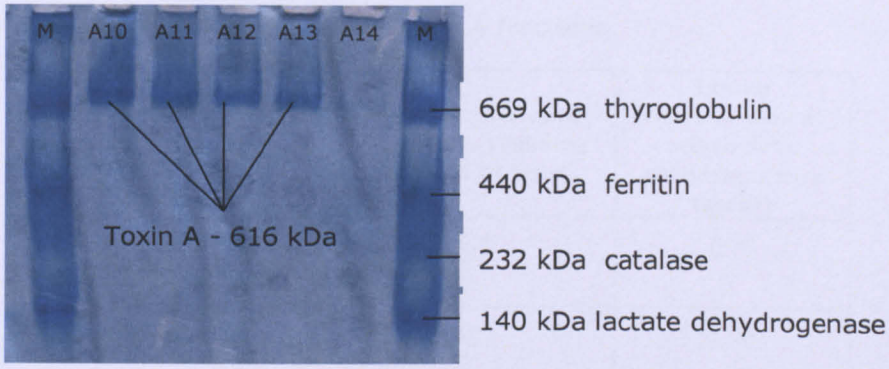

Figure 3-2 Native PAGE gel of purified toxin A fractions

Electrophoresis was performed on five fractions of purified toxin A, on a 5 % resolving gel. A high weight molecular protein mixture (Amersham Biosciences) (M) containing 76 µg of thyroglobulin (Mw 669 000 Da), 50 µg of Ferritin (Mw 440 000 Da), 36 µg of Catalase (Mw 232 000 Da), 48 µg of lactate dehydrogenase (Mw 140 000 Da) and 40 µg of Albumin (Mw 66 000) was used as a marker. Toxin A exists as a dimer and therefore a single band was seen close to the thyroglobulin band at 669 kDa.

As can be visualised in Figure 3-2 comparison of sample bands against the high molecular weight protein marker shows a single distinct band at approximately 600 kDa, corresponding to a dimer of 308 kDa toxin A protein.

3.2.3 Cytotoxic activity of purified toxin A

As discussed in Chapter 2 section 2.4.3 the cytotoxic activity of purified toxin A is determined using the Vero cell assay and the cytotoxicity titre is determined following the incubation of Vero cell monolayers to serial dilutions of toxin A for 24 h. At 24 h, the lowest serial dilution to induce 50% rounding in each fraction was identified (Table 3-1). The concentration of purified toxin A that elicited the cytotoxic effect were calculated to be within the range of 0.58 – 400 pg/ml.

Table 3-1 Cytotoxic activity of purified toxin A fractions

Batch	Fraction	Concentration (mg/ml)	Maximal dilution at which 50% rounding visible at 24 hours	Lowest concentration at which 50% rounding occurs (pg/ml)
16	A10	0.77	10^{-9}	0.77
	A11	1.70	10^{-9}	1.70
	A12	0.58	10^{-9}	0.58
	A13	0.31	10^{-8}	3.1
	A14	0.17	10^{-7}	17
	A15	0.38	10^{-7}	38
	B1	0.04	10^{-6}	400
	B2	0.04	10^{-6}	400

3.3 Intestinal epithelial cell response to *C. difficile* toxin A

Early experiments investigated the time- and dose-dependent response of intestinal epithelial cells Caco-2 and HT29 to various concentrations of purified toxin A.

Using a previously characterized fraction of toxin A with a known pre-frozen concentration of 1.16 mg/ml, the toxin concentration was checked for possible degradation during storage using the Nanodrop at 280 nm and diluted in cell specific medium to give 1000 ng/ml; 100 ng/ml; 10 ng/ml; 1 ng/ml and 0.1 ng/ml. Removing the medium from Caco-2 and HT29 cells grown to confluence, 1 ml of each diluted concentration was added (in triplicate) to the cells and the plates re-incubated at 37°C, 5% CO_2. Control wells were also prepared, containing media only. Morphological assessments using light microscopy were made at 30 minutes, 1 h, 2 h, 4 h, 6 h, 24 h, 48 h and 72 h as described in Chapter 2.

3.3.1 Cell cytotoxicity established using MTT assay

Cell cytotoxicity was measured in Caco-2 and HT29 cells incubated with varying concentrations of *C. difficile* toxin A at 48 h and 72 h using the MTT assay as described in Chapter 2, section 2.7.1

3.3.2 Cell viability using Trypan Blue Exclusion Assay

Cell viability was measured in Caco-2 and HT29 cells incubated with varying concentrations of *C. difficile* toxin A at 48 h and 72 h using the Trypan blue exclusion assay as described in Chapter 2, section 2.7.2.

3.3.3 Propidium Iodide staining and cell cycle analysis

Cell cycle analysis was performed on Caco-2 and HT29 cells incubated with 100 ng/ml of toxin A for 4, 8, 24, 48 and 72 hours using propidium iodide and flow cytometry as described in Chapter 2, section 2.7.3. Toxin-exposed cells were compared with cells cultured with control medium, seeded at the same time and obtained at the same time points as those cultured in the presence of the toxin.

This experiment was also repeated to investigate the response of HT29 cells to 10 000 ng/ml toxin A.

3.3.4 Labelling of Toxin A

To investigate the uptake of *Clostridium difficile* toxin A the protein was labelled using AlexaFluor^{488} Protein Labelling kit (Invitrogen) and size exclusion purification resin (Bio-Rad) to separate unincorporated due from the labelled toxin A.

3.3.4.1 Preparation of toxin A and conjugate

With a starting toxin A concentration of 2 mg/ml the Tris buffer was removed with three PBS exchanges (mixing 1 ml PBS with 500 µl toxin A and centrifuged for 20 minutes at 5000 g). The Alex Fluor^{488} was resuspended in 120 µl of PBS and a 1 M sodium bicarbonate solution prepared. Adding 50 µl of 1M sodium bicarbonate solution and 30 µl of dissolved AlexaFluor^{488} to the 500 µl of 2 mg/ml toxin A – the reaction was stirred for 1 hour in darkness at room temperature.

3.3.4.2 Preparation of size exclusion purification resin

Bio-Gel P-30 is a porous polyacrylamide bead gel prepared by copolymerization of acrylamide and N,N'-methylene-bis-acrylamide. The gel is extremely hydrophilic; essentially free of charge allowing for efficient filtration of the toxin A sample, and; the narrow distribution of bead diameter providing excellent resolution and molecular weight discrimination. Using the fine size exclusion resin (BioGel P-30, Bio-Rad) designed to separate free dye from proteins with MW >40 kDa, a 10X stock elution buffer was prepared (0.1 M potassium phosphate, 1.5 M NaCl, 2 mM sodium azide, pH7.2) and a 1X dilution made. The resin powder was gradually added to the buffer and gently stirred to ensure uniform suspension of beads and allowed to hydrate for 12 hours at room temperature. Following hydration half of the supernatant was removed and the resin sample degassed for 5-10 minutes with occasional swirling of the contents. With the addition of two bed volumes of degassed buffer the gel was gently swirled to suspend any fine particles and when 90-95% of the gel settled the supernatant containing the fine particles was removed by suction. This process was completed 3-4 times until 90% of the fine particles were removed.

3.3.4.3 Preparation of size exclusion purification resin column

The column was prepared as detailed in Figure 3-3. The elution buffer (1X) was prepared from 10X stock elution buffer (0.1 M potassium phosphate, 1.5 M NaCl, 2 mM sodium azide, pH7.2) and the resin prepared as described on page 109. Gently stirring the resin to ensure homogenous suspension the resin was carefully pipetted into the column until the resin was approximately 3 cm from the top, allowing excess buffer to drain into the column bed.

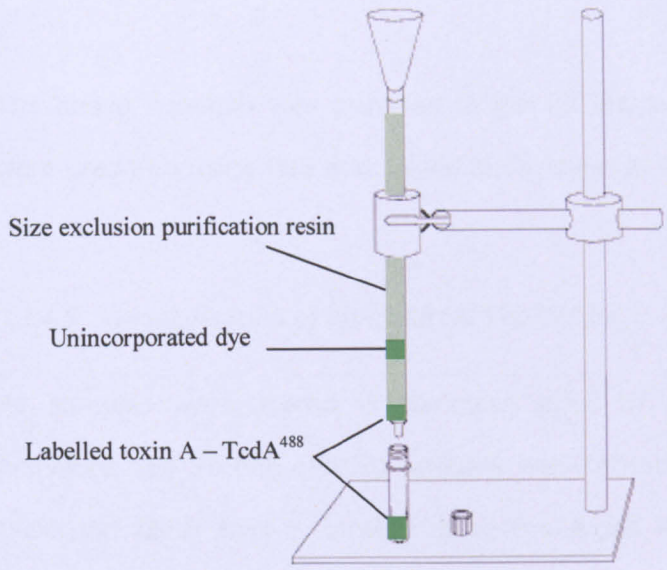

Figure 3-3 Column assembly for toxin labeling

Image adapted from AlexaFluor^{488} Protein Labelling Kit instructions (Invitrogen).

3.3.4.4 Separation of labelled toxin A TcdA^{488} from incorporated dye

The reaction mixture was loaded into the column and allowed to enter the column resin. The vial containing the mixture was rinsed with 100 µl of elution buffer and also applied to the column. With the mixture embedded in the resin, elution buffer was slowly added until the labelled protein had been eluted. Two bands were viewed travelling through the resin representing the separation of labelled toxin from unincorporated dye. 500 µl fractions were collected until both bands were eluted. The first band contained labelled toxin A and all eluted 500 µl samples containing fluorescent dye were pooled and concentrated. The protein conjugate concentration was established using Bradford assay and the degree of labelling (moles of dye per mole of protein) of toxin A with AlexaFluor^{488} established taking the absorbance measured at 495 nm and inserting that value and the protein concentration into the following equation:

moles of dye per mole of protein = Abs at 495 nm/71,000 x protein conc.

The above equation was provided in the kit instruction. Stock solutions were prepared using PBS and stored in darkness at 4°C.

3.3.4.5 Quantification of internalised $TcdA^{488}$ by flow cytometry

All samples were stored in darkness prior to analysis. Fluorescent Activated Cell Sorting (FACS) analysis was carried out using the Becton Dickinson LSRII flow cytometer using the Argon 488 nm laser. Median fluorescence intensity was recorded from 10,000 events (excitation 488-494 nm, detection 519 nm). See representative scatter plots and histogram in Figure 3-4.

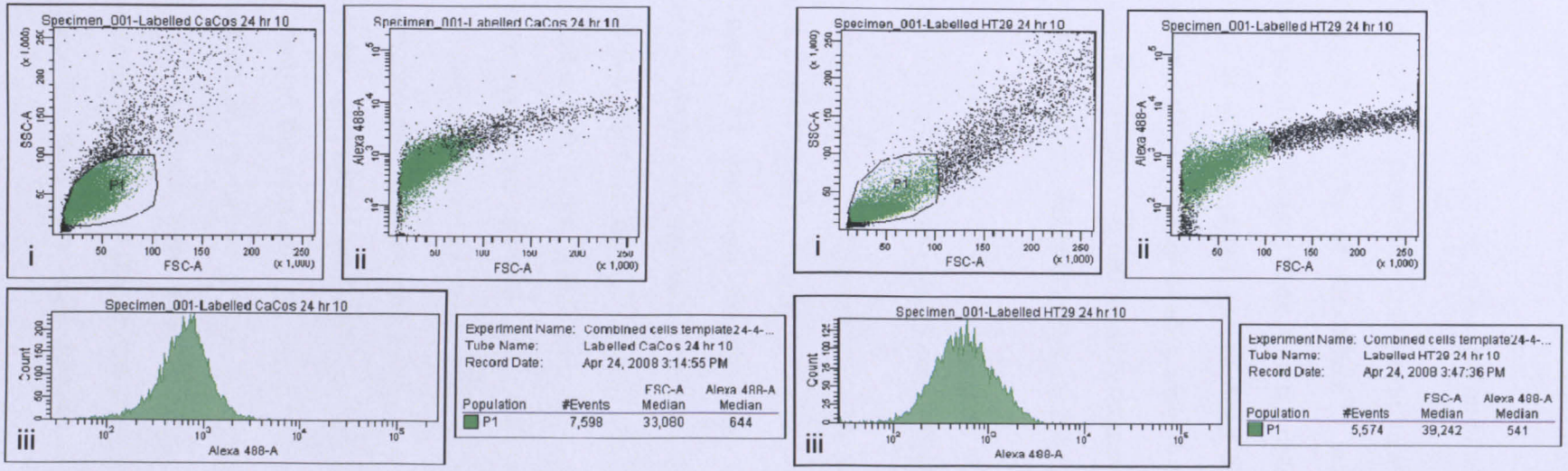

A) Representative plot of Caco-2 cells 24 h 10µg/ml TcdA^{488} B) Representative plot of HT29 cells 24 h 10µg/ml TcdA^{488}

Figure 3-4 Representative scatter plot and histogram of Median Fluorescence Intensity (MFI)

i. Representative Scatter plot showing forward and side scatter; ii. Forward scatter and Alexa-^{488}-A; iii) histogram showing count and Alexa-^{488}-A of Caco-2 cells treated with 10 µg/ml of TcdA^{488} for 24 h. B)i. Representative Scatter plot showing forward and side scatter; ii. Forward scatter and Alexa-^{488}-A; iii) histogram showing count and Alexa-^{488}-A of HT29 cells treated with 10 µg/ml of TcdA^{488} for 24 h.

3.3.5 Internalisation of Tcd^{488} by intestinal epithelial cells HT29 & Caco-2

3.3.5.1 Biological activity of labeled and unlabeled toxin A

In view of the possibility that toxin labelling may affect its biological activity, the activity of AlexaFluor^{488} labelled toxin A ($TcdA^{488}$) was compared with unlabeled toxin A on the cells of interest. Caco-2 and HT29 cultured in 96 well plates as described in 2.5.2.7 were incubated with either unlabeled toxin A or labelled toxin A at 10 000, 1 000 and 100 ng/ml or control medium and cell viability assessed at 48 hours using the MTT assay as previously detailed in section 2.7.1.

3.3.5.2 Cell culture with $TcdA^{488}$ and fixing of cells

Initial experiments investigated the dose dependent uptake of $TcdA^{488}$ by Caco-2 and HT29 cells at 24h. HT29 and Caco-2 cells were seeded in 24 well plates as previously described and grown to confluence. When confluent, media was replaced with either labelled toxin A at 2 000, 5 000 and 10 000 ng/ml or control medium for 24 h. Dilutions were prepared using cell specific media. After 24 h the media was removed from all wells and cells trypsinized with 200 µl of 0.25% trypsin were pooled and placed into labelled eppendorf's. The eppendorf containing the media together with any non-adherent cell was pelleted by centrifugation at 1000 rpm for 5 minutes and 100 µl of 0.25% of trypsin added to the pellet. After trypsinisation the cells from the wells were transferred into the respective eppendorfs and a further 1.5 ml of warmed media added to wash out trypsin. The cells were pelleted at 1000 rpm for 5 minutes and resuspended in 400 µl of DMEM (2% FCS)/4% formaldehyde solution for 5 minutes. The cells were again pelleted at 1000 rpm for 5 minutes and

resuspended in 0.5% formaldehyde in labelled FACS tubes. The tubes were kept in darkness until fluorescence was measured and median fluorescence intensity reported.

All subsequent experiments were conducted using 5000 ng/ml and 10000 ng/ml of $TcdA^{488}$ and median fluorescence intensity recorded in control and toxin exposed cells after 1 h, 2 h, 5 h and 24 h using the above method.

3.3.5.3 Visualisation of internalized $TcdA^{488}$

To visualize the internalization of $TcdA^{488}$ by HT29 and Caco-2 cytospins of cells in control medium and following incubation with 10 000 ng/ml $TcdA^{488}$ for 24 h were prepared. In brief, HT29 and Caco-2 cells incubated with 10 000 ng/ml $TcdA^{488}$ for 24 h were fixed in formaldehyde and stored at 4 °C. Glass slides were labelled and place into the metal holder and blotting paper placed on top. Transferring 100 µl of HT29 samples and 250 µl of Caco-2 samples into the plastic cup, the cup was then clamped into place and placed into cytospin centrifuge (Shandon Cytospin 2). The cells were spread onto the glass slides using centrifugal force of 1000 rpm for 8 minutes and stored in darkness overnight prior to mounting.

Cells were mounted with a small drop of glycerol and a small glass coverslip on top. Excess glycerol was wiped away and the perimeter of the slip sealed with clear varnish. $TcdA^{488}$ uptake was visualised and micrographs taken using fluorescent microscope (Nikon Eclipse TE2000-S). Fluorescent and phase contrast micrographs were taken and can be viewed in Figure 3-12.

3.3.6 Rho protein expression

Investigation of Rho signalling in intestinal epithelial cells was completed using whole cell lysates from HT29 and Caco-2 cells in control and toxin A treated samples and the Western blot technique using Rho specific antibodies for detection. See Chapter 2 section 2.8. The proteins investigated included Rac-1, Rho A and Rho B. β-actin was used as a loading control.

In brief, HT29 and Caco-2 intestinal epithelial cells were incubated with 1000 ng/ml toxin A or control medium for 0 h, 4 h, 8 h and 24 h. A 48 h timepoint was also included for HT29 cells but not Caco-2, due to extreme loss of viable cells. A Western blot was completed for each protein to be investigated, including a loading control. A colour scan was made of each Western blot.

3.4 Epithelial cell response to *C. difficile* toxin A

3.4.1 Dose dependent response in HT29 and Caco-2 cells to toxin A – 0.1 – 1 000 ng/ml

Initial experiments investigated the response of intestinal epithelial cells, Caco-2 and HT29 to varying concentrations of *C. difficile* toxin A ranging 0.1 ng/ml through to 1 000 ng/ml. Morphological assessments were made at 1 h – 72 h and viability of cells following exposure to toxin A or control media at 48 and 72 hours.

Subsequent experiments were completed using Caco-2 and HT29 cells and *C. difficile* toxin A at 100 ng/ml, 1000 ng/ml or 10000 ng/ml. Cellular viability and cytotoxic effect was established at 48 and 72 hours post toxin exposure and compared against untreated (control) cells.

3.4.2 Alterations to cell morphological

Morphological assessment was made using light microscopy as described in Chapter 2, and the cells in each well categorized into one of three morphological stages; no visible rounding; 50% visible rounding and 100 % visible rounding. The percentage rounding was ascertained by observing the rounded cells in ten random high power fields and taking the subjective mean of these ten observations. Attachment and signs of cell death will also be noted. Photographic representation of these stages in each cell line can be viewed in Figure 3-5.

Assessments were made at 1 hr, 2 hr, 4 hr, 24 hr, 48 hr and 72 hr post toxin A exposure. Cell rounding occurred in a time- and dose-dependent

manner occurring marginally earlier, by 1 hr, and at lower concentrations in Caco-2 cells (Table 3-2).

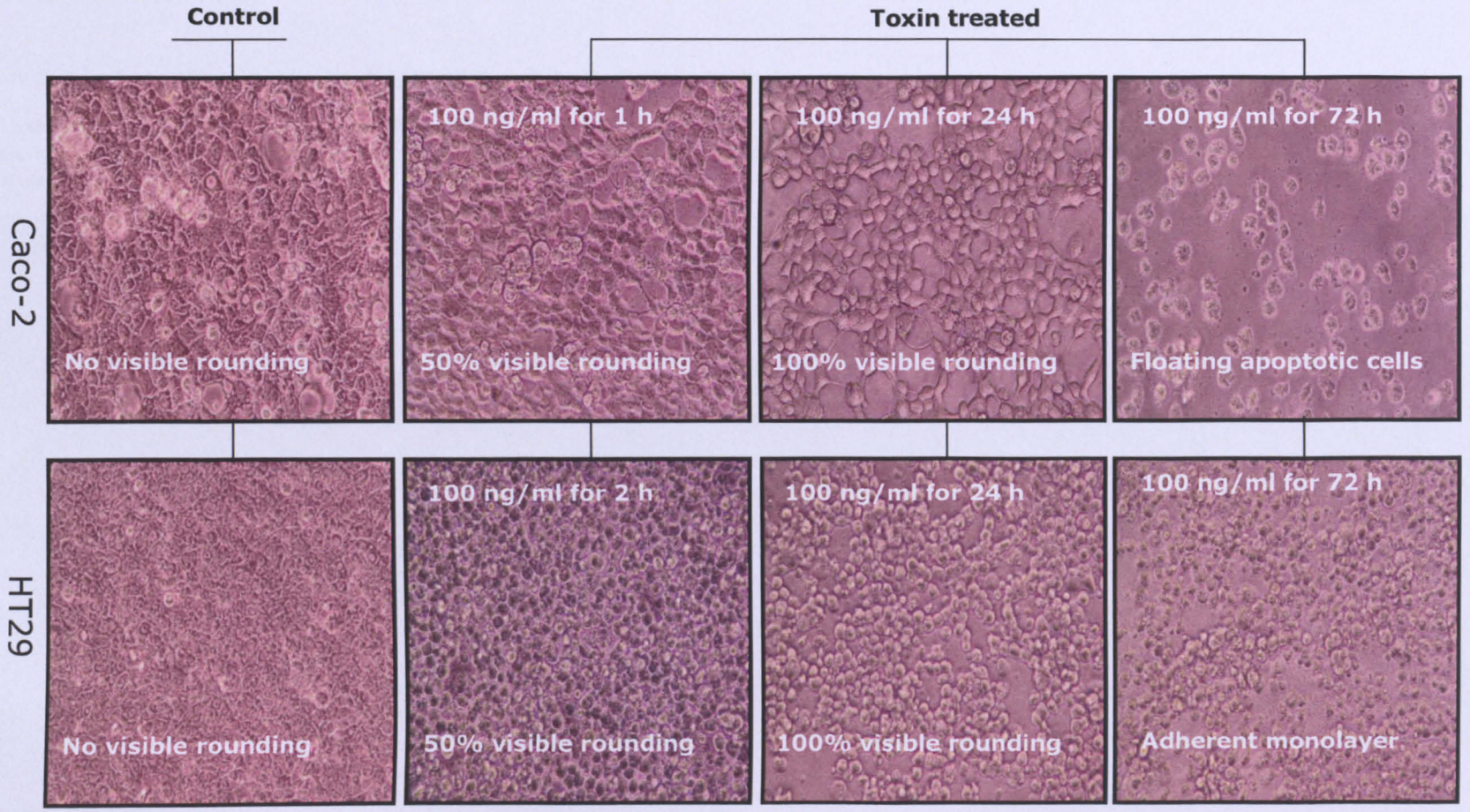

Figure 3-5 Representative phase contrast images of Caco-2 and HT29 cells incubated with *C. difficile* toxin A

The data is representative of seven experiments completed in triplicate. The 'control' images are taken from untreated cells cultured in DMEM. The percentage rounding was ascertained by observing the rounded cells in ten random high power fields and taking the subjective mean of these ten observations.

Table 3-2 Cell rounding in intestinal epithelial cells to *C. difficile* toxin A

Cell rounding; 100% (+) or 50% (+/-) in Caco-2 and HT29 cells in response to varying concentrations of toxin A. The data is representative of three experiments completed in triplicate. The percentage rounding was ascertained by observing the rounded cells in ten random high power fields and taking the subjective mean of these ten observations.

Toxin A (ng/ml)	Duration of toxin A exposure											
	1 hour		2 hours		4 hours		24 hours		48 hours		72 hours	
	Caco-2	HT29	Caco-2	HT29	Caco-2	HT29	Caco-2	HT29	Caco-2	HT29	Caco-2	HT29
0.1	-	-	-	-	-	-	+	-	+	+/-	+	+/-
1.0	-	-	-	-	+	-	+	+/-	+	+	+	+
10	-	-	+/-	-	+	+/-	+	+	+	+	+	+
100	+/-	-	+/-	+/-	+/-	+/-	+	+	+	+	+	+
1000	+/-	+/-	+	+/-	+	+/-	+	+	+	+	+	+

3.4.3 Investigation of cellular viability using the MTT assay

Cell viability was established after 48 h and 72 h toxin A exposure using the MTT assay as previously described. (Chapter 2, section)

3.4.3.1 Caco-2 cellular viability – 0.1 ng/ml – 1 000 ng/ml toxin A

Caco-2 intestinal epithelial cells exposed to *C. difficile* toxin A showed a reduction in mitochondrial dehydrogenase activity, which reflects cell viability, in a time and dose dependent manner. A significant reduction in cell viability was seen when Caco-2 cells were exposed to concentrations of toxin ≥ 100 ng/ml at 48 hours and ≥ 10 ng/ml after 72 hours when compared to control (untreated cells), Table 3-3. Cells exposed to concentrations < 10 ng/ml presented with some loss of cell viability, however not significantly so, even after 72 hour exposure to the toxin (Table 3-3).

3.4.3.2 HT29 cellular viability – 0.1 – 1 000 ng/ml toxin A

HT29 intestinal epithelial cells exposed to *C. difficile* toxin A showed a reduction (not statistically significant) in mitochondrial dehydrogenase activity, which reflects cell viability, at 48 hours in a dose dependent manner; however by 72 hours mitochondrial dehydrogenase activity increased to levels found in control (untreated cells) (Table 3-3).

No significant difference was noted between 48 and 72 hours or at any concentration when compared against control (untreated cells) at either time point (Table 3-3 B).

Table 3-3 Mitochondrial dehydrogenase activity (MDA) in Caco-2 and HT29 cells to *C. difficile* toxin A (0.1-1000 ng/ml)

MTT assay for mitochondrial dehydrogenase activity (expressed as OD 570 nm) in (A) Caco-2 cells and (B) HT29 cells exposed to varying concentrations of toxin A for 48 h and 72 h. Data in table presents mean (±SEM) of 3 experiments performed in triplicate. ** = $p<0.01$ * = $p<0.05$ when compared with control

A

Conc. (ng/ml)	Period of exposure (h)	
	48	72
Control	0.2217 ± 0.0157	0.2733 ± 0.0191
0.1	0.1860 ± 0.0395	0.1920 ± 0.0185
1	0.2037 ± 0.0194	0.1700 ± 0.0364
10	0.1807 ± 0.0043	0.1037 ± 0.0362 *
100	0.0910 ± 0.0252 *	0.0580 ± 0.0380 *
1000	0.0460 ± 0.0180 *	0.0293 ±0.0264 **

B

Conc. (ng/ml)	Period of exposure (h)	
	48	72
Control	0.3273 ± 0.0238	0.2983 ± 0.0104
0.1	0.3193 ± 0.0295	0.2897 ± 0.0184
1	0.3147 ± 0.0294	0.3000 ± 0.0063
10	0.2943 ± 0.0177	0.2937 ± 0.0234
100	0.2957 ± 0.0463	0.306 ± 0.0180
1000	0.2907 ± 0.0395	0.3117 ±0.0130

3.4.3.3 Comparison of viability in cells exposed to C. difficile toxin A

With a significant difference in cellular response observed in Caco-2 cells exposed to toxin A >100 ng/ml from 48 hours onwards, future experiments were completed to compare the response of Caco-2 and HT29 cells to 100 and 1 000 ng/ml toxin A.

Caco-2 and HT29 cells were grown to confluence and incubated with either 100 ng/ml, 1 000 ng/ml toxin A or control media. Morphological changes were noted and found to be similar to that reported in Table 3-2. Cell cytotoxicity was measured using the MTT assay as previously described. Cell viability was assessed using the Trypan Blue Exclusion assay, see 2.7.2; together with Propidium Iodide analysis by flow cytometry of DNA content, see 2.7.3.

3.4.3.4 Significant loss of mitochondrial dehydrogenase activity

Supporting earlier results, cell cytotoxicity as measured using the MTT assay (n=7) established a highly significant (p= <0.0001) loss of mitochondrial dehydrogenase activity in Caco-2 cells incubated with ≥100 ng/ml purified toxin A from 48 h when compared with control (untreated) cells (Table 3-4 and Figure 3-6 A). In contrast, and supporting initial experiments the mitochondrial dehydrogenase activity in toxin treated HT29 cells remained similar to control (untreated) cells at concentrations ≤1 000 ng/ml toxin A (Table 3-4 and Figure 3-6 B).

Table 3-4 Mitochondrial dehydrogenase activity (MDA) in Caco-2 and HT29 cells to *C. difficile* toxin A (100-1000 ng/ml)

MTT assay for mitochondrial dehydrogenase activity (expressed as OD 570 nm) in Caco-2 and HT29 cells exposed to varying concentrations of toxin A for 48 h and 72 h. Data in table presents mean (±SEM) of 7 experiments performed in triplicate. *** = $p<0.000\ 1$ when compared with control

Conc. (ng/ml)	Period of exposure (h)			
	Caco-2		HT29	
	48	72	48	72
Control	0.3527 ± 0.0439	0.3722 ± 0.0440	0.4542 ± 0.0355	0.4434 ± 0.0527
100	0.1774 ± 0.0410 ***	0.1274 ± 0.0298 ***	0.4294 ± 0.0513	0.4346 ± 0.0491
1000	0.1266 ± 0.0333 ***	0.1021 ± 0.0280 ***	0.4286 ± 0.0512	0.4376 ± 0.0500

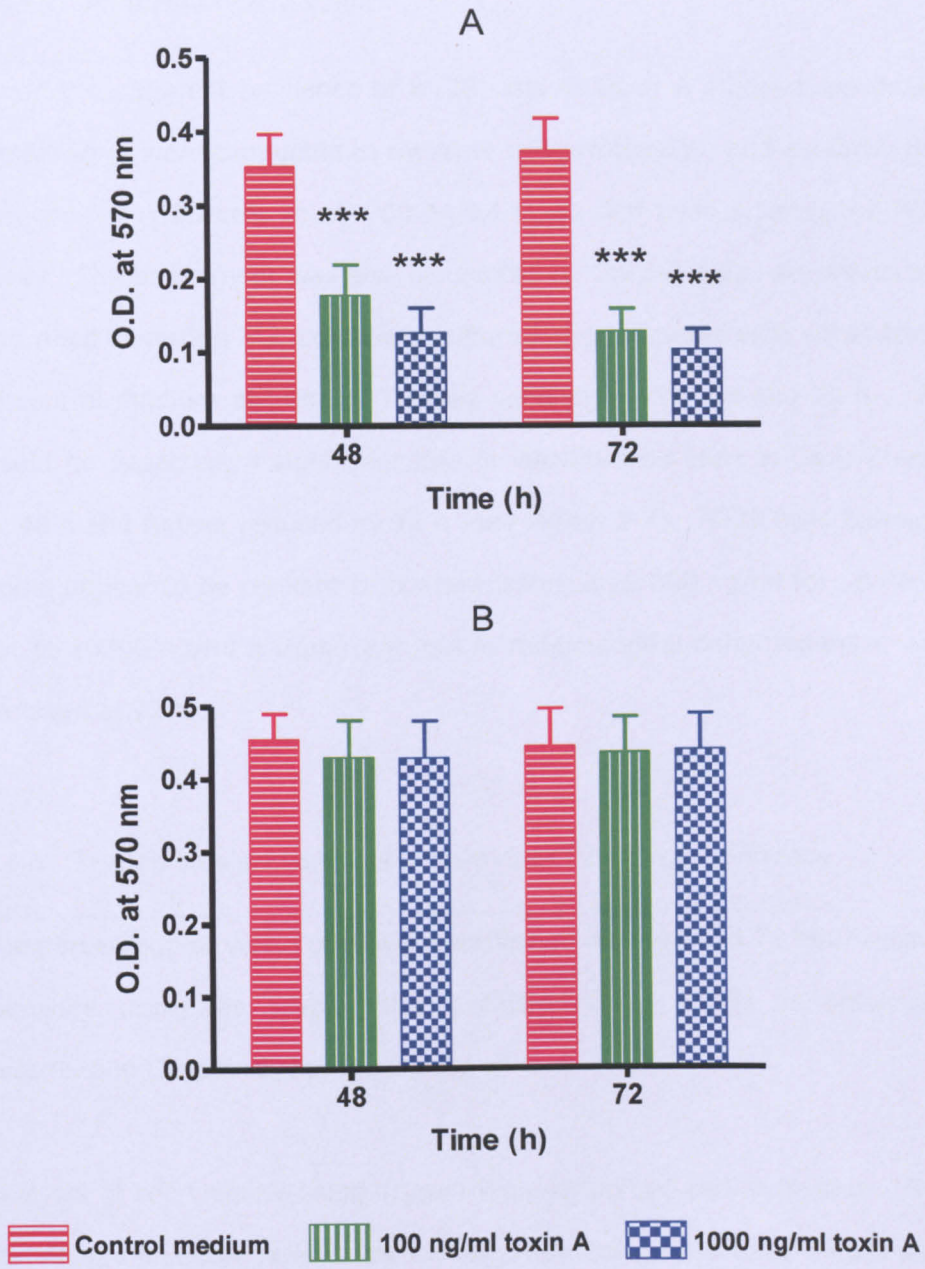

Figure 3-6 Mitochondrial dehydrogenase activity (MDA) in Caco-2 and HT29 to *C. difficile* toxin A (100-1000 ng/ml)

MTT assay for mitochondrial dehydrogenase activity (expressed as OD 570 nm) in Caco-2 (A) and HT29 (B) cells exposed to varying concentrations of toxin A for 48 h and 72 h. Data in figures represent mean (±SEM) of 7 experiments performed in triplicate. ***= $p<0.0001$ when compared with control.

3.4.3.5 Resilience of HT29 cells

Given the apparent resilience of HT29 cells to toxin A induced cell death experiments were conducted to measure cell cytotoxicity and establish the response of HT29 cells to 10 000 ng/ml of purified toxin A using the MTT assay. The experiment was also completed on Caco-2 cells. As previously described in section 3.3, cells were cultured and incubated with either toxin or control medium and the MTT assay conducted after 48 and 72 h. As would be expected, a significant loss in viability was seen in Caco-2 cells by 48 h and further reduced by 72 h (see Figure 3-7). HT29 cells however would appear to be resilient to concentrations ≤10 000 ng/ml for up 48 h, but at 10000 ng/ml a significant loss in mitochondrial dehydrogenase was reported at 72 h.

3.4.4 Trypan blue exclusion assay provides supportive evidence

The percentage of viable cells was established after 48 and 72 hour toxin A exposure using the Trypan blue exclusion assay (n=3) as previously described in Chapter 2, section 2.7.2.

Analysis of cell viability using Trypan Blue supported earlier findings. The percentage of viable cells is low with a great many dead Caco-2 cells seen (Figure 3-8 A). This correlates with the large reduction in mitochondrial dehydrogenase activity reported earlier in Caco-2 cells (Table 3-3). As would be expected the percentage of non stained (viable) HT29 cells was high with very few blue stained (dead) HT29 cells observed (Figure 3-8 B). This correlates with the small reduction in mitochondrial dehydrogenase activity reported earlier in HT29 cells (Table 3-3).

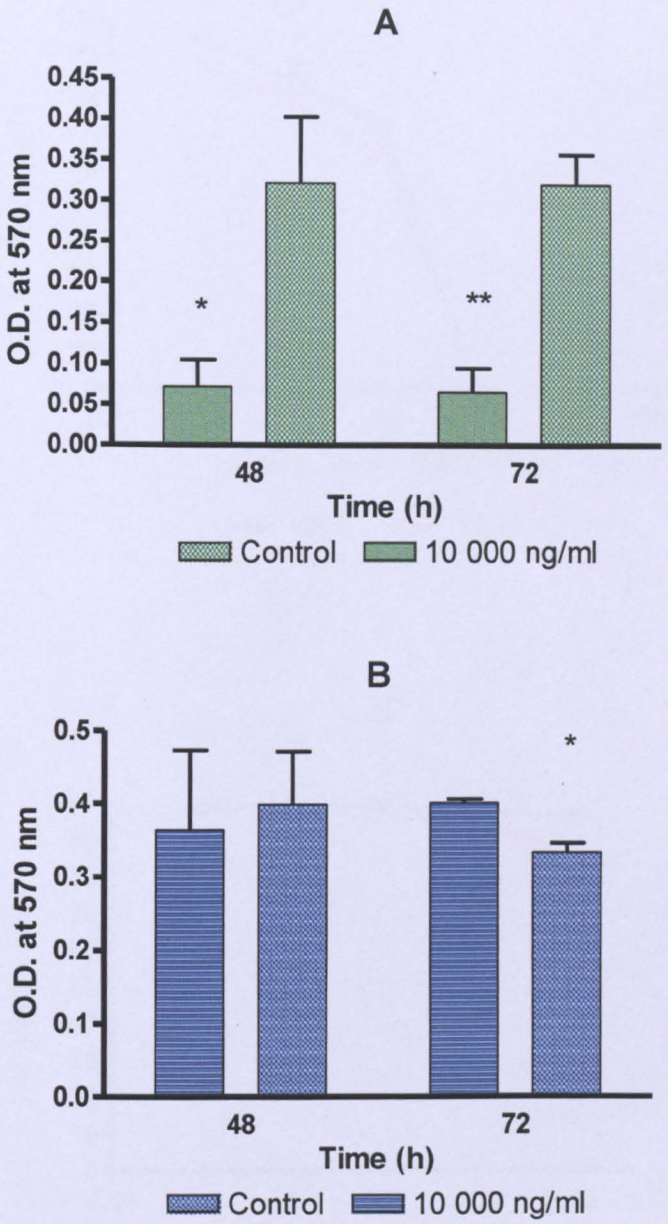

Figure 3-7 Mitochondrial Dehydrogenase Activity (MDA) in Caco-2 and HT29 cells to *C. difficile* toxin A (10,000 ng/ml)

MTT assay for mitochondrial dehydrogenase activity (expressed as OD 570 nm) in Caco-2 (A) and HT29 (B) cells exposed to 10 000 ng/ml of toxin A for 48 h and 72 h. Data in figures represent mean (±SEM) of 3 experiments performed in triplicate. *= $p<0.05$ **=$p<0.001$ when compared with control.

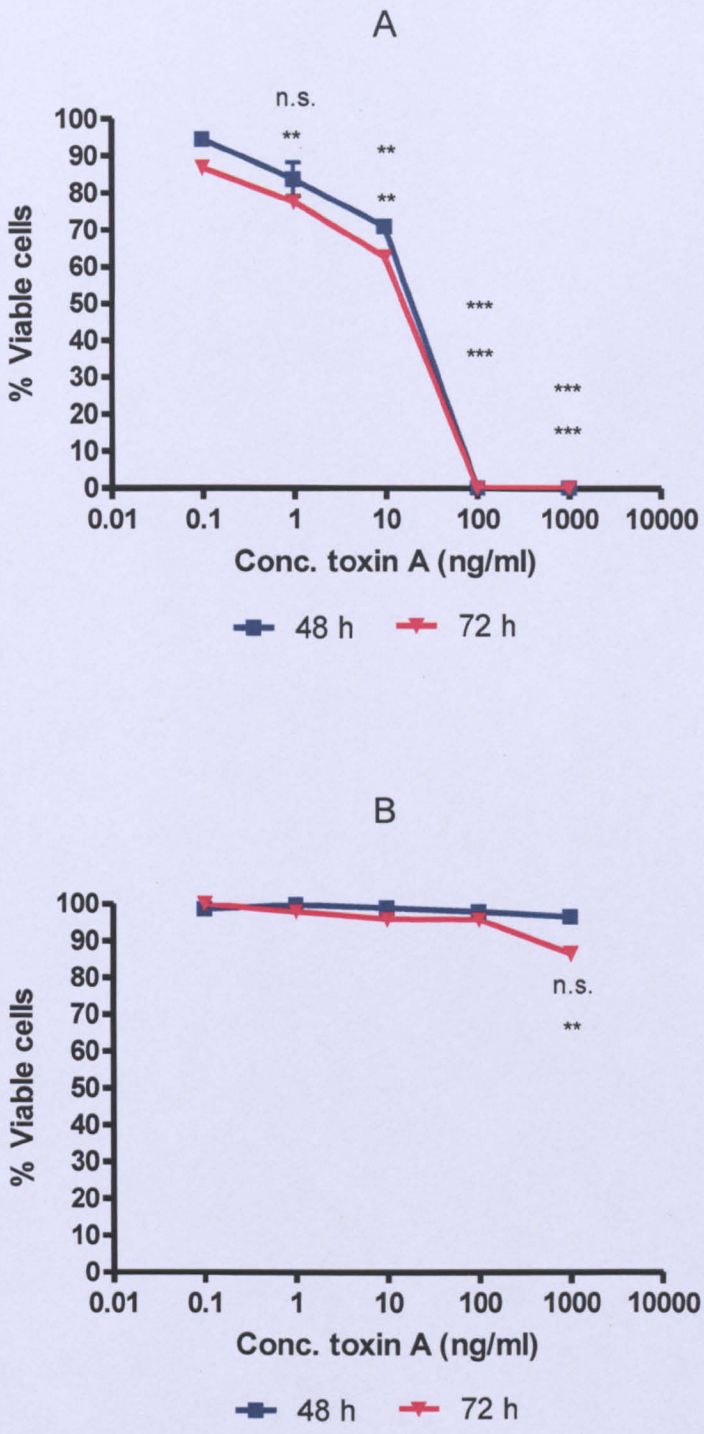

Figure 3-8 Cell viability assessed using Trypan Exclusion Assay in Caco-2 and HT29 cells to *C. difficile* toxin A (0.1-1000 ng/ml)

Assessment of Caco-2 (A) and HT29 (B) cell viability following exposure to toxin A for 48 h or 72 h. Proportions of cells that have not taken up trypan blue are expressed as % viable cells. Data in figures represent mean (±SEM) of 3 experiments performed in triplicate. *** = $p<0.0001$ and ** = $p<0.01$ n.s. = not significant when compared with control

3.4.5 Propidium Iodide staining and measurement using FACS confirm cell loss

As described in Chapter 2, 2.7.3, Caco-2 and HT29 cells incubated with 100 ng/ml toxin A or control media were fixed at 8 h, 24 h, 48 h and 72 h, stained with Propidium Iodide and fluorescence emitted assessed by flow cytometry. Using WinMDI 2.9 and cell cycle analysis programme Cyclhred as described in Chapter 2 section 2.7.3 the number of events in the sub-G1 region was ascertained and this number presented as a percentage of the total events recorded, comparing the percentage events in the sub-G1 region in toxin A-treated cells with control (untreated) cells.

As can be viewed in Figure 3-9 A, an increase in the % Sub-G1 cells is evident from 4 hours in toxin A-treated Caco-2 cells when compared with control cells, the increase in sub-G1 events becoming more prominent from 24 h onwards and significant increase noted at 72 h [mean toxin 46.76% (±SEM 7.36) vs control 12.32% (±2.81) $p<0.05$]. In contrast, and as would be expected from above findings, the % of sub-G1 events in toxin A-exposed HT29 cells was similar to control (untreated) cells until 72 h, when a significant increase was noted when compared with control cells [toxin 23.04% (±5.15) vs control 7.97% (±1.53) $p<0.05$], see Figure 3-9 B.

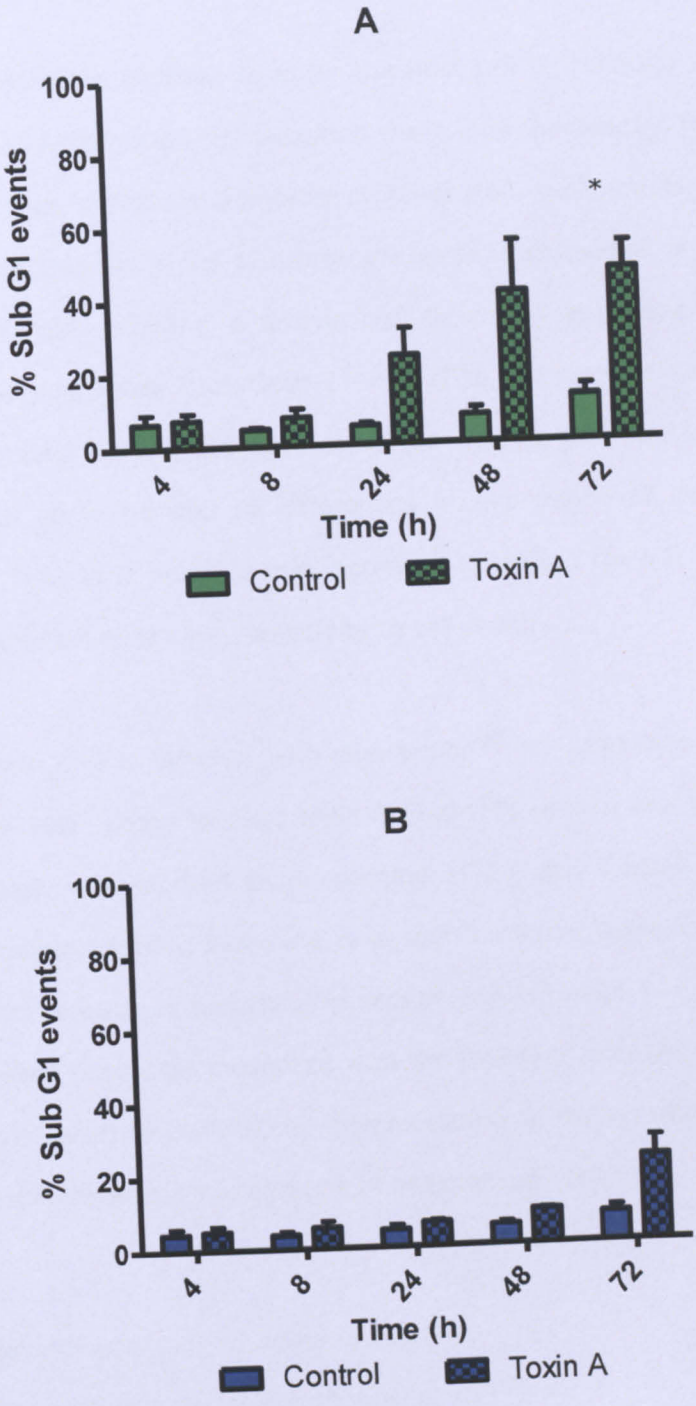

Figure 3-9 DNA analysis of Propidium iodide stained Caco-2 and HT29 cells incubated with *C. difficile* toxin A, 100 ng/ml

Assessment of Caco-2 (A) and HT29 (B) sub G1 region of the cell cycle following exposure to toxin A for 48 h or 72 h. Percentage of sub-G1 events calculated using total events and number of events in the sub-G1 region when analysed using Cylchred. Data in figures represent mean (±SEM) of 3 experiments performed in triplicate.

3.4.5.1 Uptake of toxin A ($TcdA^{488}$) is similar in intestinal epithelial cells

C. difficile toxins are believed to enter the host cell by receptor mediated endocytosis and following internalization the toxins inactivates Rho family of small GTPases, which are eukaryote switches that modulate downstream signalling. Inactivation of the Rho proteins leads to disruption of the actin cytoskeleton, cell rounding and eventual death by apoptosis. It can therefore be postulated that Caco-2 and HT29 cell specific sensitivities occur as a result of differing abilities of the cells to take up/ internalise toxin (which could be due to differences in expression of cell surface receptors). Thus, it is possible that increased uptake of toxin A by Caco-2 cells could explain its greater sensitivity to cell death.

Purified toxin A was labelled with AlexaFluor^{488} as described in section 3.3.4, page 108. Using labelled toxin A ($TcdA^{488}$) uptake and subsequent internalisation was studied by incubating HT29 and Caco-2 cells with $TcdA^{488}$ or control media; fixing the cells with formaldehyde and measuring emitted fluorescence as described in section 3.3.4.5 page 111. Cytospins were prepared from cells incubated with the labelled toxin and fluorescent micrographs taken to confirm the internalisation of the labelled toxin, see Figure 3-12 Fluorescent micrographs of internalised $TcdA^{488}$.

3.4.5.2 Biological activity reduced in $TcdA^{488}$

In view of the possibility that toxin labelling may affect its biological activity, the ability of AlexaFluor^{488} labelled toxin A ($TcdA^{488}$) to induce cell death in Caco-2 and HT29 cells, was compared with unlabelled toxin A (see section 3.3.5.1, page 113).

As previously demonstrated, at concentrations $\geq$1000 ng/ml toxin A (TcdA) induced a significant reduction in the mitochondrial dehydrogenase activity in Caco-2 cells, but not HT29 cells, see Figure 3-10 A & B. Whilst the labelled toxin exerted a similar effect on the Caco-2 cells, a significant reduction in mitochondrial dehydrogenase activity was only seen at 10 000 ng/ml (Figure 3-10 A) suggesting that the labelling process may have reduced the biological activity of the toxin.

In order to have the greatest probability of detecting differences (between Caco-2 and HT29 cells) in uptake of $TcdA^{488}$ it was decided to expose them to 5 000 ng/ml and 10 000 ng/ml labelled toxin A for up to 24 h.

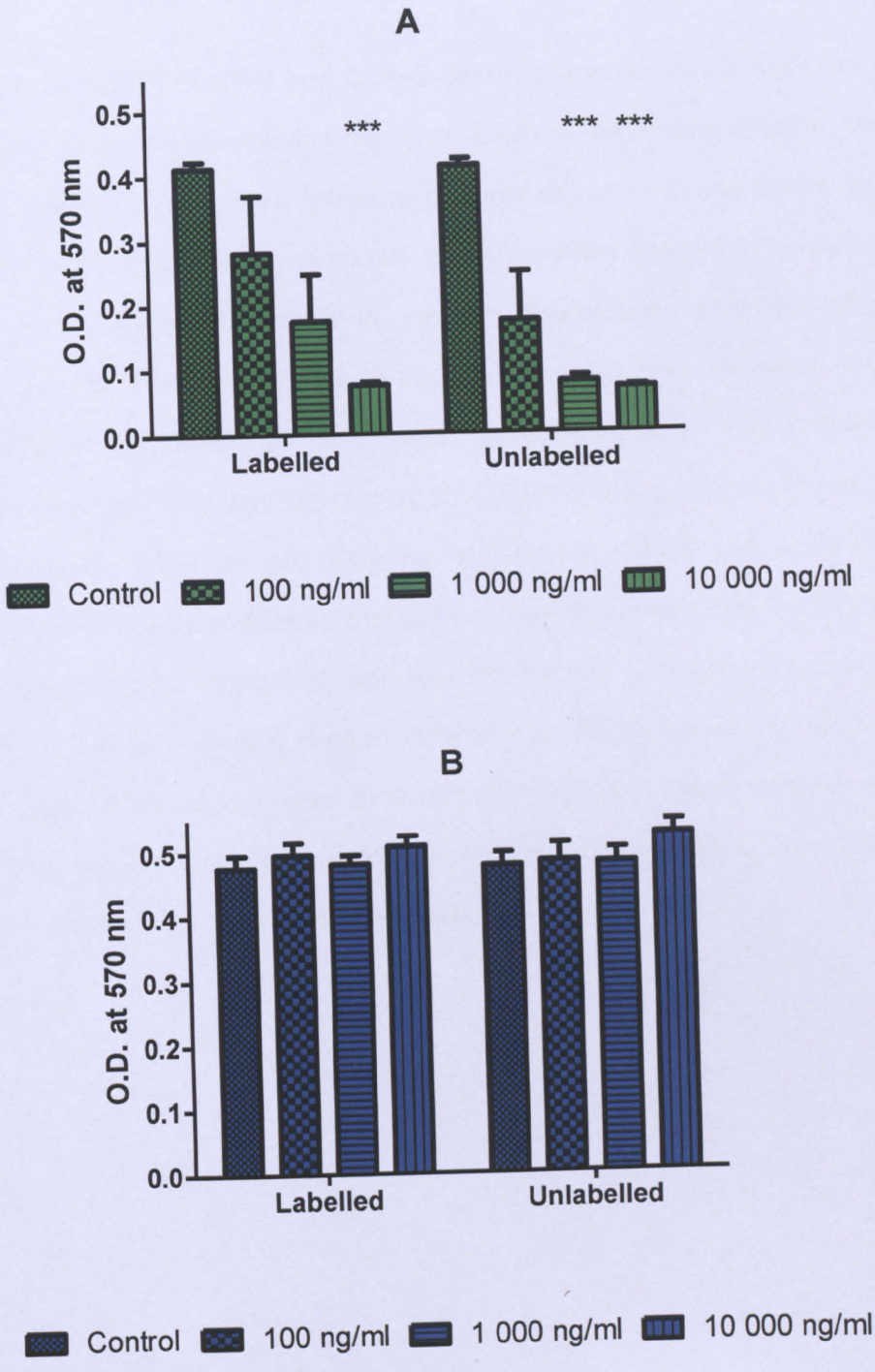

Figure 3-10 Mitochondrial dehydrogenase activity (MDA) in Caco-2 and HT29 cells to *C. difficile* toxin A and TcdA^{488}

Assay for mitochondrial dehydrogenase activity (expressed as OD 570 nm) in Caco-2 (A) and HT29 (B) cells exposed to either labelled toxin A (TcdA^{488}) or unlabelled toxin A (TcdA) for 48 h to compare biological activity. Data in figures represent mean (±SEM) of 3 experiments performed in triplicate. *** $p = 0.005$ when compared with control

3.4.5.3 *Internalisation of TcdA^{488} by Caco-2 and HT29 cells*

Uptake of TcdA^{488} in HT29 and Caco-2 cells occurred in a time dependent manner, as can be observed in the representative histograms detailing the mean median fluorescence intensity of three separate experiments, see Figure 3-13. Considering the uptake and subsequent internalisation, there was no significant difference in medium fluorescence intensity when corrected for auto-fluorescence in Caco-2 and HT29 cells incubated with identical concentrations of TcdA^{488}, see Figure 3-11 A & B. With evidence to suggest that the toxin is entering the cell and the subsequent median fluorescence intensity not differing significantly when the cells are compared it can be postulated that the cell-specific sensitivities may not be attributable to the amount of toxin entering the cell. Our previous findings suggest a significant and marked difference in the responses by the two cell types following exposure to *C. difficile* toxin A. Taken together the findings suggest that the disparity in toxin induced cell death in Caco-2 and HT29 cells may be due to an intracellular mechanism.

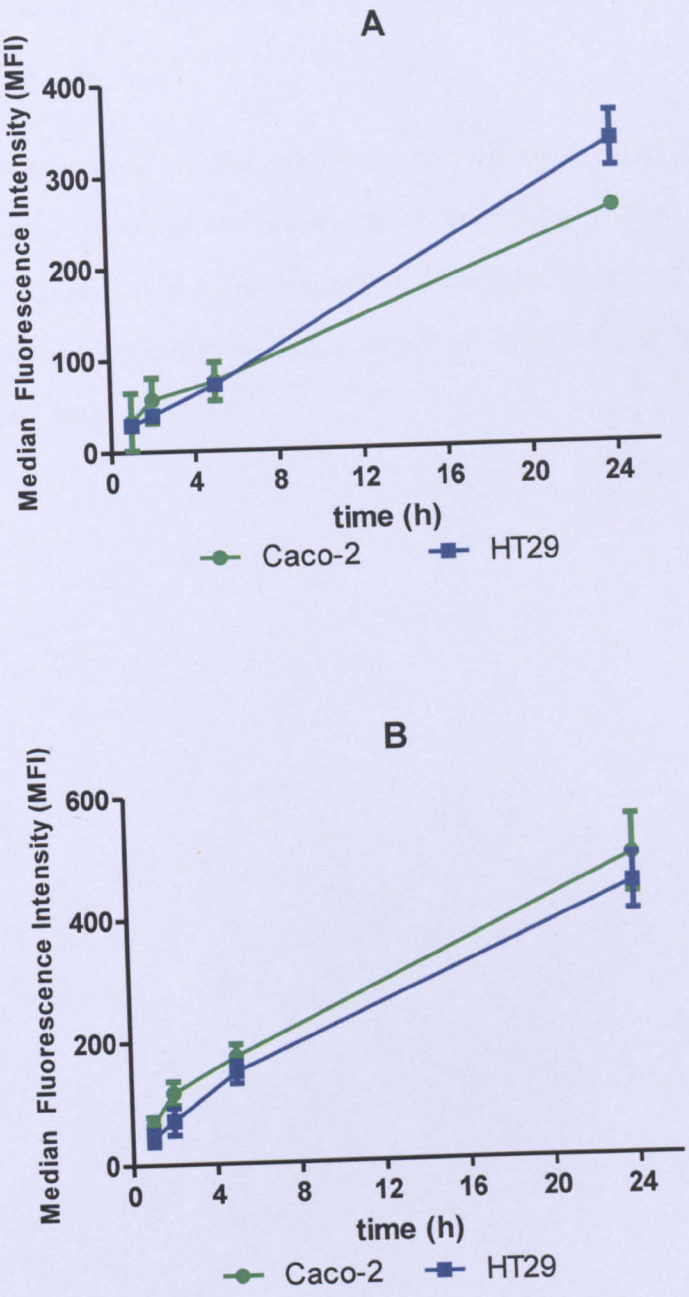

Figure 3-11 Median Fluorescence Intensity (MFI) of Caco-2 and HT29 cells incubated with TcdA^{488}

Median fluorescence intensities (MFI's) of Caco-2 and HT29 cells exposed to 5,000 ng/ml (A) and 10,000 ng/ml (B) of fluorescently-labelled toxin A for 1, 2, 5 and 24 h. MFI was calculated after subtracting auto-fluorescence in cells cultured in control medium only. Data presented as mean (±SEM) of 3 experiments

3.4.5.4 Cytospin preparation and fluorescent Microscopy confirmed toxin internalization

Fluorescence emitted by the cells when corrected for auto-fluorescence was as a direct result of the labelled toxin being internalized. This can as can be visualised in the fluorescent micrographs taken from cytospins prepared following incubation with 10µg/ml of $TcdA^{488}$ for 24 hours (Figure 3-12, page 136).

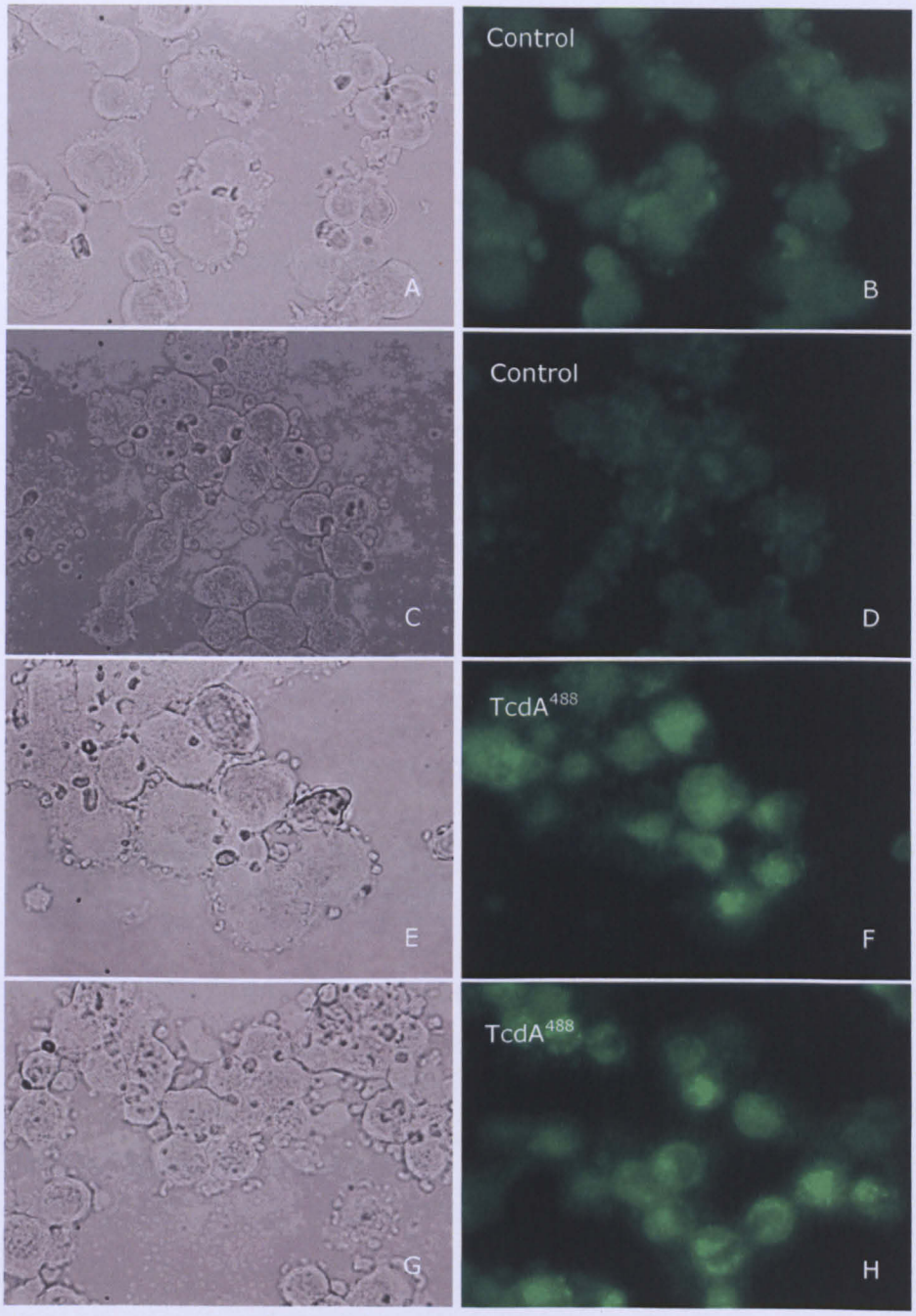

Figure 3-12 Fluorescent micrographs of internalised TcdA^{488}

Phase contrast and corresponding fluorescent micrographs of Caco-2 (A&B, E&F) and HT29 (C&D, G&H) cells cultured for 24 h in the absence or presence of fluorescently-labelled toxin A (10,000 ng/ml). After washing and detachment, cytospin preparations of the cells were studied by phase contrast and fluorescence microscopy. A greater intensity of fluorescence is visible in cells exposed to labelled toxin A, compared to auto-fluorescence displayed by controls cells cultured in medium only.

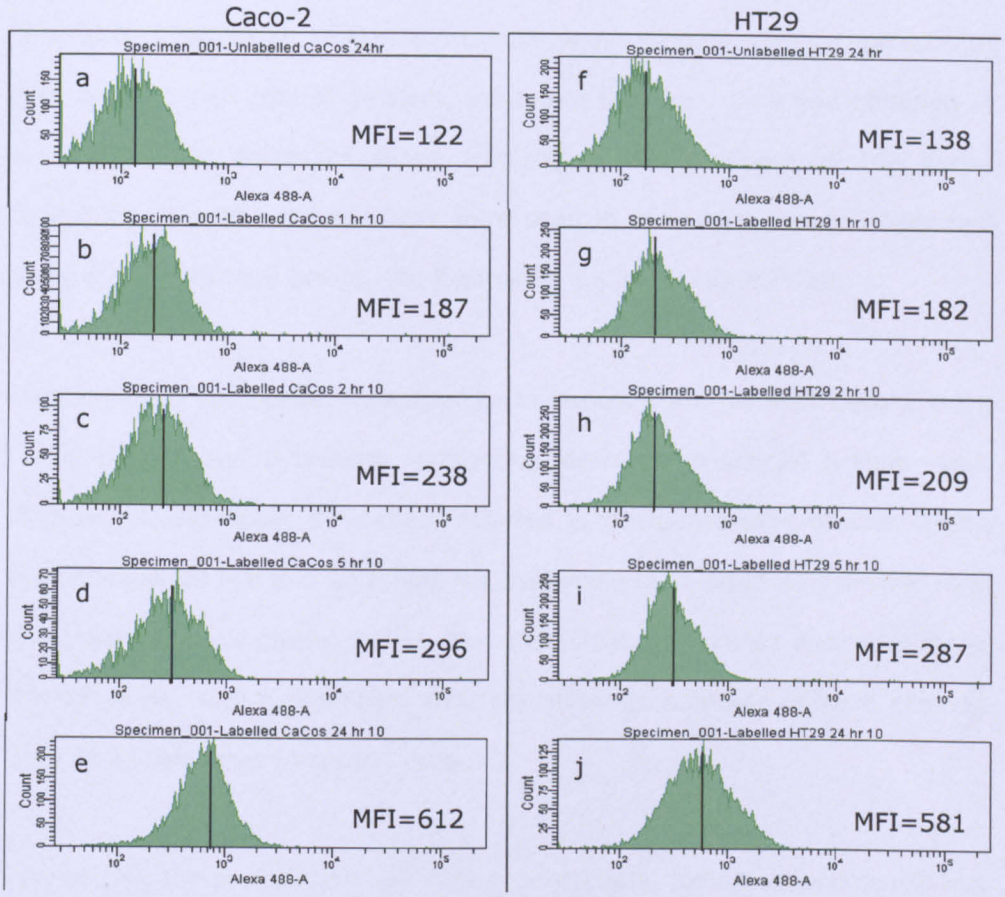

Figure 3-13 Representative histograms of Median Fluorescence Intensity (MDI) of Caco-2 and HT29 cells incubated with TcdA^{488}

Representative histograms of Caco-2 (a-e) and HT29 cells (f-j) incubated with 10,000 ng/ml of labelled *C. difficile* toxin A (TcdA^{488}) for 1 h (b&g), 2 h (c&h), 5 h (d&i) and 24 h (e&j) or control medium (a&f). MFI – median fluorescence intensity is presented as mean (±SEM) of 3 experiments.

3.4.6 Role of epithelial cell cycle in susceptibility to *C. difficile* toxin A induced cell death

Studies were undertaken to determine whether certain phases of the cell cycle are under- or over-represented at various time points following exposure to *C. difficile* toxin A. For these studies, cell cycle analysis was performed by flow

cytometry at 4 h, 8 h, 24 h, 48 h and 72 hours after exposure to toxin A as described in Chapter 2, section 2.7.3. Toxin-exposed cells were compared with cells cultured with control medium, seeded at the same time and obtained at the same time points as those cultured in the presence of the toxin. Statistically significant differences were seen in individual phases of the cell cycle at different time points, see Figures 5a-e Caco-2; 6a-e HT29.

Comparison of cell cycle profiles of toxin exposed and control Caco-2 cells, Figure 3-14 A and B provide contrasting views up to the 24 h time-point. However, a significant difference recorded in the percentage of cells in the G0/G1 region at 4 h and 24 h was not supported by a significant difference in any other cell cycle phase until at 72 h a significant difference was recorded in the G2 phase, with a significant reduction in the percentage of toxin exposed cells when compared to control cells.

Considering the profiles of HT29 cells in control and toxin exposed conditions, a similar contrasting profile is visible up to 24 h with cells incubated in the control medium leaving the G0/G1 phase up to 24 h and the toxin exposed cells appearing to stop cycling, with minimal movement evident in the cell cycle phases, as can be viewed in Figure 3-15. This is supported by a significant increase in the number of toxin exposed HT29 cells in the G0/G1 region and a significant reduction in the corresponding toxin exposed HT29 cells in the S-phase when compared against untreated cells.

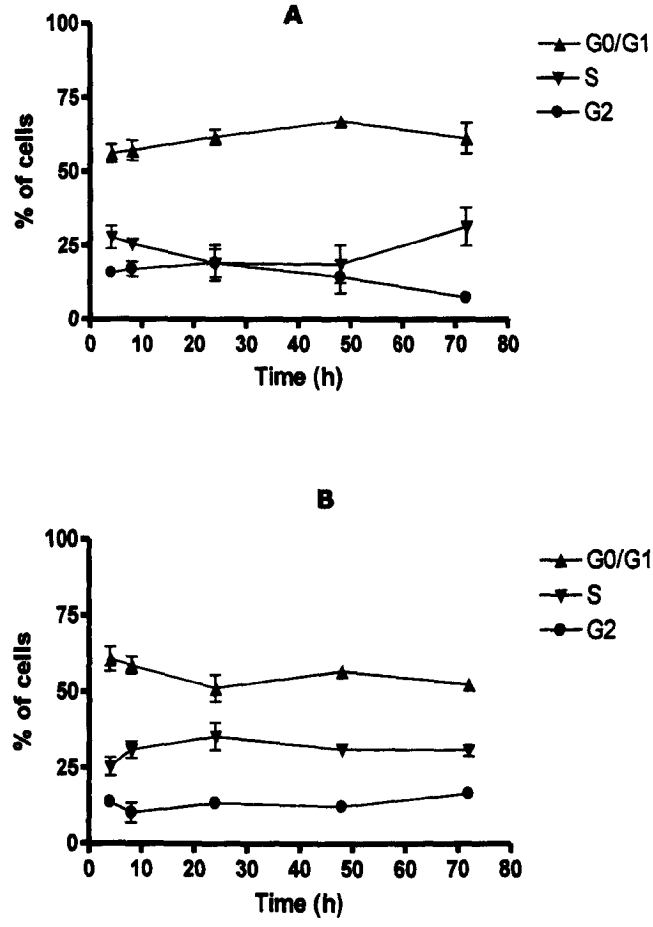

Figure 3-14 Whole cell cycle analysis of Caco-2 cells incubated with *C. difficile* toxin A (100 ng/ml)

Using PI stained Caco-2 cells incubated with 100 ng/ml of *C. difficile* toxin A (A) or control medium (B) for 4 h, 8 h, 24 h, 48 h and 72 h, the cells were sorted using FACS and the resulting scatterplot gated to remove debris. Using only the gated events the percentage of cells in each phase of the cell cycle was calculated using Cyclhred. Data presented as % (± SEM) of cells in G0/G1, S and G2 phase n=3. This data reflects viable cells only and does not reflect the cells lost to cell death

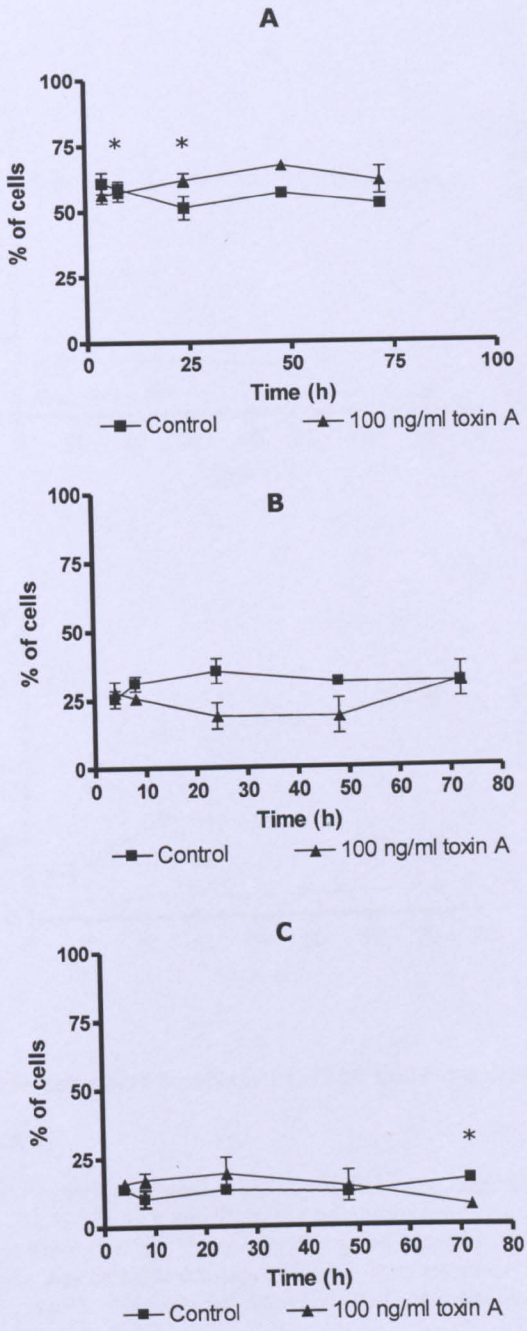

Figure 3-15 Individual phase cell cycle analysis of Caco-2 cells incubated with *C. difficile* toxin A (100 ng/ml)

Percentage of Caco-2 cells in G0/G1 (A) S-phase (B) and G2 (C), comparison of toxin treated and control cells at 4, 8, 24, 48 and 72 h. Data presented as % ± SEM n=3 *=p=<0.05 PI stained cells were sorted using FACS and the resulting scatterplot gated to remove debris. Using only the gated events the percentage of cells in each phase of the cell cycle was calculated using Cyclhred. This data reflects viable cells only and does not reflect the cells lost to cell death

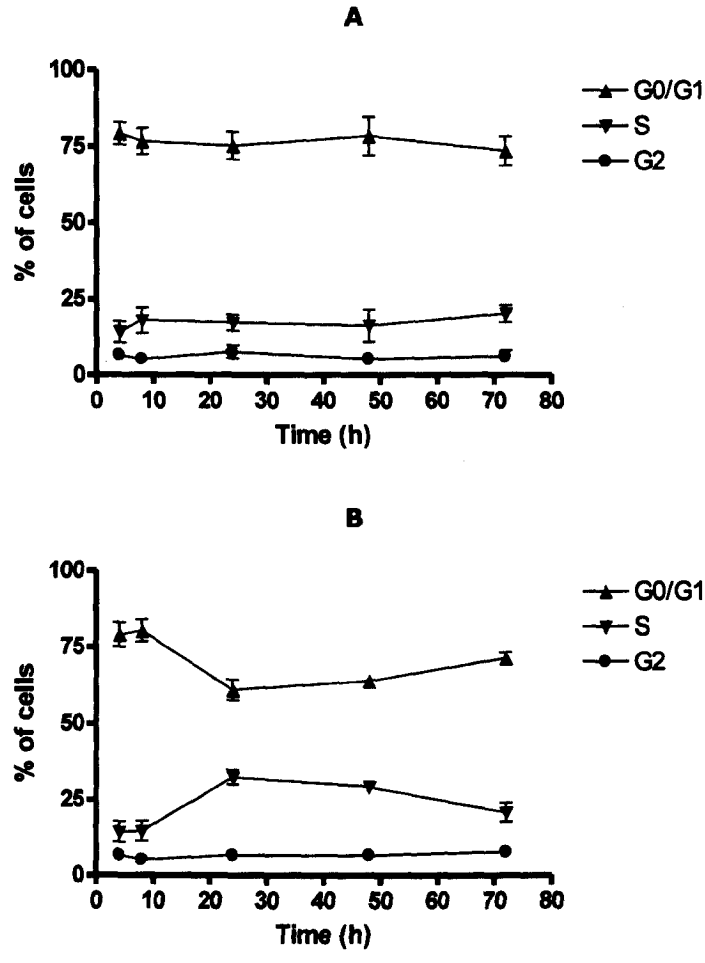

Figure 3-16 Whole cell cycle analysis of HT29 cells incubated with *C. difficile* toxin A (100 ng/ml)

Using PI stained HT29 cells incubated with 100 ng/ml of *C. difficile* toxin A (A) or control medium (B) for 4 h, 8 h, 24 h, 48 h and 72 h, the cells were sorted using FACS and the resulting scatterplot gated to remove debris. Using only the gated events the percentage of cells in each phase of the cell cycle was calculated using Cyclhred. Data presented as % (± SEM) of cells in G0/G1, S and G2 phase n=3. This data reflects viable cells only and does not reflect the cells lost to cell death

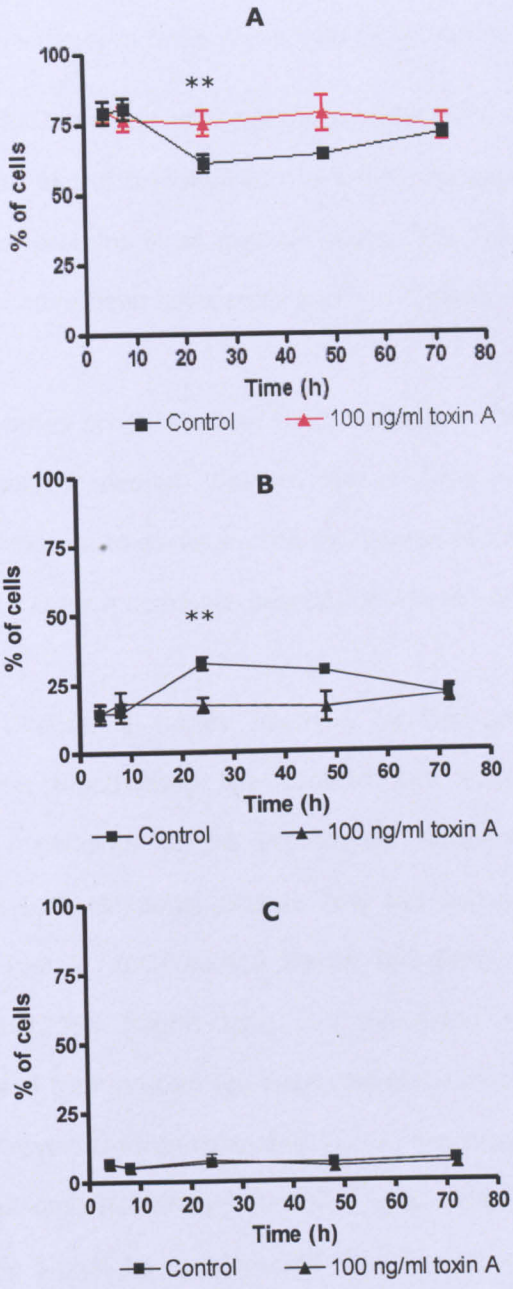

Figure 3-17 Individual phase cell cycle analysis of HT29 incubated with *C. difficile* toxin A (100 ng/ml)

Percentage of HT29 cells in G0/G1 (A) S-phase (B) and G2 (C), comparison of toxin treated and control cells at 4, 8, 24, 48 and 72 h. Data presented as % ± SEM n=3 **=p=<0.01 PI stained cells were sorted using FACS and the resulting scatterplot gated to remove debris. Using only the gated events the percentage of cells in each phase of the cell cycle was calculated using Cyclhred. This data reflects viable cells only and does not reflect the cells lost to cell death

3.4.7 Substrate specificity in toxin A exposed intestinal epithelial cells

Rho, Rac-1 and Cdc42 are the intracellular targets for *C. difficile* toxins and utilizing UDP-glucose as the co-substrate the toxins are capable of maintaining these key molecular proteins in an inactive state. The mechanisms that lead to their inactivation have been covered in detail in Chapter 1.

Using whole cell lysates prepared from HT29 and Caco-2 cells incubated with either toxin A or control medium Western Blot analysis was completed using protein specific antibodies to ascertain the expression of Rac-1 and Rho A, see Chapter 2, section 2.8 for a complete description of methods used.

As discussed in Chapter 1 toxins released by the bacterium *C. difficile* glucosylate, therein inactivating the protein and disrupting downstream signalling. This is believed to be irreversible modification. The Rac-1 (MAB3735, Mouse IgG, Millipore) detects only the non-glucosylated (active) protein, whereas Rho A (26C4:sc-418 Mouse IgG Santa Cruz Biotechnology Inc.) and Rho B (2098 Rabbit IgG, Cell Signalling Technology) detects endogenous levels of total protein (glucosylated and non-glucosylated). It has been reported however, that glucosylated Rho A is promptly degraded by the intracellular proteasome (Genth, Huelsenbeck et al. 2006) and therefore it is presumed that the signal being identified from the Rho A antibody is non-glucosylated (active) Rho A.

As can be seen in Figure 3-18, a reduction in non-glucosylated Rac-1 expression can be observed from as early as 3 hrs in both cell types when

compared to the control (untreated) lysate at 0 h. This loss continued through to 48 h.

Total RhoA (glucosylated and non-glucosylated) expression in toxin treated Caco-2 cells remained consistent when compared to the control (untreated) cell lysate at 0 h. The consistent expression of Rho A in toxin treated Caco-2 cells was still evident after 24 h. In contrast, a slight reduction in Rho A expression in toxin treated HT29 cells was evident at 3 h and further reductions were noted at 8 h, 24 h and 48 h when compared to control (untreated) cell lysate at 0 h.

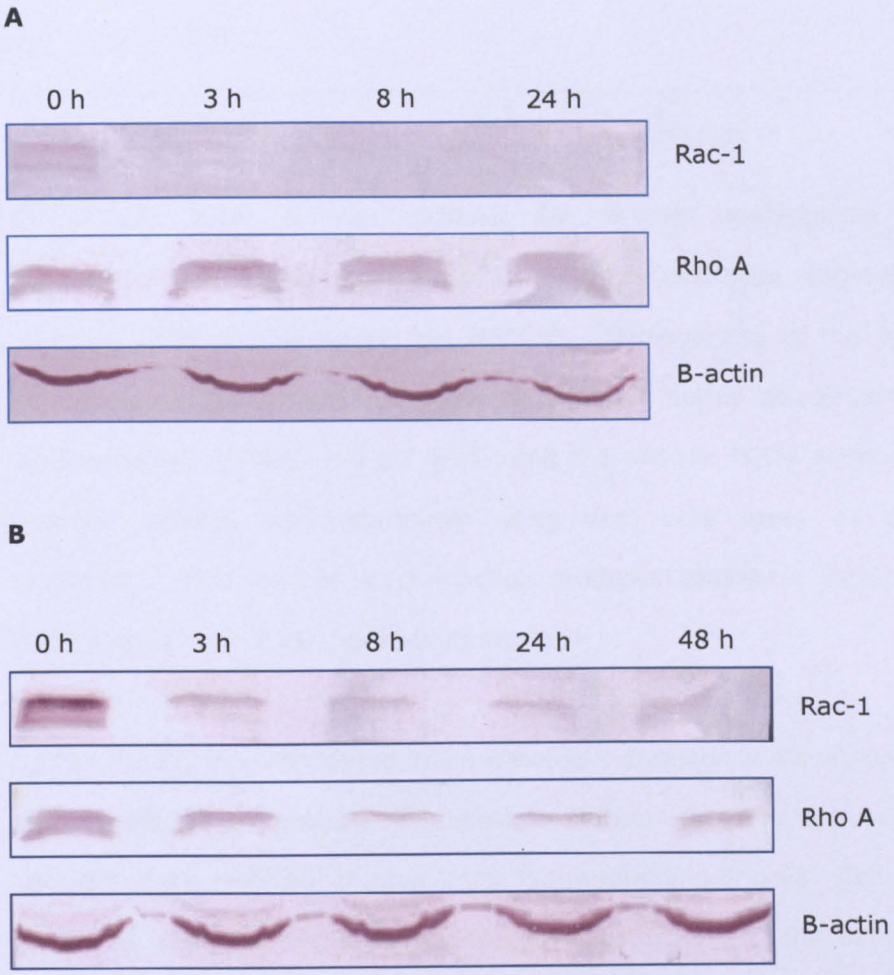

Figure 3-18 Expression of Rac-1, RhoA and beta-actin in control and C. difficile toxin A exposed Caco-2 (A) and HT29 (B) cells

Intestinal epithelial cell monolayers were cultured in medium only (0 h) or in the presence of 1,000 ng/ml toxin A for 3 h, 8 h, 24 h and 48 h (in HT29 cells only). Lysates of cells were electrophoresed on SDS-PAGE gels and following transfer onto PVDF membranes, immunostaining was performed using antibodies specific for RhoA, beta-actin or non-glucosylated form of Rac1. Equal loading of the lanes is illustrated by beta-actin-immunoreactive bands of similar size. The figures are representative of five experiments.

3.5 Discussion

3.5.1 Purification and Characterisation of *C. difficile* toxin A

C. difficile toxin A was purified by bovine thyroglobulin affinity chromatography followed by two sequential anion exchange chromatography steps on DEAE Sepharose FF and Mono Q. Homogeneity of the toxin was confirmed by the presence of a single band on native polyacrylamide gel electrophoresis (PAGE) and dot blot using the specific PCG4 antibody. The cytotoxic activity was determined using Vero cells assay as described previously. This method of purification produces consistent yields of pure toxin ranging from 0.06 mg/ml-2.33 mg/ml.

As has already been discussed, toxin A exerts a dramatic effect on mammalian cell morphology. Perhaps the most important of these alterations and considered the hallmark of intoxication is the rounding of cells. Cell rounding occurs in response to the toxin entering the target cell and subsequently inactivating Rho, Rac and Cdc42, small GTPases pivotal in ultra-structure maintenance and downstream signalling.

This chapter looked at the response of two human intestinal epithelial cell lines exposed to varying concentrations of toxin A. Caco-2 cells (colonic epithelial adenocarcinoma cell line), phenotypically similar to mature enterocytes (Sambuy, De Angelis et al. 2005) and HT29 cells (colonic epithelial adenocarcinoma cell line) were cultured to confluence and exposed to a range of the toxin A concentrations (10000 - 0.1 ng/ml).

Visible cell rounding was first noted just 1 hour after Caco-2 cells were exposed to ≥1000 ng/ml of toxin A. Cell rounding in HT29 was also visible 1 hour after exposure, although only at the highest of concentrations; 10,000 ng/ml. A similar pattern of responses was noted throughout the experiment suggesting that cell rounding occurred in a time- and dose- dependent manner with no major difference in morphological change observed in Caco-2 and HT29 cells.

Another important observation made during this study involved the integrity of the cell monolayers. The integrity of both monolayers were observed at given time-points and whilst the Caco-2 monolayers appeared disrupted within the first 24 hours, particularly at concentrations ≥100 ng/ml, HT29 monolayers remained intact throughout, even after 72 hour exposure at the highest concentrations. These observations will be discussed in more detail alongside cellular viability.

To establish cell viability and cytotoxicity of a given entity on the host it has been suggested that multiple methods be employed, each of which considering a different mechanism or feature of cell death (Galluzzi, Aaronson et al. 2009). With this in mind the cellular viability of Caco-2 and HT29 cells to *C. difficile* toxin A was investigated using the MTT assay; trypan blue exclusion assay; propidium iodide staining of DNA content and visual inspection using light microscopy.

Metabolic activity was investigated using the MTT assay and the ability of metabolizing cells to cleave the soluble tetrazolium salt and thereby producing

insoluble purple formazan crystals that when solubilised could be quantified spectrophometrically .

Caco-2 cell monolayers treated with a range of toxin A concentrations resulted in a time and dose dependent reduction in mitochondrial dehydrogenase activity. Mitochondrial dehydrogenase activity is reported to be a direct reflection of cellular viability (Mosmann 1983). These findings mirror observations reported previously (Mahida, Makh et al. 1996) and have also been reported in studies considering the effects of *C. difficile* toxin A on cells within the lamina propria (Mahida, Galvin et al. 1998).

Mitochondrial dehydrogenase activity was significantly reduced in toxin treated Caco-2 cells (0.1774 ±0.0418 and 0.1266 ±0.0333), 100 ng/ml and 1000 ng/ml respectively (mean ± SEM p=<0.001) after 48 hours when compared with untreated control cells (0.3527 ±0.0439). By 72 hours, a further reduction was observed at concentrations ≥100ng/ml (0.1274 ±0.0298 and 0.1021 ±0.0280) 100 ng/ml and 1000 ng/ml respectively, when compared with control (untreated) cells (0.3722 ±0.0440) (mean ±SEM p=<0.01).

In contrast, only a very small reduction in cell viability was observed in HT29 monolayers at 48 hours and 72 hours using ≤1000 ng/ml cell viability.

Investigations using 10,000 ng/ml confirmed my previous findings with mitochondrial dehydrogenase activity in Caco-2 cells significantly reduced when treated with toxin A and HT29 cells showing no significant reduction.

The dramatic reduction observed in Caco-2 cells and the minimal effect of toxin A observed in HT29 cells was supported by the use of an additional viability assay. Using the trypan blue exclusion assay, the percentage of viable cells was calculated, as previously discussed. The trypan blue assay supported my earlier findings and suggests that the MTT results were an accurate reflection of cell viability.

The MTT assay and trypan blue exclusion assay were further supported by cell cycle analysis of cells exposed to toxin A. Using propidium iodide staining the DNA content in cells was measured using FACS and the percentage events in the sub-G1 region established. A time dependent increase in the % sub G1 events was evident in Caco-2 cells becoming statistically significant by 72 h ($p<0.05$). Of interest, a significant increase in % sub G1 events was also reported in HT29 cells when compared with control (untreated) cells ($p<0.05$).

To summarize, *Clostridium difficile* toxin A exerts a cell specific effect, in which Caco-2 display greater susceptibility than HT29 cells.

These early findings raised a number of questions and perhaps the most pertinent at this stage are; i) Why are Caco-2 cells more sensitive to toxin A and/or why are HT29 cells more resilient?; and ii) are the mechanisms that result in cell death and cell rounding temporally distinct in these cell lines?

The sensitivities of Caco-2 have been commented upon previously; Mahida and colleagues found that Caco-2 cells were more sensitive than T84 (epithelial cell line) cells, detaching earlier and presenting an early decline in mitochondrial dehydrogenase (Mahida, Makh et al. 1996). In this same study,

Mahida proposed the following sequence of events resulting from the intoxication of confluent epithelial cell lines with *C. difficile* toxin A; cell rounding, detachment of the monolayer from the matrix coating (pseudo basement membrane) and subsequently death by apoptosis (Mahida, Makh et al. 1996). This sequence of events has been developed over the past 11 years however the pathway to apoptosis induced by *C. difficile* toxin A and the reasons for the specific sensitivities to *C. difficile* toxins still remains largely undefined.

The toxin enters the target cell by receptor mediated endocytosis and a possible explanation for the differential rounding patterns and cell viability seen in the two cell lines may be explained by the ability of the target cell to internalize the toxin. Tucker and colleagues reported cells expressing large volumes of the tri-saccharide receptor were more susceptible to the cytopathic effects of toxin A (Tucker, Carrig et al. 1990).

Using fluorescently labelled toxin A, internalisation of the toxin by HT29 and Caco-2 was investigated. Labelling the toxin reduced some of the original bioactivity and therefore higher concentrations were used to maximise the response. Studying the response of Caco-2 and HT29 to 5,000 ng/ml and 10,000 ng/ml of $TcdA^{488}$, cells were exposed for various periods of time. The successful internalisation of the labelled toxin was shown in cytospin preparations and extracellular labelled toxin excluded as a possible effect on our results. Toxin uptake was dose and time dependent in both cell types, with no obvious saturation evident at the concentrations and timescales used. Comparison of the two cell types failed to establish a significant difference in

the amount of toxin being internalised and can therefore not be used to explain the cell specific differences attributed to toxin A.

The cell rounding caused by the inactivation of Rho, Rac and Cdc42; the subsequent detachment from the basement membrane and cell death are suggested to be temporally distinct events. However, a number of studies have looked at the pathways to apoptosis induced by *C. difficile* toxin A, some argue that the inactivation of Rho results in the activation of caspases and thus induces apoptosis (Hippenstiel, Schmeck et al. 2002); some argue that apoptosis is independent of this activation and have identified a caspase independent mechanism (Carneiro, Fujii et al. 2006) and to confuse the issue further; others claim that both Rho inactivation and caspase independent signalling facilitate apoptosis in cells exposed to *C. difficile* toxin A. It may be that the pathway to apoptosis is also cell specific.

Caco-2 cells rounded slightly earlier than HT29 cells, but a significant disparity has been found in the ability of toxin A to induce cell death in Caco-2 cells but not in HT29 cells. As we have shown no difference in the amount of toxin being taken into the cell then intracellular processing may provide the explanation. The early loss of monolayer integrity observed in Caco-2 cells would support the early loss of the regulatory switch, Rho. What remains to be ascertained is whether the dramatic decrease in cell viability was the result of the cell rounding and detachment from the basement membrane or mediated by other independent signalling mechanisms i.e. caspases.

Once inside the target cell, toxin A exerts it effect by inactivating a number of small GTPases, namely Rho, Rac-1 and Cdc42. These proteins are key

molecular switches that regulate various different pathways and functions within the cell. A number of studies have suggested that substrate specificity may be cell specific. A recent study has shown that inactivation of Rho A (but not Rac-1) is required to induce cell death in response to *C. difficile* toxin B in basophilic leukaemia cells (Huelsenbeck, Dreger et al. 2007). It is possible therefore that toxin A induces greater inactivation of Rho A in Caco-2 cells than HT29 cell. Other studies, (Fritz and Kaina 2001) and (Liu, Cerniglia et al. 2001) suggest that RhoB, which is negatively regulated by RhoA, is the main regulator of cell death.

I therefore postulate that the target substrates for *C. difficile* toxin A in Caco-2 and HT29 cells may be different. My initial plan was to investigate the expression of RhoA, RhoB and Rac-1 in toxin exposed cells but after months of optimisation, investigation of Rho B was abandoned due undetectable RhoB concentration levels in the cell types under investigation. The RhoB antibody was shown to be active, and specific binding to RhoB expressed in control lysates (mouse brain) was shown using Western Blot analysis. Analysis of Rho expression was therefore limited to Rac-1 and RhoA.

As would be expected and in line with cell rounding a reduction in non-glucosylated Rac-1 was apparent in both cell types from 3 hr and continued to reduce to 72 h. The similarity in cell rounding; loss of non-glucosylated Rac-1 in response to *C. difficile* toxin A is in stark contrast to the viability of Caco-2 and HT29 cells. This disparity would suggest that Rac-1 is associated with morphological changes that result in cell rounding but not cell death. The expression of RhoA in Caco-2 cells remained consistent throughout with no reduction in expression. In contrast, expression of RhoA in HT29 cells is

shown to reduce slightly from 3 hr and this reduction continues through to 72 h. These findings further support a cell specific response but contradict our earlier suggestion that RhoA may regulate cell death, if this was so we would have expected a reduction in Rho A expression in Caco-2 cells but not in HT29 cells.

Rho proteins are linked with many biochemical and biological functions within the host cell; one of which being the cell cycle and more specifically G1 progression and mitosis (Jaffe and Hall 2005). A recent study (Nottrott, Schoentaube et al. 2007) suggests that cells in G0/G1 phase of cell cycle may be more sensitive to toxin A-induced cell death. Using propidium iodide staining we investigated the cell cycle phases in toxin exposed and control cells using a dedicated cell cycle programme, CycIhred to elicit any cell specific sensitivities. Whole cycle profiles show an increase in G0/G1 cells in Caco-2 cells until 48 hrs (a significant increase being reported at 4 and 24 h) and this appears mirrored by a decrease in S-phase cells. This would suggest that G0/G1 cells may not be progressing into S-phase or not leaving G0/G1. As would be expected a decrease in S phase cells would indicate a progression through to G2 and this is shown by an increase in G2. From 24 h onwards a steady decline in G2 cells is reported. However by 48 h the events in the G0/G1 region are declining and S-phase events are increasing – suggesting that progression previously delayed or halted is now occurring. As would be expected Caco-2 whole cycle profiles from control cells show a progression from G0/G1 into S, with a decrease in G0/G1 and an increase in S phase events and as the S-phase decreases an increase in G2 is noted. Of interest however is, despite the simultaneous increase in S-phase events a significant reduction in G2 events in toxin exposed cells is reported and suggests that the

cells may not be progressing through S-phase or are not passing the G2 checkpoint by 72 h. It is therefore possible that Caco-2 cells are more sensitive in the G0-GI phase evidenced by their lack of progression into S-phase. This would not however be true in HT29 cells incubated with toxin A; these cells also appear to remain in G0/G1 phase when compared with control profiles. A very small decrease in G0/G1 events is seen between 4-8 hours and this is correlated by an increase in S-phase events however there would appear to be limited movement of G0/G1 into S-phase events from 8 h. By 24 h a significant difference in the percentage of G0/G1 and S-phase events is recorded, with a significant increase in G0/G1 cells and a significant decrease in S-phase cells when compared with control.

Whilst a significant difference is not evident at all time-points, cell cycle progression is fluid and whilst progression may be delayed in toxin treated cells the control cells will be proliferating as normal and progressing through all stages of the cell cycle.

To summarize, this chapter has described the response of two intestinal epithelial cell types to varying concentration of purified toxin A. In doing so, it has been established that Caco-2 cells are more sensitive to toxin induced cell death. Investigations to elucidate the reasons for this cell specific sensitivity initially considered a possible difference in the uptake of the toxin into the cell. The incubation of cells with identical concentrations of fluorescently labelled toxin A for various time points failed to provide a explanation. Both cells internalised the toxin at a similar rate with no significant difference evident. Looking for an intracellular explanation, expression of RhoA and Rac-1, two of the key GTPases inactivated in target cells were investigated. Using whole cell

lysates from cells incubated with either toxin A or control medium Western Blot analysis established a time dependent loss of non-glucosylated Rac-1 in both cell types. RhoA expression in Caco-2 cells remained constant following incubation with toxin A, however a slight time dependent loss of RhoA occurred in HT29 cells incubated with toxin A. The cell cycle is regulated by Rho proteins and consideration of cell cycle progression was also investigated with some interesting findings.

CHAPTER 4

4 Establish methodology for purification of toxin B

4.1 Introduction

Toxin B is designated a cytotoxin (Tucker, Carrig et al. 1990) and whilst the molecular weight has been reported to range from 50-300 kDa, DNA sequence determination shows the molecular mass to be 270 (kDa) (Barroso, Wang et al. 1990; von Eichel-Streiber, Laufenberg-Feldmann et al. 1990). The amino acid sequence of the toxins A and B shows some 63% homology (von Eichel-Streiber, Laufenberg-Feldmann et al. 1990; von Eichel-Streiber, Laufenberg-Feldmann et al. 1992). Despite this similarity, significant differences are evident.

Having successfully purified *C. difficile* toxin A and after completing experiments on both intestinal epithelial cells and primary intestinal myofibroblasts and establishing some very interesting responses, my interest naturally turned to the possible response of these cells to *C. difficile* toxin B. Would I observe a similar cell specific response? Whilst *C. difficile* toxin B can be purchased as a lyophilized powder, it is expensive and given the variability in cytotoxic activity noted by others (Banno, Kobayashi et al. 1984; Mitchell, Laughon et al. 1987) it may not reflect the same biological activity as in-house toxin B purified from the reference strain used in the toxin A purification. In addition, in-house purification of toxin B would provide a stronger starting platform for comparative studies of responses to toxin A and B. The in-house purification of toxin B has proven difficult due to the close homology and elution patterns of toxins A and B and as observed by others the persistence

of a contaminating protein that would appear to form a complex with the toxin B protein (Meador and Tweten 1988).

Aim: To successfully purify *Clostridium difficile* toxin B at sufficient yield and biological activity to permit investigations into epithelial cell and myofibroblast response to toxin B, comparative and combined (A+B) investigations.

4.2 Material and Methods

Using the most recent protocol held within the Institute, outlined in the flow diagram in Figure 4-1, several runs were completed to establish techniques and highlight problem areas. Using this protocol, *Clostridium difficile* toxin B is purified by bovine thyroglobulin affinity chromatography followed by ammonium sulphate precipitation and two sequential anion exchange chromatography steps on ready prepared DEAE Sepharose FF and Mono-Q. Homogeneity of the toxin is established on SDS polyacrylamide gel electrophoresis (PAGE) and dot blot using the specific monoclonal antibody for toxin B. Cytotoxic activity was determined using the Vero cell assay.

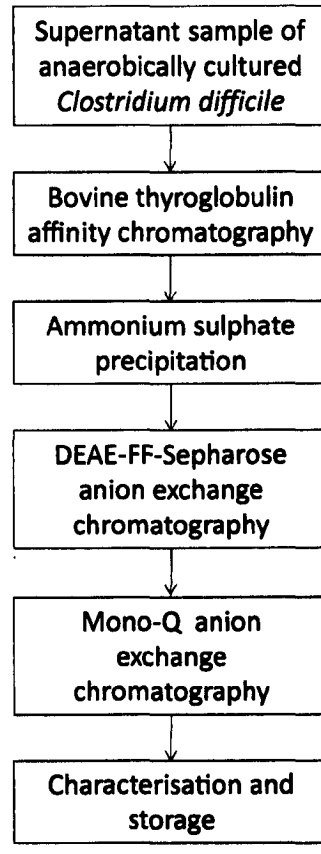

Figure 4-1 Flow diagram of current *C. difficile* toxin B purification protocol

4.2.1 Bacterial Culture

4.2.1.1 Bacterial strains

Clostridium difficile, VPI 10463 (Toxinotype 0), a widely used reference strain was chosen for this study as it expresses the genes *tcdA* and *tcdB* and produces active forms of toxin A and toxin B proteins.

4.2.2 Recovery, growth and harvesting of bacteria

As described under 'Toxin A purification', Chapter 2, 2.2 *Clostridium difficile* spores were retrieved from long-term storage; vegetative bacteria destroyed and resultant solution streaked onto blood agar plates and incubated anaerobically. Colonies isolated on blood agar were added to brain heart infusion broth, incubated anaerobically at 37°C for two days and the purity of the culture was checked by re-streaking the culture onto blood agar and the subsequent identification of pure *C. difficile* colonies. Five flasks were prepared and 5 ml of the bacterial harvest was added to each flask and incubated anaerobically at 37°C for 3-4 days. The contents of the dialysis tubing were centrifuged and the bacterial pellet removed. The remaining supernatant was syringe filtered (0.2 µm filter used) and to prevent protein degradation, the serine protease inhibitor, 4-(2-Aminoethyl) benzenesulfonyl fluoride hydrochloride (AEBSF, Sigma) was added and the supernatant samples stored at 4°C. Another five flasks were prepared as above and all the supernatant pooled prior to application to the bovine thyroglobulin column.

4.2.3 Protein purification chromatography

4.2.3.1 Bovine thyroglobulin affinity chromatography column

Using the specific binding to the carbohydrate sequence Galα1-3Galβ1-4GlcNAc found on bovine thyroglobulin, *C. difficile* toxin A is selected for and removed from the supernatant using repeated applications to the column. The column was prepared as described in Chapter 2, page 73.

As described on pages 2.3.1, the column was washed with TBS and the filtered supernatant applied to column overnight at 4 °C. Unbound supernatant was washed from the column with TBS at 4°C and the column then transferred to 37°C and allowed to warm for an hour. The toxin A bound to thyroglobulin was eluted with warm TBS and the column washed with acidic buffer and basic buffer. The process was repeated to remove as much toxin A from the supernatant sample as possible. The column was finally washed and stored.

4.2.4 Protein Precipitation using Ammonium Sulphate

The addition of salt, (<0.15M) termed 'salting in' increases the solubility of globular proteins and at higher concentrations salt solubility of the protein usually decreases leading to precipitation, termed 'salting out' (Green 1955). This theory was applied for the selective precipitation of proteins. Using the toxin A depleted *C. difficile* supernatant previously stored at 4°C, 471g/L of ammonium sulphate was added to achieve 70% saturation and the solution stirred at room temperature for 30 minutes. The solution was subsequently

centrifuged at 5000 rpm for 30 minutes and the precipitate collected. The pelleted precipitate was re-suspended in 50mM Tris buffer (pH 7.4) and 113.9g/L of ammonium sulphate was added to achieve 20% saturation. The solution was stirred at room temperature for 30 minutes and centrifuged at 5000 rpm for 30 minutes. The supernatant was kept and 160.9g/L of ammonium sulphate added to obtain 50% saturation. The solution was stirred at room temperature for 30 minutes and subsequently centrifuged at 5000 rpm for 30 minutes. The supernatant was discarded and the pellet re-suspended in 25 ml 50 mM Tris buffer (pH 7.4). To remove excess salt, the protein/Tris solution was dialysed against 50mM Tris buffer overnight at 4°C.

4.2.5 Anion-exchange chromatography

Anion exchange chromatography uses the positively charged beads inside the column to bind the negatively charged protein of choice. This ionic interaction is subsequently broken and the protein is eluted using a NaCl gradient, see Figure 2-2.

Using AKTA PK900 Purifier (GE Healthcare) two sequential anion exchange chromatography runs were completed using DEAE-Q-Sepharose (Amersham Biosciences, Uppsala, Sweden) and Mono Q columns (Amersham Biosciences).

The protocol for the purification of toxin B using the DEAE-Q-Sepharose column is identical to that for toxin A, with a linear salt gradient being used to elute the proteins. The Mono-Q protocol however, employs a linear 0-1 M salt

gradient for the purification of toxin A and a stepped 0-1 M gradient in the toxin B purification protocol.

The presence of toxin B and remaining contaminating toxin A in the eluted fractions can be confirmed by the specific binding of mouse PCG-4 monoclonal antibody to *C. difficile* toxin A and binding of specific Mab monoclonal antibody to toxin B using Vectastain Universal Elite ABC kit (Vector) and VIP Substrate kit for peroxidase (Vector). Two identical membranes were prepared, one to identify toxin A contamination and the other to confirm the presence of toxin B. The method employed was identical to that previously described on page 79 except the toxin A membrane was incubated with PCG-4 (125 µg/ml diluted 1:10) and the toxin B membrane incubated with anti-toxin B antibody (1 mg/ml diluted 1:1000). The toxin B fractions were pooled and dialysed against 20 mM Tris buffer overnight at 4°C.

The pooled fractions were syringe filtered using a 0.2 µm filter and degassed using helium. The sample was injected into the super loop and this time passed through a Mono-Q (quaternary amine, a strong anionic exchanger) column and fractions eluted using 0-1M NaCl gradient. After immuno-histochemical analysis using Dot blot as described previously, toxin B containing fractions were pooled and concentrated using centrifugal filter devices (Millipore) with a 100kDa molecular weight cut-off (MWCO) as described in section 4.2.6.1 page 164 to achieve maximum concentration.

Characterisation of the toxin B was then performed as previously described for toxin A purification. In addition western blot analysis was completed to

confirm the homogeneity of the protein sample. Results from an early representative run are shown in section 4.3.1.

4.2.6 Protein characterisation

Total protein concentration was established using the Bradford Assay.

Cytotoxicity was assessed using the Vero assay as detailed in Chapter 2, 2.4.3.

4.2.6.1 Ultra filtration and concentration

To reduce the volume and concentrate the samples from 15 ml to 1 ml the samples were filtered and concentrated using a 100 kDa molecular weight cut-off filter, (Vivaspin 15, Millipore) as per the manufacturer's instruction. The retentate was held in the filter and removed using a fine needle and syringe. Smaller volume, 500 µl ultra filtration, (Amicon, Millipore) devices were also used and the retentate recovered by reversing the filter device into a clean eppendorf and pulsing to retrieve concentrated sample.

4.2.7 SDS PAGE gel and Western Blot

An SDS-PAGE gel and Western Blot analysis was used to ascertain homogeneity of purified samples. A detailed description of the materials and methods can be found in Chapter 2, 2.8.

4.2.8 Native PAGE gel and Coomassie/Silver Staining

A Native PAGE gel was used to establish homogeneity of purified samples. A detailed description of the materials and methods can be found in Chapter 2, 2.4.4.

4.2.9 Purified toxin B – Storage

Aliquots of purified toxin were stored at 4°C and -80°C in the presence or absence of 20% glycerol and the cytotoxicity checked prior to use.

4.3 Results

4.3.1 Purification of *Clostridium difficile* toxin B using old protocol

Toxin B was purified by bovine thyroglobulin affinity chromatography and ammonium sulphate precipitation followed by two sequential anion exchange chromatography steps on DEAE Sepharose FF and Mono-Q as outlined earlier. Results from a representative run are given below.

4.3.1.1 DEAE anion exchange chromatography

Figure 4-2 profiles the application of crude supernatant to the DEAE column, the NaCl gradient applied and the resulting elution of protein. Arrows detail toxin positive fractions identified following a confirmatory dot blot. Comparison of Figure 4-2, the elution profile from the DEAE column and Figure 4-3, dot blot give clear evidence of an elution overlap of toxin A and B.

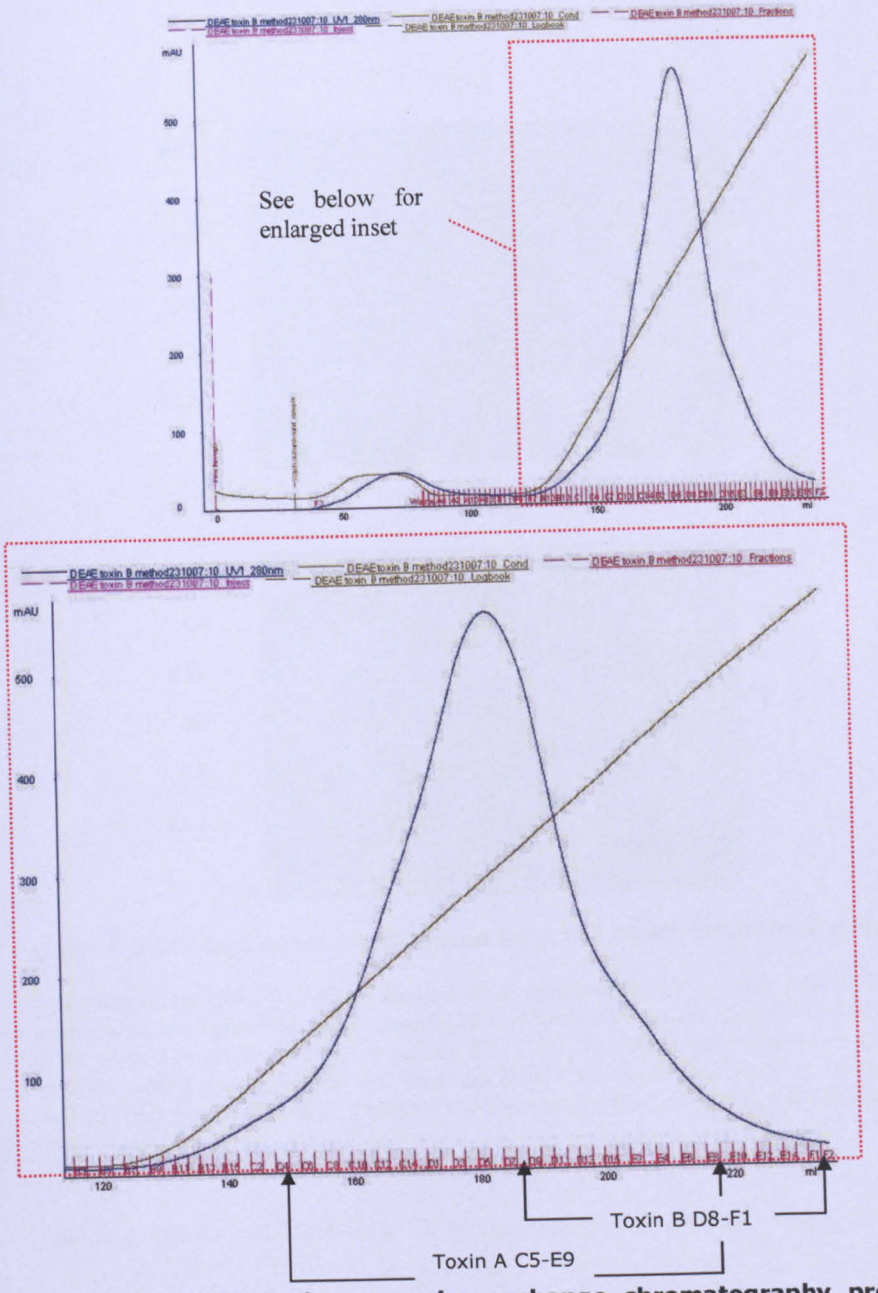

Figure 4-2 DEAE-Sepharose anion-exchange chromatography profile of *C. difficile* toxin A purification

Whole profile (top) and enlarged inset (bottom). X axis displays mAU values measured at 280 nm; Y axis details volume passing through the column and fractions. The peak represents purified protein eluted between fraction B10 and F2. Toxin A was found in eluted fraction C5-E9. Toxin B was found in eluted fractions D8-F1. The linear line crossing the peak represents the 0-1.0 M NaCl gradient used to elute the bound protein.

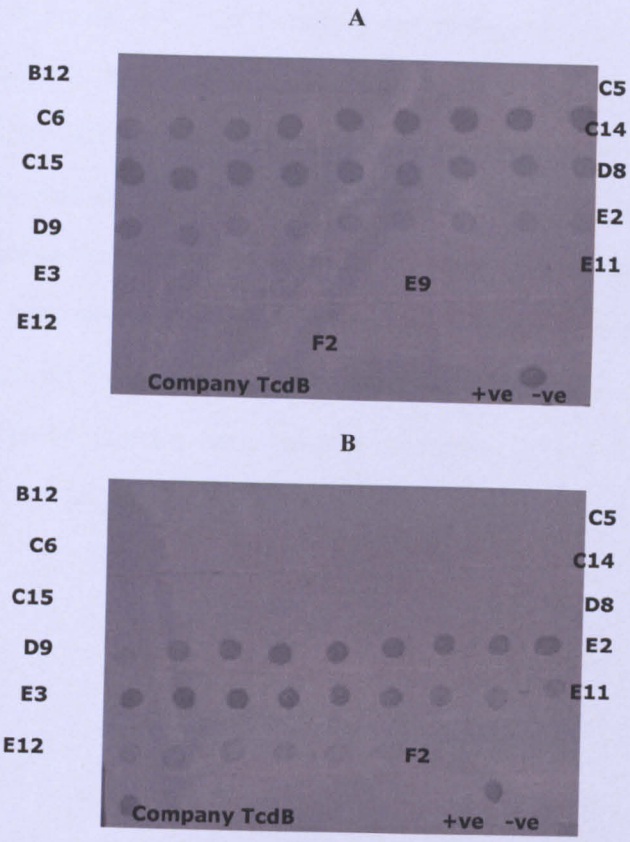

Figure 4-3 Dot blot of fractions eluted from the DEAE-Sepharose column

Application of fractions B12-F2 to nitrocellulose membrane together with positive and negative controls were incubated with either specific PCG-4 for toxin A membrane (A) or Mab monoclonal for the toxin B membrane (B). Fractions C5 – E9 (A) were confirmed to be toxin A when compared with positive control and fractions D8-F2 (B) were confirmed to be toxin B when compared with positive control. Fractions D8-E9 contains toxins A and B when referenced against positive controls.

Toxin B positive fractions D11-F2 were pooled and dialysed overnight.

4.3.1.2 Mono-Q anion exchange chromatography

Dialysed fractions D11-F2 were applied to the Mono-Q column and fractions eluted using a stepped NaCl gradient 0-0.7 M with a 15 ml plateau at 0.7M

increasing 0.7-1 M. Several peaks eluted from the column as can be visualised in Figure 4-4. Confirmatory dot blots were completed, see Figure 4-5, to establish the presence/absence of toxins A and B in the sample. As with the DEAE dot blots two identical dot blots were prepared and processed using either specific PCG-4 for toxin A (A) or Mab toxin B (B) to ascertain toxin B positive/toxin A negative fractions. Fractions B3-E6 expressed a trace of toxin A when referenced against the control. Looking at the Anti B dot blot, Fractions B11-F12 contains toxin B. From these results it would appear that fractions B11-E6 contain both toxin A and toxin B and E7-F12 is toxin B positive/toxin A negative.

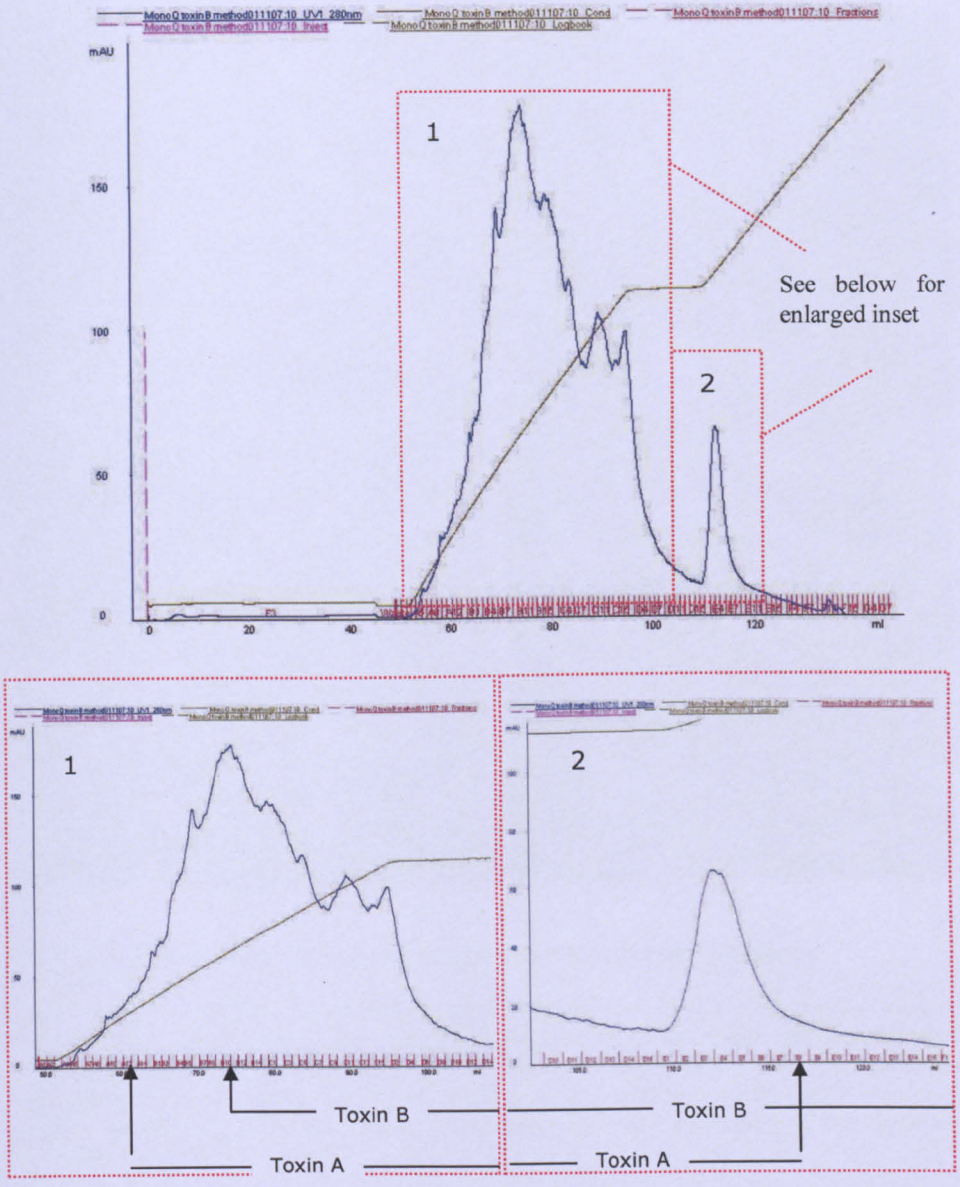

Figure 4-4 Mono-Q anion exchange chromatography of *C. difficile* toxin A purification.

Whole profile (top) and enlarged insets (bottom). X axis displays mAU values measured at 280 nm; Y axis details volume passing through the column and fractions. Two peaks eluted from the column, the first eluting at fractions A6-D14, the other eluting in fractions D15-E11. The stepped line crossing the peak represents the NaCl gradient (0-0.7M with a 15 ml plateau and 0.7-1.0M) used to elute the bound protein. Immunohistochemistry of fractions found fractions B3-E6 to contain toxin A and fractions B11-F12 to contain toxin B.

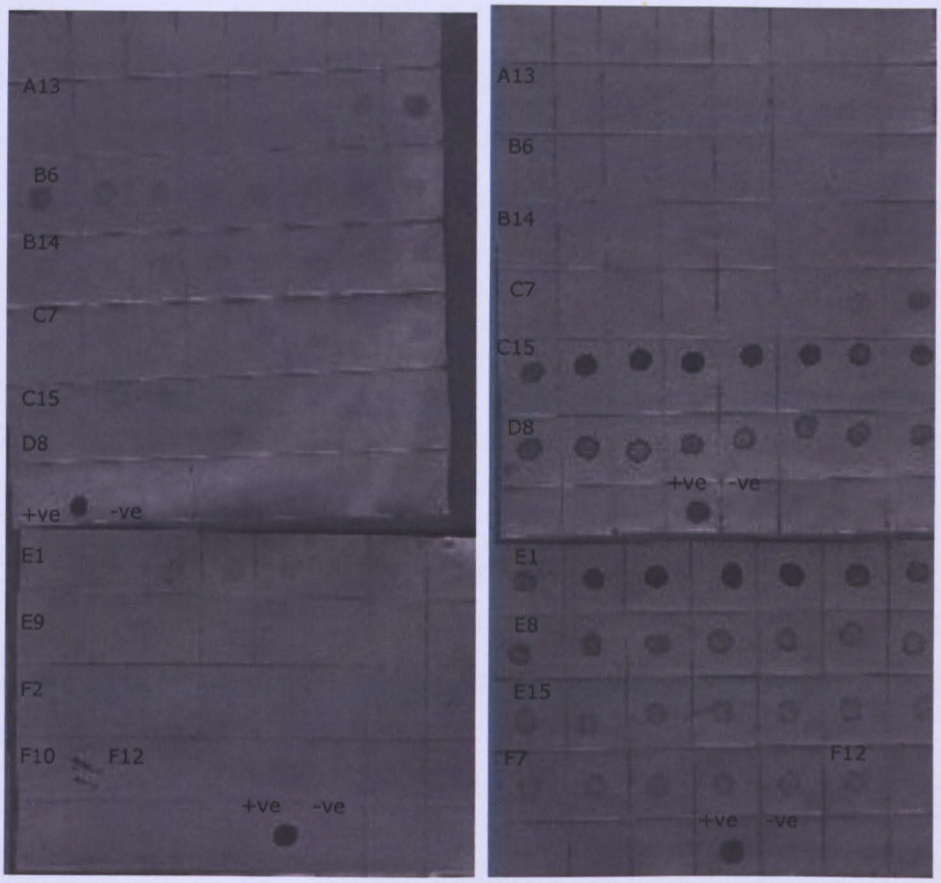

Figure 4-5 Dot blot of fractions eluted from the Mono-Q column

Application of fractions A5-F12 to nitrocellulose membrane together with positive and negative controls were incubated with either specific PCG-4 for toxin A membrane (A) or Mab toxin B for the toxin B membrane (B). Fractions B3 – E6 (A) were confirmed to be toxin A when compared with positive control and fractions B11-F12 (B) were confirmed to be toxin B when compared with positive control. The obvious overlap may represent some cross reactivity but essentially the fractions also contain toxin A.

4.3.1.3 Concentration and filtration

Toxin B containing fractions eluted from the Mono-Q column were pooled and concentrated as described in the methods, page 164. Total protein concentration was established using the Bradford Assay and bovine albumin standards, as 107.2 µg/ml. A Native PAGE gel stained with Coomassie blue

revealed a very faint band above 250 kDa. Western Blot analysis using specific Mab toxin B was completed, no visible banding was evident. Identifying low protein concentration as a factor further centrifugal concentration of protein was completed, this however resulted in a lower protein concentration 65 µg/ml, possibly due to protein degradation. Another Native PAGE gel stained with Coomassie blue revealed very faint above 250 kDa when compared against marker and a smaller molecular weight band between 70 and 50 kDa. Western blot analysis using specific Mab toxin B revealed no visible banding. Amino acid sequence analysis of the bands found in the Coomassie stained NATIVE gel was completed to ascertain if the proteins in the gel represented the protein of interest and a fragment of the protein of interest. The excised bands were not the protein of interest or a fragment.

Three runs were completed using the above protocol. Two variations were introduced during these three runs. The first was to increase the volume of bacterial supernatant used; with 5 flasks being used in run 1; 10 flasks in runs 2 and 3. The second variation was to pool toxin B positive / toxin A negative fractions in runs 1 and 2; in run 3 all toxin B positive fractions were pooled, to avoid any loss of toxin B and increase the final yield. The production of toxin B by the bacteria is far less than toxin A production.

As can be observed in the above results, a number of issues were identified following the purification of toxin B using the above protocol.

- Toxin A was still present in the supernatant despite two runs through the bovine thyroglobulin column.
- The close elution and therefore contamination of toxin B fractions with toxin A at the DEAE Sepharose stage
- Poor final yield – too small/too weak for characterisation to be completed

The current protocol takes three weeks from bacterial culture to purified protein sample. Reducing this time would limit protein degradation and loss of biological activity. The current protocol allowed toxins A and B to be eluted in the same peak resulting in either a reduced amount of toxin B because some of the fractions contained toxin A or a higher concentration of B which was contaminated with toxin A. The issues outlined above have been added to the protocol flow chart, see Figure 4-6.

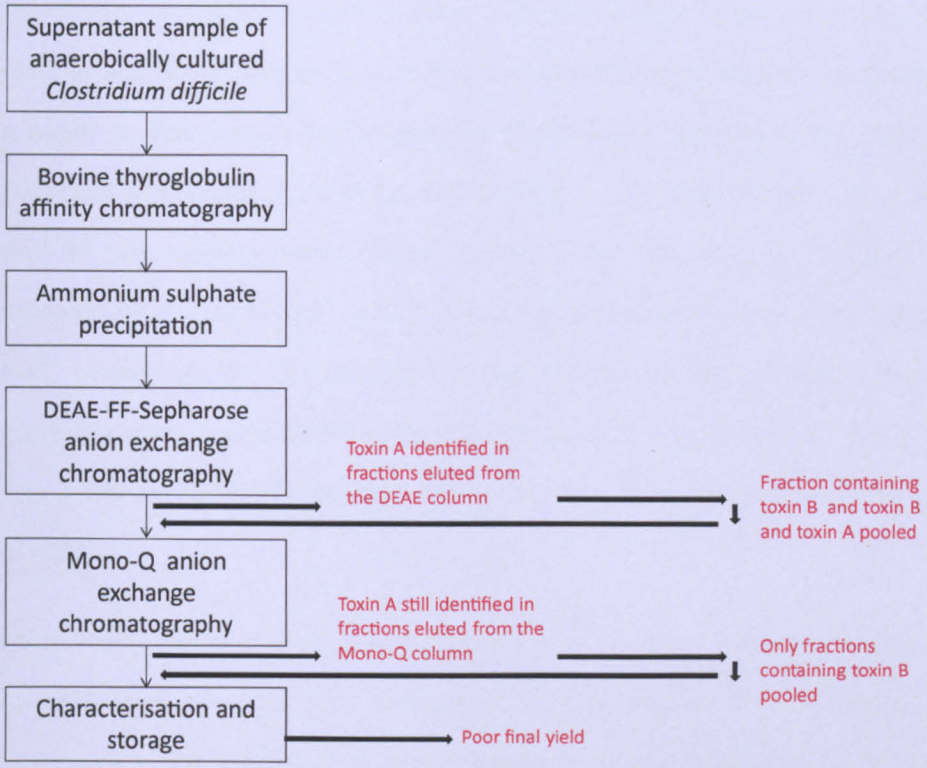

Figure 4-6 Flow diagram identifying problem areas in the current protocol used for toxin B purification.

Current protocol issues highlighted in red..

4.3.2 Separation of toxin A and toxin B using revised protocol

Investigation of elution patterns established that toxins A and B eluted in the same peak but eluted at different concentrations of NaCl. Toxin A eluted first at an average concentration of 12.5 mS/cm for approximately 75 mls and toxin B eluted at an average concentration of 29 mS/cm, some 34 mls after toxin A for an average of 46 mls.

Identifying a common elution pattern in the earlier runs using the DEAE column and the subsequent comparison of these results against the literature, a paper by Pothoulakis and colleagues (Pothoulakis, Barone et al. 1986), our DEAE column protocol was adjusted to introduce a step in the salt gradient and an intermediary wash of the column. The gradient ran 0-0.3 M NaCl followed by a 150ml wash at 0.3 M NaCl and then increased from 0.3-1.0 M NaCl (Figure 4-7). In addition to the change to our protocol, Buffer A currently used in the DEAE purification of toxin B was changed from 20 mM Tris buffer to 50 mM Tris buffer, in line with the buffer used by Pothoulakis et al (ibid).

To increase the final yield it was decided to grow more bacterial supernatant and therefore three batches of flasks (5 off), giving a total of 15 flasks, were prepared. This extended the purification time by one week, with AEBSF inhibitor added to batch 2 and 1 and stored for one or two week at 4°C, respectively.

Using a larger volume of supernatant, the sample was prepared as previously described and subsequently applied to the DEAE-FF column and the sample eluted using the revised protocol and 50 mM Tris buffer. The eluted fractions were applied to dot blot and comparison of the elution profile (Figure 4-7) with the toxin A and toxin B dot blots (Figure 4-8) confirmed the two separate peaks of protein eluted from the column were toxin A positive – toxin B negative in the first peak and toxin B positive – toxin A negative in the second peak. Toxin A was found in fractions D4-H10 and toxin B was found in fractions J7-L13.

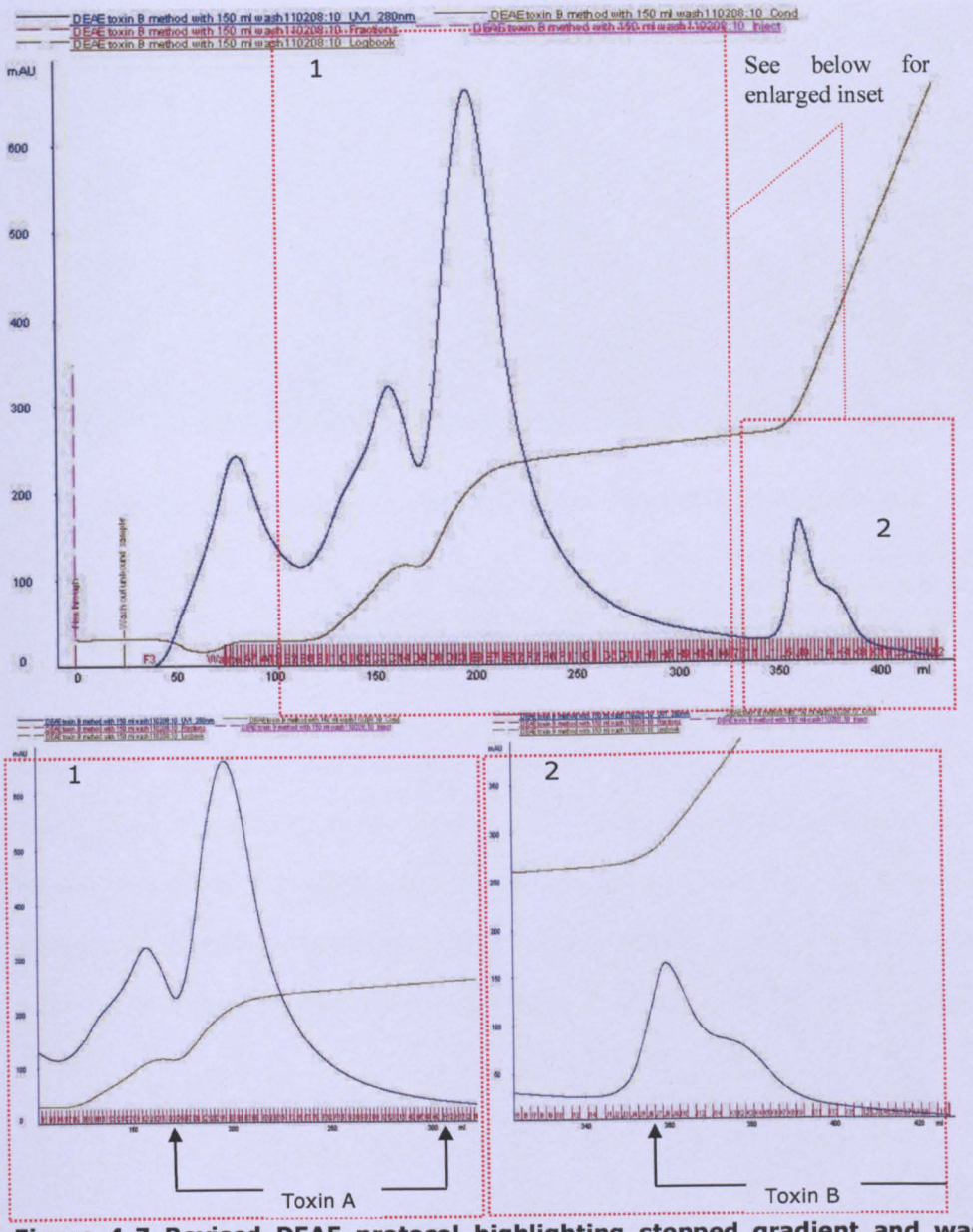

Figure 4-7 Revised DEAE protocol highlighting stepped gradient and wash segment

Whole profile (top) and enlarged insets (bottom) showing the elution of protein measured at A^{280} (Y axis) into designated fractions (X axis). The peaks represent purified protein. Toxin A was found in eluted fraction D4-H10 (Inset 1) and Toxin B was found in eluted fractions J7-L13 (Inset 2). The linear line crossing the peak represents the revised protocol with stepped NaCl gradient at 0.3 M, intermediary 150 ml wash and return to linear gradient 0.30 to 1.0 M NaCl to elute the bound protein.

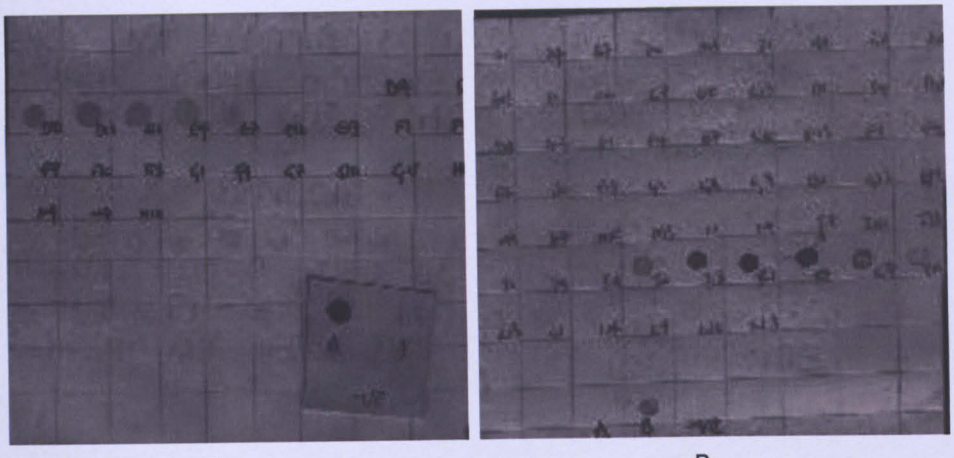

A B

Figure 4-8 Dot blot of fractions eluted from the DEAE-Sepharose column

Application of fractions A1-L13 to nitrocellulose membrane together with positive and negative controls were incubated with either specific PCG-4 for toxin A membrane (A) or Mab toxin B for the toxin B membrane (B). Fractions D4 – H10 (A) were confirmed to be toxin A when compared with positive control and fractions J7-L13 (B) were confirmed to be toxin B when compared with positive control.

The revised DEAE protocol was used in all future purifications. With the toxins successfully separated, toxin B positive - toxin A negative fractions were pooled, dialysed overnight and applied to Mono-Q column as previously described. The Mono-Q elution profile can be viewed in Figure 4-9. Dot blot analysis of eluted fractions identified toxin B in C12-D7 and E1-F4 (Figure 4-10).

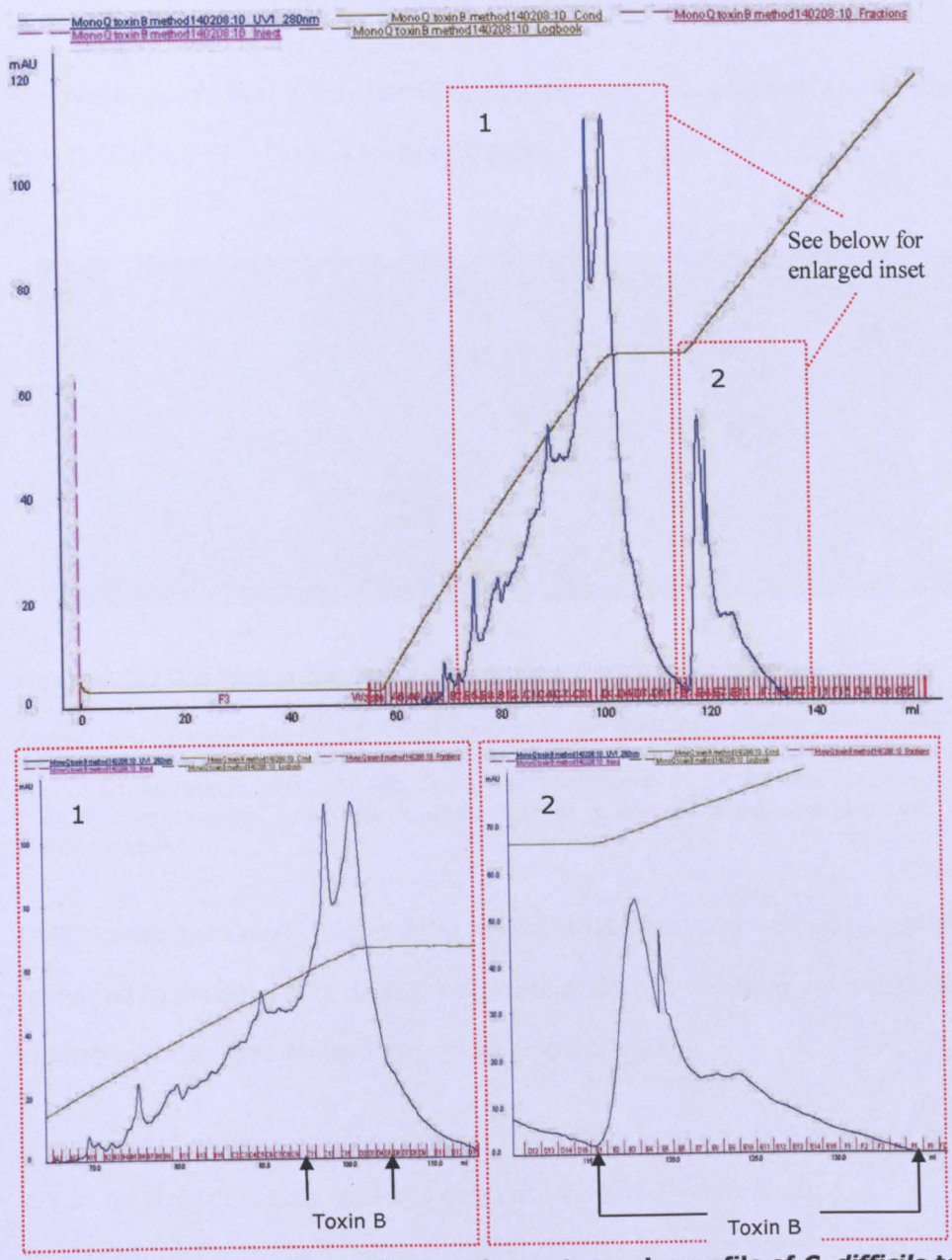

Figure 4-9 Mono-Q anion-exchange chromatography profile of *C. difficile* toxin B purification

X axis displays mAU values measured at 280 nm; Y axis details volume passing through the column and fractions. Two peaks eluted from the column, the first eluting at fractions A11-D11, and the other peak eluting in fractions E1-F4. The stepped line crossing the peak represents the NaCl gradient (0-0.7M with a 15 ml plateau and 0.7-1.0M) used to elute the bound protein. Fractions C12-D7 and E1-F4 were confirmed to be toxin B when compared with positive control.

The presence of toxin B was confirmed by immuno-histochemistry in fractions C12-D7 and E1-F4. Toxin A was not traced.

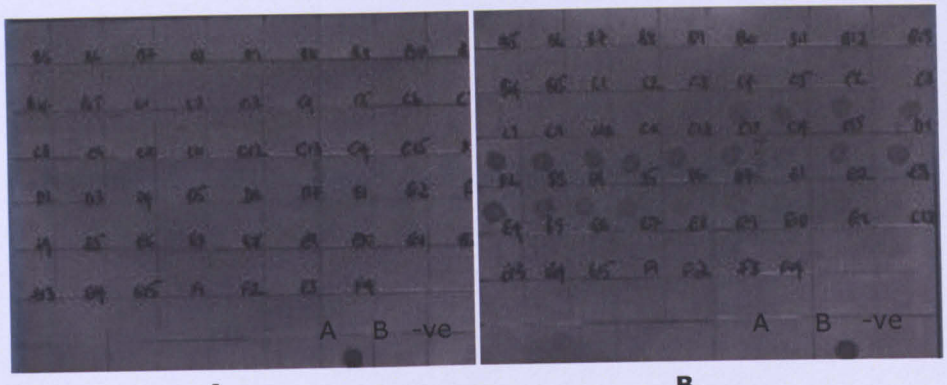

Figure 4-10 Dot blot of fractions eluted from the Mono-Q column

Application of fractions B5-D7 and E1-F4 to nitrocellulose membrane together with positive and negative controls were incubated with either specific PCG-4 for toxin A membrane (A) or Mab toxin B for the toxin B membrane (B). Fractions C12- D7 and E1- F4 (B) were confirmed to be toxin B when compared with positive control. Toxin A was not found when compared with positive control.

Utilising the increased yield and the revised DEAE protocol we had successfully managed to produce enough toxin B positive/toxin A negative sample to allow characterization, see revised flow chart (Figure 4-11).

4.3.3 Protein characterization - concentration and cytotoxicity

Characterisation of toxin B positive fractions established protein concentration ranging 4 – 52 ug/ml (pooled concentration 32 ug/ml) and cytoxicity (50 % rounding at 24 hours) ranging 10^{-2}- 10^{-4}. Pooled fractions were concentrated as previously described into two 1 ml aliquots and protein concentration established as 239 and 200 ug/ml and cytoxicity on Vero cells (50% rounding

at 24 hours) at 10^{-8}. These samples were run on Native PAGE gel and stained with Coomassie Blue and Silver.

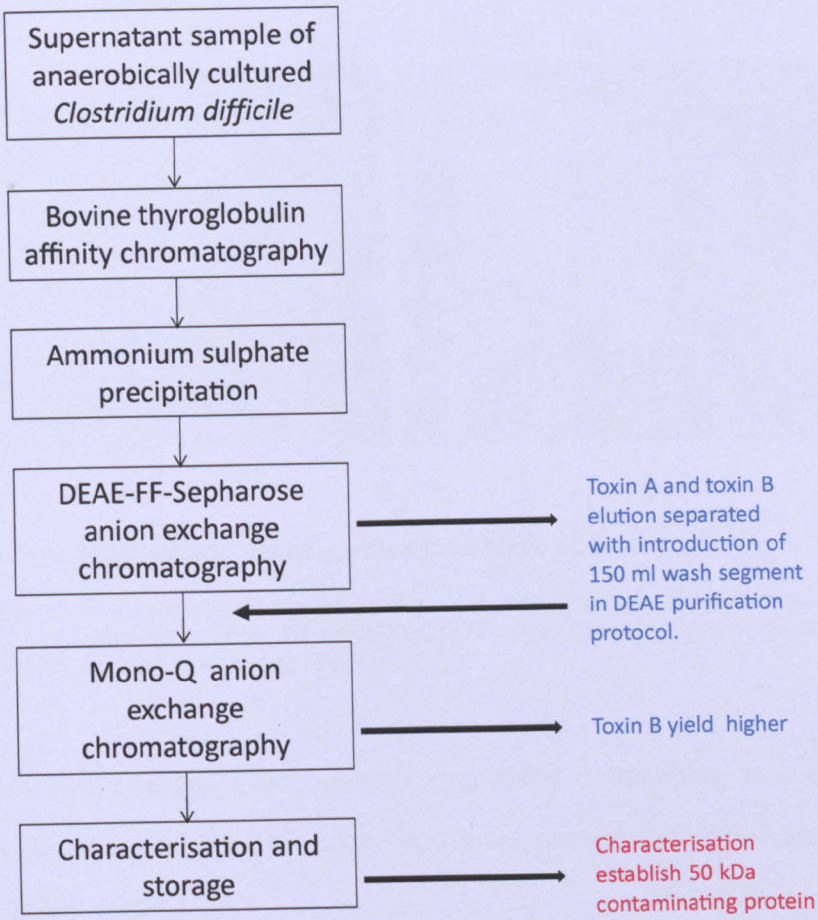

Figure 4-11 Flow diagram identifying problem areas and areas optimized.

Current protocol issues highlighted in red and optimization highlighted using blue text.

4.3.4 Homogeneity

Silver and Coomassie stained Native PAGE gels identified two bands, see Figure 4-12. As was expected identical bands were found in both samples. Proteomic analysis established the two bands using mass spectrometry to be

an enolase, mass 46 kDa and a heat shock protein, mass 58 kDa. Further proteomic investigation found that whilst toxin B was not present in the gel toxin B was present at the gel interface and had not migrated through the gel.

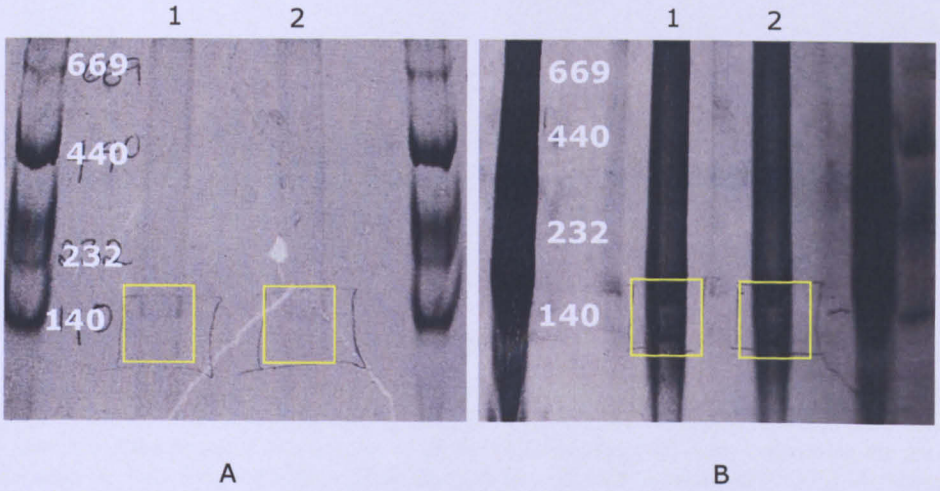

Figure 4-12 Native PAGE gel of purified *C. difficile* toxin B

Native PAGE gel stained with A) Coomassie Blue or B) Silver staining. Identical bands found in sample 1 and 2, highlighted inside the yellow box, the first band appearing just above the 140kDa marker and the second below the 140 kDa marker.

Western blot analysis using specific Mab toxin B identified a number of positive bands and using the specific PCG-4 antibody confirmed the absence of toxin A, see Figure 4-13.

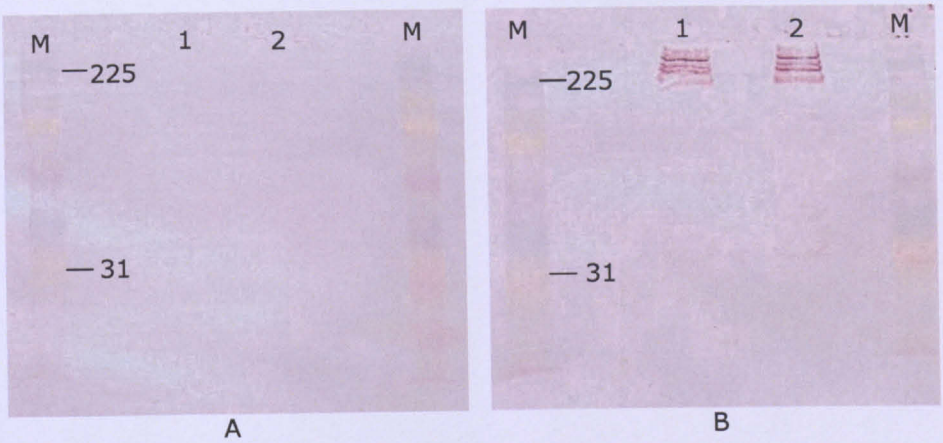

Figure 4-13 Western blot analysis of purified *C. difficile* toxin B

Western blot analysis of toxin B samples 1 and 2 incubated with A) PCG-4 specific antibody for toxin A and B) Mab toxin B antibody specific for toxin B. The membranes confirm the absence of toxin A and the presence of a number of toxin B immuno-reactive bands confirming the presence of toxin B. Full Weight Rainbow Molecular Marker (GE Life Sciences RPN800E) Marker colour reference (M); Blue - 225 kDa, Red – 150 kDa, Green – 102 kDa, Yellow – 76 kDa, Purple – 52 kDa, Blue – 38 kDa, Orange – 31 kDa.

The simultaneous completion of Coomassie stained SDS-PAGE and Western blot found a number of bands present in the Coomassie stained gel which were also evident in the Western blot incubated with Mab toxin B, see Figure 4-14, but as was expected a number of contaminating bands were identified on the Coomassie stained SDS-PAGE that were not evident on the western blot incubated with toxin B specific antibody. These results confirm the contaminating proteins highlighted in the proteomics report.

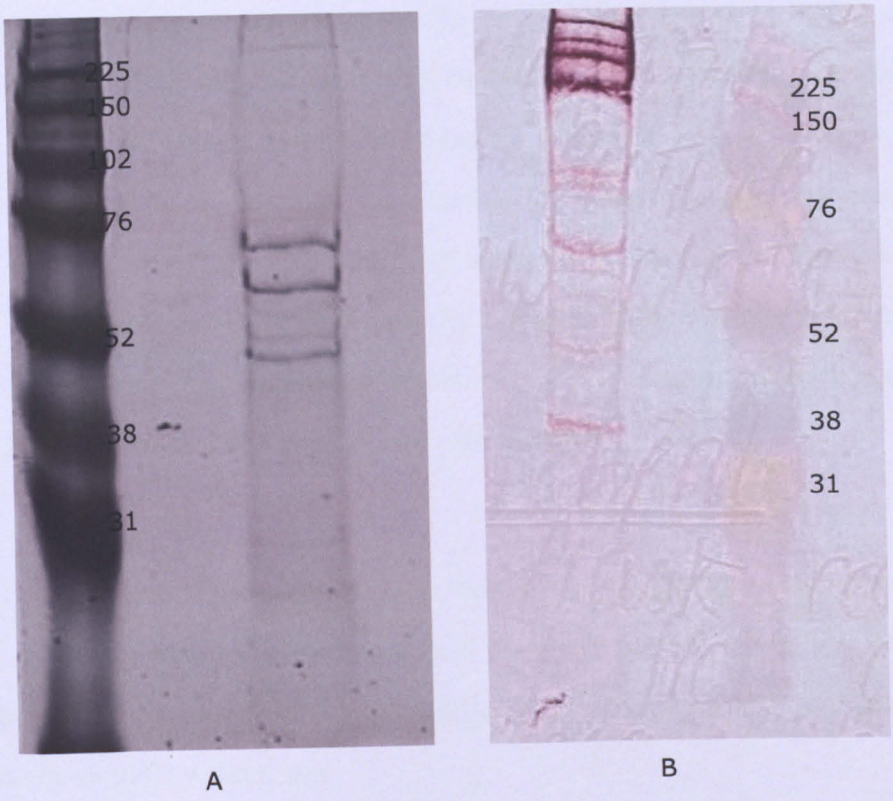

Figure 4-14 SDS PAGE gel of purified *C. difficile* toxin B

7.5% SDS-PAGE gel stained with Coomassie blue (A) and the simultaneous transfer of proteins for Western Blot analysis using specific Mab for toxin B (B). Full Weight Rainbow Molecular Marker (GE Life Sciences RPN800E) Colour reference; Blue - 225 kDa, Red – 150 kDa, Green – 102 kDa, Yellow – 76 kDa, Purple – 52 kDa, Blue – 38 kDa, Orange – 31 kDa.

With the separation of toxin A and the increased yield allowing characterisation our focus moved to the other contaminating proteins eluting with the toxin B.

4.3.5 Removal of contaminating proteins

Starting with a fresh batch of bacterial supernatant I used the revised DEAE method, see Figure 4-7. Fractions eluted from the column formed two clear

peaks and comparing the elution profile and dot blot the second peak was identified as containing the protein of interest, toxin B. Taking a sample of each fraction we sought to establish if the contaminants co-elute, elute at the beginning; middle or end of our chosen peak. This was established by running the samples on a 7.5% SDS-PAGE and staining with Silver, the scanned gel can be observed in Figure 4-16 and the strength of the contaminating band corresponds with the increase in protein eluted. It would therefore appear that the contaminants appear to elute with the toxin.

Until recently the application of pooled fractions were dialysed against 20mM Tris, applied to the Mono-Q column and then the proteins eluted using a 0-0.5M NaCl gradient with a 40 ml continuum at 0.5M followed by a second gradient on 0.5-1M NaCl, see

which provides an elution profile from the Mono-Q. This protocol successfully eluted toxin B from the column, however analysis of homogeneity confirmed the co-elution and toxin B together with the contaminants, see Figure 4-14. Taking a sample from the beginning, middle and end of each peak; three peaks in total; giving nine samples it was established that the contaminant was found in the first two peaks. The eluted fractions were cytotoxic when applied to Vero cells and toxin B positive when reference against a positive control on a dot blot. The fractions were concentrated up using concentrator columns with a 100 kDa molecular weight cut-off. The contaminant was not removed with this filter therefore it would appear that either the contaminant forms a complex with toxin B or that it may form a homo-oligomer.

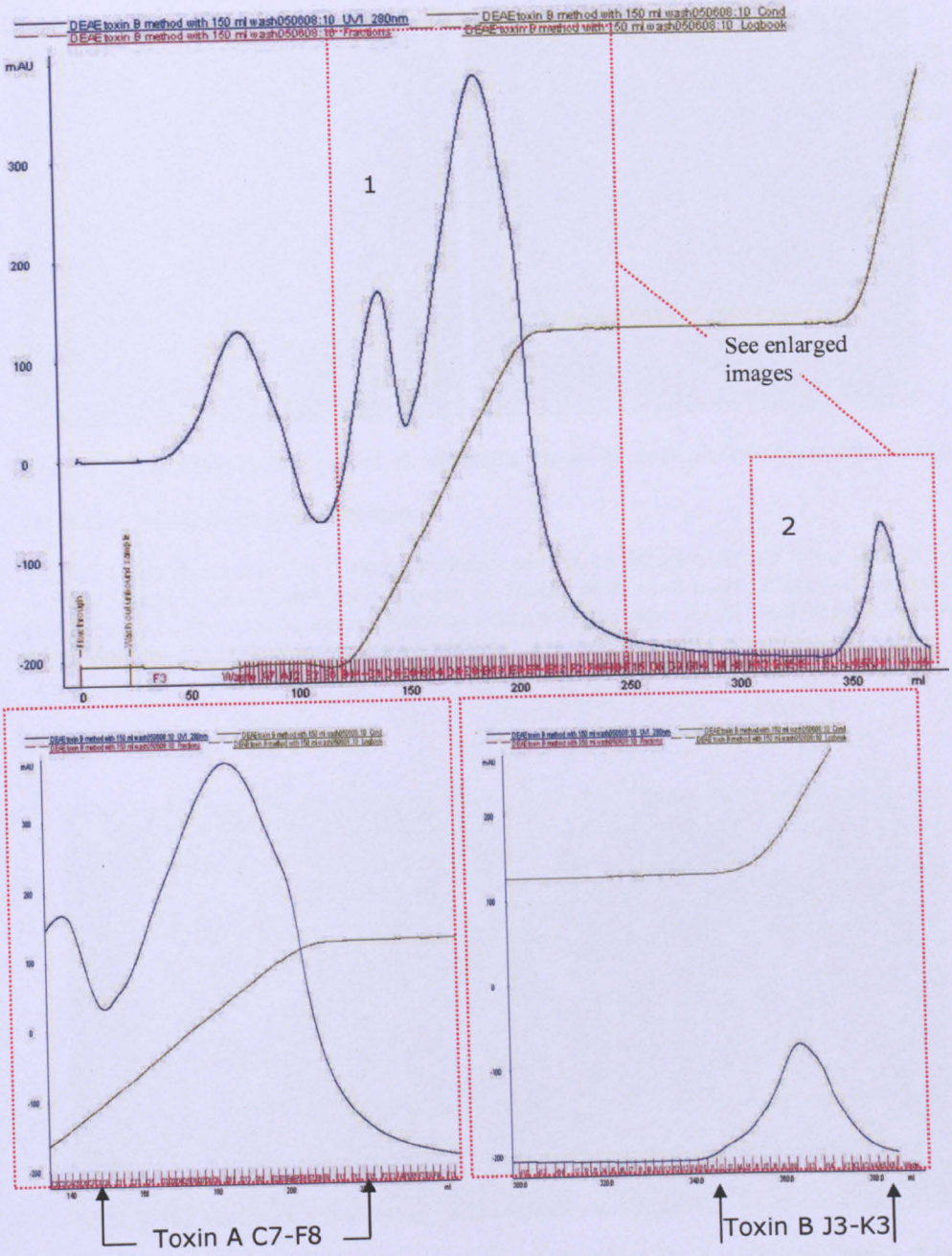

Figure 4-15 DEAE Sepharose anion exchange chromatography profile

Whole profile (top) and enlarged insets (bottom) X axis displays mAU values measured at 280 nm; Y axis details volume passing through the column and fractions. The peaks represent purified protein. Toxin A was found in eluted fractions C7-F8 and toxin B was found in eluted fractions J3-K3. The linear line crossing the peaks represents the revised protocol with stepped NaCl gradient at 0.3M, intermediary 150 ml wash and return to a linear gradient 0.3-1.0 M to elute the bound protein.

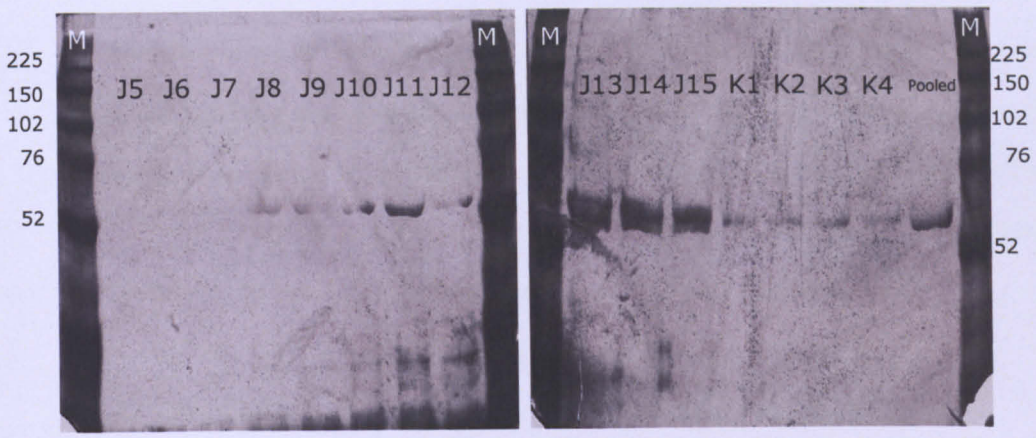

Figure 4-16 SDS-PAGE gel of *C. difficile* toxin B containing fractions eluted from the DEAE-Sepharose column

Fractions were denatured with 2-mercaptoethanol and run on SDS-PAGE and Silver stained. As previously viewed the contaminant is between 52-76 kDa in size and elutes throughout the toxin B positive peak with the band strength corresponding with the peak in. M (Full Weight Rainbow Molecular Marker (GE Life Sciences RPN800E)).

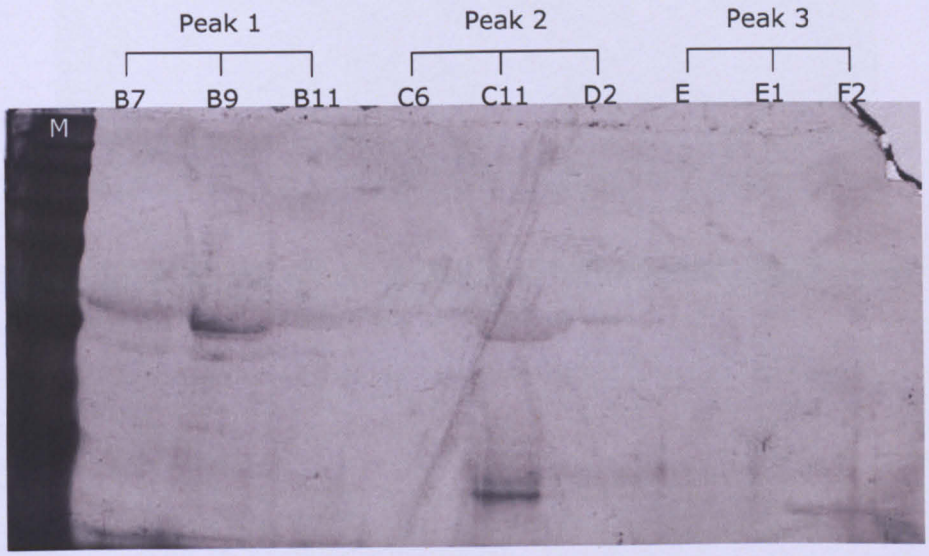

Figure 4-17 SDS-PAGE gel of fractions containing *C. difficile* toxin B and contaminant eluted from the Mono-Q column

Fractions denatured with 2-mercaptoethanol, run on 7.5% SDS-PAGE and Silver stained. As previously viewed the contaminant is between 52-76 kDa in size. The fractions analysed were taken from the beginning, middle and end of the three peaks eluted from the Mono-Q. The contaminant can be observed in the first two peaks but not the third. M (Full Weight Rainbow Molecular Marker (GE Life Sciences RPN800E))

To identify whether this complex could be successfully reduced to two separate proteins the solution containing toxin B and the contaminant was incubated with either 2-mercaptoethanol, DTT or PBS at room temperature for 1 hour. Following the incubation the solution was concentrated using the 100 MWCO filters, run on an SDS-PAGE and silver stained, see Figure 4-18.

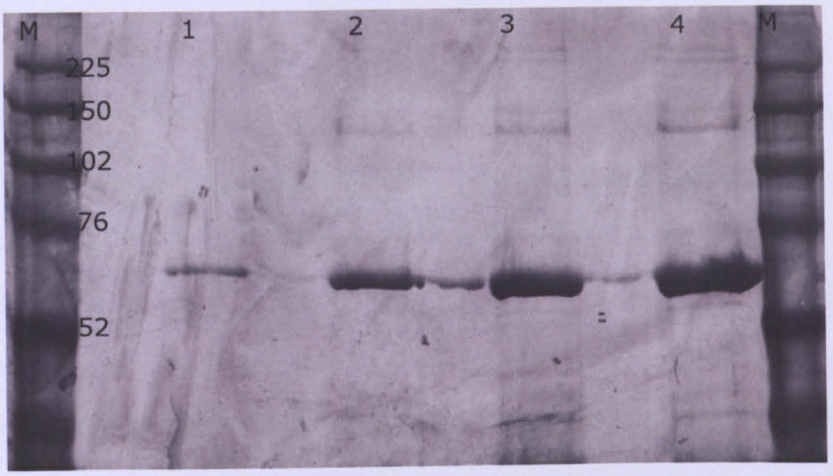

Figure 4-18 SDS-PAGE gel of contaminant removal from toxin B positive fractions

Comparison of immuno-histochemistry and the earlier SDS-PAGE fractions C11-D11 were pooled and following a 1 hr incubation with PBS (1 and 2); DTT (3) or 2-mercaptoethanol (4), samples 2, 3 and 4 were concentrated using 100 MWCO filters and ran on a SDS-PAGE. The gel was stained with silver and scanned. M (Full Weight Rainbow Molecular Marker (GE Life Sciences RPN800E)).

The addition of reducing agents DTT (1 mmol/litre) or 2-Mercaptoethanol (5% v/v) for 1 hour prior to concentrating did not denature the contaminant and was not removed using the 100 MWCO filter, see Figure 4-18.

Having established a solution to the separation of toxins A and B, it was now important to resolve the issue of contamination. Further review of the literature identified a possible solution. The contaminating proteins have been reported previously. Meador and Tweten found that two contaminating proteins were eluted with toxin B, the first which was only occasionally eluted was a 45kDa protein and the other a 50 kDa protein that regularly contaminated toxin B purification attempts (Meador and Tweten 1988). Establishing that the 50 kDa protein was neither cytotoxic nor a fragment of toxin B, Meador and Tweten successfully managed to remove both of these contaminants and maintain the cytotoxicity of the purified toxin B. Instead of using a Tris based buffer, Meador and Tweten combined Tris and Calcium chloride and used this buffer solution to dialyse the toxin solution prior to the Mono-Q purification and as a buffer throughout the application and elution of the proteins from the Mono-Q column. In addition to the alteration made to the buffer, the gradient used was slightly different and the flow rate was also reduced.

In line with the method used by Meador and Tweten, toxin B positive fractions from our revised DEAE method were dialysed against 10 mM Tris 50 mM CaCl buffer pH 8, our current stepped gradient removed and the flow rate reduced to 0.5 ml/min, see Figure 4-20. Figure 4-19 updates the protocol flow diagram with the current stage of toxin B optimization.

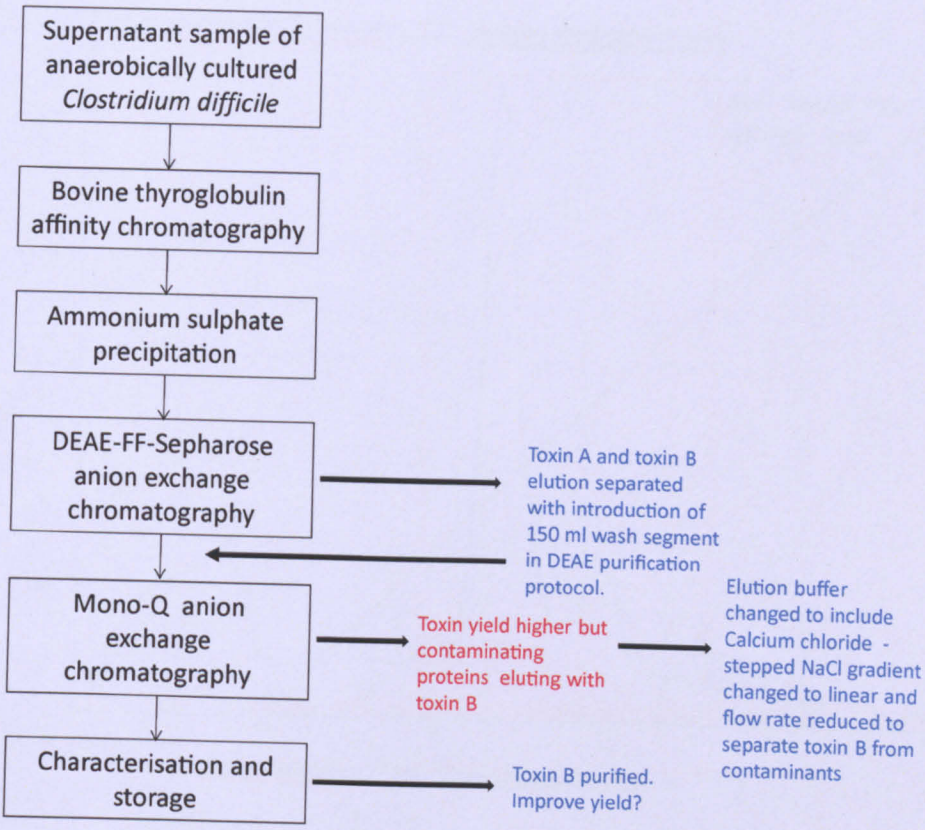

Figure 4-19 Flow diagram identifying problem areas and areas optimized.

Current protocol issues highlighted in red and optimization highlighted using blue text.

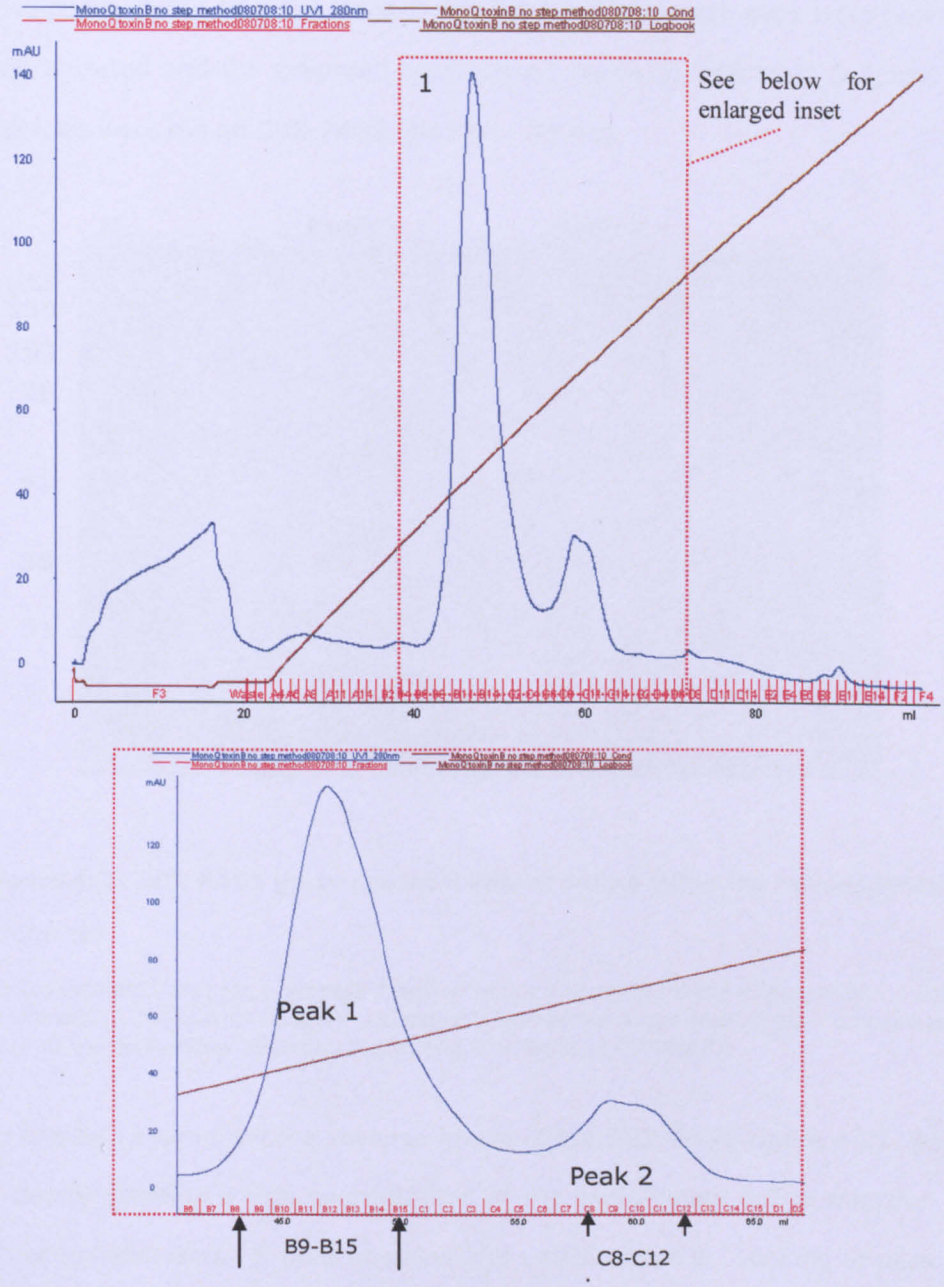

Figure 4-20 Revised Mono-Q protocol highlighting the linear salt gradient

Whole profile (top) and enlarged inset (bottom). Showing the elution of protein measured at A^{280} (Y axis) into designated fractions (X axis) of the revised protocol which removed the step at 0.7 M and reduced the flow rate to 0.5 ml/min. Two peaks eluted from the column, the peak 1 eluting at fractions B9-B15, and peak 2 eluting in fractions C8-C12. The line crossing the peak represents the NaCl gradient (0-1.0 M) used to elute the bound protein.

Two peaks eluted from the Mono-Q and fractions from each peak were pooled, concentrated and the proposed contaminant (peak 1) and toxin B (peak 2) samples were run on SDS-PAGE and silver stained.

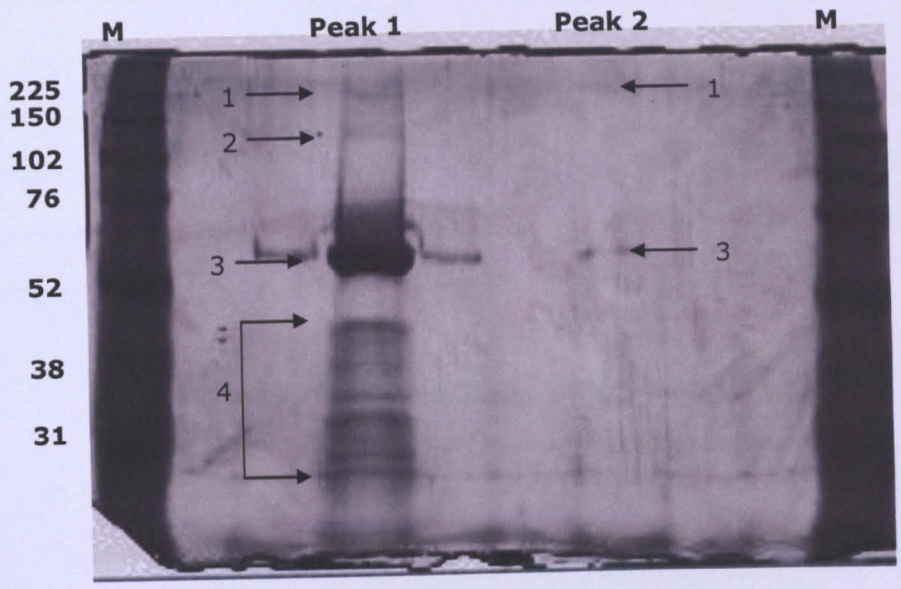

Figure 4-21 SDS-PAGE gel of pooled fractions eluted using the revised Mono-Q protocol

Pooled fractions from peak 1 and peak 2 derived from the Mono-Q column (Figure 4-20). 1) Toxin B estimated at 250 kDa 2) unknown contaminant 3) unknown contaminant 4) other contaminants. M (Full Weight Rainbow Molecular Marker (GE Life Sciences RPN800E))

As can be viewed from the scanned image of the SDS-PAGE Figure 4-21, peak 1 clearly contains a high concentration of the contaminant and a selection of other contaminants. It does however also contain toxin B. Looking at peak 2, this peak contains toxin B, it may still contain traces of the contaminant.

Cytotoxicity of the fractions prior to pooling confirmed the above with cytotoxicity being recorded in fractions taken from the first peak. The second

peak was also cytotoxic - but a higher cytotoxic effect was noted. Cytotoxicity was reduced in fractions pooled to make peak 2 and failed to be increased in fractions pooled into peak 1. This would suggest that activity is being lost as a result of degradation of toxin B and/or through the process of concentration.

Peak 1 was also run on Native PAGE to ascertain size of the contaminant. From the scanned image and the proposed positioning of the molecular marker, the contaminant would appear to be around between 140 and 232 kDa in size and may represent a homo-oligomer.

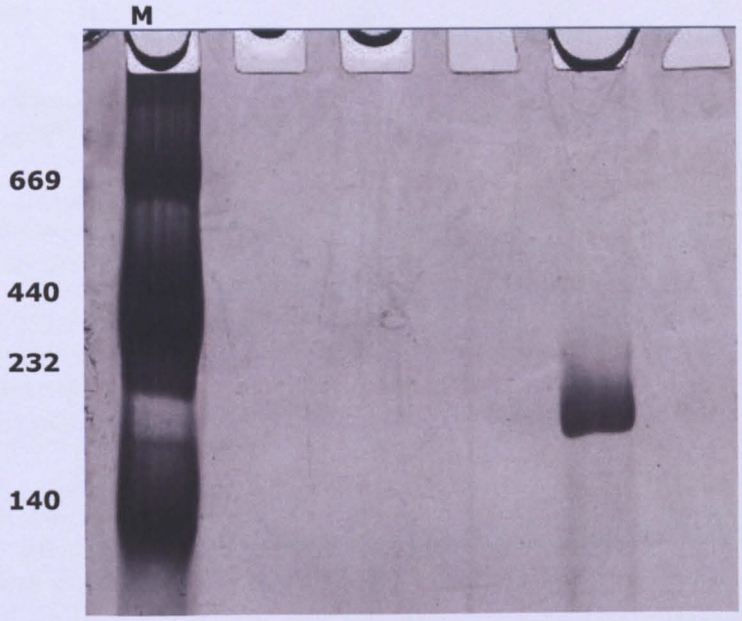

Figure 4-22 Native PAGE gel of contaminant (pooled peak 1 fractions) eluted from the Mono-Q column using the revised protocol.

A high weight molecular protein mixture (Amersham Biosciences) (M) containing 76 µg of thyroglobulin (Mw 669 000 Da), 50 µg of Ferritin (Mw 440 000 Da), 36 µg of Catalase (Mw 232 000 Da), 48 µg of lactate dehydrogenase (Mw 140 000 Da) and 40 µg of Albumin (Mw 66 000) was used as a marker and comparison of the contaminant against the known molecular weights seen the contaminant is between 140-232 kDa.

To increase overall yield and prevent loss of biological activity it was decided to withdraw the thyroglobulin step and proceed immediately to ammonium sulphate precipitation. In addition, five more flasks were purchased and 10 flasks could be harvested in one week, limiting protein degradation and loss of cytotoxic activity. Using the revised protocol as detailed in Figure 4-23 *Clostridium difficile* toxin B was successfully purified.

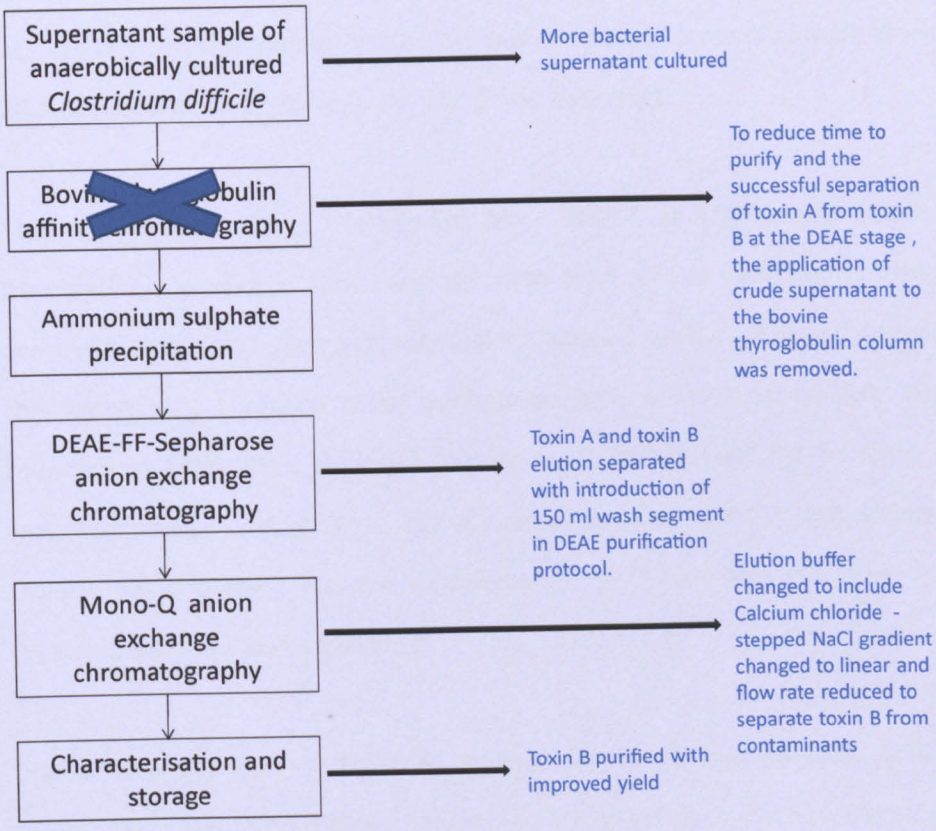

Figure 4-23 Flow diagram of final optimized protocol for purification of *C. difficile* toxin B.

Optimization highlighted using blue text.

4.4 Stability and cytotoxic activity of *Clostridium difficile* toxin B

The successful purification of *Clostridium difficile* toxin B has enabled experiments investigating the response of intestinal epithelial cells types and primary colonic myofibroblasts to be conducted. Toxin B is reported to particularly susceptible to degradation and early loss of biological activity (Meador and Tweten 1988) with storage at -80°C in 20% glycerol reported as the best method of storage. Investigating biological activity in a batch of purified toxin B using the Vero assay as described previously, the cytotoxic activity of toxin B stored at 4°C in Tris buffer and an identical sample stored in 20% glycerol in 20 µl aliquots at -80°C was assessed.

The cytotoxic activity of the purified toxin stored at 4°C in Tris buffer was assessed on a weekly basis for the first four weeks and then fortnightly thereafter; the total period of assessment was 12 weeks. The cytotoxicity of this batch was assessed upon purification with a cytotoxicity titre 100 % rounding at 10^{-24}. The cytotoxic activity remained at 10^{-24} for 1 month after which a gradual reduction in activity was recorded. After two months of storage at 4°C the cytotoxic activity was 10^{-14} and by the third month cytotoxic activity had fallen to 10^{-4}

Due to the shortage of toxin B; analysis of the frozen samples was only completed twice, the cytotoxic activity being established prior to freezing and checked after one week.

The remaining purified toxin B from this batch was used in experiments investigating the intestinal epithelial cell response to toxin B and as discussed in Chapter 5, the cytoxicity of this batch of toxin B stored at -80°C had lost considerable biological activity, with the pre-frozen titre established at a concentration of 10^{-24} and the defrosted toxin B sample at 10^{-5} when the cytotoxicity was checked.

My characterization of purified toxin B supports early findings which highlight the instability of the purified toxin, however my findings suggest the purified toxin can be stored for at least eight weeks before a reduction in biological activity is observed. Unless otherwise stated, all toxin B experiments were conducted with purified toxin stored at 4°C in Tris buffer and the cytotoxic activity established using Vero cells as discussed previously prior to application.

4.5 Discussion

In contrast to toxin A purification, which has been successfully purified within the institute over many years, toxin B purification has proven more difficult. The initial aim of my protocol was to see if toxin B could be purified after depletion of toxin A via the thyroglobulin column. Whilst the thyroglobulin column removed most of the toxin A, a considerable amount of toxin A was still found in supernatant samples even after two consecutive applications to the column and ammonium sulphate precipitation. This was supported by a confirmatory dot blot of fractions eluted from the DEAE column indicating strong immunoreactivity to the PCG-4 antibody. The inclusion of a stepped

salt gradient with an extended wash segment resulted in the successful separation of toxin A and toxin B. With other modifications to the protocol, namely the change to the buffer used and a reduction in the flow rate used during the elution of toxin from the Mono-Q column, toxin B has been purified with only minor contamination. Removal of the thyroglobulin column and an increase in starting supernatant has ensured a greater yield and the reduction in purification time has resulted in greater cytoxicity activity in purified toxin B.

The successful purification of toxin B has allowed studies on Caco-2 and HT29 cells to be carried out and comparative studies of the responses to toxin A, B and A+B by primary colonic myofibroblasts.

CHAPTER 5

5 Caco-2 cells are more sensitive to toxin B-induced cell death than HT29 cells

5.1 Introduction

The primary target of luminal *C. difficile* toxins is believed to be the intestinal epithelial cells and as discussed in the introduction to Chapter 3 the response of epithelial cells may determine the severity of mucosal inflammation. Following on from my toxin A investigations on intestinal epithelial cells my interest naturally turned to epithelial cell response to toxin B.

Our understanding of the role of toxin B in the pathogenesis of *Clostridium difficile* associated disease (CDAD) has become clearer over the last thirty years. With early claims suggesting the bacteria only produced one cytotoxin, early animal experiments suggested only toxin A mediated *C. difficile* associated diarrhoea and enterocolitis whilst others argued that toxin B was unable to elicit disease in the absence of toxin A. In 1995 Reigler reported that the human colon was 10 times more sensitive to toxin B than A and may therefore be more important in *C. difficile* pathogenesis (Riegler, Sedivy et al. 1995). It was in 2003, after the isolation of toxin A-negative toxin B-positive toxigenic strains, that toxin B was considered as a major virulence factor in CDAD (Johnson, Sambol et al. 2003; Komatsu, Kato et al. 2003; Rupnik, Kato et al. 2003). This belief was supported by Savidge and colleagues who by generating a chimeric animal model using human intestinal xenografts found that toxin B caused similar pathophysiological response to that observed with toxin A (Savidge, Pan et al. 2003). What is clear today is toxin B is a powerful cytotoxin

which is significantly more potent than the enterotoxic activity of toxin A. Investigation of epithelial response to toxin B will complement my research, comparing my observations of epithelial cell responses with the response of these cell types to toxin B.

Utilising a similar mechanism to toxin A, toxin B secreted by toxigenic *Clostridium difficile* into the lumen preferentially binds to receptors located on the basolateral surface of the host cell (Stubbe, Berdoz et al. 2000). The toxin is then internalised by receptor mediated endocytosis and following acidification the catalytic domain is translocated into the cytosol whereby it inactivates small GTPases, Rho, Rac and CDC-42 (Just, Fritz et al. 1994; Just, Selzer et al. 1995). The inactivation of these key molecular switches alters cell signalling and ultra structural maintenance leading to dramatic changes in cell physiology (Just and Gerhard 2004; Jaffe and Hall 2005).

Early research reported dramatic phenotypic alterations in non-intestinal epithelial cells exposed to *C. difficile* toxin B which appeared to occur as a secondary response to the toxin induced actin re-organisation (Mitchell, Laughon et al. 1987; Fiorentini, Fabbri et al. 1998). Interested in the response of intestinal epithelial cells to toxin B, Hecht cultured T84 cells reported a similar response in T84 cells to that reported in non-intestinal epithelial cells. T84 cells rounded and barrier function was reduced due to a toxin induced alteration at the tight junction but cell death was not reported. (Hecht 1992).

Looking to further investigate the cellular response to toxin B, Chaves Olarte investigated the response of Don and T84 cells to toxins A and B

(Chaves-Olarte, Weidmann et al. 1997) and reported toxin B to be 1,000 times more potent than toxin A and microinjection of toxins A and B established that this difference was due to greater enzymatic activity of toxin B and to a lesser extent, toxin binding. Supporting these findings Ciesla et al found a significant catalytic difference when comparing UDP-glucose hydrolysis in toxin B and toxin A exposed cells (Ciesla and Bobak 1998).

Comparing the morphological changes induced by toxins A and B in a selection of cultured cells, Donta et al reported toxin B as more active than toxin A and of particular interest, they also reported no significant difference in the cellular sensitivities across the cell types to toxin B (Donta, Sullivan et al. 1982). In contrast, a greater variation in cellular response was reported in toxin A exposed cells (Donta, Sullivan et al. 1982). Of particular interest, a similar comparative study conducted by Fiorentini et al suggested the origin and proliferative rate of the target cell may also contribute to the toxin B induced response (Fiorentini, Fabbri et al. 1998). Using IEC-6, Int407, HT29 and A431, Fiorentini revealed toxin B to be a time and dose dependent inducer of apoptosis. Comparative research using rabbit ileal loops and cultured cells established some contrasting and competing evidence. Whilst toxin A and B produce an additive effect on cultured cells, exposure of rabbit ileal loops to A and B worked in synergy to cause disease only at high doses (Fiorentini, Fabbri et al. 1998).

The aim of this work is to compare responses to *C. difficile* toxin B by Caco-2 and HT29 human intestinal epithelial cells.

5.2 Materials and methods

5.2.1 Purification of toxin B

Toxin B was purified using the revised protocol as outlines in Chapter 4. In brief, toxin B was by ammonium sulphate precipitation of cultured *C. difficile* (VPI 10463) supernatant samples followed by two sequential anion exchange chromatographic steps as detailed in Chapter 4, 4.3. Protein concentration and cytotoxic activity were established prior to use.

As highlighted in Chapter 4, purified toxin B is extremely fragile with degradation and loss of biological activity observed within one week of purification. It has therefore been essential to assess cytotoxic activity and protein concentration prior to commencing any experiments. Section 5.4.1 of this Chapter will highlight the importance of establishing protein concentration and biological activity of toxin B before experimentation.

5.2.2 Early experiments

Having already investigated the response of intestinal epithelial cells to *C. difficile* toxin A and establishing a cell specific response in which Caco-2 cells are more sensitive to toxin A-induced cell death, I was interested to see if this sensitivity was also apparent when the cells were exposed to toxin B. Intestinal epithelial cells, Caco-2 and HT29 were grown to 70% confluence in 24-well plates and using similar toxin B concentrations to those used in early toxin A experiments, morphological assessments were made at 1, 2, 3, 24, 48 and 72 hours. Cell viability was assessed using the MTT assay at 72 hours.

5.2.2.1 *Effect of seeding densities on epithelial cell response*

Caco-2 and HT29 cells were seeded at 4.5 x 10^5, 9.0 x 10^4 and 2 x 10^4 and grown for 24 hours. At 24 hours, the media was replaced with 1000 ng/ml toxin B in DMEM supplemented for either Caco-2 or HT29 cells and morphological assessments made at 1 h, 2 h, 4 h and 24 h.

5.2.2.2 *Intestinal epithelial cell and Vero cell response compared*

As previously discussed the African Green Monkey (Vero) cell response is the gold standard cell type used to establish the cytotoxicity of *C. difficile* toxins. Using, Caco-2, HT29 and Vero cells seeded in 96 well plates cellular responses were recorded at 24 h and 48 h. Toxin B was taken from two separate batches and serial dilutions were prepared with either a starting concentration of 10,000 ng/ml or 1,000 ng/ml in the less concentrated batch samples. Morphological assessments were made at 24 h and 48 h. Cytotoxicity was recorded as lowest possible concentration to induce 50% rounding at 24 h and 48 h.

The findings from these experiments were used to structure future work using *C. difficile* toxin B.

5.3 Epithelial cell response to *Clostridium difficile* toxin B

Caco-2 and HT29 cells were seeded, grown to 40% confluence and exposed to serial dilutions of toxin B ranging from 1 000 ng/ml through 10 ng/ml, prepared using a previously characterized fraction of toxin B with a known concentration of 0.73 mg/ml and a pre-experimental cytotoxicity

titre of at least 10^{-16} at 24 hours. Cells were incubated with toxin B for 72 h. Morphological assessments were made hourly from 1 h to 72 h.

5.3.1 Cell cytotoxicity established using MTT assay

Cell cytotoxicity was measured in Caco-2 and HT29 cells incubated with varying concentrations of *C. difficile* toxin B at 48 h and 72 h using the MTT assay as described in Chapter 2, section 2.7.1.

5.3.2 Propidium Iodide staining and cell cycle analysis

Cell cycle analysis was performed on Caco-2 and HT29 cells incubated with 1000 ng/ml of toxin B for 8, 24, 48 and 72 hours using propidium iodide and flow cytometry as described in Chapter 2, section 2.7.3. Toxin-exposed cells were compared with cells cultured with control medium, seeded at the same time and obtained at the same time points as those cultured in the presence of the toxin.

5.3.3 Rho protein expression

Investigation of Rho signalling in intestinal epithelial cells was completed using whole cell lysates from HT29 and Caco-2 cells in control and toxin B treated samples and the western blot technique using Rho specific antibodies for detection. See Chapter 2 section 2.8. The proteins investigated included Rac-1, RhoA. β-actin was used as a loading control.

HT29 and Caco-2 intestinal epithelial cells were incubated with 1,000 ng/ml toxin B or control medium for 0 h, 3 h, 8 h, and 24 h. A western

blot was completed for each protein to be investigated, including a loading control. A colour scan was made of each western blot.

5.4 Results Intestinal epithelial cell response to *C. difficile* toxin B

5.4.1 Initial experiments identified low biological activity in toxin B

Early experiments investigated the morphological changes and cell viability of intestinal epithelial cells to *Clostridium difficile* toxin B. Using a toxin sample with a pre-frozen cytotoxicity of titre of 10^{-24}, serial dilutions were performed as previously described and applied to sub-confluent epithelial cells, Caco-2 and HT29. Morphological assessments were made at 1, 2, 3, 24, 48 and 72 hours. With only minimal rounding after 24 hours at the highest concentrations, cytotoxic activity of this thawed batch of toxin B was rechecked in Vero cells. The thawed sample had lost considerable biological activity and the new titre was 10^{-5}. It was not until 48 hours that 50 % rounding was visible at 1000 ng/ml and at 72 hours rounding had risen to 100% and 50% at the two highest concentrations 1000 ng/ml and 100 ng/ml, respectively. Given the limited biological activity seen, it was decided to only complete the cell viability assay at 72 h. As can be viewed in Figure 5-1 A, a small (not statistically significant) dose dependent reduction of cell viability measured using the MTT assay was apparent in Caco-2 cells exposed to toxin B. HT29 cells provided an inconclusive picture with lower concentrations displaying a reduction but the highest concentration giving an increase in mitochondrial dehydrogenase activity and hence cell viability. It is worth noting that the reduction or increase in mitochondrial dehydrogenase activity is not statistically significant, see Figure 5-1 B. Comparison of mitochondrial dehydrogenase activity in untreated control and toxin treated cells at 1000

ng/ml for 72 hours (Figure 5-2) confirmed a small (non-significant) reduction in cell viability of Caco-2 cells exposed to 1000 ng/ml for 72 hours and a small (non-significant) increase in cell viability of HT29 cells exposed to the same concentration for 72 hours.

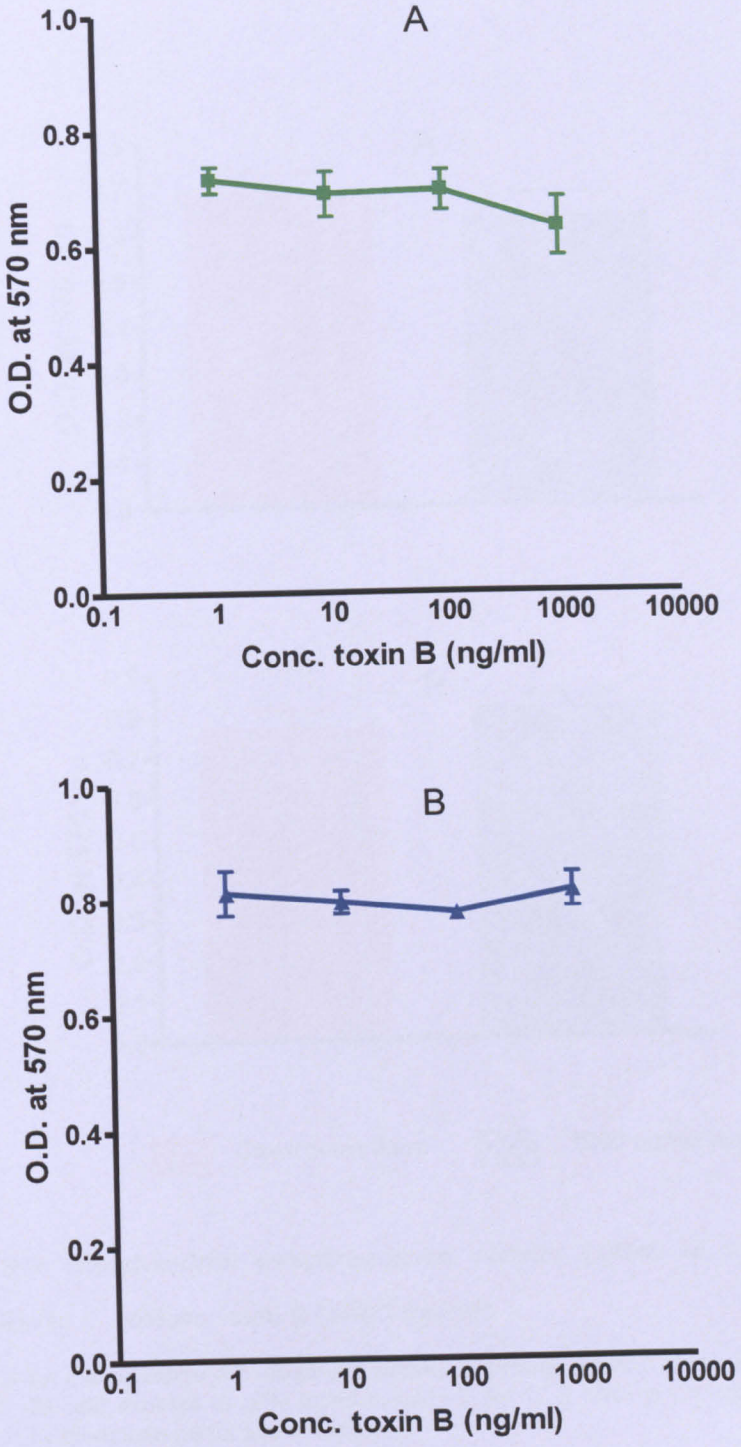

Figure 5-1 Mitochondrial dehydrogenase activity (MDA) in Caco-2 and HT29 cells to *C. difficile* toxin B (1-1000 ng/ml)

MTT assay for mitochondrial dehydrogenase activity (expressed as OD 570 nm) in (A) Caco-2 cells and (B) HT29 cells exposed to varying concentrations of toxin B for 72 h. Data in figures represent mean (±SEM) of 3 experiments performed in triplicate.

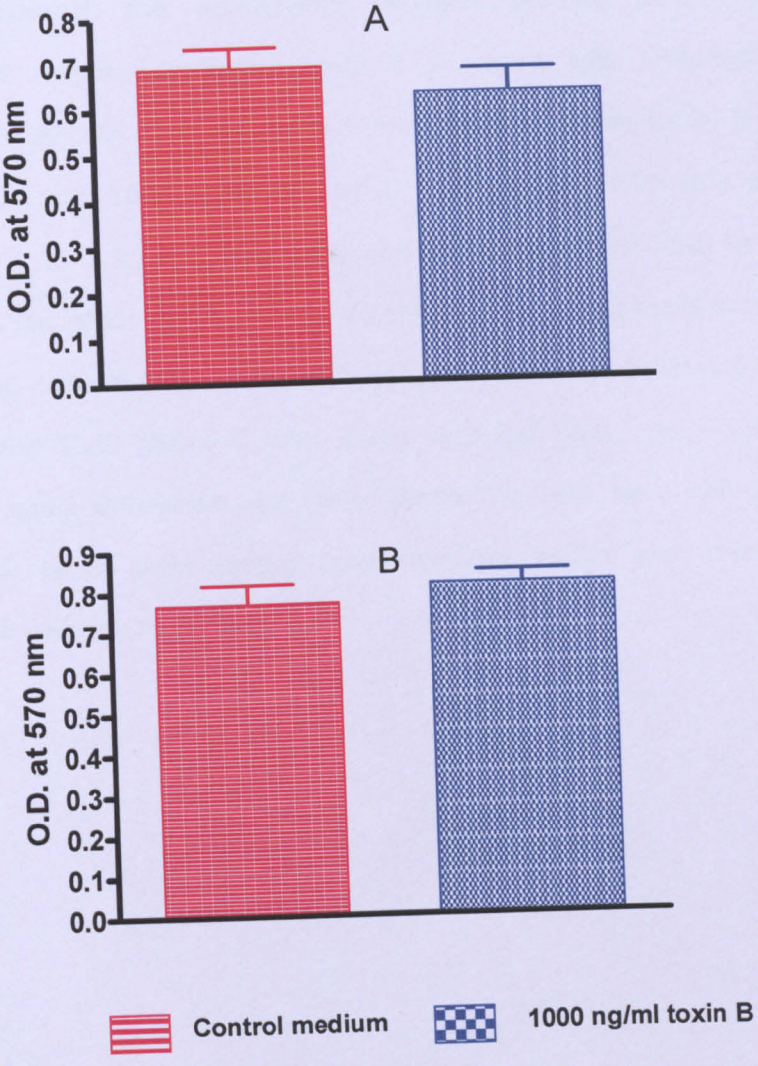

Figure 5-2 Mitochondrial dehydrogenase activity (MDA) in Caco-2 and HT29 cells to *C. difficile* toxin B (1000 ng/ml)

MTT assay for mitochondrial dehydrogenase activity (expressed as OD 570 nm) in Caco-2 (A) and HT29 (B) cells exposed to 1000 ng/ml of toxin B for 72 h. Data in bars represent mean (±SEM) of 3 experiments performed in triplicate.

5.4.2 Seeding density and % confluence on epithelial cell response.

Establishing loss of biological activity as the primary reason for the response observed, the relationship between seeding density and morphological response following toxin B exposure was investigated. Caco-2 and HT29 cells were seeded at three densities, grown for 24 h and then incubated with 1000 ng/ml of toxin B. Caco-2 and HT29 cells were observed at 1 h, 2 h, 4 h and 24 h and percentage rounding, to the nearest 10% recorded. As can be viewed in Table 5-1, using these seeding densities and subsequent cell monolayer confluence no difference was observed using 1000 ng/ml of toxin B for each cell type. As would be expected a small difference was noted when the cells were compared against each other with Caco-2 cells rounding earlier and rounding percentage increasing to a higher rate.

Table 5-1 Seeding density and percentage cell rounding in Caco-2 and HT29 cells to *C. difficile* toxin B

Percentage rounding in Caco-2 and HT29 cells seeded at 4.5×10^5, 9.0×10^4 and 2.0×10^4. Percentage cell rounding assessed at 1 h, 2 h, 4 h and 24 h post toxin exposure. All cells exposed to 1000 ng/ml toxin B.

	Seeding density (cells / ml)													
	4.5×10^5					9.0×10^4					2.0×10^4				
	% rounding				% confluence at 24 h	% rounding				% confluence at 24 h	% rounding				% confluence at 24 h
Exp (h)	1	2	4	24		1	2	4	24		1	2	4	24	
Caco-2	10	20	50	100	70 %	10	20	50	100	45 %	10	20	50	100	35 %
HT29	0	10	30	100	75 %	0	10	40	100	55 %	0	10	40	100	45 %

5.4.3 Cytotoxic comparison of Caco-2 and HT29 cells to *C. difficile* toxin B

Subsequent experiments investigated the response of intestinal epithelial cells, Caco-2 and HT29, to varying concentrations of *C. difficile* toxin B ranging 10 ng/ml through to 1 000 ng/ml. A new batch of purified toxin B was used and the cytotoxicity established prior to starting the experiment as 10^{-16} (lowest dilution to induce 50% rounding at 24 h). Morphological changes were assessed from 1 h - 72 h and cellular viability/cytotoxic effect established at 24, 48 and 72 h.

5.4.3.1 Alterations to cell morphological

Morphological assessment was made using light microscopy and the cells in each well categorized into one of three morphological stages; no visible rounding; 50% visible rounding and 100 % visible rounding. Detailed phase contrast micrographs of toxin treated and control HT29 and Caco-2 cells can be observed in Figure 5-3, Figure 5-4, Figure 5-5, Figure 5-6, Figure 5-7, Figure 5-8 and Figure 5-9. Cell rounding occurred in a time- and dose-dependent manner with 50% and 100% rounding observed in Caco-2 cells after 1 h incubation with 100 ng/ml and 1000 ng/ml, respectively. Rounding in HT29 was first observed at 2 h to 1000 ng/ml, see Table 5-2. As observed with *C. difficile* toxin A, an increase in non-adherent Caco-2 cells was observed from 24 h (Figure 5-7) to 1000 ng/ml and by 72 h (Figure 5-9) most cells appeared to be floating with morphological characteristics of non-viable cells. In contrast to the observed adherence of HT29 cells incubated with *C. difficile* toxin A, cell incubated with 1000 ng/ml toxin B appeared to be losing adherence with some cells observed floating at 48 h (Figure 5-8) and 72 h (Figure 5-9).

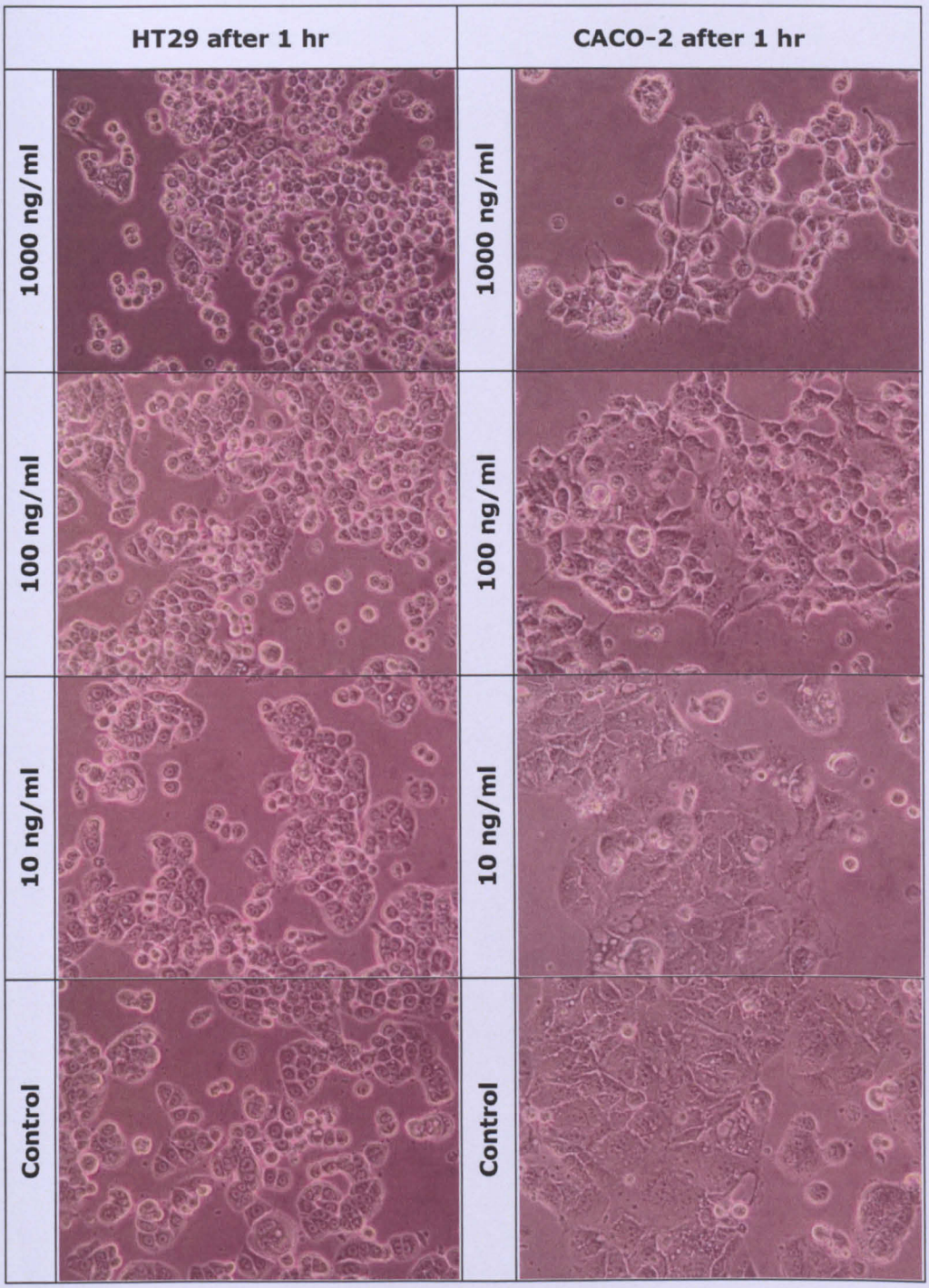

Figure 5-3 Phase contrast micrographs of Caco-2 and HT29 cells incubated with *C. difficile* toxin B for 1 h

Intestinal epithelial cells Caco-2 and HT29 grown to 40% confluence were incubated with purified toxin B (10-1000 ng/ml) or control medium.

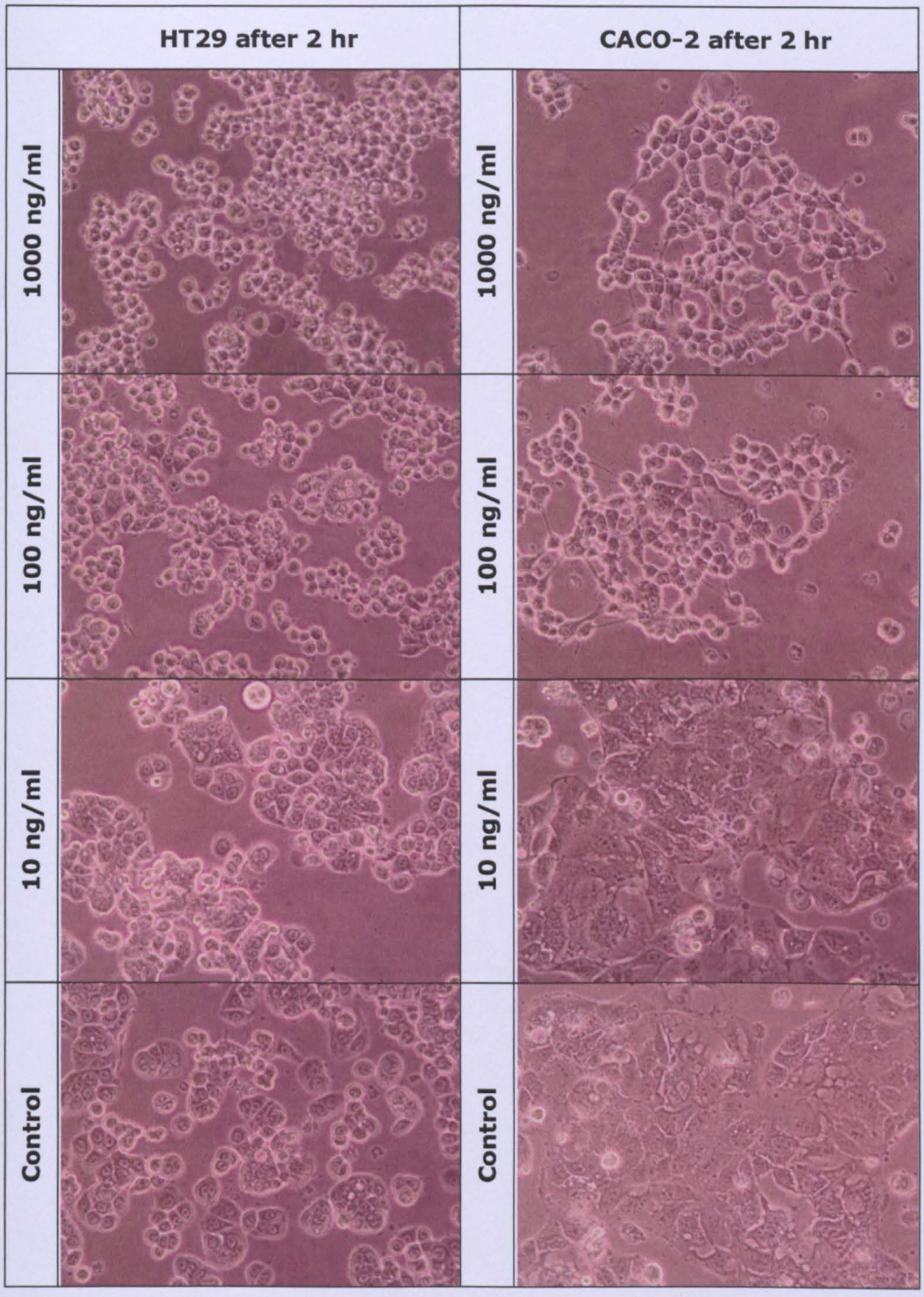

Figure 5-4 Phase contrast micrographs of Caco-2 and HT29 cells incubated with *C. difficile* toxin B for 2 h

Intestinal epithelial cells Caco-2 and HT29 grown to 40% confluence were incubated with purified toxin B (10-1000 ng/ml) or control medium.

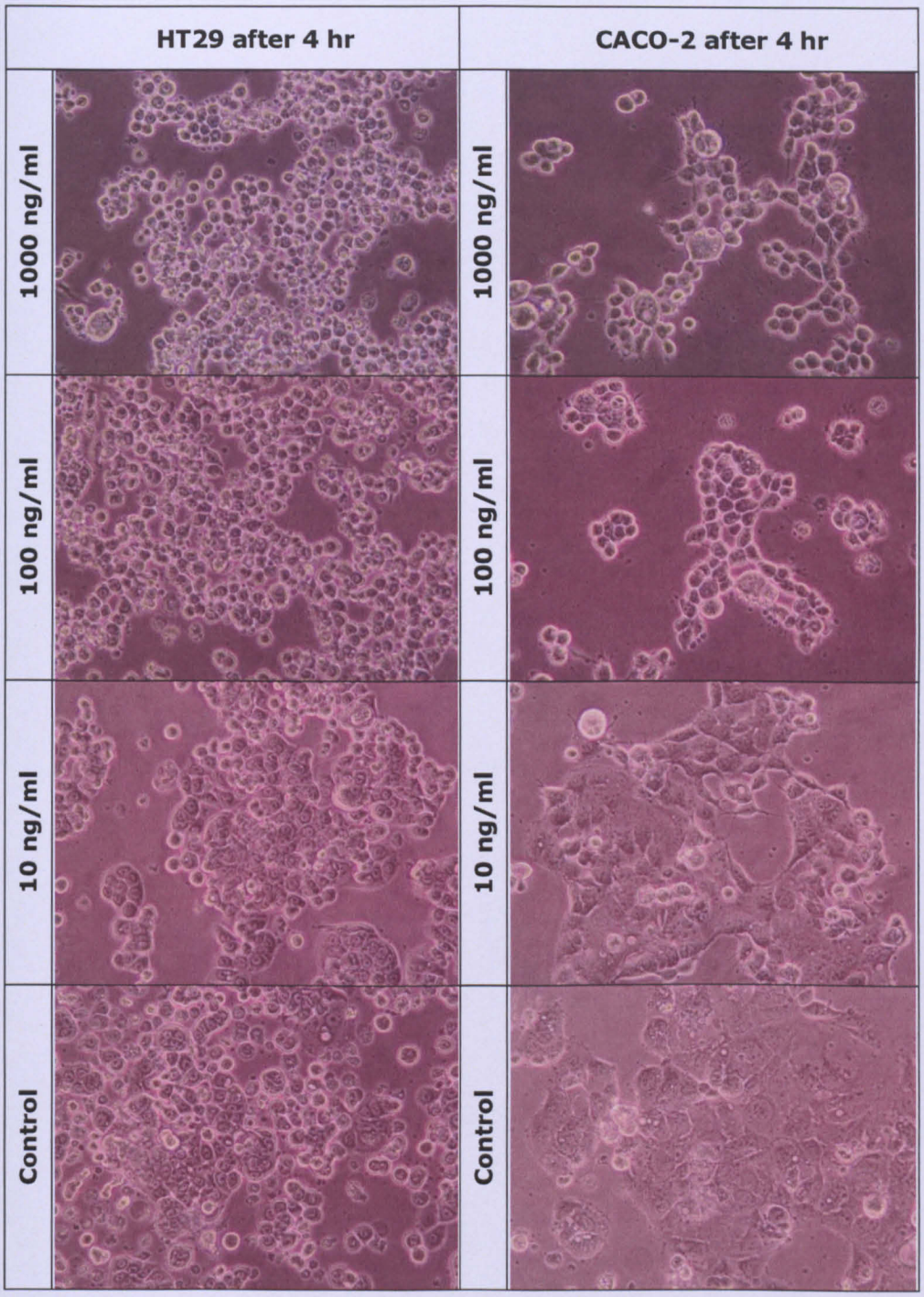

Figure 5-5 Phase contrast micrographs of Caco-2 and HT29 cells incubated with *C. difficile* toxin B for 4 h

Intestinal epithelial cells Caco-2 and HT29 grown to 40% confluence were incubated with purified toxin B (10-1000 ng/ml) or control medium.

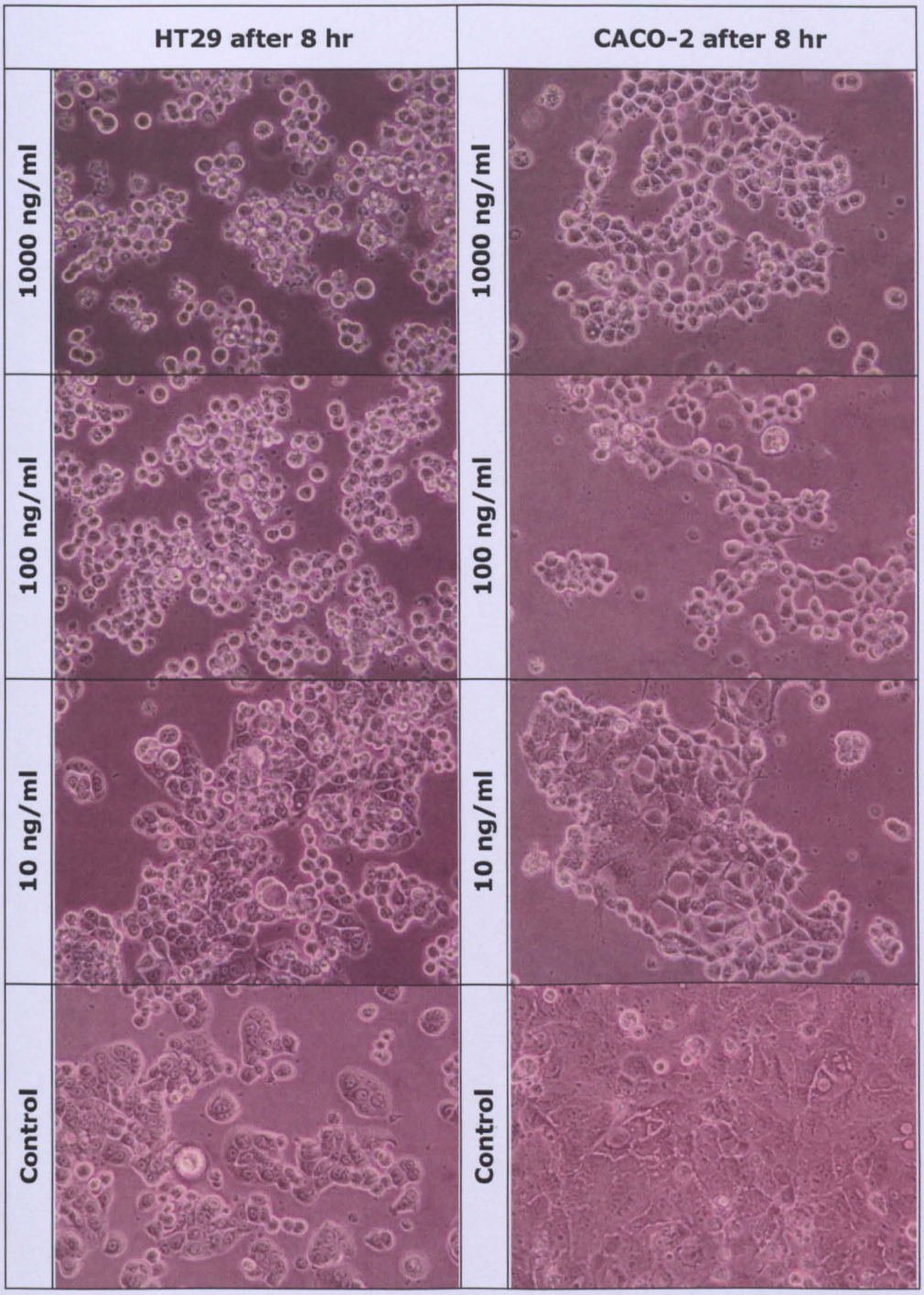

Figure 5-6 Phase contrast micrographs of Caco-2 and HT29 cells incubated with *C. difficile* toxin B for 8 h

Intestinal epithelial cells Caco-2 and HT29 grown to 40% confluence were incubated with purified toxin B (10-1000 ng/ml) or control medium.

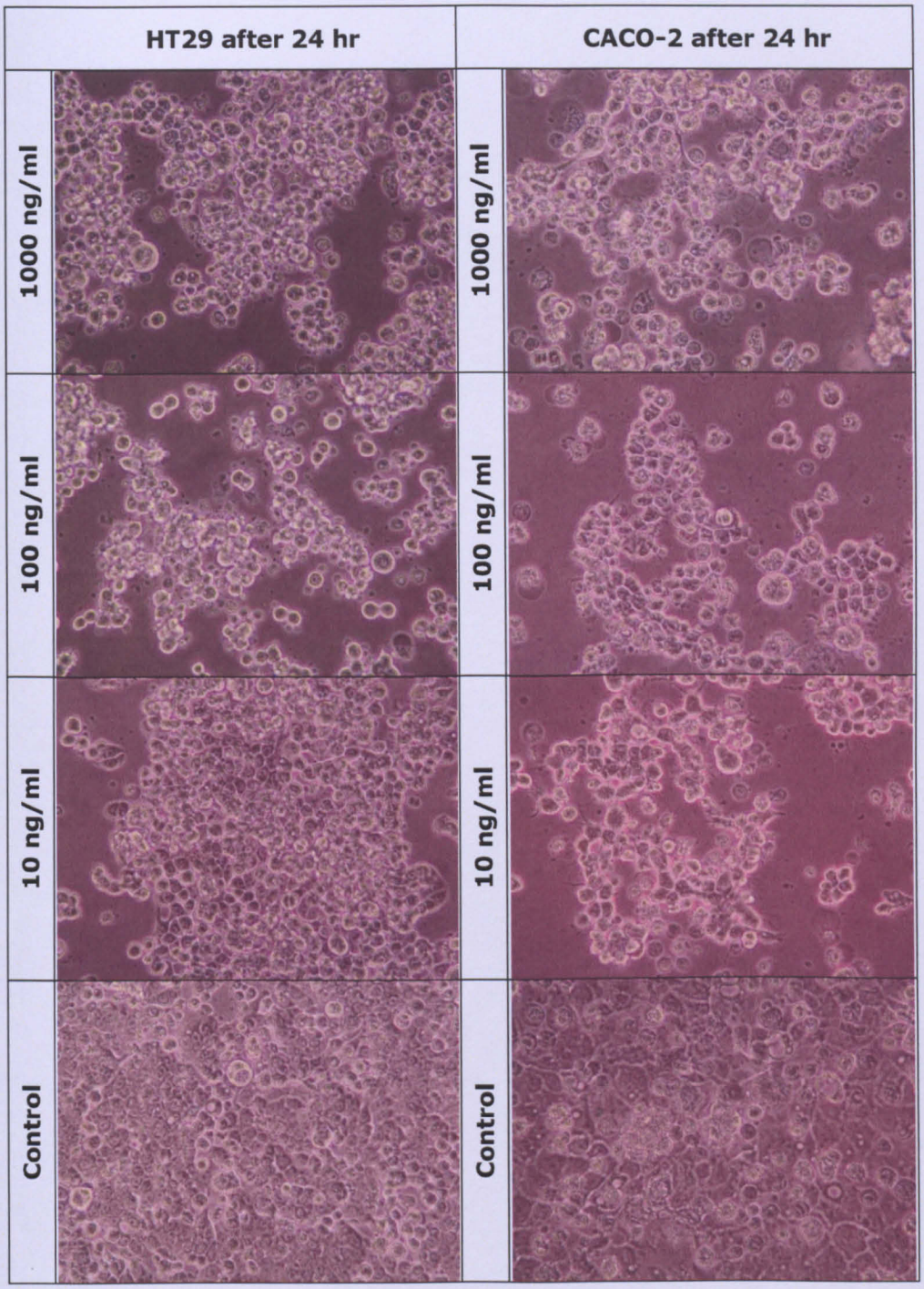

Figure 5-7 Phase contrast micrographs of Caco-2 and HT29 cells incubated with *C. difficile* toxin B for 24 h

Intestinal epithelial cells Caco-2 and HT29 grown to 40% confluence were incubated with purified toxin B (10-1000 ng/ml) or control medium.

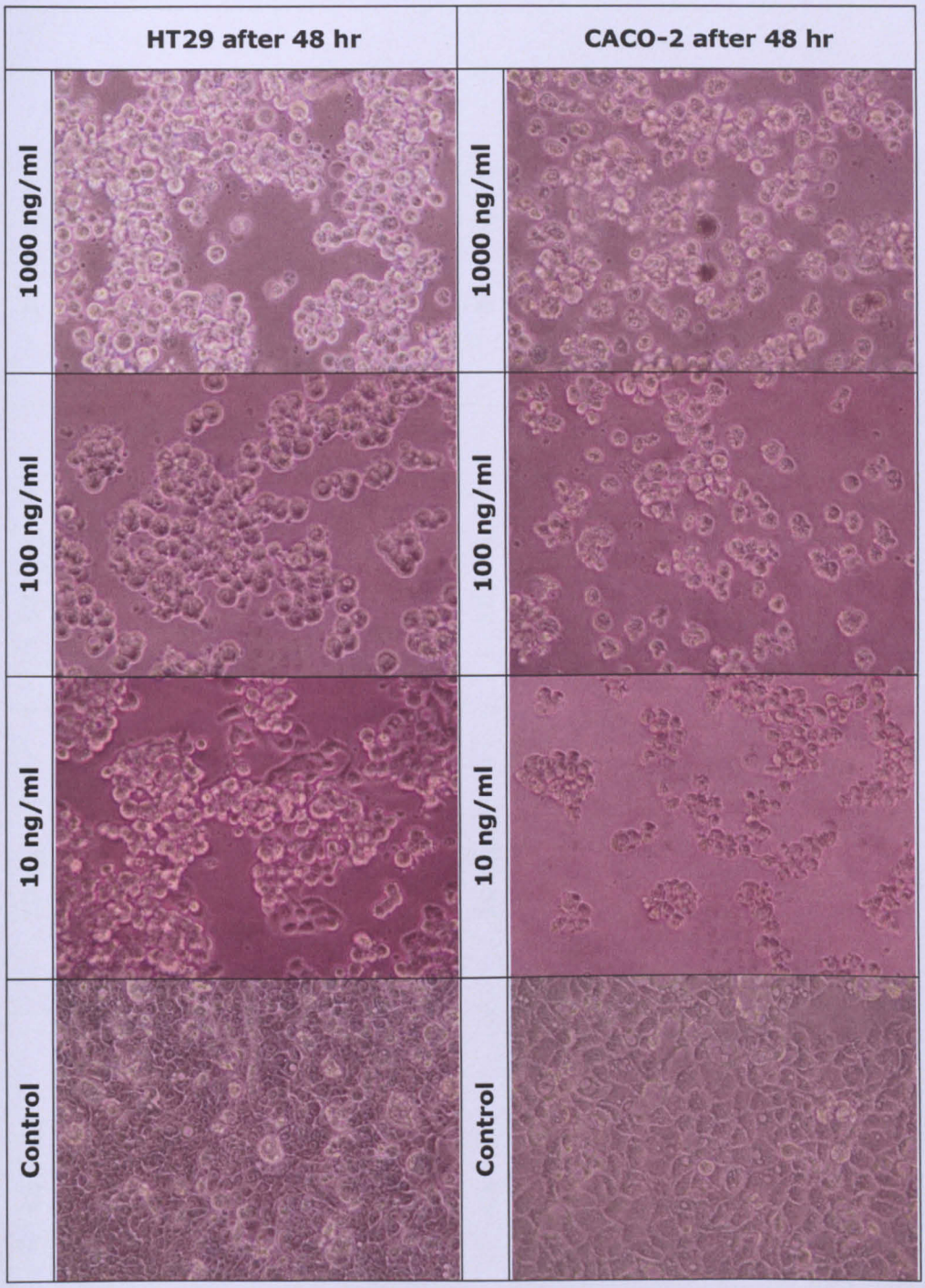

Figure 5-8 Phase contrast micrographs of Caco-2 and HT29 cells incubated with *C. difficile* toxin B for 48 h

Intestinal epithelial cells Caco-2 and HT29 grown to 40% confluence were incubated with purified toxin B (10-1000 ng/ml) or control medium.

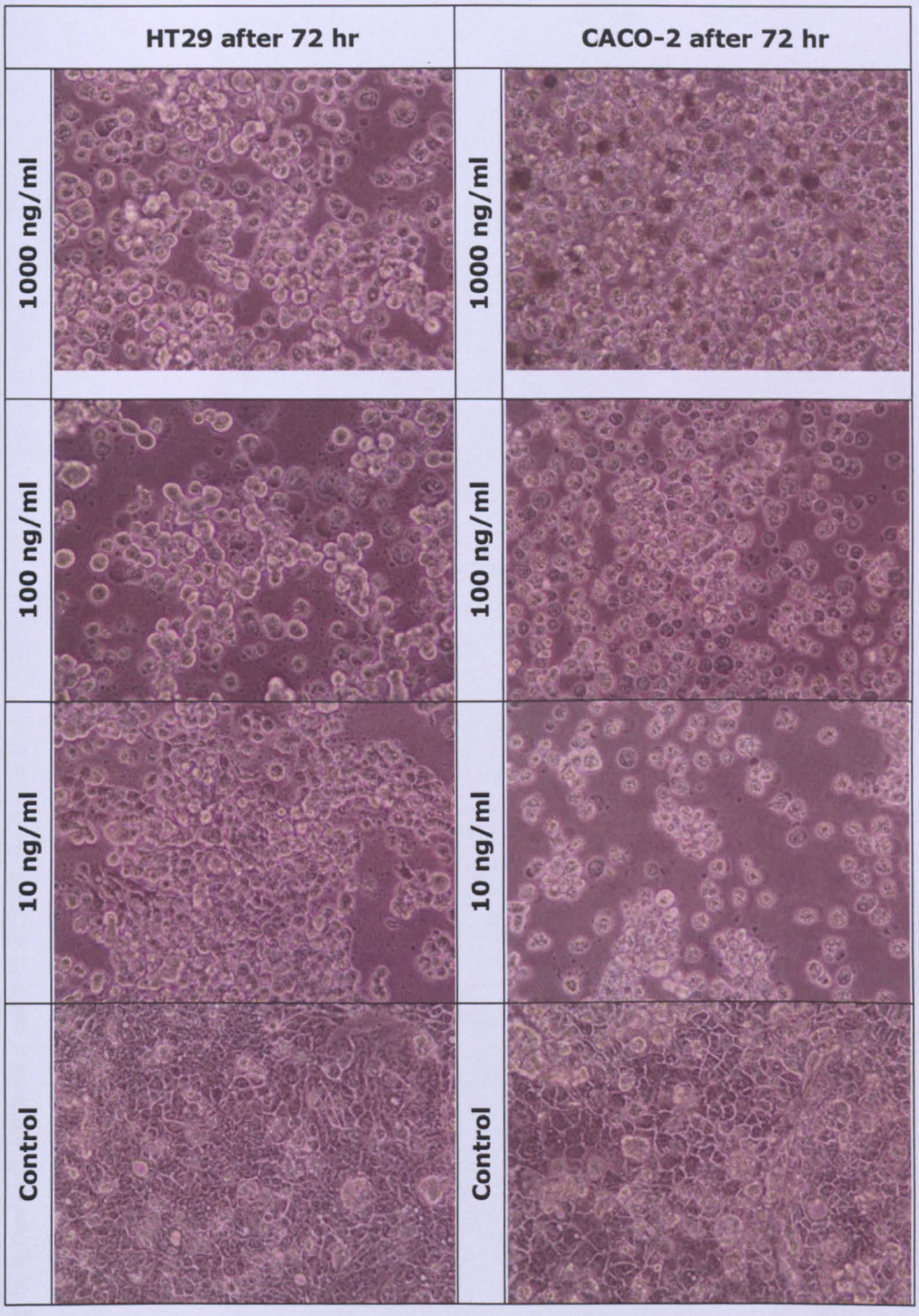

Figure 5-9 Phase contrast micrographs of Caco-2 and HT29 cells incubated with *C. difficile* toxin B for 72 h

Intestinal epithelial cells Caco-2 and HT29 grown to 40% confluence were incubated with purified toxin B (10-1000 ng/ml) or control medium.

Table 5-2 Cell rounding in intestinal epithelial cells to *C. difficile* toxin B

Cell rounding; 100% (+) or 50% (+/-) in Caco-2 and HT29 cells in response to varying concentrations of toxin B. The data is representative of three experiments completed in triplicate. The percentage rounding was ascertained by observing the rounded cells in ten random high power fields and taking the subjective mean of these ten observations.

Toxin B (ng/ml)	Duration of toxin B exposure													
	1 hour		2 hours		4 hours		8 hours		24 hours		48 hours		72 hours	
	Caco-2	HT29	Caco-2	HT29	Caco-2	HT29	Caco-2	HT29	Caco-2	HT29	Caco-2	HT29	Caco-2	HT29
10	-	-	-	-	+/-	-	+/-	-	+	+/-	+	+	+	+
100	+/-	-	+	-	+	+	+	+	+	+	+	+	+	+
1000	+	-	+	+	+	+	+	+	+	+	+	+	+	+

5.4.4 Investigation of cellular viability using the MTT assay

Cell viability was established after 24 h, 48 h and 72 h (Chapter 2, 2.7.1).

5.4.4.1 Caco-2 cellular viability – 10 ng/ml – 1 000 ng/ml toxin B

Caco-2 intestinal epithelial cells exposed to *C. difficile* toxin B showed a reduction in mitochondrial dehydrogenase activity, which reflects cell viability, in a time and dose dependent manner. A significant reduction in cell viability was seen when Caco-2 cells were exposed to concentrations of toxin ≥1000 ng/ml at 48 hours, at 72 hrs highly significant reduction in cell viability was observed when compared to control (untreated cells) (Table 5-3). Of interest, although a dose dependent response was observed at the later time points, cellular viability in Caco-2 cells remained fairly consistent at 24 hours with minimal reduction in cell viability when the concentration of toxin B was increased, see Figure 5-10 A. Cells exposed to concentrations <1000 ng/ml presented with some loss of cell viability, however not significantly so, even after 72 hour exposure to the toxin (Table 5-3 A).

5.4.4.2 HT29 cellular viability – 10 to 1 000 ng/ml toxin B

HT29 intestinal epithelial cells exposed to *C. difficile* toxin B showed a small reduction in mitochondrial dehydrogenase activity reflecting a time dependent loss of cell viability by 72 hours, see Table 5-3. No significant difference was noted at 24 h 48 h or 72 h at any concentration when compared against control (untreated cells), see Table 5-3 B. Observing Figure 5-10 B, a dose dependent response was not observed as viability remained largely constant across all three concentrations investigated.

Table 5-3 Mitochondrial dehydrogenase activity (MDA) in Caco-2 and HT29 cells to *C. difficile* toxin B (10-1000 ng/ml)

MTT assay for mitochondrial dehydrogenase activity (expressed as OD 570 nm) in (A) Caco-2 cells and (B) HT29 cells exposed to varying concentrations of toxin B for 24 h, 48 h and 72 h. Data in table presents mean (±SEM) of 3 experiments performed in triplicate. ** = $p<0.01$ * = $p<0.05$ when compared with control (Cytotoxicity of toxin B on Vero cells 10^{-16})

A

Conc. (ng/ml)	Period of exposure (h)		
	24	48	72
Control	0.4613 ± 0.0198	0.4450 ± 0.0092	0.4187 ± 0.0171
10	0.4623 ± 0.0196	0.4597 ± 0.0035	0.4227 ± 0.0073
100	0.4537 ± 0.0191	0.4350 ± 0.0158	0.3817 ± 0.0189
1000	0.4693 ± 0.0174	0.3880 ± 0.0074 **	0.2633 ± 0.0209 *

B

Conc. (ng/ml)	Period of exposure (h)		
	24	48	72
Control	0.4927 ± 0.0030	0.4730 ± 0.0116	0.4753 ± 0.0092
10	0.4933 ± 0.0134	0.4840 ± 0.0059	0.4693 ± 0.0159
100	0.4783 ± 0.0128	0.4680 ±0.0100	0.4490 ± 0.0030
1000	0.4943 ± 0.0113	0.4943 ± 0.0030	0.4653 ± 0.0104

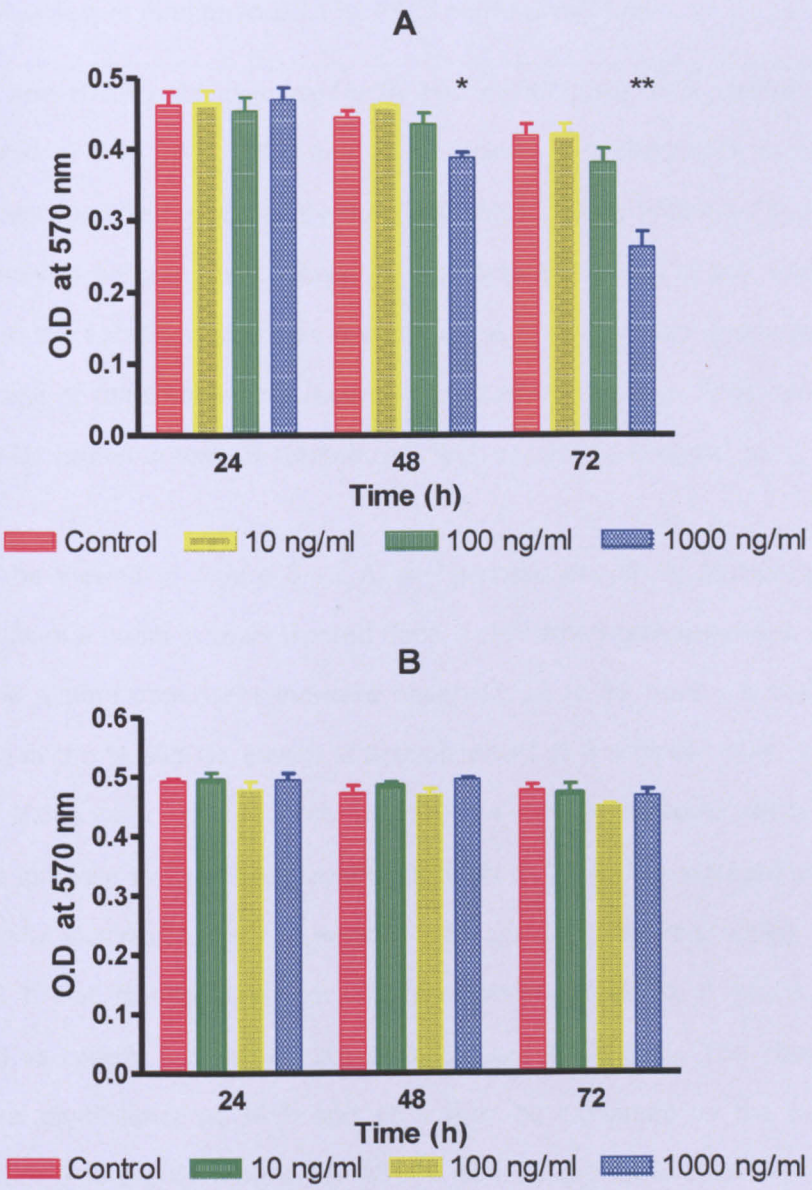

Figure 5-10 Mitochondrial dehydrogenase activity (MDA) in Caco-2 and HT29 cells to *C. difficile* toxin B (10-1000 ng/ml)

MTT assay for mitochondrial dehydrogenase activity (expressed as OD 570 nm) in Caco-2 (A) and HT29 (B) cells exposed to varying concentrations of toxin B for 24 h, 48 h and 72 h. Data in bars represent mean (±SEM) of 3 experiments performed in triplicate. *= $p<0.05$ **= $p<0.01$ when compared with control.

5.4.5 Analysis of PI stained DNA by FACS confirm cell loss

Caco-2 and HT29 cells incubated with 100 ng/ml toxin B or control media were fixed at 8 h, 24 h, 48 h and 72 h, stained with Propidium Iodide and fluorescence emitted assessed by flow cytometry. Using WinMDI 2.9 and cell cycle analysis programme Cyclhred as described in Chapter 2 the number of events in the sub-G1 region was ascertained and this number presented as a percentage of the total events recorded, comparing the percentage events in the sub-G1 region in toxin B-treated cells with control (untreated) cells.

As can be viewed in Figure 5-11 A, an increase in the % Sub-G1 cells is evident from 8 hours in toxin treated Caco-2 cells when compared with control cells and a time dependent increase observed up to 72 hour. A significant increase in the % sub-G1 events is first observed at 8 h [mean toxin 13.44% (±SEM 2.38) vs control 3.77% (±0.52) $p=<0.05$], however despite the obvious increase in % sub G1 events through to 72 h, the increase was not statistically significant when compared with control (untreated cells) at 24h and 48 h but statistical significance was observed at 72 h [toxin 22.03 (±6.53) vs control 3.37% (±0.20) $p<0.05$], see Table 5-4. The absence of statistical significance at 24 h and 48 h may be explained by the range of results [24 h % sub G1 events 8%-23% & 48 h % sub G1 events 5% - 38 %] in toxin B exposed Caco-2 cells. By comparison a small (non-significant) time dependent increase in percentage of sub-G1 events in toxin B exposed HT29 cells is noted when compared with control (untreated) cells, see Figure 5-11 B.

Table 5-4 Sub-G1 events in toxin treated Caco-2 and HT29 cells

Percentage of sub-G1 events in toxin treated (100 ng/ml toxin B [Batch J2C, cytotoxic activity on Vero cells $x10^{-88}$]) and control (untreated cells at 8, 24, 48, and 72 h. Percentage calculated using total events and number of events in the sub-G1 region when analysed using Cyclhred. Data in figures represent mean (±SEM) of 3 experiments performed in triplicate. * $p<0.05$ when compared with control

		Caco-2		HT29	
		Control (untreated)	100 ng/ml toxin B	Control (untreated)	100 ng/ml toxin B
Period of exposure (h)	8	3.765 ± 0.5189	13.440 ± 2.376 *	3.125 ± 1.068	4.661 ± 2.420
	24	3.821 ± 0.3928	14.150 ± 4.836	4.324 ± 1.973	6.718 ± 4.631
	48	4.183 ± 0.2575	21.920 ± 9.550	5.221 ± 1.785	8.864 ± 3.930
	72	3.374 ± 0.2019	22.030 ± 6.531 *	5.369 ± 2.000	9.993 ± 4.047

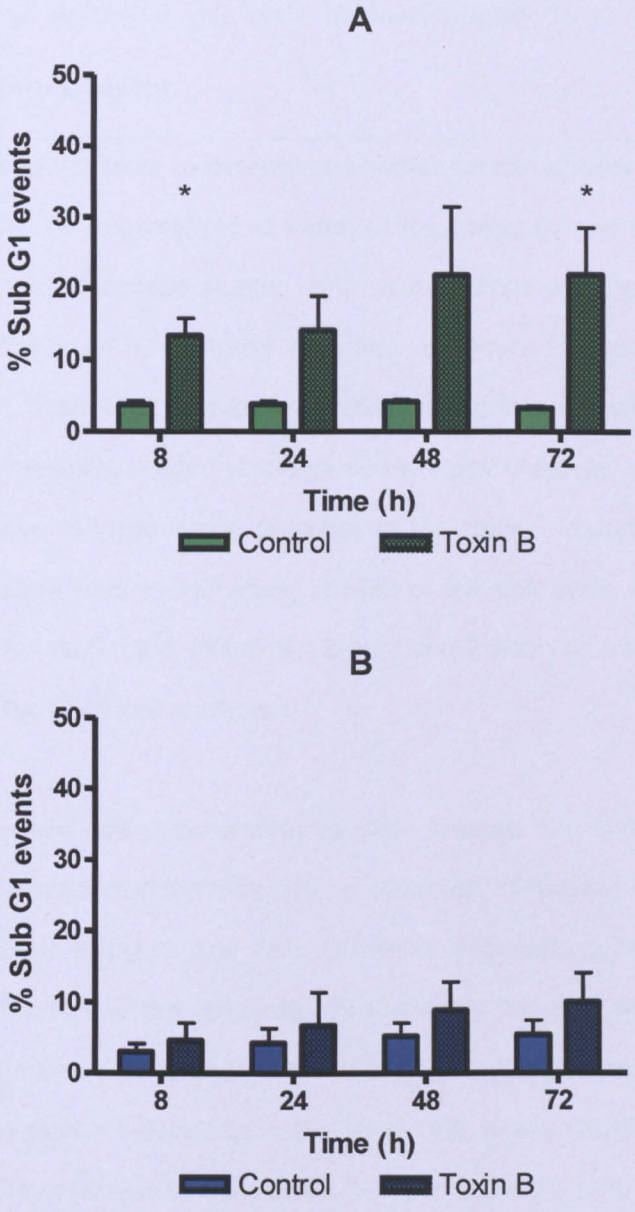

Figure 5-11 Percentage of sub-G1 events in Caco-2 and HT29 cells incubated with *C. difficile* toxin B (100 ng/ml)

Assessment of Caco-2 (A) and HT29 (B) events in the sub-G1 region of the cell cycle following exposure to 100 ng/ml toxin B (J2C, cytotoxic activity on Vero cells $x10^{-88}$) at 8, 24, 48 and 72 h. Percentage of sub-G1 events calculated using total events and number of events in the sub-G1 region when analysed using Cyclhred. Data in figures represent mean (±SEM) of 3 experiments performed in triplicate.

5.4.6 Role of epithelial cell cycle in susceptibility to *C. difficile* toxin B induced cell death

Studies were undertaken to determine whether certain phases of the cell cycle are under- or over-represented at various time points following exposure to *C. difficile* toxin B. For these studies, cell cycle analysis was performed by flow cytometry at 8 h, 24 h, 48 h and 72 h after exposure to toxin B as described in Chapter 2, page 94. Toxin-exposed cells were compared with cells cultured with control medium, seeded at the same time and obtained at the same time points as those cultured in the presence of the toxin. Statistically significant differences were seen in individual phases of the cell cycle at different time points, see Figure 5-12 & Figure 5-13 for Caco-2 analysis and Figure 5-14 & Figure 5-15 for HT29 cell analysis.

Comparing whole cell cycle profiles in toxin treated and control (untreated) Caco-2 cells a notable difference can be observed. Studying Figure 5-12, the profile produced using control cells (A) show a smooth parallel progression through each phase of the cell cycle. In stark contrast the cell phases in toxin B exposed Caco-2 cells change dramatically (B). Considering each phase of the cycle a significant decrease in the % of cells in the G0/G1 region (Figure 5-13 A) of the cycle was evident at 48 h [mean toxin 27.10% (±SEM 2.83) vs control 44.17% (±5.62) $p<0.05$] and 72 h [toxin 26.23 (±2.83) vs control 46.40% (±5.13) $p<0.05$] when compared with untreated G0/G1 events. Also of interest the % S-phase cells (Figure 5-13 B) in toxin treated cells was significantly lower at 8 hour [toxin 26.13% (±5.50) vs control 46.17 (±4.84) $p<0.05$], by 48 hours the % of cells in S-phase was similar to control cells.

Mirroring the S-phase response in toxin exposed Caco-2 cells the % toxin treated cells in the G2 region (Figure 5-13 C) was significantly higher than control at 8 h [toxin 48.3% (±6.38) vs control 15.6% (±1.56) $p<0.05$] and 72 h [toxin 47.3% (±8.00) vs control 16.07% (±2.18) $p<0.05$].

Whole cell cycle profiles of toxin treated and control (untreated) HT29 cells appear similar upon initial inspection (Figure 5-14 A & B), however an overall decrease in HT29 cells in the G0/G1 region can be observed and this reduction becomes significant 72 h exposure [toxin 59.60% (±0.69) vs control 77.267 (±3.19) $p<0.05$]; (Figure 5-15 A). The % of cells in the S-phase of the cell cycle remains similar in toxin treated and control cells (Figure 5-15 B). Of particular interest the % of toxin B exposed HT29 cells in the G2-phase of the cell cycle increased at 8 h and remained higher than control cells through to 72 h (Figure 5-15 C), statistical significance was observed at 8 h [toxin 26.17% (±3.04) vs control 9.1% (±1.03) $p<0.05$] and 72 h [toxin 22.23 % (±4.06) vs control 6.67% (±1.64) $p<0.05$] when compared with control (untreated cells).

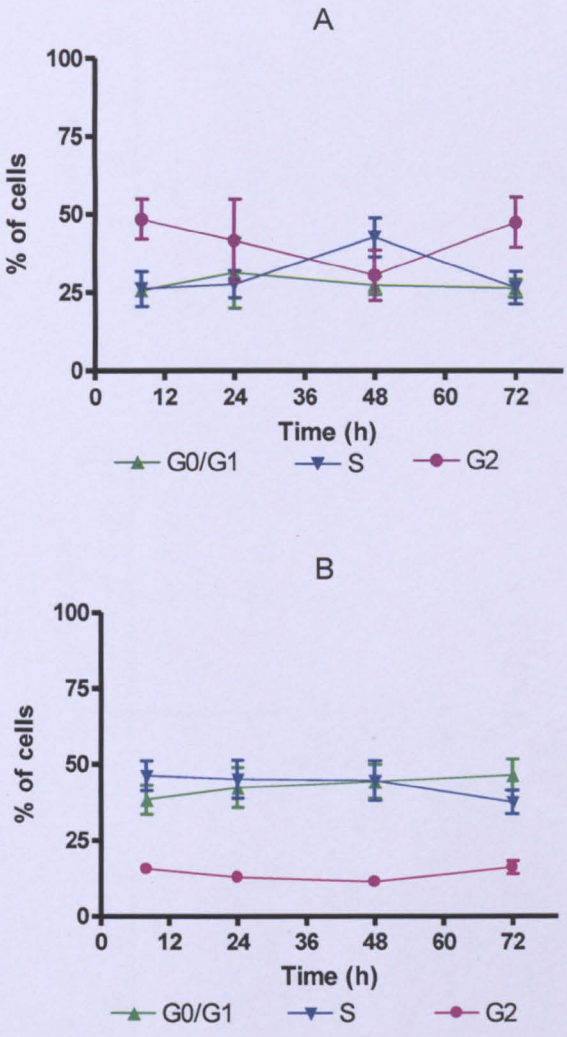

Figure 5-12 Whole cell cycle analysis of Caco-2 cells incubated with *C. difficile* toxin B (100 ng/ml)

Using PI stained Caco-2 cells incubated with 100 ng/ml of *C. difficile* toxin B (J2C, cytotoxic activity on Vero cells $x10^{-88}$) (A) or control medium (B) for 4 h, 8 h, 24 h, 48 h and 72 h, the cells were sorted using FACS and the resulting scatterplot gated to remove debris. Using only the gated events the percentage of cells in each phase of the cell cycle was calculated using Cyclhred. Data presented as % (± SEM) of cells in G0/G1, S and G2 phase n=3. This data reflects viable cells only and does not reflect the cells lost to cell death

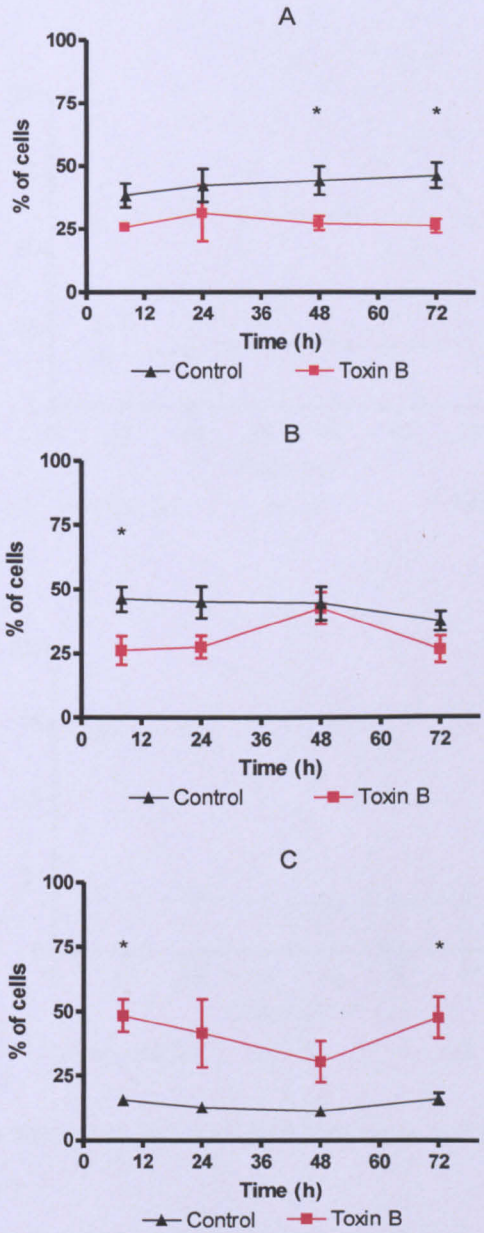

Figure 5-13 Individual phase cell cycle analysis of Caco-2 cells incubated with *C. difficile* toxin B (100 ng/ml)

Percentage of Caco-2 cells in G0/G1 (A) S-phase (B) and G2 (C), comparison of toxin treated and control cells at 8 h, 24 h, 48 h and 72 h. Toxin B from J2C, cytotoxic activity on Vero cells $x10^{-88}$. Data presented as % ± SEM n=3 *=p=<0.05 PI stained cells were sorted using FACS and the resulting scatterplot gated to remove debris. Using only the gated events the percentage of cells in each phase of the cell cycle was calculated using Cyclhred. This data reflects viable cells only and does not reflect the cells lost to cell death

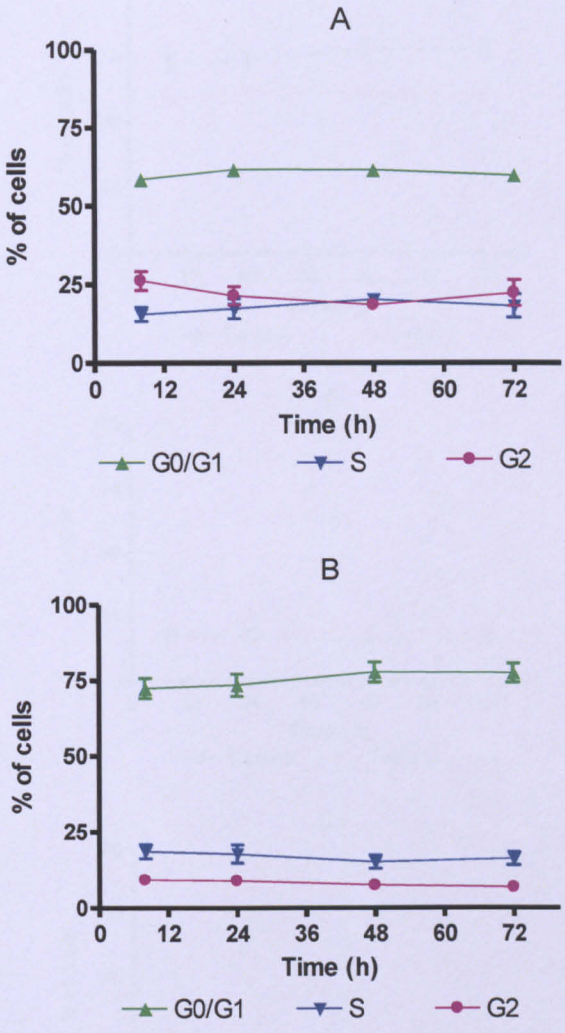

Figure 5-14 Whole cell cycle analysis of HT29 cells incubated with *C. difficile* toxin B (100 ng/ml)

Using PI stained HT29 cells incubated with 100 ng/ml of *C. difficile* toxin B (from J2C, cytotoxic activity on Vero cells $x10^{-88}$) (A) or control medium (B) for 4 h, 8 h, 24 h, 48 h and 72 h, the cells were sorted using FACS and the resulting scatterplot gated to remove debris. Using only the gated events the percentage of cells in each phase of the cell cycle was calculated using Cyclhred. Data presented as % (± SEM) of cells in G0/G1, S and G2 phase n=3. This data reflects viable cells only and does not reflect the cells lost to cell death

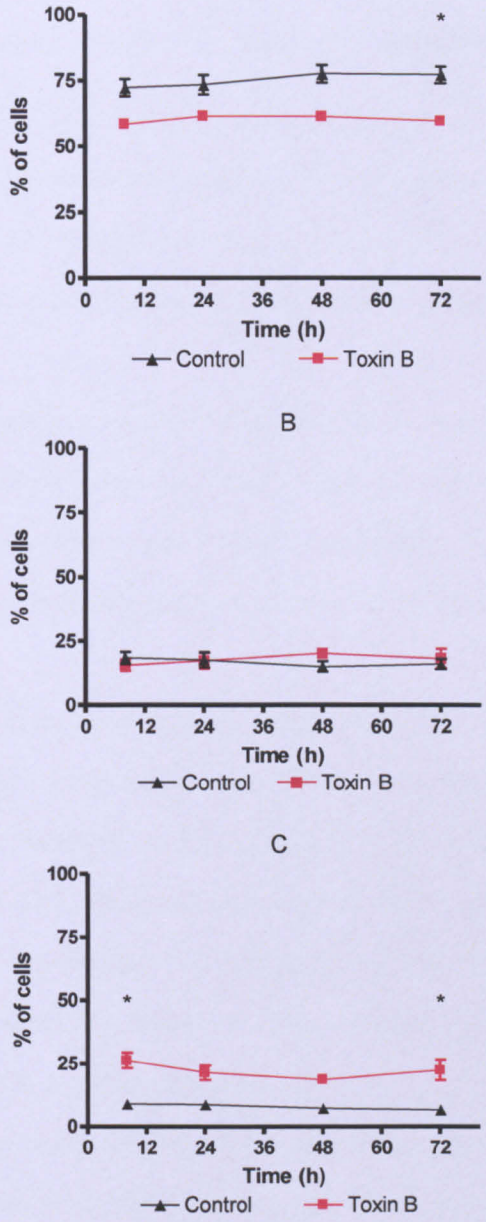

Figure 5-15 Individual phase cell cycle analysis of HT29 cells incubated with *C. difficile* toxin B (100 ng/ml)

Percentage of HT29 cells in G0/G1 (A) S-phase (B) and G2 (C), comparison of toxin treated and control cells at 4, 8, 24, 48 and 72 h. Toxin B from J2C, cytotoxic activity on Vero cells $x10^{-8}$. Data presented as % ± SEM n=3 *=p=<0.05 PI stained cells were sorted using FACS and the resulting scatterplot gated to remove debris. Using only the gated events the percentage of cells in each phase of the cell cycle was calculated using Cyclhred. This data reflects viable cells only and does not reflect the cells lost to cell death

5.4.7 Substrate specificity in toxin B intestinal epithelial cells

Rho, Rac-1 and Cdc42 are the intracellular targets for *C. difficile* toxins and utilizing UDP-glucose as the co-substrate the toxins are capable of maintaining these key molecular proteins in an inactive state. The mechanisms that lead to their inactivation have been covered in detail in Chapter 1.

Using whole cell lysates prepared from HT29 and Caco-2 cells incubated with either toxin B or control medium, Western Blot analysis was completed using protein specific antibodies to ascertain the expression of Rac-1 and Rho A, see Chapter 2, section 2.8 for a complete description of methods used.

As discussed in Chapter 1 toxins released by the bacterium *C. difficile* glucosylate, therein inactivating the protein and disrupting downstream signalling. This is believed to be an irreversible modification. The Rac-1 (MAB3735, Mouse IgG, Millipore) detects only the non-glucosylated (active) protein, whereas Rho A (26C4:sc-418 Mouse IgG Santa Cruz Biotechnology Inc.) detects endogenous levels of total protein (glucosylated and non-glucosylated). It has been reported however, that glucosylated Rho A is promptly degraded by the intracellular proteasome (Genth, Huelsenbeck et al. 2006) and therefore it is presumed that the signal being identified from the Rho A antibody is non-glucosylated (active) Rho A. As can be seen in, a reduction in non-glucosylated Rac-1 expression can be observed from as early as 3 hrs in both cell types when compared to the control (untreated) lysate at 0 h. This loss continued through to 24 h.

Total RhoA (glucosylated and non-glucosylated) expression in toxin treated Caco-2 cells remained consistent when compared to the control (untreated) cell lysate at 0 h. The consistent expression of Rho A in toxin treated Caco-2 cells was still evident after 24 h. In contrast, a reduction in Rho A expression in toxin treated HT29 cells was evident at 3 h and further reductions were noted at 8 h, 24 h when compared to control (untreated) cell lysate at 0 h.

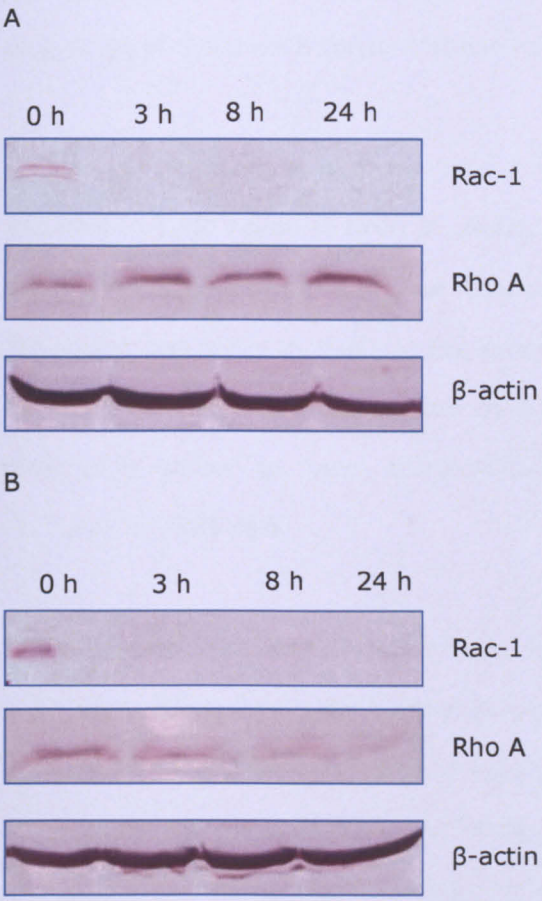

Figure 5-16 Expression of Rac-1, RhoA and beta-actin in control and *C. difficile* toxin B exposed Caco-2 (A) and HT29 (B) cells

Intestinal epithelial cell monolayers were cultured in medium only (0 h) or in the presence of 1,000 ng/ml toxin B for 3 h, 8 h and 24 h. Lysates of cells were electrophoresed on SDS-PAGE gels and following transfer onto PVDF membranes, immunostaining was performed using antibodies specific for RhoA, beta-actin or non-glucosylated form of Rac1. Equal loading of the lanes is illustrated by beta-actin-immunoreactive bands of similar size. The figures are representative of five experiments.

5.5 Discussion

This chapter looked at the response of two human intestinal epithelial cell lines exposed to varying concentrations of toxin B. Caco-2 cells (colonic epithelial adenocarcinoma cell line), phenotypically similar to mature enterocytes (Sambuy, De Angelis et al. 2005) and HT29 cells (colonic epithelial adenocarcinoma cell line) were cultured to confluence and exposed to a range of the toxin B concentrations (1000 - 10 ng/ml).

Visible cell rounding was first noted just 1 hour after Caco-2 cells were exposed to 1000 ng/ml of toxin B. Rounding in HT29 cells was visible 2 hour after exposure also at the highest concentration used. A similar pattern of responses was noted throughout the experiment suggesting that cell rounding occurred in a time- and dose- dependent manner, with Caco-2 rounding only marginally earlier to lower concentrations when compared with the cell rounding in HT29 cells.

Whilst loss of monolayer integrity was reported in Chapter 3 when Caco-2 cells were exposed to toxin A, toxin B exposed cells were only grown to sub-confluence prior to exposure and therefore the effect of toxin B on monolayer integrity cannot be discussed. As briefly highlighted, the early experiments using toxin B were conducted using near confluent monolayers of Caco-2 and HT29 and the basolateral location of toxin B receptors may have contributed to the lack of response observed in these experiments. It is worth noting that attachment of cells to the pseudo basement membrane (culture plate) was effected in Caco-2 cells incubated with toxin B. Toxin B exposed Caco-2

cells detached from the basement membrane by 48 h and the majority of HT29 cells were still attached even after 72 h exposure to 1000 ng/ml toxin B.

Cellular viability of Caco-2 and HT29 cells to *C. difficile* toxin B was investigated using the MTT assay and propidium iodide staining of DNA content and visual inspection using light microscopy.

Caco-2 cell monolayers treated with a range of toxin B concentrations resulted in a time and dose dependent reduction in mitochondrial dehydrogenase activity after 24 h. Of particular interest is the mitochondrial dehydrogenase activity of Caco-2 cells exposed to varying concentrations of toxin B during the first 24 h – a very small reduction is visible in cells exposed to 100 ng/ml, however mitochondrial dehydrogenase activity of cells exposed to 10 ng/ml and 1000 ng/ml was similar to that in control (untreated cells).

Mitochondrial dehydrogenase activity was significantly reduced in Caco-2 cells (0.3880 ±0.0074) exposed to 1 000 ng/ml toxin A (mean ± SEM p=<0.001) after 48 hours when compared with untreated control cells (0.4450 ±0.0092). By 72 hours, a further reduction was observed at 1 000 ng/ml (0.1274 ±0.0298) when compared with control (untreated) cells (0.4187 ±0.0171) (mean ±SEM p=<0.01).

In contrast, only a very small reduction in cell viability was observed in HT29 monolayers exposed to ≤1000 ng/ml for 72 hours.

The MTT assay was supported by DNA fragmentation assessed by flow cytometry (Nicoletti, Migliorati et al. 1991) to toxin B. Using propidium iodide staining the DNA content in cells was measured using FACS and the percentage events in the sub-G1 region established. A time dependent increase in the % events in the sub-G1 region was evident in Caco-2 cells with over 22% of all events being in the sub-G1 region at 72 h when exposed to 100 ng/ml toxin B. The difference in response to toxin B may be explained by the two different batches of toxin B; early experiments were completed using a batch of toxin with a cytotoxicity titre of 10^{-16} and the PI experiments completed using a batch with a titre of 10^{-88}. This was lower than the % of cells in the sub-G1 region of toxin A exposed cells and this may partly be explained by the lower concentration of toxin used (100 ng/ml toxin B v 1000 ng/ml toxin A). To a lesser extent, a time dependent increase in the % sub G1 events was seen in HT29 cells when compared with control (untreated) cells.

Similar to the responses observed in toxin A exposed Caco-2 and HT29 cells – a cell specific effect is evident with Caco-2 cells displaying a greater susceptibility to toxin B induced cell death than HT29 cells. This supports earlier work completed by Fiorentini who suggested the origin and proliferative rate of the target cell may contribute to toxin B induced cell death (Fiorentini, Fabbri et al. 1998). Contradicting this Donta et al reported insignificant cellular sensitivities across cell types to toxin B (Donta, Sullivan et al. 1982). The differences across studies may be explained by differing cytotoxicity of toxins used.

Raising similar questions to those considered in Chapter 3 my interest will centre on the obvious disparity in cellular responses to *C. difficile* toxin B. Comparison of the cell specific response to toxin A and toxin B will be discussed in Chapter 7.

As discussed in some detail in the introduction, *C. difficile* toxins enter the host cell by receptor mediated endocytosis. Toxin B binds to unknown receptor believed to be located on the basolateral surface of the host cell. Having established similar internalisation of toxin A into our host cells; the fragility and volume of purified toxin B did not make labelling a realistic option and therefore direct assessment of toxin B internalisation was not investigated. It may therefore be possible that the disparity seen in Caco-2 cells may be explained by a greater number of toxin B receptors and more toxin B entering the target cell, however the inactivation of the intracellular protein and loss of Rac-1 was largely similar, suggesting similar uptake.

Supporting our findings, cell rounding caused by the inactivation of Rho, Rac and Cdc42; and cell death have been suggested to be temporally distinct events. I have reported similarities in cell rounding to toxin B exposure but significantly different cellular viability in Caco-2 and HT29 cells. Studying the response of Hela and MCF cells to toxin B, Qa'Dan and colleagues found two distinct pathways to cell death; a caspase independent and; caspase dependent pathway to apoptosis (Qa'Dan, Ramsey et al. 2002). Using a caspase inhibitor delayed cell death but the cells still rounded, similarly insertion of the enzymatic region of toxin B into cells failed to stimulate caspase 3 yet the cells rounded and progressed to cell death. This would

suggest that caspase independent apoptosis occurred as a result of substrate inactivation (Qa'Dan, Ramsey et al. 2002).

Caco-2 cells rounded slightly earlier than HT29 cells, but a significant disparity has been found in the ability of toxin B to induce cell death in Caco-2 cells but not in HT29 cells. As I have been unable to investigate toxin internalisation our attention has turned to intracellular processing for a possible explanation. The early loss of monolayer integrity observed in Caco-2 cells would support the early loss of the regulatory switch, Rho. What remains to be ascertained is whether the dramatic decrease in cell viability was the result of the cell rounding and detachment from the basement membrane or mediated by other independent signalling mechanisms i.e. caspases.

Once inside the target cell, toxin B exerts it effect by inactivating a number of small GTPases, namely Rho, Rac-1 and Cdc42. A number of studies have suggested that substrate specificity may be cell specific. A recent study has shown that inactivation of RhoA (but not Rac-1) is required to induce cell death in response to *C. difficile* toxin B in basophilic leukaemia cells (Huelsenbeck, Dreger et al. 2007). It is possible therefore that toxin B induces greater inactivation of Rho A in Caco-2 cells than HT29 cell. Other studies, (Fritz and Kaina 2001) and (Liu, Cerniglia et al. 2001) suggest that RhoB, which is negatively regulated by RhoA, is the main regulator of cell death.

As discussed in Chapter 4, substrate specificity is suggested to be cell specific and I therefore postulate the target substrates for *C. difficile* toxin B in Caco-2

and HT29 cells may be different. Investigating the expression of Rac1 and in line with cell rounding, a reduction in non-glucosylated Rac-1 was apparent in both cell types from 3 hr, suggesting a similar level of internalization of toxin B. This reduction continued through 24 h. The expression of Rho A in Caco-2 cells remained consistent throughout with no reduction in expression. In contrast, expression of Rho A in HT29 cells is shown to reduce from 8 hr and this reduction continues through to 24 h. These findings further support a cell specific response but contradicts the findings of others, suggesting Rho A may regulate cell death (Huelsenbeck, Dreger et al. 2007), if RhoA regulated cell death a reduction in Rho A expression in Caco-2 cells would have been observed. Huelsenbeck and colleagues investigated the response in a different cell type and therefore the substrate specificity argued by my findings is supported.

Rho proteins are linked with many biochemical and biological functions within the host cell; one of which being the cell cycle and more specifically G1 progression and mitosis (Jaffe and Hall 2005). Using propidium iodide staining I investigated the cell cycle phases in toxin exposed and control cells using a dedicated cell cycle programme; Cychred, to elicit any cell specific sensitivities. Whole cycle profiles showed a small increase in the percentage of G0/G1 cells in toxin exposed Caco-2 cells to 24 h followed by a decrease through to 72 hours. A small increase in S-phase cells is noted from 8-24 h followed by a moderate increase to 48 h and a decrease to 72 h. The G2 phase mirrored the S-phase profile, decreasing rapidly to between 24 and 48 h and increasing again through to 72 h. This shows that cells are progressing from S-phase into G2-phase successfully. With a gradual reduction in G2 cells

through to 48 h we would also expect an increase in G0/G1 events, the absence of this indicates that cells are failing to pass the G2 checkpoint and undergo mitosis.

If we consider specifically the stages of the cell cycle and compare toxin and control cells we can see an overall decrease in the percentage of toxin exposed cells in the G0/G1 region, becoming significant after 48 and 72 h. The S-phase also saw an overall reduction in the percentage of toxin exposed cells through to 48 h, being significant at 8 h. However between 24 and 48 h, the percentage of toxin B exposed cells in the S-phase increases to match the percentage of control cells in S-phase. A decrease in both control and toxin treated cells in S-phase is seen through to 72 h. Mirroring the S-phase pattern in toxin B exposed Caco-2 cells; the percentage of G2 cells is greater when compared with control (untreated) cells in the G2-phase throughout 8-72 h, a significant difference being noted at 8 and 72 h. This mirroring would suggest that cells are successfully entering G2 but the rapid decline in G0/G1 events would suggest that Caco-2 cells are more sensitive to toxin B induced cell death in G0/G1 or perhaps the cells do not enter G0/G1; failing to pass the M1 checkpoint due to poor spindle alignment and undergoing programmed cell death.

Whole cycle profiles of HT29 cells look remarkably similar with the percentage of G0/G1 events remaining constant throughout 8-72 h. Running almost parallel to the G0/G1 profile the S-phase and G2-phase profiles do not change dramatically with a small increase in the percentage of G2 events. To get a better understanding of what is happening with the HT29 cells incubated with

toxin B comparison of each stage of the cell cycle is needed. A reduction in the percentage of cells in the G0/G1 region is observed throughout, becoming significantly different at 72 h. Interestingly S-phase profiles appear very similar in control and treated HT29 cells. In contrast the percentage of toxin treated cells in the G2 region is lower than control cells, being significantly different at 8 and 72 h. With a consistent reduction in G0/G1 events and increase in G2 events it would appear that cells are progressing through the cycle and arresting in G2. These finding were also reported by others, however they also reported that HT29 cells underwent cell death in response to toxin exposure (Nottrott, Schoentaube et al. 2007). The use of recombinant toxin may explain the notable differences in cell death (Nottrott, Schoentaube et al. 2007).

Whilst a significant difference is not evident at all time-points, cell cycle progression is fluid and whilst progression may be delayed in toxin treated cells the control cells will be proliferating as normal and rotating through all stages of the cell cycle.

To summarize, this chapter has described the response of two intestinal epithelial cell types to varying concentration of purified toxin B. In doing so, it has been established that Caco-2 cells are more sensitive to toxin induced cell death. Investigation to elucidate the reasons for this cell specific sensitivity initially considered a possible difference in the uptake of the toxin into the cell but as discussed previously biological fragility of toxin B did not permit this to be investigated. Looking for an explanation intracellularly, expression of Rho A and Rac-1, two of the key GTPases inactivated in target cells was

investigated. Using whole cell lysates from cells incubated with either toxin B or control medium Western Blot analysis established a time dependent loss of non-glucosylated Rac-1 in both cell types. Rho A expression in Caco-2 cells remained constant following incubation with toxin B, however a time dependent loss of occurred in HT29 cells incubated with toxin B. The cell cycle is regulated by Rho proteins and consideration of cell cycle progression was also investigated with some supporting evidence.

CHAPTER 6

6 Primary colonic myofibroblast response to *C. difficile* toxins

6.1 Introduction

Intestinal myofibroblasts represent a distinct sub-population of cells that are located below the intestinal epithelium, separated by a porous basement membrane (Powell, Mifflin et al. 1999). The intestinal myofibroblast has characteristics of both the smooth muscle cell and the fibroblast, strongly expressing alpha-smooth muscle actin and vimenten respectively. Myofibroblasts play an important role in the maintenance of normal mucosal functions and in inflammation, repair and fibrosis (Powell, Mifflin et al. 1999).

Fundamental processes rely on a complex network of cell to cell, cell to extracellular matrix and chemical messenger interactions and the intestinal myofibroblast regulate a number of fundamental interactions in the gastrointestinal tract (Powell, Mifflin et al. 1999; Powell, Mifflin et al. 1999).

The cells play an important role in organogenesis of the intestine (Simon-Assmann, Kedinger et al. 1995) by secreting soluble mediators and growth factors the myofibroblasts promote epithelial growth, proliferation and differentiation (McKaig, Makh et al. 1999). Myofibroblasts are also responsible for contraction to release fluid from the gastric glands (Synnerstad, Ekblad et al. 1998) and motility in the intestinal villi (Joyce, Haire et al. 1987). In addition, myofibroblasts regulate epithelial functions

such as electrolyte transport and barrier function (Beltinger, McKaig et al. 1999).

The myofibroblast is also a key facilitator of the repair and inflammatory processes when the intestine is damaged or attacked by a pathogen or toxic agent (Powell, Mifflin et al. 1999).

Damage and loss of epithelial cells lining the intestinal tract triggers a repair process called restitution (Silen and Ito 1985; Podolsky 1997). This mechanism is promoted by Prostaglandin COX-1 and COX-2 activation and growth factors released from myofibroblasts (Blikslager, Roberts et al. 1997). The residual epithelial cells either side of the denuded space move along the basement membrane, forming new tight junctions and restoring the luminal barrier (McKaig, Makh et al. 1999). If the damage or assault penetrates the basement membrane, a complex ordered repair process is activated (Wallace and Granger 1996). The early release of chemical signals activates the myofibroblasts leading to cell motility and contraction to reduce the wound area (Moore, Carlson et al. 1989). The subsequent release of matrix proteins and growth factors induce a chain of events starting with angiogenesis and tissue remodelling followed by epithelial cell proliferation and differentiation (Wallace and Granger 1996). After granulation and scar formation myofibroblasts undergo apoptosis (Desmouliere, Redard et al. 1995). Whilst matrix molecules produced by myofibroblasts assist in wound healing unregulated production of the molecules results in tissue fibrosis (Border and Noble 1994; Kovacs and DiPietro 1994).

Myofibroblasts are avid producers of chemokines and cytokines and play a major role in the inflammatory response being able to accentuate or diminish an inflammatory reaction (Fiocchi 1997; Roberts, Nadler et al. 1997; Strong, Pizarro et al. 1998). Through the expression adhesion molecules on their cell surface, myofibroblasts invite other cells of the immune system to join them to facilitate a pooled inflammatory response (Saada, Pinchuk et al. 2006).

Given my interest in the mucosal cell response to *C. difficile* toxins I have investigated the response of intestinal epithelial cells to toxins A and B and following the disruption of the epithelial cell barrier the toxins would encounter cells of the lamina propria. It has previously been shown that myofibroblasts provide protection to intestinal epithelial monolayers against loss of barrier function in response to low concentrations of toxin A, via TGF-beta secretion (Johal, Solomon et al. 2004) and of particular interest, the responses by primary intestinal myofibroblasts to *C. difficile* toxins remain to be characterized.

The aim of this work is to investigate and compare responses to *C. difficile* toxins A and B by primary human colonic myofibroblasts.

6.2 Materials and methods

6.2.1 Purification, preparation and application of toxin A and B

Toxin A was purified as detailed in Chapter 2. Toxin B was purified by ammonium sulphate precipitation of cultured *C. difficile* (VPI 10463) supernatant samples followed by two sequential anion exchange chromatographic steps as detailed in Chapter 4.

Using previously characterized fractions of toxin A and toxin B, protein concentration and cytotoxicity was investigated again prior to use as described previously.

Purified toxin was subsequently diluted using warm DMEM, supplemented for use with myofibroblasts, Caco-2 or HT29 cells. The existing media covering the confluent cell monolayers was gently aspirated and discarded and the medium containing varying concentrations of toxin A, toxin B or toxin A + B was placed onto the cells in each well and the plates re-incubated at 37°C, 5% CO_2. Each concentration was completed in triplicate with control wells.

6.2.2 Primary colonic myofibroblast response to *C. difficile* toxin A – a comparison using intestinal epithelial cells, HT29 and Caco-2

Early experiments investigated the responses of myofibroblasts (derived from histologically normal colonic mucosal samples) to *C. difficile* toxin A alongside identical experiments using intestinal epithelial cell lines – HT29 and Caco-2. Whilst myofibroblasts are a primary cell type with features of smooth muscle/fibroblasts like cells and a distinctive phenotype, Caco-2

and HT29 are carcinoma derived intestinal epithelial cells, it was considered that the responses provided by the cell lines would provide a 'real time' benchmark of sensitivity to *C. difficile* toxin A and in the absence of primary epithelial cells; provide a direct comparison of mucosal cell responses to *C. difficile* toxin A.

Intestinal myofibroblasts, Caco-2 and HT29 cells were seeded in 24 well plates, grown to confluence and exposed to either 100 ng/ml or 1000 ng/ml of toxin A (cytotoxicity titre 50% rounding at 10^{-94} on Vero cells at 24 h) or control medium. Morphological assessments were made by phase contrast light microscopy and micrographs taken at 1, 2, 3, 24, 48 and 72 h. Cell viability was assessed using the MTT assay. Two plates for each cell type were prepared; the first plate was incubated with toxin for 48 hrs; and the second for 72 hrs.

6.2.3 Morphological changes over the time-course

Morphology of cells incubated with toxin A (cytotoxicity titre 50% rounding at 10^{-94} on Vero cells at 24 h) were investigated as described in the Chapter 2, at various time points (1 h through to 72 h) and micrographs taken. Morphological changes were described as percentage rounding and specific signs of apoptosis, necrosis noted.

6.2.4 Cell cytotoxicity

Cell cytotoxicity was assessed at 48 h and 72 h using the MTT assay as described in Chapter 2, section 2.4.3.

6.2.5 Propidium Iodide staining and cell cycle analysis

Establishing that cell numbers were insufficient using 3 wells of a 24 well plate per treatment and time-point subsequent cell cycle experiments were completed using 2 wells of a 6 well plate. Cell cycle analysis was performed on myofibroblasts incubated with either 1000 ng/ml of toxin A (cytotoxicity titre 50% rounding at 10^{-14} at 24 h) or control medium for 8, 24, 48 and 72 hours using propidium iodide and flow cytometry as described in Chapter 2, section 2.7.3. Toxin-exposed cells were compared with cells cultured with control medium, seeded at the same time and obtained at the same time points as those cultured in the presence of the toxin.

6.2.6 Rho protein expression

Investigation of Rho signalling in intestinal myofibroblasts was completed using whole cell lysates from cells in control and toxin A treated samples and the western blot technique using Rho specific antibodies for detection. The proteins investigated included Rac-1, RhoA and β-actin was used as a loading control. The Rac-1 (MAB3735, Mouse IgG, Millipore) detects only the non-glucosylated (active) protein, whereas Rho A (26C4:sc-418 Mouse IgG Santa Cruz Biotechnology Inc.) detects endogenous levels of total protein (glucosylated and non-glucosylated). It has been reported however, that glucosylated Rho A is promptly degraded by the intracellular proteasome (Genth, Huelsenbeck et al. 2006) and therefore it is presumed that the signal being identified from the Rho A antibody is non-glucosylated (active) RhoA.

Myofibroblasts were incubated with 1 000 ng/ml toxin A (cytotoxicity titre 50% rounding at 10^{-94} at 24 h) or control medium for 4 h and 24 h. A Western blot was completed for each protein to be investigated, including a loading control. A colour scan was made of each western blot.

6.2.7 Smooth muscle actin expression in toxin A exposed myofibroblasts

To investigate the expression and distribution of smooth muscle actin in myofibroblasts incubated with 1000 ng/ml toxin A (cytotoxicity titre 50% rounding at 10^{-14} at 24 h) or control medium. Myofibroblasts were cultured on glass coverslips placed into a 24 well plate and grown to confluence as previously described. Upon confluence the cells were exposed to toxin A for 3, 6, 24 and 48 hours or control medium. After each time point the toxin was removed and the glass coverslip gently removed from the well and fixed in acetone for 1 minute. The coverslip was allowed to dry before being placed into a fresh 24 well plate, wrapped in foil and stored at -20 °C. The plate was removed from the freezer and the coverslips incubated with monoclonal anti-α smooth muscle actin (Clone 1A4, Sigma) in TBS p.H. 7.5 (1:500) for 1 h. The primary antibody was removed and the coverslips washed five times with TBS p.H. 7.5; covered with biotinylated secondary antibody (containing blocking serum and biotinylated affinity purified anti-mouse immunoglobulin) and incubated at room temperature for 30 minutes. The biotinylated secondary antibody binds to the primary antibody, monoclonal anti-α smooth muscle actin.

The preformed avidin/biotinylated horseradish peroxidase macromolecular complex was prepared and left to incubate for 30 minutes before use. The biotinylated secondary antibody was washed off and the pre-prepared

avidin/biotin complex pipetted into each well, covering the coverslips. The coverslips were left to incubate at room temperature for 30 minutes.

The coverslips were washed a further five times to remove the avidin/biotin complex. The horseradish peroxidase was visualized using peroxidase substrate (VIP Substrate Kit, Vector), when prepared the peroxidase substrate was pipetted onto the slips. Leaving the membrane to develop for two minutes, the peroxidise substrate was removed and the coverslips washed with water to remove the peroxidise and end the reaction.

The coverslips were counterstained using Gill's Hematoxylin, in brief, water covering coverslips was removed and enough Gill's Hematoxylin was put into each well to immerse the coverslips. The counter stain was removed after 1 minute and any excess removed by washing with water. The glass coverslips were gently removed from the plate and each coverslip was passed through a graded series of ethanol solutions and finally zylene. The coverslips were then mounted onto glass slides with DPX mountant and left to dry overnight before inspection.

The slides were visualised for immuno-stained cells using phase contrast microscopy and micrographs taken at various magnifications.

6.2.8 Recovery of intestinal myofibroblasts pre-exposed to toxin A

Given the apparent resilience of myofibroblasts to *Clostridium difficile* toxin A and their paracrine functioning in the lamina propria studies were designed to see if myofibroblasts could recover from toxin A exposure.

Reviewing earlier observations 100% rounding could be achieved after 3 hours to 1000 ng/ml and therefore myofibroblasts grown to confluence in 6 well plates were pre-exposed to toxin A 1000 ng/ml (cytoxicity titre of 50% rounding at 24 h on Vero cells 10^{-94}) for 3 h, 24 h and 48 h followed by washing and culture in medium only. The medium was replaced three times a week. The cells were observed at 3 hours and then once a week using phase contrast microscopy for signs of recovery and micrographs taken.

6.3 Intestinal Myofibroblast response to *C. difficile* toxin B

Following the successful purification of *Clostridium difficile* toxin B investigations to ascertain the myofibroblast response to this toxin were commenced. Toxin B was re-characterised prior to use as described in section 6.2.1 page 246.

Intestinal myofibroblasts were exposed to either 10 ng/ml, 100 ng/ml or 1000 ng/ml of toxin B or control medium; morphological assessments made and cell cytotoxicity assessed using the MTT assay as outlined in section 6.2.2 pages 246 to 247.

6.3.1 Cell cytotoxicity

Cell cytotoxicity, following the incubation of myofibroblasts with 10 ng/ml, 100 ng/ml or 1000 ng/ml toxin B or control medium (cytotoxicity titre 50% rounding at 10^{-47} at 24 h), was assessed at 24 h, 48 h, and 72 h using the MTT assay (measuring mitochondrial dehydrogenase activity in metabolising cells).

6.3.2 Propidium Iodide staining and cell cycle analysis

Cell cycle analysis was performed on myofibroblasts incubated with either 1000 ng/ml of toxin B (cytotoxicity titre 50% rounding at 10^{-94} at 24 h) or control medium for 8, 24, 48 and 72 hours using propidium iodide and flow cytometry. Toxin-exposed cells were compared with cells cultured with control medium, seeded at the same time and obtained at the same time points as those cultured in the presence of the toxin.

6.3.3 Rho protein expression

Investigation of Rho signalling in intestinal myofibroblasts was completed using whole cell lysates prepared from cells in control and toxin B (cytotoxicity titre 50% rounding at 10^{-14} at 24 h) treated samples and the Western blot technique using Rho specific antibodies for detection. The proteins investigated included non-glucosylated Rac-1 and total (glucosylated and non-glucosylated) Rho A. β-actin was used as a loading control.

Myofibroblasts were incubated with 1 000 ng/ml toxin B or control medium for 4 h and 24 h. A western blot was completed for each protein to be investigated and a colour scan was made of each western blot.

6.3.4 Smooth muscle actin expression in toxin B exposed myofibroblasts

The expression and distribution of smooth muscle actin in myofibroblasts was re-investigated using confluent cells incubated with 1000 ng/ml toxin B (cytotoxicity titre 50% rounding at 10^{-54} at 24 h) for 3 h, 6 h, 24 h and 48 h; or control medium. The methods for which are identical to those

used in toxin A investigation of smooth muscle actin and is described in section 6.2.7 page 249.

6.3.5 Hoechst 33812 staining of toxin B exposed myofibroblasts

To investigate signs of apoptosis in toxin B exposed myofibroblasts, cells were grown on glass coverslips to confluence and incubated with either 1000 ng/ml or 100 ng/ml toxin B (cytotoxicity titre 50% rounding at 10^{-94} at 24 h) or control medium for 48 h and 72 h. At the given time-points the toxin/media was removed and the coverslips fixed in 100 % acetone by immersing the slips in the acetone for 1 minute. The excess acetone was gently blotted and the slips allowed to dry before storing in a fresh 24 well plate covered with foil at -20°C.

The plate was removed from the freezer and the glass coverslips stained with Hoechst stain (1:10 Hoechst 33812 and PBS, (Sigma)) for 15 minutes at room temperature. The stain was removed and the coverslips washed three times using PBS. The coverslips were gently removed from the plate and mounted onto glass slides using a 1:1 glycerol:PBS solution. The slides were observed immediately using the fluorescent microscope (Nikon Eclipse TE2000-S). Fluorescent and corresponding phase contrast micrographs were taken.

6.3.6 Recovery of intestinal myofibroblasts to *C. difficile* toxin B

After observing recovery in intestinal myofibroblasts to *C. difficile* toxin A, identical experiments were conducted using toxin B. With similar time course changes in myofibroblast morphology to toxins A and B, pre-exposure with toxin B was kept to 3 hours using 1000 ng/ml toxin B. As

before, myofibroblasts grown to confluence in 6 well plates were pre-exposed to toxin B 1000 ng/ml (cytotoxicity titre 50% rounding at 10^{-47} at 24 h) for 3 h, 24 h and 48 h followed by washing and culture in medium only. The medium was replaced three times a week. The cells were observed at 3 hours and then once a week using phase contrast microscopy for signs of recovery and micrographs taken.

6.3.7 Comparative response to *C. difficile* toxins A and B

Observing a difference in the response elicited by intestinal myofibroblasts to toxins A and B, I wanted to ensure that our observations were not as a result of the toxins being studied separately and the possible effect of using different myofibroblast isolates in our observed response. With this in mind, cell cytoxicity (MTT) and morphological assessments were repeated using identical myofibroblast isolates seeded at the same time and toxin A and toxin B experiments run simultaneously.

It has been reported that toxin B is more cytotoxic than toxin A (Riegler, Sedivy et al. 1995). With this in mind one might expect myofibroblasts to be more sensitive to toxin B, however having already established that toxin B was in fact no more cytotoxic than A on intestinal epithelial cell type, HT29, further investigations were completed to compare the cytotoxicity of toxins A & B on myofibroblasts. As outlined in Chapter 2, the 'gold standard cytoxicity assay' for *C. difficile* toxins is the African Green Monkey (Vero) cell bioassay. In brief, Vero cells seeded in a 96 well plates were cultured for 24 hours and serial dilutions of toxins A & B 10^{-1} through 10^{-95} prepared and applied to the Vero cells. After 24 hours the assay is read

and the lowest serial dilution to induce 50% rounding at 24 hours recorded.

With the titre for each toxin established, three serial dilutions, 10^{-3}, 10^{-5} and 10^{-7} were prepared as described in 6.2.1 page 246 for each toxin and applied simultaneously to confluent myofibroblasts and Vero cells. Morphological assessments were made by light microscopy and micrographs taken at 1, 2, 3, 24, 48 and 72 h and a comparison of cytotoxicity of toxins A & B ascertained.

6.3.7.1 Morphological changes over the time-course

Morphology of cells incubated with toxin B (cytotoxicity titre 50% rounding at 10^{-57} at 24 h) were investigated as described in the Chapter 1 - Material and methods at various time points (1 h through to 72 h) and micrographs taken. Morphological changes were described as percentage rounding and specific signs of apoptosis, necrosis noted.

6.3.8 Scanning Electron Microscopy

To obtain an in-depth picture of the morphological changes induced by *C. difficile* toxins, myofibroblasts were grown on Thermanox cover-slips placed into the wells of a 24 well culture plate. The cells were grown to confluence as previously described and incubated with 1000 ng/ml of toxin A (cytotoxicity titre 50% rounding at 10^{-94} at 24 h), toxin B (cytotoxicity titre 50% rounding at 10^{-47} at 24 h) or control medium for 24 hours. Following the 24 h period the media/toxin was removed and the wells gently washed with warmed PBS. The cells were then fixed with 3% gluteraldehyde by gently pippetting 500 µl of the solution into each well –

submerging the Thermanox slide. The plates were stored at 4 °C until processing.

Removing the plates from storage the slides were washed three times with 0.1 M Phosphate / Cacodylate buffer and post fixed in 1% osmium tetroxide for 30 minutes in the fume cupboard. The slides were washed 5 x 1 minute using distilled water and then dehydrated using a graded series of ethanol solutions (2 x 15 min using 50% ethanol; 2 x 15 min using 70% ethanol; 2 x 15 min using 90% ethanol; and finally 3 x 20 min using 100% ethanol). The remaining traces of ethanol evaporated and Hexamethyldisilazane was added to each well to cover the slip. The slides were incubated with the Hexamethyldisilazane for 2 x 15 minutes and slips/wells left to dry overnight in the fume hood.

The following morning the dry slides were carefully removed and mounted onto aluminium stubs using sticky carbon tabs and placed in the dessicator until coating. The samples were coated with gold using the Sputter Coater and viewed on the scanning electron microscope (JEOL 840).

6.3.9 Small G Protein Activation Assay (RhoA – colorimetric) – G-LISA™

The RhoA G-LISA™ (Cytoskeleton Inc, USA) is an enzyme linked immunosorbent assay (ELISA) based activation assay that measures RhoA activity in cells. RhoA is a small GTPase that acts as a molecular switch by cycling from a GDP bound (inactive) to a GTP (active) form, its function has been described previously. *C. difficile* toxins A and B inactivate this key molecular switch by keeping the protein in its inactive form. Using the Rhotekin – RBD (Rho binding domain) protein, which only binds to the

active (GTP bound) form of RhoA, the G-LISA is able to measure the level of GTP-loaded RhoA (active form) in cells. The kit provides all the necessary reagents and the only additional product sourced was the ultrapure water (Sigma Ltd, Poole, UK) used to reconstitute the reagents.

All reagents were reconstituted and stored according to the manufacturers guidelines.

Three different myofibroblast isolates were revived, grown to 90% confluence, split as previously described and 20,000 cells per well seeded into 3 off 6 well plates. The cells were grown to 70% confluence over three days and the media changed the day after seeding. To investigate the inactivation of RhoA, four different conditions were prepared; incubation with toxin A; incubation with toxin B; serum starved (inactivates cellular RhoA); and control. The serum starved condition was achieved by washing the cells in serum (FCS) free medium, incubating the cells in fresh medium containing 0.5% serum (FCS) overnight and at the start on the experiment replacing the medium for serum free. Toxin A and toxin B were diluted to 1000 ng/ml using DMEM supplemented with 10% FCS, 0.1% NEAA and PSG and applied to cells for 4 h. The medium was also replaced on the control wells.

After 4 h, all medium was removed; the wells washed with ice cold PBS and the cell culture plates placed on ice. The cells were lysed using 100 µl ice cold lysis buffer and a cell scraper, the same 100 µl of buffer was transferred across wells of the same condition to achieve a higher protein concentration and placed into ice cold eppendorfs. Samples were subsequently centrifuged at 4°C for 2 minutes at 5000g and the lysate

removed, placed into clean ice-cold eppendorfs, snap frozen and stored at -80 °C. 20µl of each lysate was left on ice to establish protein concentration. Protein concentration was ascertained using the Precision Red protein assay (supplied with the kit). In brief, 10 µl of each sample and a blank (lysis buffer) was placed into a 96 well plate (induplicate) and 300 µl Precision Red added to each well. After 1 minute the absorbance was read at 600 nm using the plate reader (BioRad). After subtracting the blank absorbance value, the reading was multiplied by 3.75 as per the instructions. The value calculated was the protein concentration. Protein concentrations ranged from 1.2 – 1.6 mg/ml.

The frozen samples were defrosted and diluted to 1 mg/ml using ice cold lysis buffer and placed on ice. With the assay preparation and lysate collection complete the G-LISA was carried out according to manual supplied with the kit. Each sample was measured in duplicate and a RhoA positive control, supplied with the kit was also used. The level of active RhoA is measured with absorbance set at 490 nm and the samples compared against the positive control.

6.4 Results

6.4.1 Primary colonic myofibroblast response to *C. difficile* toxin A – benchmarking against intestinal epithelial cell responses.

Preliminary experiments investigated the response of intestinal myofibroblasts to *C. difficile* toxin A at two concentrations, 100 and 1000 ng/ml. These concentrations have been to shown to cause cell rounding in both HT29 and Caco-2 cells and induce cell death in Caco-2 cells. Using the two intestinal epithelial cell types and the myofibroblasts, simultaneous

experiments were set up and the morphological response and cell viability in response to toxin A recorded. Morphological changes were assessed from 1 h – 72 h using light microscopy and the cells in each well categorized into one of three morphological stages; no visible rounding; 50% visible rounding and 100 % visible rounding. Tabular confirmation of rounding can be found in Table 6-1 and representative micrographs of myofibroblasts at each of these stages can be viewed in Figure 6-1. Cellular viability was established at 48 and 72 hours post toxin exposure.

6.4.1.1 Dose and time dependent change in cell morphology

As was previously observed in Caco-2 and HT29 cells a time and dose dependent response was recorded, this response also being recorded in the intestinal myofibroblasts with 50% rounding visible after just 3 hours, see Table 6-1. Of particular interest, myofibroblasts incubated with toxin A appear to initially transform into a stellate shape before rounding, see Figure 6-1 c and a small number of these cells can still be viewed even after 48 h, image d.

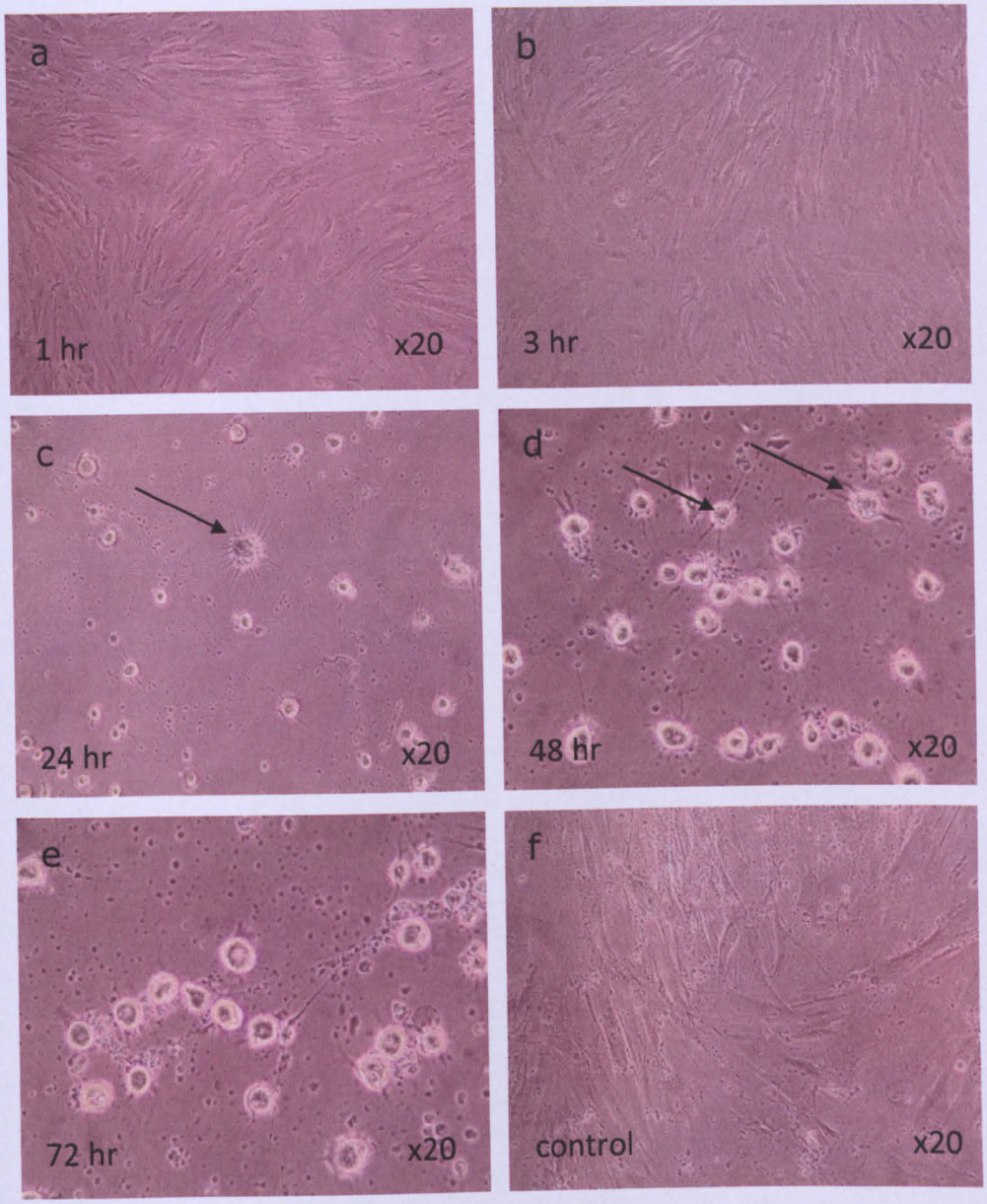

Figure 6-1 Phase contrast micrographs of primary colonic myofibroblasts to *C. difficile* toxin A

Representative images taken from three experiments using different patient isolates. Cells incubated with either control medium (f) or 1000 ng/ml toxin A from 1 hour through 72 hour (a-e). Arrow indicate cells in stellate form.

Table 6-1 Cell rounding in intestinal epithelial cells (Caco-2 and HT29) and primary colonic myofibroblasts to *C. difficile* toxin A

Percentage cell rounding in Caco-2 and HT29 cells and Myofibroblasts in response to 100 and 1000 ng/ml of toxin A. The percentage of rounded cells was ascertained by counting the rounded cells in ten random high power fields and taking the mean of these ten observations and reporting the value to the nearest 10%.

Toxin A (ng/ml)	Duration of toxin A exposure																				
	1 hour			2 hours			3 hours			8 hours			24 hours			48 hours			72 hours		
	Caco-2	HT29	Myofib	Caco-2	HT29	Myofib	Caco-2	HT29	Myofib	Caco-2	HT29	Myofib	Caco-2	HT29	Myofib	Caco-2	HT29	Myofib	Caco-2	HT29	Myofib
100	50	0	0	60	50	0	70	60	0	100	70	0	100	100	100	100	100	100	100	100	100
1000	60	10	0	100	60	0	100	70	10	100	70	70	100	100	100	100	100	100	100	100	100

6.4.1.2 Investigation of cellular viability using the MTT assay

Cell viability was established after 48 and 72 hour toxin A exposure using the MTT assay.

As previously reported in Chapter 3, Caco-2 intestinal epithelial cells exposed to *C. difficile* toxin A showed a significant reduction in mitochondrial dehydrogenase activity (Figure 6-2 A), which reflects cell viability, in a time and dose dependent manner. Mitochondrial dehydrogenase activity in HT29 cells remained largely similar with no reduction observed even at the highest concentration, see Figure 6-2 B.

Using the intestinal epithelial cell types as a benchmark for sensitivity the myofibroblast would appear to be as resilient as HT29 cells to ≤1000 ng/ml toxin A, (see Figure 6-2 B and C) with no reduction in mitochondrial dehydrogenase activity in myofibroblasts exposed to 100 ng/ml and 1000 ng/ml toxin A at 48 and 72 h.

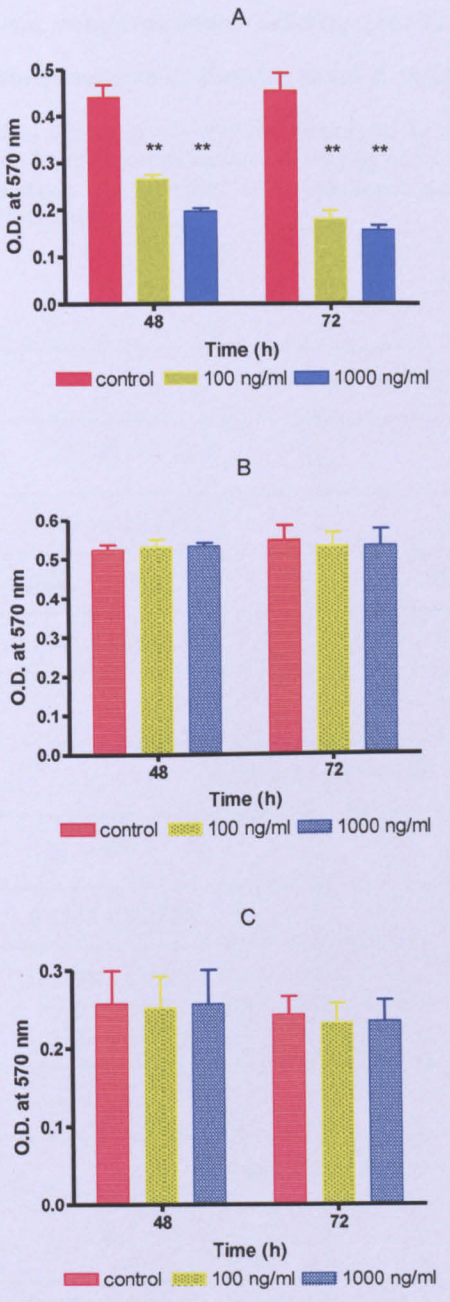

Figure 6-2 Mitochondrial dehydrogenase activity (MDA) in Caco-2, HT29 and primary colonic myofibroblasts to *C. difficile* toxin A (100- 1000 ng/ml)

MTT assay for mitochondrial dehydrogenase activity (expressed as OD 570 nm) in (A) Caco-2 cells (B) HT29 cells (C) Myofibroblasts exposed to 100 and 1000 ng/ml toxin A for 48 h and 72 h. Data in figures represent mean (±SEM) of 4 experiments performed in triplicate. ** = $p<0.01$ when compared with control

Table 6-2 Mitochondrial dehydrogenase activity (MDA) in Caco-2, HT29 and primary colonic myofibroblasts to *C. difficile* toxin A (100-1000 ng/ml)

MTT assay for mitochondrial dehydrogenase activity (expressed as OD 570 nm) in (A) Caco-2 cells, (B) HT29 cells and (C) Myofibroblasts exposed to varying concentrations of toxin B for 48 h and 72 h. Data in table presents mean (±SEM) of 4 experiments performed in triplicate. ** = $p<0.01$ when compared with control

A

Conc. (ng/ml)	Period of exposure (h)	
	48	72
Control	0.4405 ± 0.0253	0.4538 ± 0.0381
100	0.2648 ± 0.0082 **	0.1795 ± 0.0168 **
1000	0.1965 ± 0.0057 **	0.1568 ± 0.0091 **

B

Conc. (ng/ml)	Period of exposure (h)	
	48	72
Control	0.5230 ± 0.0127	0.5468 ± 0.0365
100	0.5298 ± 0.0175	0.5310 ± 0.0325
1000	0.5320 ± 0.0076	0.5320 ± 0.0416

C

Conc. (ng/ml)	Period of exposure (h)	
	48	72
Control	0.2570 ± 0.0419	0.2423 ± 0.0230
100	0.2518 ± 0.0405	0.2313 ± 0.0241
1000	0.2560 ± 0.0437	0.2328 ± 0.0264

6.4.1.3 Propidium Iodide staining and assessment of DNA fragmentation by flow cytometry

As described in section 6.2.5 page 248, Myofibroblasts incubated with toxin A or control media were fixed at 8 , 24, 48 and 72 h; stained with Propidium Iodide, and; fluorescence emitted measured by fluorescent activated cell sorting (n=3). Using WinMDI 2.9 and cell cycle analysis programme Cyclhred as described in Chapter 2, page 94 the number of events in the sub-G1 region was ascertained and a percentage of events in the sub-G1 region calculated against total events and presented as % of sub-G1 events in toxin treated cells against control (untreated) cells (Table 6-3).

As can be viewed in Figure 6-3, a small time dependent increase in the percentage of cells in the sub-G1 region can be observed, peaking at 72 h [mean toxin 4.2 (±SEM 0.936) vs control 0.807 (± 0.030) $p<0.05$], a significant increase was observed when compared against control. Representative DNA profiles of toxin and control cells indicate the majority of cells displayed DNA profiles of viable cells, see Figure 6-4.

Table 6-3 DNA analysis of Propidium iodide stained myofibroblasts incubated with *C. difficile* toxin A, 100 ng/ml

Percentage of sub-G1 events in toxin treated (1000 ng/ml toxin A) and control (untreated cells at 8, 24, 48, and 72 h. Percentage calculated using total events and number of events in the sub-G1 region when analysed using Cyclhred. Data in figures represent mean (±SEM) of 3 experiments performed in triplicate. n.s.= not significant.

		% of sub-G1 events in myofibroblasts		
		Control (untreated)	1000 ng/ml toxin A	p
Period of exposure (h)	8	2.313 ± 0.902	0.885 ± 0.135	n.s.
	24	2.114 ± 0.808	1.385 ± 0.131	n.s.
	48	0.576 ± 0.165	2.140 ± 0.210	n.s.
	72	0.807 ± 0.030	4.216 ± 0.936	0.0219

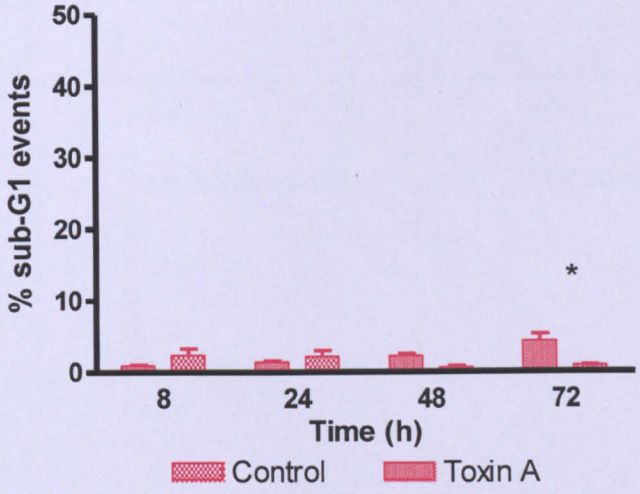

Figure 6-3 DNA analysis of Propidium iodide stained primary colonic myofibroblasts incubated with *C. difficile* toxin A, 1000 ng/ml

Assessment of myofibroblast sub G1 region of the cell cycle following exposure to 1000 ng/ml toxin A at 8, 24, 48 and 72 h. Percentage of sub-G1 events calculated using total events and number of events in the sub-G1 region when analysed using Cyclhred. Data in figures represent mean (±SEM) of 3 experiments performed in triplicate. * $p<0.05$

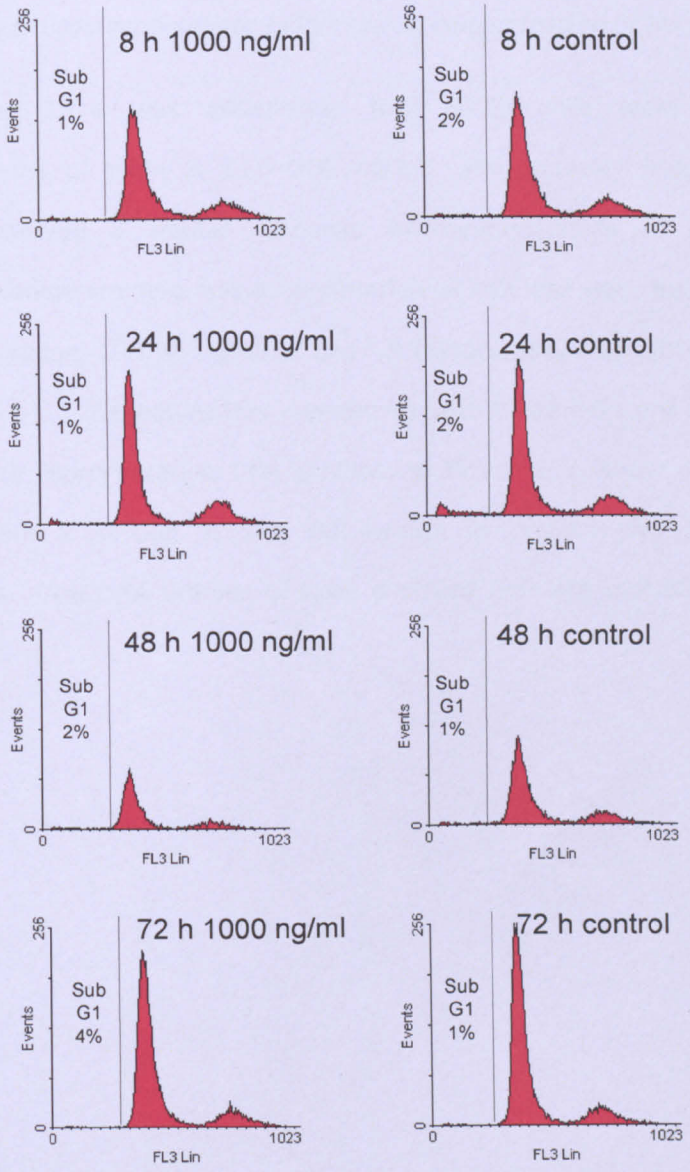

Figure 6-4 Representative DNA fluorescent profiles of propidium iodide stained myofibroblasts incubated with *C. difficile* toxin A (1000 ng/ml)

Cells cultured in the absence or presence of toxin A (1000 ng/ml, cytotoxicity titre 50% rounding at 10^{-14} at 24 h) for 8, 24, 48 and 72 h. Histograms represent data from all events produced using raw FACS data and WinMDI 2.9 scatterplots gated for single cells excluding cell debris at given timepoints. The sectioned part of the histogram shows events in the sub-G1 region and the other two peaks represent cells in the G0/G1 and G2 regions, respectively. The S phase events are found between the two peaks. Data for events in the sub-G1 region represent means of three experiments performed in triplicate.

6.4.1.4 Myofibroblast response to increasing concentration of toxin A

In Chapter 3, it was established that HT29 cells were resilient to concentrations of toxin A ≤10 000 ng/ml, with minimal loss of viability. Having observed a similar response in myofibroblasts at 1000 ng/ml, propidium iodide staining and determination of cell loss was repeated using a ten-fold increase, 10 000 ng/ml of toxin A (cytotoxicity titre 50% rounding at 10^{-18} at 24 h). Repeating this experiment with three different myofibroblast isolates, the representative DNA profiles, in Figure 6-5, show no loss of cell viability with a similar % sub G1 events in control and toxin treated histograms. The DNA profiles of toxin exposed cells are indicative of normal viable cells.

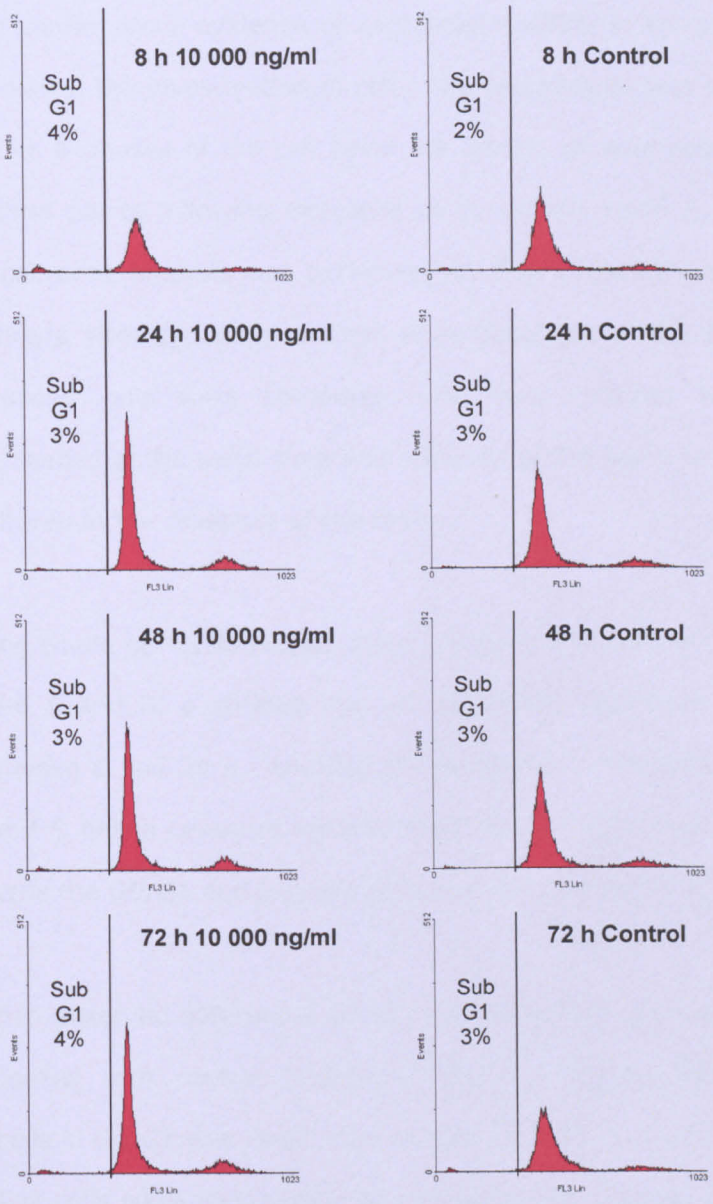

Figure 6-5 Representative DNA fluorescent profiles of propidium iodide stained myofibroblasts incubated with *C. difficile* toxin A (10000 ng/ml)

Cells cultured in the absence or presence of toxin A (10000 ng/ml, cytotoxicity titre 50% rounding at 10^{-18} at 24 h) for 8, 24, 48 and 72 h. Histograms represent data from all events produced using raw FACS data and WinMDI 2.9 scatterplots gated for single cells excluding cell debris at given timepoints. The sectioned part of the histogram shows events in the sub-G1 region and the other two peaks represent cells in the G0/G1 and G2 regions, respectively. The S phase events are found between the two peaks. Data for events in the sub-G1 region represent means of three experiments performed in triplicate.

6.4.1.5 Cell cycle response in toxin A exposed intestinal Myofibroblasts

Providing confirmatory evidence of sustained viability in toxin A exposed myofibroblasts, the investigation of cell cycle progression was investigated to ascertain if phases of the cell cycle are under- or over-represented at various time points following exposure to *C. difficile* toxin A. For these studies, cell cycle analysis was performed by flow cytometry at 8, 24, 48 and 72 hours after exposure to toxin A as described in 6.2.5 page 248. Toxin-exposed cells were compared with cells cultured with control medium, seeded at the same time and obtained at the same time points as those cultured in the presence of the toxin.

Comparing whole cell cycle profile in toxin treated and control (untreated), Figure 6-6 A and B, a striking but not significant difference appears to occur between 8 and 24 h. Looking at the control (untreated) profile the G0/G1 and S phase contours remain apart throughout, however in toxin treated cells the G0/G1 and S phase contours clearly overlap at 24 hours.

Some small observed differences can be reported when toxin exposed cells are compared with control (untreated cells), the percentage of toxin treated cells in G0/G1 was lower than control until 48 hour where the toxin and control cells were very similar and remained so through to 72 hours. Mirroring the apparent reduction in toxin exposed myofibroblasts in G0/G1 phase, a higher percentage of toxin exposed cells in S-phase is observed. The percentages of cells in G2 phase remain similar throughout. Whilst small observations have been made no statistical significance was seen in individual phases of the cell cycle at any given time point, see Figure 6-7 A-C.

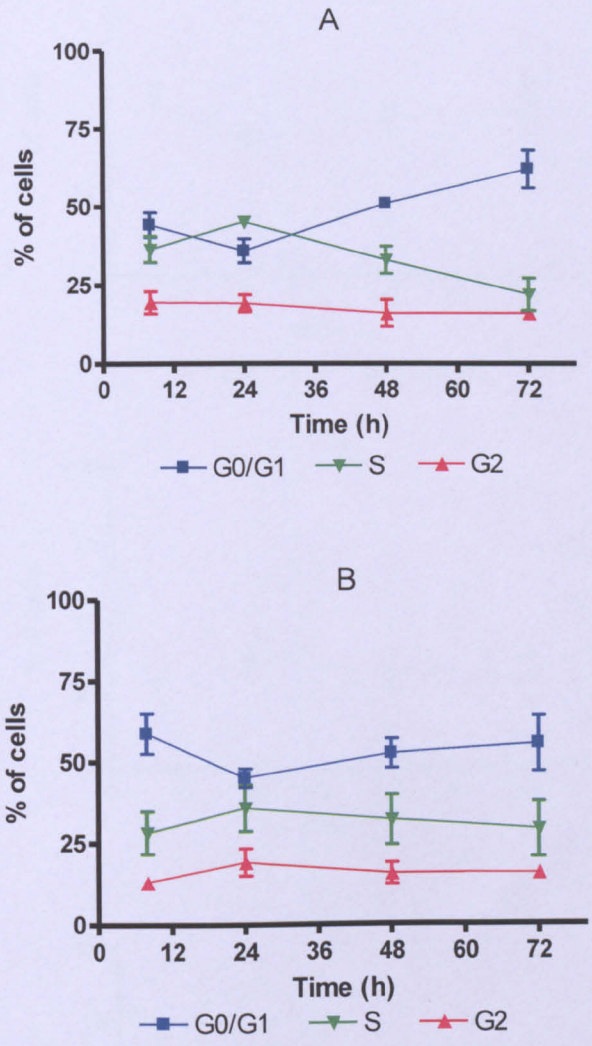

Figure 6-6 Whole cell cycle analysis of myofibroblasts incubated with *C. difficile* toxin A (1000 ng/ml)

Using PI stained myofibroblasts incubated with 1000 ng/ml of *C. difficile* toxin A (B17, cytotoxic activity on Vero cells $x10^{-14)}$ (A) or control medium (B) for 4 h, 8 h, 24 h, 48 h and 72 h, the cells were sorted using FACS and the resulting scatterplot gated to remove debris. Using only the gated events the percentage of cells in each phase of the cell cycle was calculated using Cyclhred. Data presented as % (± SEM) of cells in G0/G1, S and G2 phase n=3. This data reflects viable cells only and does not reflect the cells lost to cell death

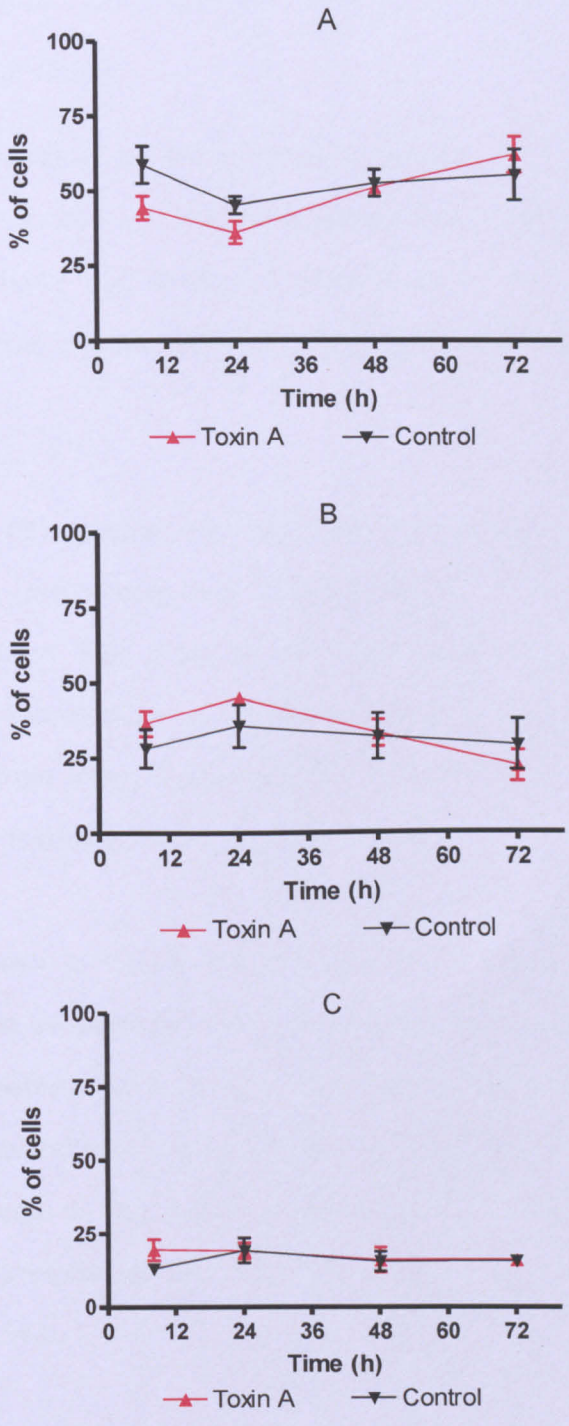

Figure 6-7 Individual phase cell cycle analysis of myofibroblasts incubated with *C. difficile* toxin A (1000 ng/ml)

Percentage of myofibroblasts in G0/G1 (A) S-phase (B) and G2 (C), comparison of toxin treated and control cells at 8 h, 24 h, 48 h and 72 h. Toxin A from B17, cytotoxic activity on Vero cells $x10^{-14}$. Data presented as % ± SEM n=3 *=p=<0.05 PI stained cells were sorted using FACS and the resulting scatterplot gated to remove debris. Using only the gated events the percentage of cells in each phase of the cell cycle was calculated using Cyclhred. This data reflects viable cells only and does not reflect the cells lost to cell death

6.4.1.6 Substrate specificity in toxin A exposed primary colonic myofibroblasts.

Rho, Rac-1 and Cdc42 are the intracellular targets for *C. difficile* toxins and utilizing UDP-glucose as the co-substrate the toxins are capable of maintaining these key molecular proteins in an inactive state. The mechanisms that lead to their inactivation have been covered in detail in Chapter 1.

Using whole cell lysates prepared from myofibroblasts incubated with either toxin A (cytotoxicity titre 50% rounding at 10^{-94} at 24 h) or control medium Western Blot analysis was completed using protein specific antibodies to ascertain the expression of non-glucosylated Rac-1 and total (non-glucosylated and glucosylated) Rho A, see Chapter 2 for a complete description of methods used.

As can be seen in Figure 6-8, a reduction in non-glucosylated Rac-1 expression can be observed from as early as 4 hrs when compared to the control (untreated) lysate at 0 h. This loss continued through to 24 h. Total Rho A expression in toxin treated myofibroblasts remained constant when compared to the control (untreated) cell lysate at 0 h. The consistent expression of Rho A in toxin treated myofibroblasts was still evident after 24 h.

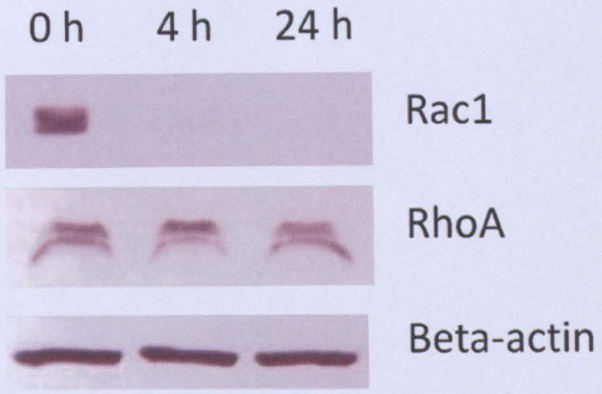

Figure 6-8 Expression of Rac-1, RhoA and beta-actin in control and C. *difficile* toxin A exposed primary colonic myofibroblasts

Myofibroblast monolayers were cultured in medium only (0 h) or in the presence of 1,000 ng/ml toxin A (cytotoxicity titre on Vero cells 50% rounding at 10^{-94} at 24 h) for 4 h and 24 h. Lysates of myofibroblasts were electrophoresed on SDS-PAGE gels and following transfer onto PVDF membranes, immunostaining was performed using antibodies specific for RhoA, beta-actin or non-glucosylated form of Rac1. Equal loading of the lanes is illustrated by beta-actin-immunoreactive bands of similar size. The figures are representative of three experiments using myofibroblasts isolated from colonic mucosal samples from three donors.

6.4.1.7 Smooth Muscle Actin distribution in toxin A exposed myofibroblasts

Immunohistochemical studies showed that the processes in toxin A exposed myofibroblasts were strongly immunoreactive for alpha-smooth muscle actin and the persistence of these immunoreactive processes was still evident at 72 h. Longitudinally arranged, α-smooth muscle actin-immunoreactive, bundles of microfilaments are seen in myofibroblasts cultured in control medium (Figure 6-9 A & B). In myofibroblasts exposed to *C. difficile* toxin A (Figure 6-9 C-L), the cell cytoplasm surrounding the nucleus and the cell processes (identified with arrows in Figure 6-9 F) are immunoreactive for α-smooth muscle actin. In addition, upon microscopic inspection of the toxin A exposed myofibroblasts, the integrity of the cell membrane remained intact throughout.

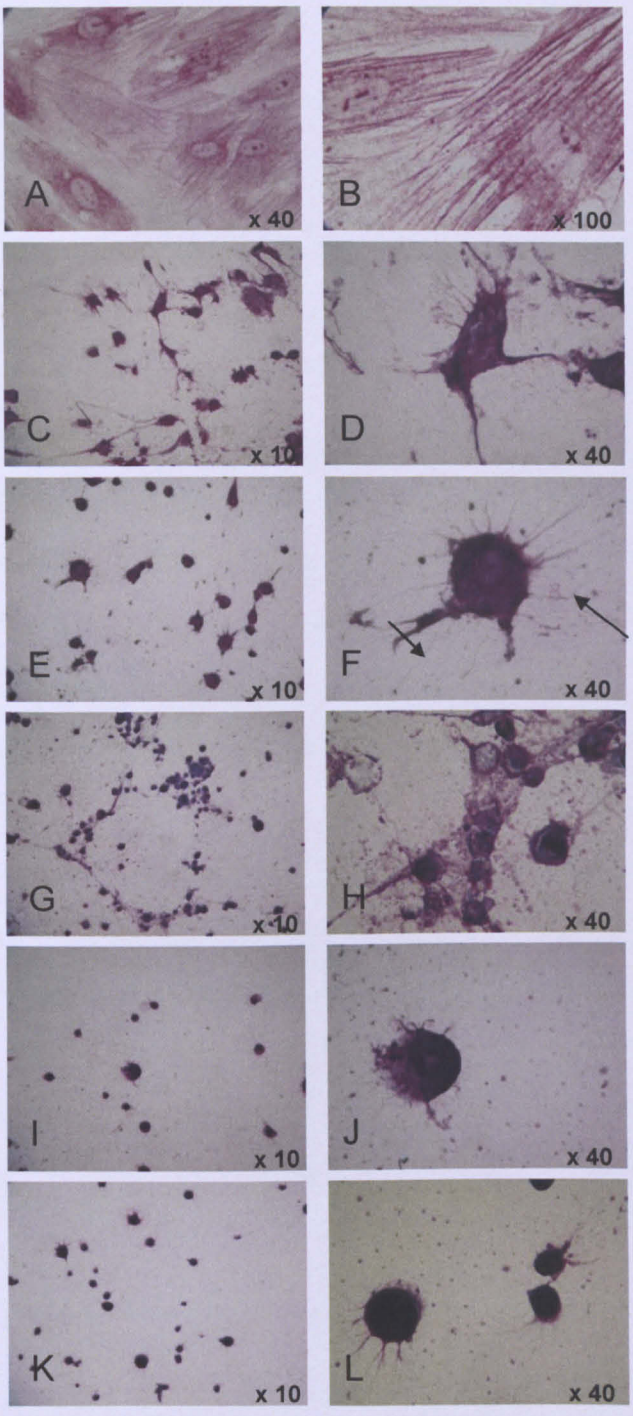

Figure 6-9 Alpha smooth muscle actin expression by *C. difficile* toxin A exposed myofibroblasts

Alpha- smooth muscle actin expression (3-72 h). Immunocytochemical studies were undertaken in monolayers of isolated normal human colonic myofibroblasts that had been cultured in medium only (A & B) or in the presence of 1,000 ng/ml toxin A (C-L). Low x10 (A-K) and High x40 and x100 (B-L) power images are shown at various time points; 3 h (C & D), 6 h (E & F), 24 h (G & H), 48 h (I & J) and 72 h (K & L). Arrows point to immunoreactive processes extending from the cell.

6.4.1.8 Recovery of Myofibroblasts exposed to C. difficile toxin A

In studies undertaken using myofibroblasts isolated from 8 different donors, morphological recovery of the cells was studied after 3 h pre-exposure to 1000 ng/ml and 10000 ng/ml toxin A followed by washing and culture in medium only. While cultured in medium, signs of recovery were observed between 2-4 weeks in myofibroblast isolates pre-exposed to toxin A (cytotoxicity titre on Vero cells 50% rounding at 10^{-14} at 24 h) for 3 h (see Figure 6-10). Myofibroblasts returned to normal morphology with the monolayers becoming fully confluent between 4 and 9 weeks. In addition, following trypsinisation and re-culture (passage in 1:3 split ratio), the toxin A-pre-exposed myofibroblasts proliferated to confluence.

Subsequent recovery experiments increased the pre-exposure time to include 24 and 48 h to 10000 ng/ml and 1000 ng/ml toxin A. The colonic myofibroblasts pre-exposed to toxin A (cytotoxicity titre on Vero cells 50% rounding at 10^{-18} at 24 h) for 3 h, 24 h and 48 h all showed signs of recovery in a dose and time dependent manner.

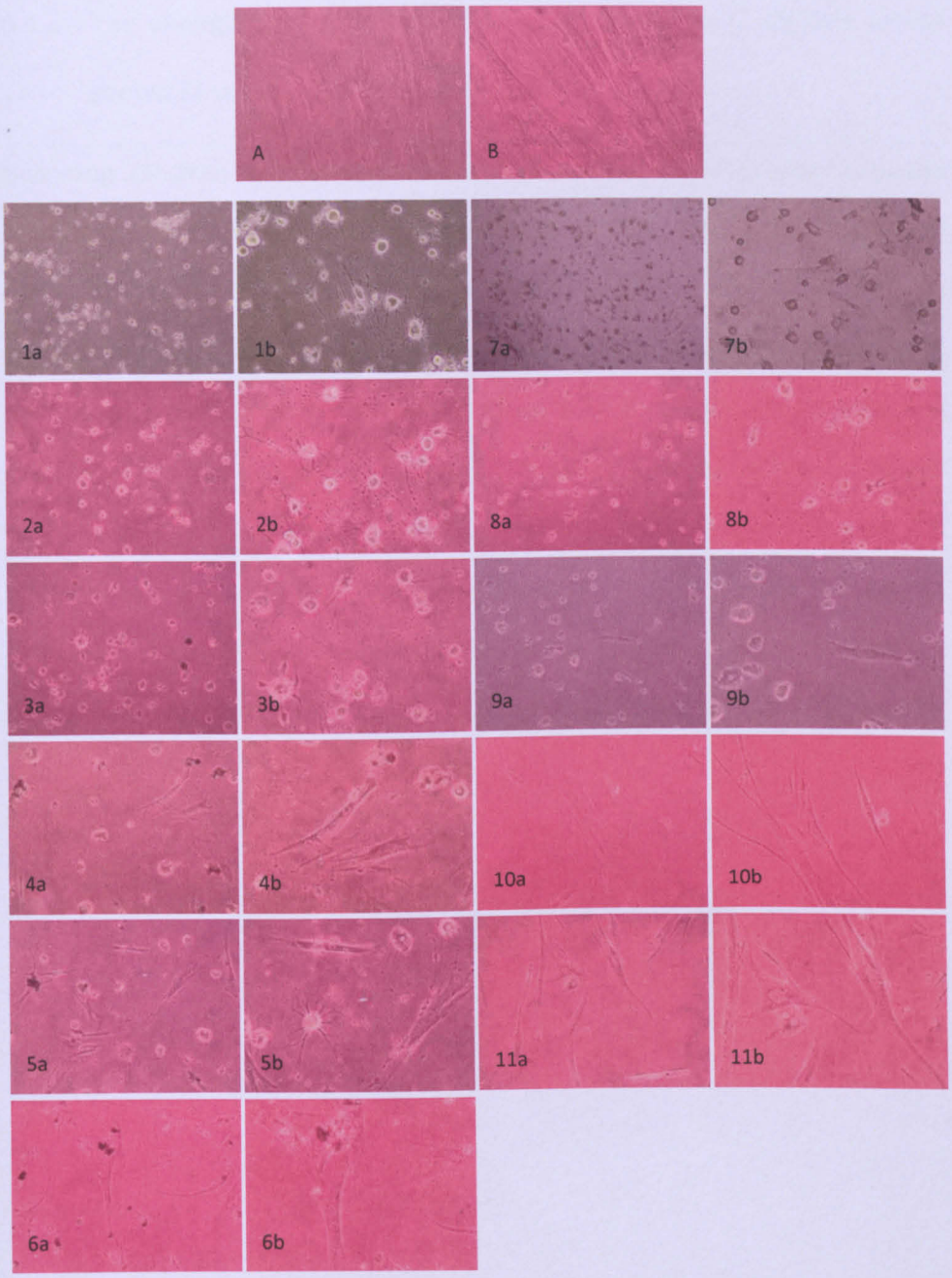

Figure 6-10 Phase contrast micrographs of recovery in myofibroblasts pre-exposed to *C. difficile* toxin A (1000-10000 ng/ml) for 3 h

Recovery in myofibroblasts following pre-exposure to 10000 ng/ml (images 1a-6b) and 1000 ng/ml (images 7a-11b). Image (A) represents low (x10) and image (B) high (x40) power micrographs of control (untreated) cells. Image 1a-b and 7a-b pre-exposure after 3 hr; 2a-b and 8a-b 1 week later; 3a-b and 9a-b 2 weeks later; 4a-b and 10a-b 3 weeks later; 5a-b and 11a-b 4 weeks; 6a-b 5 weeks

6.4.2 The changing morphology of myofibroblasts to *C. difficile* toxins shown in scanning electron micrographs.

Scanning electron micrographs of control and *C. difficile* toxin exposed myofibroblasts provide detailed evidence of the dramatic change in myofibroblast morphology. Myofibroblasts maintained in control medium spread to occupy a large surface area. By contrast cells incubated with toxin A or B change from flat cells to those with a stellate appearance and myofibroblast size reduced (Figure 6-11 A & D). The numerous processes of varying thickness can be viewed using phase contrast microscopy but additionally the scanning electron microscopy has identified distinct globular structures seen either close to the cell body or at a distance associated with processes (marked with arrows in Figure 6-11 B, C, and F).

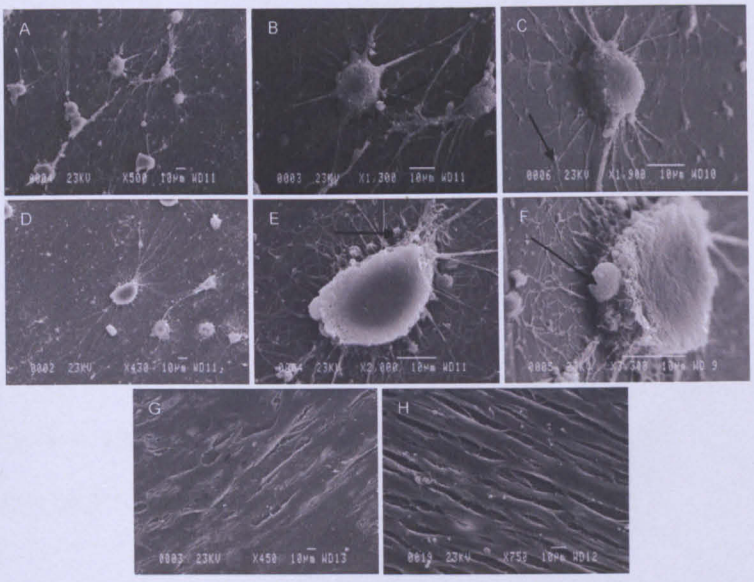

Figure 6-11 Scanning electron micrographs of *C. difficile* toxin A or toxin B exposed primary colonic myofibroblasts

Micrographs of myofibroblasts incubated with *C. difficile* toxin A (A-C) or toxin B (D-F) 1000 ng/ml or control medium (G-H) for 24 h. Arrows point to distinct globular structures seen either close to the cell body or associated at a distance to processes (further characterization of globular structures needed)

6.4.3 Results - Primary colonic myofibroblast response to *C. difficile* toxin B

With the myofibroblast response to toxin A established experiments to investigate the response of intestinal myofibroblasts to *C. difficile* toxin B were completed. Given the reported increase in cytotoxicity of toxin B three concentrations were studied, 10, 100 and 1000 ng/ml and in addition to cell viability being studied at 48 and 72 hours, a 24 hour time point was included. These concentrations have been to shown to cause cell rounding in both HT29 and Caco-2 cells and induce cell death in Caco-2 cells. Myofibroblasts were grown to confluence and the morphological response and cell viability in response to toxin B exposure recorded. Morphological changes were assessed from 1 h - 72 h using phase contrast microscopy and the cells in each well categorized into percentage cell rounding. Tabular confirmation of rounding can be found in and representative micrographs of myofibroblasts at each of these stages can be viewed in Figure 6-12. Cellular viability was established at 24, 48 and 72 hours post toxin exposure.

6.4.3.1 Dose and time dependent change in cell morphology

A time and dose dependent response was recorded in the intestinal myofibroblasts exposed to toxin B (cytoxicity titre on Vero cells at 24 h 10^{-47}), with 50% rounding visible after just 1 hour at 1000 ng/ml, see Table 6-1. As observed in toxin A exposed myofibroblasts, toxin B exposure causes an transformation into a stellate shape, see Figure 6-12, image c. By 3 hours the majority of cells were rounded (exposed to 100 or 1000 ng/ml) with only a few cells still in a stellate form. By 24 hours 100%

rounding was evident and the majority of cells appeared to be fragmented or floating in cells exposed to ≥100 ng/ml toxin B

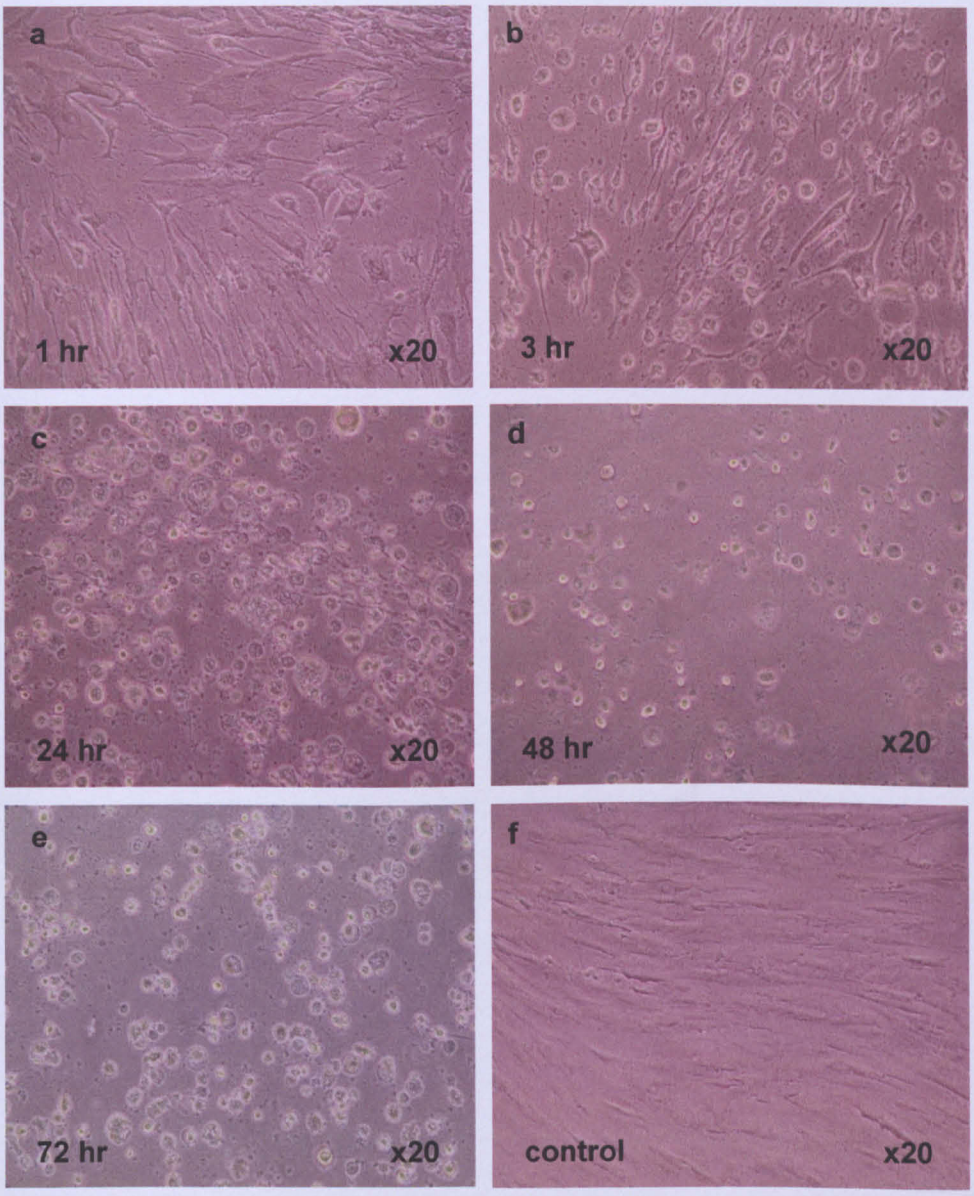

Figure 6-12 Phase contrast micrographs of myofibroblasts exposed to *C. difficile* toxin B (1000 ng/ml)

Phase contrast micrographs of primary intestinal myofibroblasts exposed to *C. difficile* toxin B. Representative image taken from three experiments using different patient isolates. Cells incubated with either control medium (f) or 1000 ng/ml toxin B (cytotoxicity titre on Vero cells at 24 h 10^{-47}) from 1 h through to 72 h (a-e).

Table 6-4 Cell rounding in primary colonic myofibroblasts to *C. difficile* toxin B

Percentage cell rounding in cells in response to 10 ng/ml 100 ng/ml and 1000 ng/ml of toxin B. Morphological changes to the cells were studied by phase contrast microscopy and the percentage of rounded cells ascertained by counting the rounded cells in ten random high power fields and taking the mean of these ten observations and reporting the value to the nearest 10%.

Toxin B (ng/ml)	Duration of toxin B exposure						
	1 h	2 hours	3 hours	8 hours	24 hours	48 hours	72 hours
10	-	-	-	60	100	100	100
100	-	-	80	100	100	100	100
1000	70	90	100	100	100	100	100

6.4.3.2 *Investigation of cellular viability using the MTT assay*

Having observed a consistent response to toxins A and B in intestinal epithelial cells, with a significant reduction of cell viability in toxin exposed Caco-2 cells and resilience in HT29 cells to both toxins the results for toxin B exposed myofibroblasts were of particular interest. The myofibroblast responses to *C. difficile* toxin B resulted in a time and dose dependent loss of mitochondrial dehydrogenase activity, see Figure 6-13. At 10 ng/ml, a small loss was apparent but not statistically significant, see Table 6-5.

In stark contrast to the responses reported in toxin A exposed myofibroblasts (Figure 6-2 page 263), mitochondrial dehydrogenase activity as a measure of cell viability in myofibroblasts was significantly reduced following exposure to 100 ng/ml and 1000 ng/ml as early as 24 hour when compared against control (untreated cells) [100 ng/ml mean 0.2001 (±SEM 0.0144) vs control 0.3941 (±0.0105) p= <0.05; 1000 ng/ml 0.1774 (±0.0065) vs control 0.3941 (±0.0105) p= <0.01] and a continued loss seen through 48 hour [100 ng/ml 0.1834 (±0.0382) vs control 0.4078 (±0.0037) p=<0.05; 1000 ng/ml 0.1719 (± 0.0295) vs control 0.4078 (±0.0037) p=<0.05] and 72 hours [100 ng/ml 0.1437 (±0.0170) vs control 0.3117 (±0.0177) p=<0.01; 1000 ng/ml 0.1411 (±0.0201) vs control 0.3117 (±0.0177) p=<0.05].

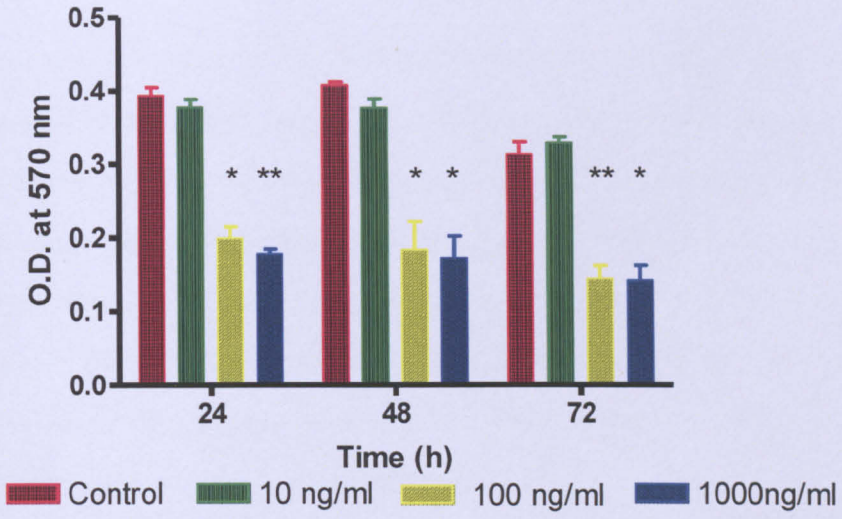

Figure 6-13 Mitochondrial dehydrogenase activity (MDA) in myofibroblasts exposed to C. difficile toxin B (10-1000 ng/ml)

MTT assay for mitochondrial dehydrogenase activity (expressed as OD 570 nm) in myofibroblasts exposed to 10, 100 and 1000 ng/ml toxin B (cytotoxicity on Vero cells at 24 h 10^{-47}) for 24, 48 and 72 h. Data in figures represent mean (±SEM) of 3 experiments performed in triplicate. *=$p<0.05$ ** = $p<0.01$ when compared with control

Table 6-5 Mitochondrial dehydrogenase activity (MDA) in myofibroblasts exposed to C. difficile toxin B (10-1000 ng/ml)

MTT assay for mitochondrial dehydrogenase activity (expressed as OD 570 nm) in myofibroblasts exposed to varying concentrations of toxin B for 24, 48 h and 72 h. Data in table presents mean (±SEM) of 3 experiments performed in triplicate. *=$p<0.05$ ** = $p<0.01$ when compared with control

Conc. (ng/ml)	Period of exposure (h)		
	24	48	72
Control	0.3941 ± 0.0105	0.4078 ± 0.0037	0.3117 ± 0.0177
10	0.3771 ± 0.0109	0.3760 ± 0.0121	0.3286 ± 0.0075
100	0.2001 ± 0.0144 *	0.1834 ± 0.0382 *	0.1437 ± 0.0170 **
1000	0.1774 ± 0.0065 **	0.1719 ± 0.0295 *	0.1411 ± 0.0201 *

6.4.3.3 PI staining and measurement using FACS confirm cell loss

As described in section 2.7.3, Myofibroblasts were incubated with toxin B (cytotoxicity titre on Vero cells at 24 h 10^{-94}) or control media were fixed at 8 , 24, 48 and 72 h; stained with Propidium Iodide, and; fluorescence emitted measured by fluorescent activated cell sorting (n=3). Using WinMDI 2.9 and cell cycle analysis programme Cyclhred as described in Chapter , the number of events in the sub-G1 region was ascertained and this number presented as a percentage of the total events recorded, comparing the percentage events in the sub-G1 region in toxin A-treated cells with control (untreated) cells.

As can be viewed in Figure 6-14 a time dependent increase in the percentage of cells in the sub-G1 region is observed in toxin treated cells, becoming statistically significant at 72 hours [1000 ng/ml 35.150 (±1.310) vs control 0.800 (±0.019) p=<0.01]. Although not statistically significant 13% of the total events were sub-G1 events at 48 hours, see Table 6-6. Supporting the MTT data, representative DNA profiles of toxin B exposed myofibroblasts clearly show DNA fragmentation due to apoptotic death at 48 hour and 72 hour, see Figure 6-15.

Table 6-6 DNA analysis of Propidium iodide stained primary colonic myofibroblasts incubated with *C. difficile* toxin B (1000 ng/ml)

Percentage of sub-G1 events in toxin treated (1000 ng/ml toxin B) and control (untreated cells at 8, 24, 48, and 72 h. Percentage calculated using total events and number of events in the sub-G1 region when analysed using Cyclhred. Data in figures represent mean (±SEM) of 3 experiments performed in triplicate. n.s.= not significant.

		% of sub-G1 events in myofibroblasts		
		Control (untreated)	1000 ng/ml toxin B	p
Period of exposure (h)	8	1.126 ± 0.146	1.291 ± 0.0626	n.s.
	24	1.436 ± 0.041	2.298 ± 0.243	n.s.
	48	1.168 ± 0.215	13.380 ± 3.815	n.s.
	72	0.800 ± 0.019	35.150 ± 1.310	0.0015

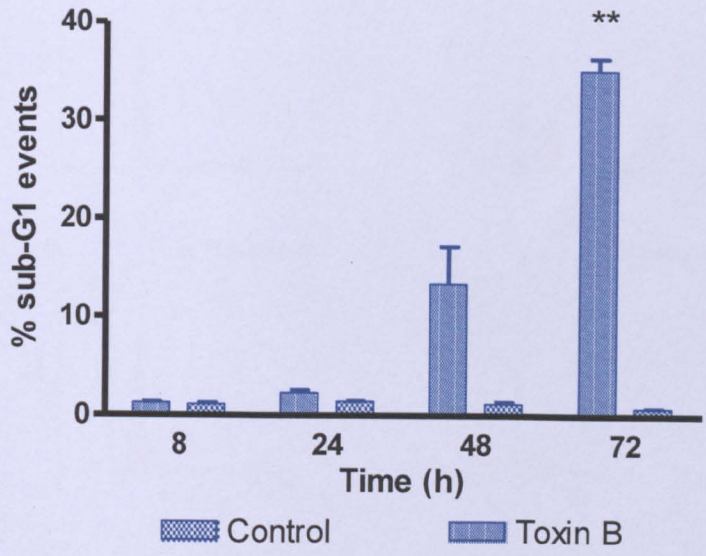

Figure 6-14 DNA analysis of Propidium iodide stained primary colonic myofibroblasts incubated with *C. difficile* toxin B, 1000 ng/ml

Assessment of myofibroblast sub G1 region of the cell cycle following exposure to 1000 ng/ml toxin B (cytotoxicity titre on Vero cells at 24 h 10^{-94}) at 8, 24, 48 and 72 h. Percentage of sub-G1 events calculated using total events and number of events in the sub-G1 region when analysed using Cyclhred. Data in figures represent mean (±SEM) of 3 experiments performed in triplicate. ** $p<0.01$

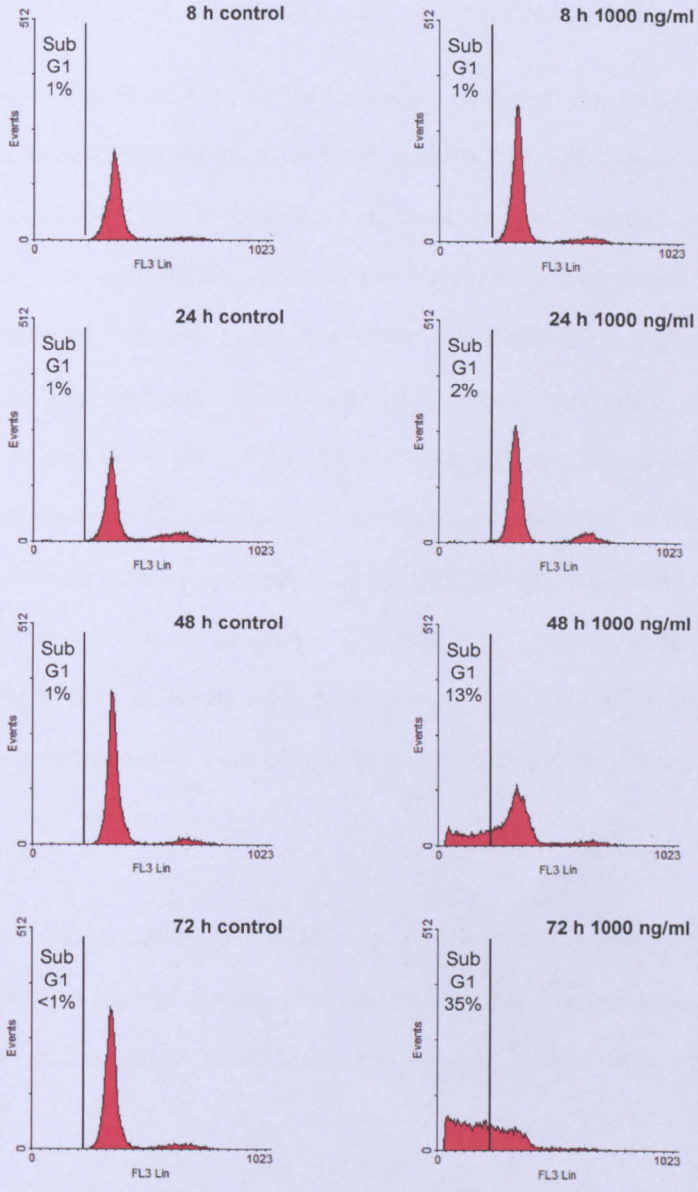

Figure 6-15 Representative DNA profiles of propidium iodide labelled myofibroblasts exposed to *C. difficile* toxin B

Cells cultured in the absence or presence of toxin B (1000 ng/ml, cytotoxicity titre 50% rounding at 10^{-94} at 24 h) for 8, 24, 48 and 72 h. Histograms represent data from all events produced using raw FACS data and WinMDI 2.9 scatterplots gated for single cells excluding cell debris at given timepoints. The sectioned part of the histogram shows events in the sub-G1 region and the other two peaks represent cells in the G0/G1 and G2 regions, respectively. The S phase events are found between the two peaks. Data for events in the sub-G1 region represent means of three experiments performed in triplicate

6.4.3.4 Cell cycle response in toxin B exposed intestinal myofibroblasts

An increase in the % events in the sub-G1 region of the cell cycle following exposure of myofibroblasts to *C. difficile* toxin B from 48 hours supported my earlier finding that toxin B reduced cell viability and induced cell death. As commented upon previously, studies by others has suggested that cells in certain phases of the cell cycle are more susceptible to toxin-induced cell death and to this end cell cycle progression was investigated to ascertain if phases of the cell cycle are under- or over-represented at various time points following exposure to *C. difficile* toxin B. For these studies, cell cycle analysis was performed by flow cytometry at 8, 24, 48 and 72 hours after exposure to toxin B as described in Chapter 2, page 94. Toxin-exposed cells were compared with cells cultured with control medium, seeded at the same time and obtained at the same time points as those cultured in the presence of the toxin.

Studying the individual Figure 6-17 and whole cycle graphs Figure 6-16 of toxin treated and control (untreated) myofibroblasts the percentage of cells in each phase at any given time point are largely similar with no identifiable differences.

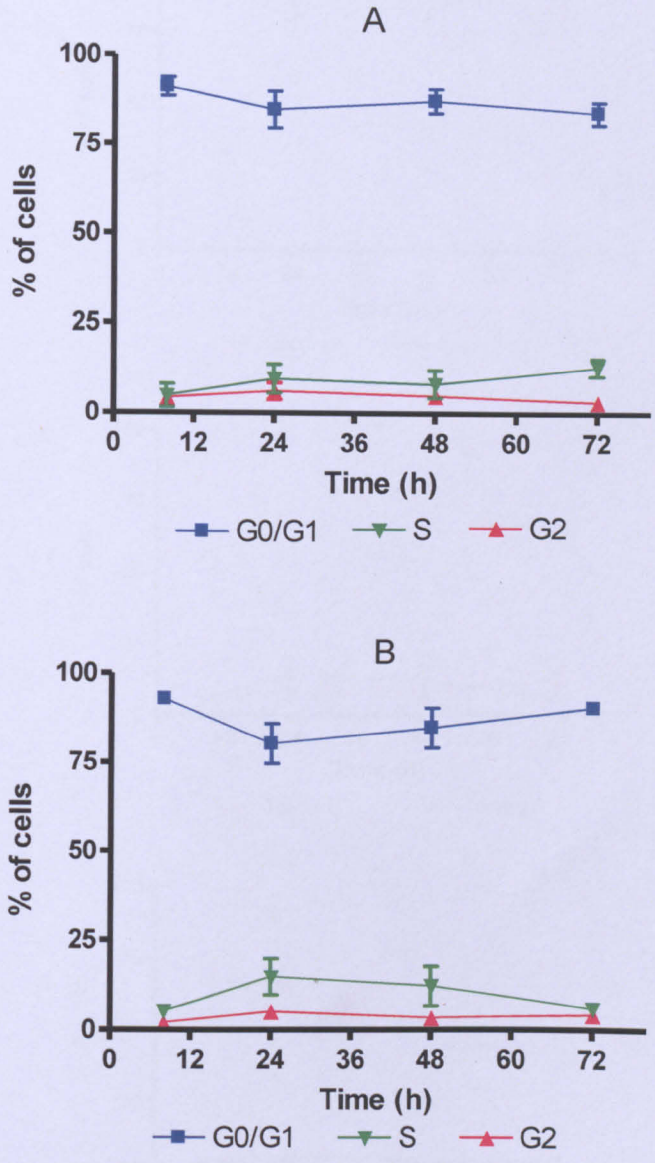

Figure 6-16 Cell cycle analysis of myofibroblasts incubated with *C. difficile* toxin B

Using PI stained myofibroblasts incubated with 1000 ng/ml of *C. difficile* toxin B (J2C, cytotoxic activity on Vero cells $x10^{-94)}$ (A) or control medium (B) for 4 h, 8 h, 24 h, 48 h and 72 h, the cells were sorted using FACS and the resulting scatterplot gated to remove debris. Using only the gated events the percentage of cells in each phase of the cell cycle was calculated using Cyclhred. Data presented as % (± SEM) of cells in G0/G1, S and G2 phase n=3. This data reflects viable cells only and does not reflect the cells lost to cell death

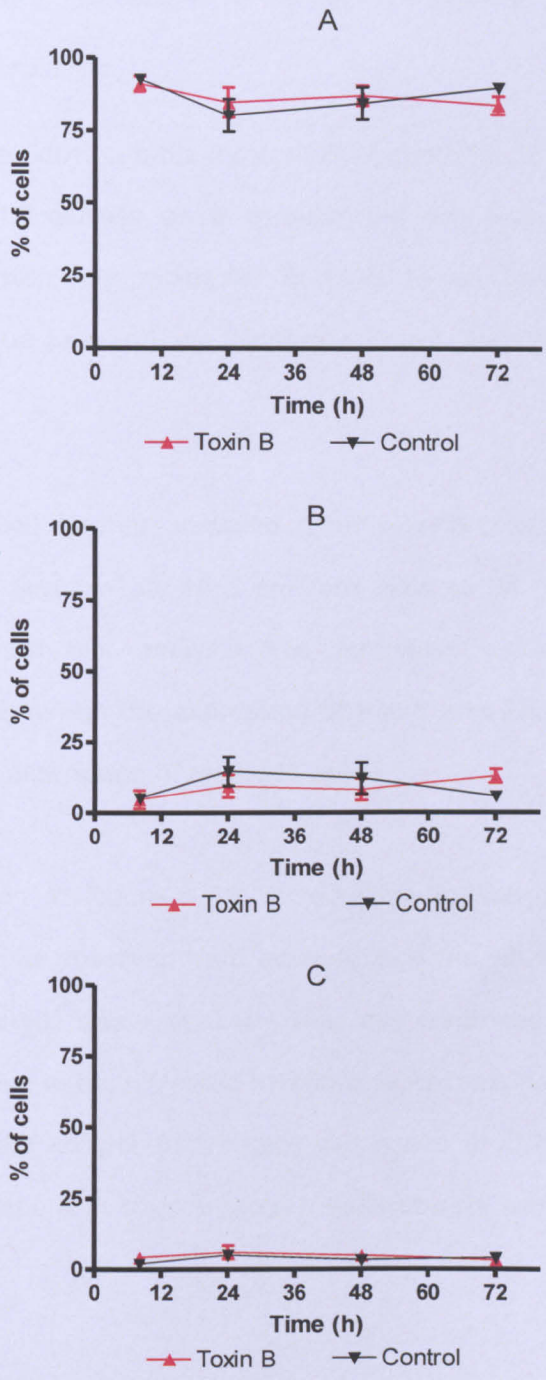

Figure 6-17 Individual phase cell cycle analysis of myofibroblasts incubated with *C. difficile* toxin B (1000 ng/ml)

Percentage of myofibroblasts in G0/G1 (A) S-phase (B) and G2 (C), comparison of toxin treated and control cells at 8 h, 24 h, 48 h and 72 h. Toxin B from J2C, cytotoxic activity on Vero cells $x10^{-94}$. Data presented as % ± SEM n=3 *=p=<0.05 PI stained cells were sorted using FACS and the resulting scatterplot gated to remove debris. Using only the gated events the percentage of cells in each phase of the cell cycle was calculated using Cyclhred. This data reflects viable cells only and does not reflect the cells lost to cell death

6.4.3.5 Substrate specificity in toxin B exposed primary colonic myofibroblasts.

Rho, Rac-1 and Cdc42 are the intracellular targets for *C. difficile* toxins and by utilizing UDP-glucose as a co-substrate the toxins are capable of maintaining these key molecular proteins in an inactive state. The mechanisms that lead to their inactivation have been covered in detail in Chapter 1.

Using whole cell lysates prepared from myofibroblasts incubated with either toxin B (cytotoxicity titre on Vero cells at 24 h 10^{-54}) or control medium Western Blot analysis was completed using protein specific antibodies to ascertain the expression of Rac-1 and Rho A, see Chapter 2 for a complete description of methods used.

As can be seen in Figure 6-18, a reduction in non-glucosylated Rac-1 expression can be observed from as early as 4 hrs when compared to the control (untreated) lysate at 0 h. This loss continued through to 24 h. Rho A expression in toxin treated myofibroblasts remained consistent when compared to the control (untreated) cell lysate at 0 h. The consistent expression of Rho A in toxin treated myofibroblasts was still evident after 24 h.

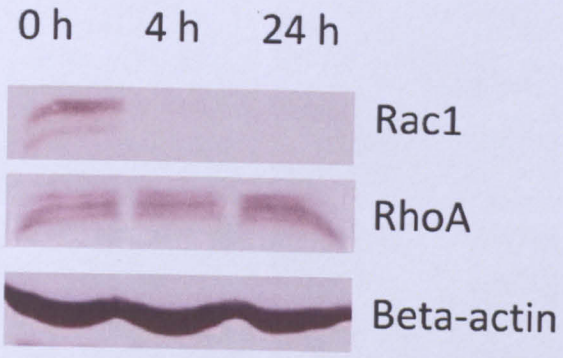

Figure 6-18 Expression of Rac1, RhoA and beta actin in control and *C. difficile* toxin B exposed myofibroblasts.

Monolayers of isolated normal human colonic myofibroblasts were cultured in medium only (0 h) or in the presence of 1,000 ng/ml toxin B (cytotoxicity titre on Vero cells at 24 h 10^{-5}) for 4 h and 24 h. Lysates of myofibroblasts were electrophoresed on SDS-PAGE gels and following transfer onto PVDF membranes, immunostaining was performed using antibodies specific for RhoA, beta-action or non-glucosylated form of Rac1. Equal loading of the lanes is illustrated by beta-actin-immunoreactive bands of similar size. The figures are representative of three experiments using myofibroblasts isolated from colonic mucosal samples from three donors.

6.4.3.6 Smooth Muscle Actin distribution in toxin B exposed myofibroblasts

Immunohistochemical studies showed longitudinally arranged, α-smooth muscle actin-immunoreactive, bundles of microfilaments in myofibroblasts cultured in control medium (A & B). The processes in toxin B exposed myofibroblasts were strongly immunoreactive for alpha-smooth muscle actin at 3 h and 6 h (C-F) and the persistence of these immunoreactive processes was evident at 24 h (G & H). By 48 h and 72 h and as observed by phase contrast microscopy (Figure 6-19) the majority of myofibroblasts exposed to toxin B (at concentration of 1000 ng/ml) had lost processes and variable immunoreactivity for α-smooth muscle actin was observed at 48 hours (I & J). At 72 hours many toxin B exposed cells appeared to have lost the integrity of their cell membranes, showing either negative or weakly positive immunoreactivity for α-smooth muscle actin and appearing non-viable (K & L).

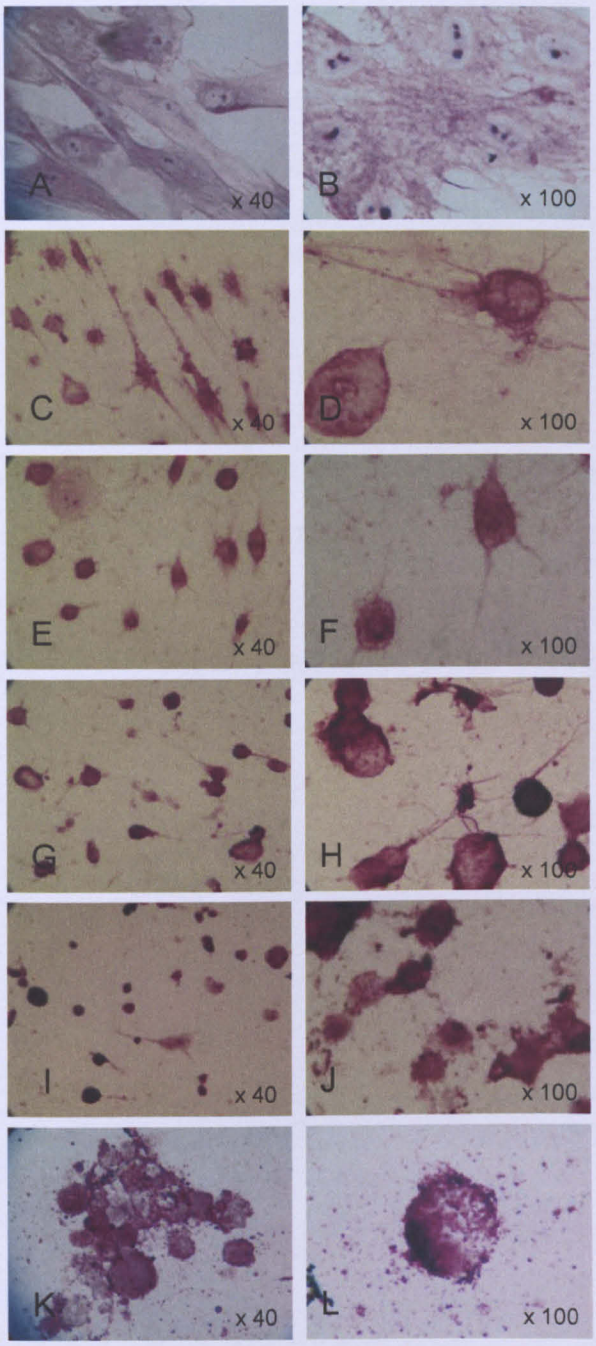

Figure 6-19 Alpha-smooth muscle actin expression by control and *C. difficile* toxin B exposed myofibroblasts (1000 ng/ml)

Immunocytochemical studies were undertaken in monolayers of isolated normal human colonic myofibroblasts that had been cultured in medium only (A & B) or in the presence of 1,000 ng/ml toxin B (cytotoxicity on Vero cells at 24 h 10^{-54}) (C-L). Low x40 (A-K) and High x100 (B-L) power images are shown at various time points; 3 h (C & D), 6 h (E & F), 24 h (G & H), 48 h (I & J) and 72 h (K & L).

6.4.3.7 Hoechst staining of toxin B exposed myofibroblasts

To investigate signs of apoptosis in toxin B exposed myofibroblasts were fixed, stained with Hoechst 33342 and mounted onto to glass slides. The slides were observed immediately using the fluorescent microscope (Nikon Eclipse TE2000-S). Fluorescent and corresponding phase contrast micrographs were taken, see Figure 6-20. Fluorescent microscopy of myofibroblasts after staining with Hoechst 33342 in control cells (A & B) and cells exposed to *C. difficile* toxin B (cytotoxicity on Vero cells at 24 h 10^{-94}), 100 ng/ml (C & D) and 1000 ng/ml (E & F). Toxin B induced morphological changes typical of apoptosis; cells with nuclear chromatin fragmentation and/or condensation are indicated by the arrow and the arrow-head, respectively.

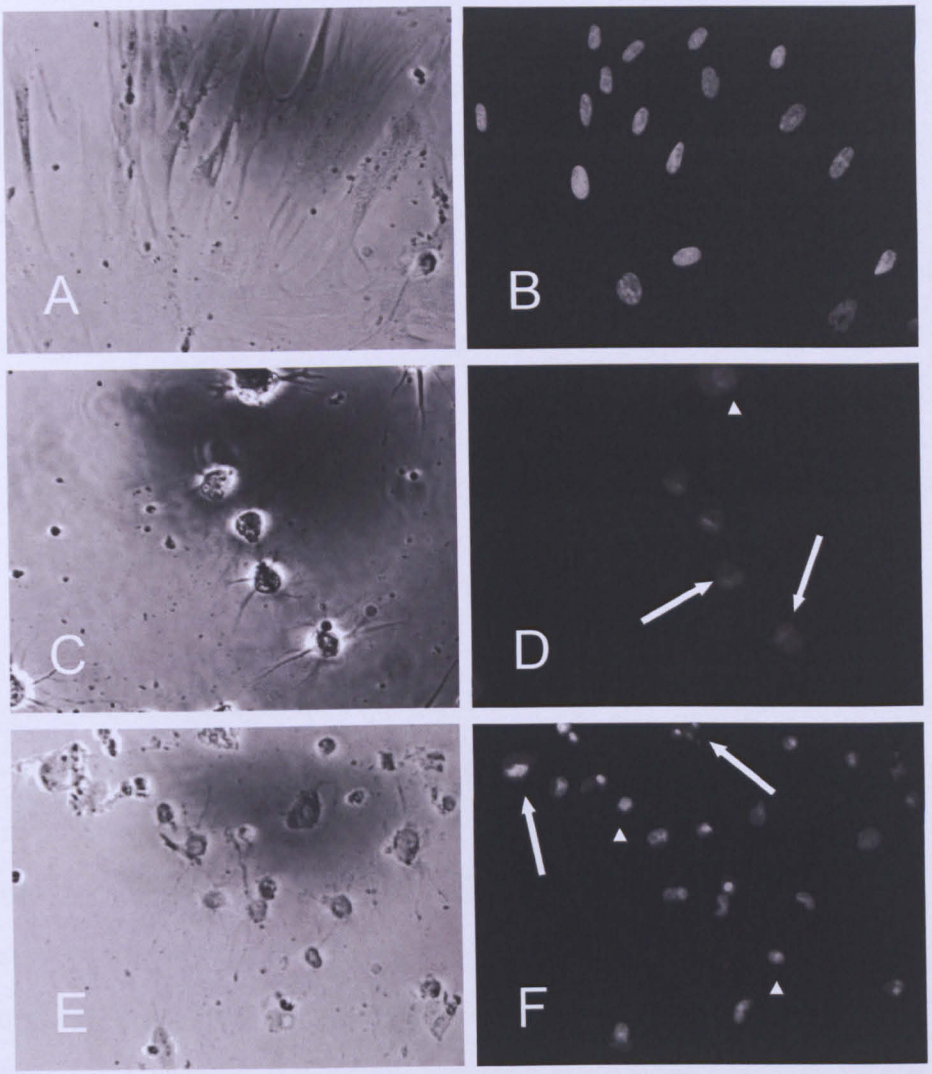

Figure 6-20 Hoechst 33342 staining of control and *C. difficile* toxin B exposed myofibroblasts (100 -1000 ng/ml)

Phase contrast and fluorescent micrographs of control (A & B) and 100 ng/ml and 1000 ng/ml toxin B exposed myofibroblasts (Cytotoxicity titre on Vero cells at 24 h 10^{-94}), (C & D) and (E & F) at 72 h, respectively. Cells with chromatin fragmentation and/or condensation are indicated by the arrow and the arrowhead, respectively.

6.4.3.8 Recovery of Myofibroblasts exposed to C. difficile *toxin B*

Conducting similar experiments to those completed using toxin A, intestinal myofibroblasts were grown to confluence in 6 well plates and pre-exposed to toxin B 1000 ng/ml for 3 hours followed by washing and culture in medium only. 100 % rounding was recorded in toxin treated wells at 3

hours. The medium was replaced three times a week. The cells were observed at 3 hours and then once a week using phase contrast microscopy. Whilst toxin A pre-exposed cells returned to a normal morphology and returned to a confluent monolayer, toxin B exposed cells failed to recover despite removal of toxin, washing and regular replacement of fresh media for nine weeks.

6.4.4 Comparative response of primary colonic myofibroblasts to *C. difficile* toxins

Having established a toxin specific response in the primary intestinal myofibroblast in the isolates studied I wanted to ensure that the response being observed was not as direct result of toxins being studied separately using different isolates or as a result of increased cytotoxicity of toxin B. Prior to completing simultaneous experiments the cytotoxicity titre of both toxin A and B was established and identical serial dilutions applied to myofibroblasts and Vero cells and the morphological response recorded.

6.4.4.1 Comparative cytotoxicity of C. difficile toxins A and B

The cytotoxicity of *C. difficile* toxin A & B was established using the bio-assay as 419 x 10^{-94} µg/ml and 750 x 10^{-94} µg/ml to induce 50% cell rounding after 24 hours, respectively. Toxins were subsequently diluted to give three different concentrations; 10^{-3}, 10^{-5} and 10^{-7} and the toxins applied to confluent myofibroblasts and Vero cells. Morphological changes were recorded as no-visible rounding, 50% rounding or 100% rounding (see Table 6-7) and micrographs taken (Figure 6-21). As observed previously a time and dose dependent response can be observed in both

myofibroblasts and Vero cells. At 10^{-5} and 10^{-7}, cell rounding occurred considerably later, in most condition the first signs of rounding did not occur until 24 hour. A largely similar response was observed in Vero cells exposed to 10^{-3} toxin A or B, toxin A achieving 100% cell rounding in 2 hours (Figure 6-21 A) and toxin B by 4 hour (Figure 6-21 K). The myofibroblast morphological response to toxins A and B was identical with cells 50% rounded by 3 hours and 100% by 4 hours (Figure 6-21 bb and jj; cc and kk).

Table 6-7 Comparison of cell rounding in myofibroblasts and Vero cells to C. difficile toxin B

Cell rounding; 100% (+) 50% (+/-) in Myofibroblasts and Vero cells in response to 419 x 10^{-3} µg/ml; 419 x 10^{-5} µg/ml; 419 x 10^{-7} µg/ml toxin A and 750 x 10^{-3}; 750 x 10^{-5}; 750 x 10^{-7} toxin B.

Duration of exposure	Vero cells						Myofibroblasts					
	Toxin A			Toxin B			Toxin A			Toxin B		
	10^{-3}	10^{-5}	10^{-7}	10^{-3}	10^{-5}	10^{-7}	10^{-3}	10^{-5}	10^{-7}	10^{-3}	10^{-5}	10^{-7}
2 h	+	-	-	-	-	-	-	-	-	-	-	-
3 h	+	-	-	+/-	-	-	+/-	-	-	+/-	-	-
4 h	+	-	-	+	-	-	+	-	-	+	-	-
6 h	+	-	-	+	-	-	+	-	-	+	-	-
24 h	+	-	-	+	+/-	-	+	-	-	+	+/-	-
30 h	+	+	-	+	+	-	+	+/-	-	+	+	-
48 h	+	+	+	+	+	-	+	+	+/-	+	+	+/-
72 h	+	+	+	+	+	+	+	+	+	+	+	+

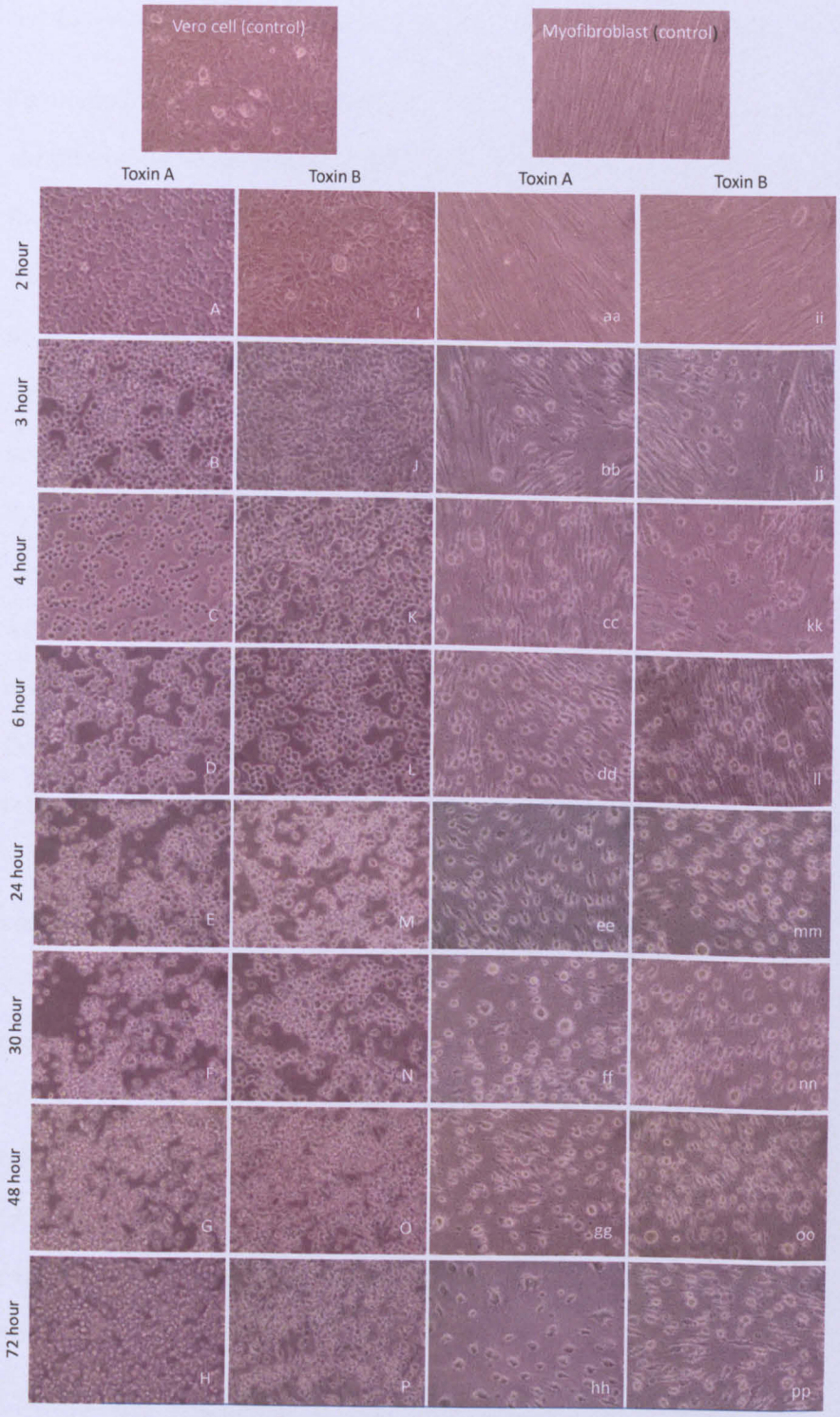

Figure 6-21 Phase contrast micrographs of myofibroblasts and Vero cells to *C. difficile* toxins A or B

Myofibroblasts (aa-pp) and African Green Monkey (Vero) cells (A-P) exposed to *C. difficile* toxin A ((419 x 10^{-3} µg ml) A-H & aa-hh) and toxin B (750 x 10^{-3} µg/ml) I-P & ii-pp) for 2 hour through 72 hour.

6.4.4.2 *Comparative viability of myofibroblasts to C. difficile toxins A & B*

To investigate the comparative viability of toxin exposed myofibroblasts simultaneous experiments were conducted investigating the response of four isolates to toxins A and B. Toxin A protein concentration measured as 419 µg/ml with cytotoxicity titre on Vero cells at 24 h of 10^{-94} and toxin B protein concentration measured as 750 µg/ml with cytotoxicity titre on Vero cells at 24 h of 10^{-94}. All isolates were cultured at the same time; seeded at similar densities; toxins applied and viability established after 24 h, 48 h and 72 h using the MTT assay.

As previously reported intestinal myofibroblasts incubated with *C. difficile* toxin A & B ≤10,000 ng/ml round in a time and dose dependent manner. Cell viability, measured using the MTT assay and the conversion of tetrazolium salts to a formazan product by mitochondrial dehydrogenase released from viable cells, was not reduced in toxin A exposed cells at concentration ≤10,000 ng/ml when compared against control (untreated) cells after 72 hours (Figure 6-22 A), [mean toxin 0.4858 (±SEM 0.0434) vs control 0.5359 (±0.0103). In contrast and supporting the results outlined in section 6.3.1 page 251, a loss in cellular viability can be observed at 24 hour to 1000 ng/ml toxin B [toxin 0.3913 (±0.0535) vs control 0.5772 (±0.0314) p=<0.01] and further reduced at 10,000 ng/ml [toxin 0.4054 (±0.0436) vs control 0.5772 (±0.0314) p=<0.01]. This loss increased at 48 hour to ≥1000 ng/ml [1000 toxin 0.3239 (±0.0172) vs control 0.5623 (±0.0299) p=<0.01]; [10,000 toxin 0.3714 (±0.0359) vs control 0.5623 (±0.0299) p=<0.001]. The loss in cell viability of myofibroblasts incubated with toxin B continued to increase through to 72 hours with a highly significant loss reported in all cells incubated with 1000 ng/ml [toxin 0.2043 (±0.0191) vs control 0.0535 (±0.0103) p=<0.001] and 10,000

ng/ml [toxin 0.2206 (±0.0126) vs control 0.0535 (±0.0103) p=<0.001], (see Figure 6-22 B). No loss of viability was seen in myofibroblasts incubated with 100 ng/ml toxin B even after 72 hour [toxin 0.4388 (±0.0631) vs control 0.0535 (±0.0103)] (Figure 6-22 B).

Comparison of cell viability in *C. difficile* toxin A and toxin B exposed myofibroblasts found a significant difference when mean absorbance of formazan product was compared (Table 6-8). The difference between toxin A and toxin B exposed cells can be viewed as early as 24 hours when myofibroblasts are incubated with ≥1000 ng/ml of toxin (Figure 6-23 B & C). The difference observed is statistically significant with cell viability being lower in toxin B exposed cells than in toxin A cells, [1000 toxin A 0.5854 (± 0.0311) vs toxin B 0.3913 (±0.5350) p<0.05; 10000 toxin A 0.6060 (±0.0443) vs toxin B 0.4054 (± 0.0436) p<0.05. By 48 hours, the difference was highly significant following exposure to 1000 ng/ml for 48 hours [toxin A 0.5838 (±0.0304) vs toxin B 0.3239 (±0.0172) p<0.001] and at 10,000 ng/ml [toxin A 0.5925 (± 0.0337) vs toxin B 0.3714 (± 0.0359) p<0.01] and this difference was also observed at 72 hours following exposure to 1,000 ng/ml [toxin A 0.4783 (± 0.0296) vs toxin B 0.2043 (±0.0191) p<0.001] and at 10,000 ng/ml [toxin A 0.4858 (±0.0434) vs toxin B 0.2206 (± 0.0126) p<0.01].

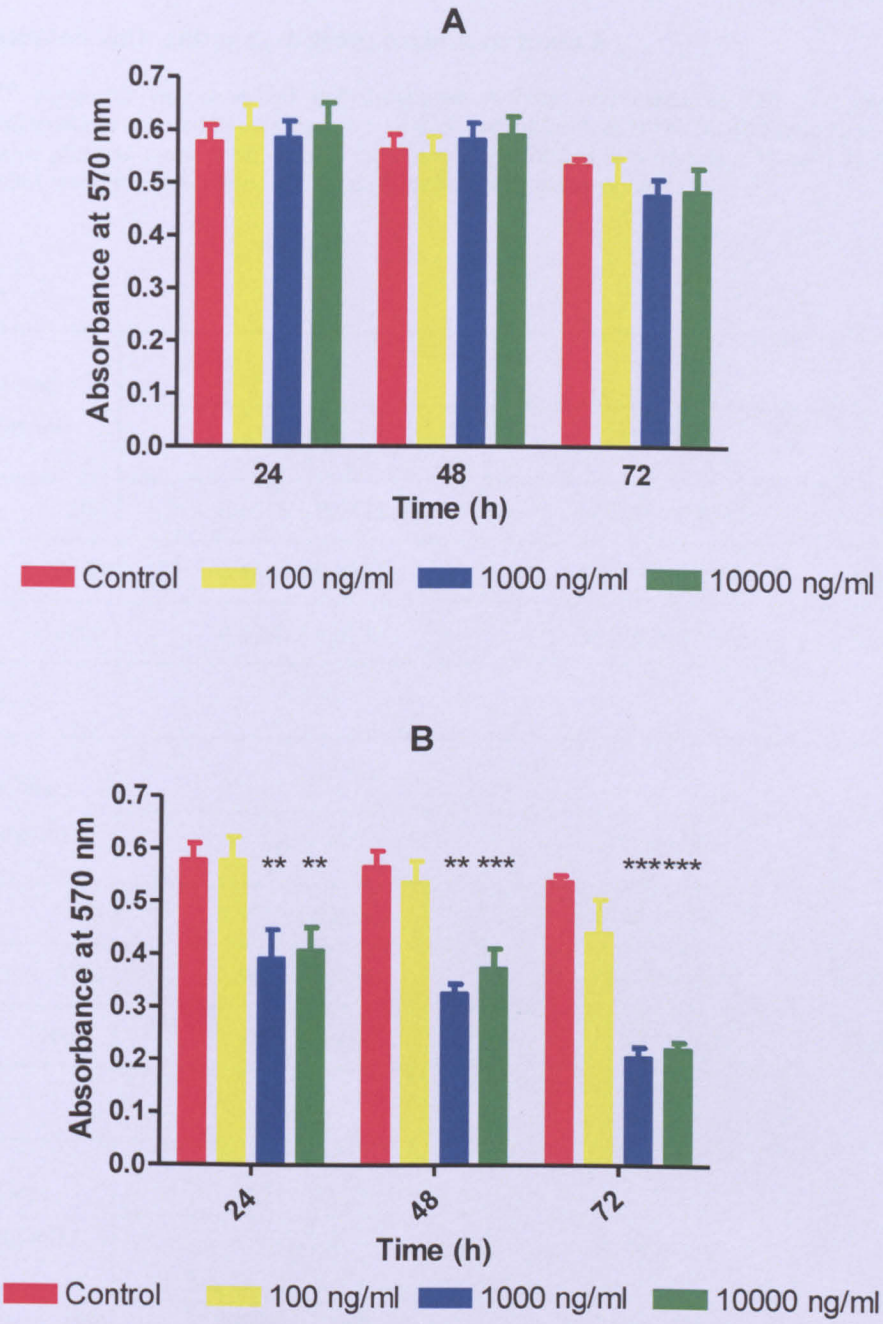

Figure 6-22 Mitochondrial dehydrogenase activity (MDA) in myofibroblasts incubated with *C. difficile* toxin A or toxin B

MTT assay for mitochondrial dehydrogenase activity (expressed as OD 570 nm) in Myofibroblasts exposed to 100, 1000 and 10000 ng/ml toxin A (A) or toxin B (B) for 24, 48 and 72 h. Data in figures represent mean (±SEM) of 3 experiments performed in triplicate. **=$p<0.01$ *** = $p<0.001$ when compared with control

Table 6-8 Mitochondrial dehydrogenase activity in myofibroblasts incubated with either *C. difficile* toxin A or toxin B

MTT assay for mitochondrial dehydrogenase activity (expressed as OD 570 nm) in Myofibroblasts exposed to varying concentrations of toxins A & B for 24, 48 h and 72 h. Data in table presents mean (±SEM) of 3 experiments performed in triplicate. **=p<0.01 *** = p<0.001 when toxin A treated and toxin B treated cells are compared.

24 h

Conc. (ng/ml)			
	Toxin A	Toxin B	P
100	0.6015 ± 0.0432	0.5769 ± 0.0432	n.s.
1000	0.5854 ± 0.0311	0.3913 ± 0.5350	0.0201
10000	0.6060 ± 0.0443	0.4054 ± 0.0436	0.0180

48 h

Conc. (ng/ml)			
	Toxin A	Toxin B	P
100	0.5537 ± 0.0340	0.5340 ± 0.3852	n.s.
1000	0.5838 ± 0.0304	0.3239 ± 0.0172	0.0003
10000	0.5925 ± 0.0337	0.3714 ± 0.0359	0.0041

72 h

Conc. (ng/ml)			
	Toxin A	Toxin B	P
100	0.4984 ± 0.0485	0.4388 ± 0.0631	n.s.
1000	0.4783 ± 0.0296	0.2043 ± 0.0191	0.0002
10000	0.4858 ± 0.0434	0.2206 ± 0.0126	0.0011

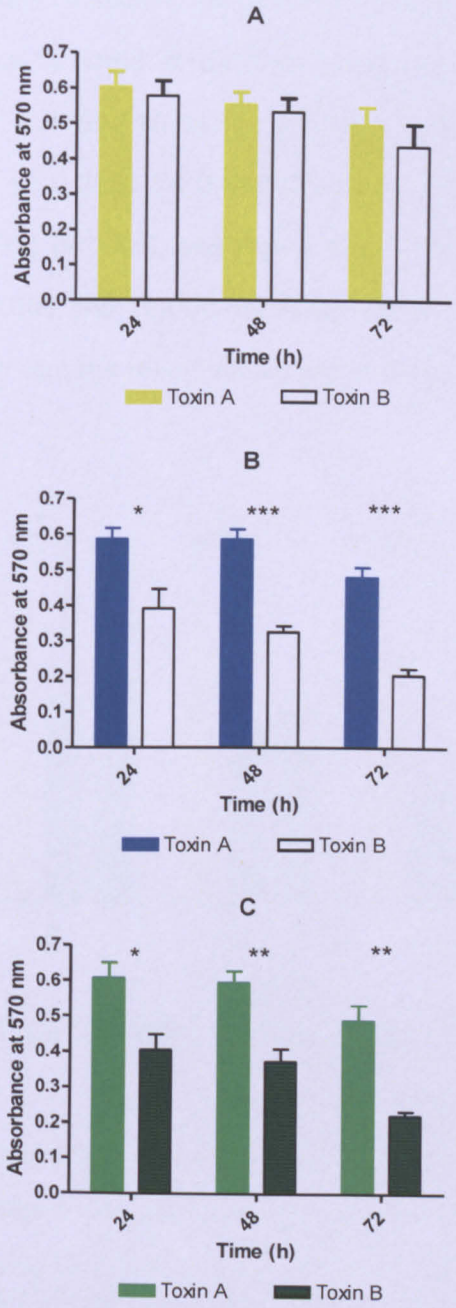

Figure 6-23 Comparison of mitochondrial dehydrogenase activity (MDA) in myofibroblasts exposed to *C. difficile* toxin A or toxin B

MTT assay for mitochondrial dehydrogenase activity (expressed as OD 570 nm) in Myofibroblasts exposed to 100 (A), 1000 (B) and 10000 (C) ng/ml toxin A or toxin B for 24, 48 and 72 h. Data in figures represent mean (±SEM) of 3 experiments performed in triplicate. *=$p<0.05$ **=$p<0.01$ *** = $p<0.001$ when toxin A treated and toxin B treated cells are compared.

Looking at the dose response in toxin B exposed myofibroblasts a significant difference is noted at all time points between 100 and 1000 ng/ml toxin B [24 h 0.5769 (±0.0432) vs 0.3913 (±0.0535) $p<0.05$; 48 h 0.5340 (± 0.0385) vs 0.3239 (± 0.0172) $p<0.01$; 72 h 0.4388 (±0.631) vs 0.2043 (± 0.0191) $p<0.05$], see Figure 6-24. However reviewing the response between 1000 and 10,000 ng/ml we see no significant difference at any time point; in fact the mean values are largely similar.

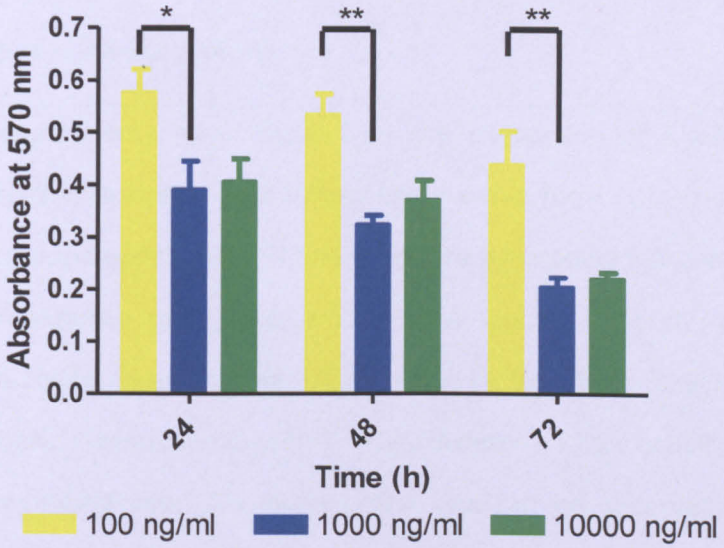

Figure 6-24 Mitochondrial dehydrogenase activity in myofibroblasts incubated with *C. difficile* toxin B – dose comparison

MTT assay for mitochondrial dehydrogenase activity (expressed as OD 570 nm) in Myofibroblasts exposed to toxin B for 24, 48 and 72 h. Data in figures represent mean (±SEM) of 3 experiments performed in triplicate. *=$p<0.05$ **=$p<0.01$ *** = $p<0.001$ when absorbance values for 100 ng/ml, 1000 ng/ml and 10000 ng/ml are compared.

If we investigate the time response to *C. difficile* toxins A & B we can see that absorbance values of formazan product reduce in a time dependent manner. Of particular interest, a notable pattern in the reduction of cell viability occurs at 1000 ng/ml and 10,000 ng/ml of toxin, see Table 6-8. In all concentrations only a moderate loss is seen at 24 hours however

between 24 and 48 hours a marked reduction is observed in both toxin A & B becoming statistical significant between 48 and 72 hours in response to 1000 ng/ml toxin A and B [48 h 0.3239 (±0.0172) vs 72h 0.2043 (± 0.0191) $p<0.01$] and 10000 ng/ml toxin B [48 h 0.3714 (±0.0359) vs 72 h 0.2206 (±0.0126) $p<0.01$]. Cell viability in control (untreated) cells remained constant throughout the experimental time course with no significant loss.

6.4.5 Investigation of RhoA activity in *C. difficile* toxin A and toxin B exposed myofibroblasts

Previous experiments have focused on the expression of RhoA in toxin exposed cells with the understanding the inactive form (GDP-bound) was rapidly degraded within the cell and therefore by producing a western blot from toxin exposed cell lysates and a RhoA specific antibody, any RhoA expression observed on the membrane would be from the active form (GTP bound) RhoA. Using the G-LISA™ (Cytoskeleton) RhoA activity in toxin exposed myofibroblasts was investigated. As can be observed in Figure 6-25 a highly significant reduction in active RhoA is observed at 4 h in myofibroblasts exposed to 1 µg/ml toxin A or toxin B when compared with control. These findings contradict earlier findings and strongly suggest that the inactivated RhoA in myofibroblasts is not rapidly degraded and the banding observed on the Western blot may in fact be the inactive form of RhoA. However, the findings are still largely similar when toxin A and toxin B RhoA activity/inactivity is compared.

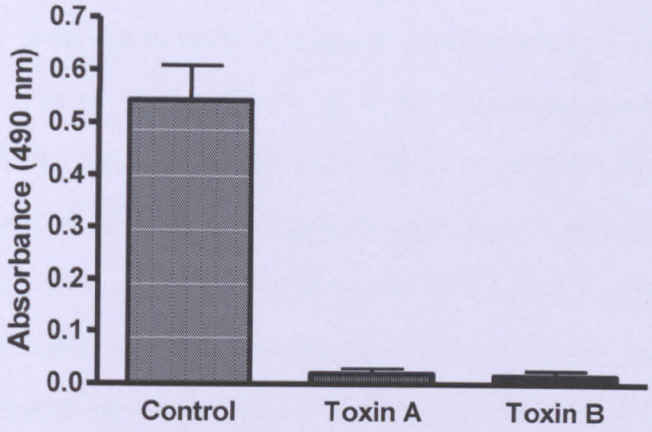

Figure 6-25 Levels of active, GTP-bound RhoA in *C. difficile* toxin-exposed myofibroblasts

Lysates were obtained from monolayers of normal human colonic myofibroblasts cultured for 4 h in medium only or in the presence of 1 μg/ml toxin A or 1 μg/ml toxin B. GTP-bound RhoA levels were quantified using an ELISA-based assay. Experiments were performed in duplicate, and the bars represent mean (SEM) absorbance values for 3 different cultures of myofibroblasts isolated from colonic mucosal samples obtained from 3 donors. The *p* value was <0.01 for the control versus toxin A or toxin B.

6.4.6 Comparative response to *C. difficile* toxins A, B or A + B

Having established that toxin A and B elicit differential effects on intestinal myofibroblasts I was interested to see if an additive effect could be induced by exposing cells to a combination of toxin A and B.

A series of experiments were conducted using three different isolates and cells exposed to either toxin A, toxin B or a combination of A + B at 100 ng/ml and 1000 ng/ml for 24, 48 and 72 hours. Combination A + B was prepared using 200 ng/ml and 2000 ng/ml of each and diluting 1:2 with the other toxin solution. Toxin A protein concentration measured as 3.17 mg/ml with cytotoxicity titre on Vero cells at 24 h of 10^{-95} and toxin B protein concentration measured as 271 μg/ml with cytotoxicity titre on Vero cells at 24 h of 10^{-25}.

Upon initial analysis of the raw data dose and time dependent loss of cell viability is observed in toxin B exposed myofibroblasts (Table 6-9) with a significant loss to 100 ng/ml at 24 h when compared with control cells [mean 0.2796 (±SEM 0.01485) vs 0.3318 (± 0.00743) $p<0.01$]. This loss increased and at 72 h a highly significant loss is seen at 100 ng/ml [0.2168 (± 0.01240) vs 0.2896 (± 0.01240) $p<0.0001$], see Figure 6-26 (a). At 24 h, cell viability in toxin A exposed myofibroblasts remained largely similar to that in control cells even at 10000 ng/ml [0.3056 (± 0.01038) vs 0.3147 (± 0.08702)]. In contrast to my previous findings, a loss in cell viability was observed at 48 h in myofibroblast exposed to 1000 ng/ml toxin A [0.2906 (± 0.00594) vs 0.3219 (± 0.00524) $p<0.01$] with a greater loss at 10000 ng/ml, [0.2544 (± 0.00300) vs 0.3219 (± 0.00524) $p<0.0001$], see Figure 6-26 B. This reduction continued through 72 h with a significant reduction seen at 100 ng/ml [0.2536 (± 0.00676) vs 0.2992 (± 0.01437) $p<0.05$], 1000 ng/ml [0.2436 (± 0.00597) vs 0.2992 (± 0.01437) $p<0.01$] and at 10000 ng/ml [0.2067 (± 0.00627) vs 0.2992 (± 0.01437) $p<0.0001$]. Reviewing the raw data for myofibroblasts exposed to toxin A+B, a time and dependent loss of cell viability is observed (see Table 6-9) with a significant loss noted at 24 h to 100 ng/ml [0.3526 (± 0.003884) vs 0.3908 (± 0.01269) $p<0.05$]. Of interest however, whilst a loss continued to be reported at 100 ng/ml, this loss was no longer significant and appeared to be decreasing with time, at 48 h [0.3044 (± 0.00689) vs 0.3457 (± 0.02017)] and by 72 h [0.2637 (± 0.00399) vs 0.2701 (± 0.01953)]. At 1000 ng/ml A+B a highly significant loss was seen at 24 h [0.2602 (± 0.00530) vs 0.3908 (± 0.01269) $p<0.0001$] decreasing to [0.1955 (± 0.00234) vs 0.3457 (±0.02017) $p<0.0001$] at 48 h and at 72 h [0.01719 (± 0.00627) vs 0.2701 (±0.01953) $p<0.0001$], see Figure 6-26 A-C.

Table 6-9 Mitochondrial dehydrogenase activity (MDA) in myofibroblasts exposed to *C. difficile* toxin A, toxin B or toxin A+B

MTT assay for mitochondrial dehydrogenase activity (expressed as OD 570 nm) in Myofibroblasts exposed to 100 ng/ml and 1000 ng/ml of toxin A, toxin B or toxin A+B for 24, 48 h and 72 h. Data in table presents mean (±SEM) of 3 experiments performed in triplicate. * $p<0.05$ ** $p<0.01$ *** $p<0.001$ when toxin treated cells are compared with control (untreated) cells.

Conc. (ng/ml)	24 h		
	Toxin A	Toxin B	Toxin A + B
Control	0.3147 ± 0.08702	0.3318 ± 0.00743	0.3908 ± 0.01269
100	0.3216 ± 0.00966	0.2796 ± 0.01485 **	0.3526 ± 0.003884 *
1000	0.3213 ± 0.00839	0.2404 ± 0.00431 ***	0.2602 ± 0.00530 ***
Conc. (ng/ml)	48 h		
	Toxin A	Toxin B	Toxin A + B
Control	0.3219 ± 0.00524	0.3310 ± 0.00754	0.3457 ± 0.02017
100	0.3050 ± 0.00615	0.2574 ± 0.01392 **	0.3044 ± 0.00689
1000	0.2906 ± 0.00594 **	0.1986 ± 0.00389 ***	0.1955 ± 0.00234 ***
Conc. (ng/ml)	72 h		
	Toxin A	Toxin B	Toxin A + B
Control	0.2992 ± 0.01437	0.2896 ±0.01240	0.2701 ± 0.01953
100	0.2536 ± 0.00676 *	0.2168 ± 0.01240 ***	0.2637 ± 0.00399
1000	0.2436 ± 0.00597 **	0.1649 ± 0.00398 ***	0.1719 ± 0.00627 ***

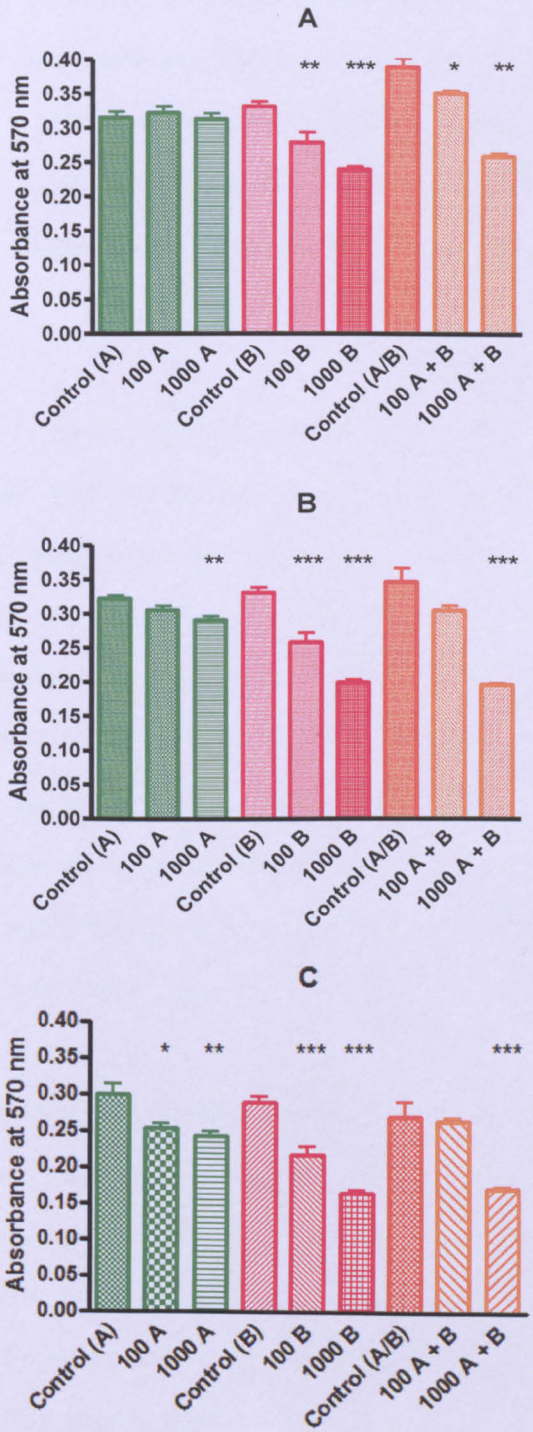

Figure 6-26 Mitochondrial dehydrogenase activity in myofibroblasts incubated with *C. difficile* toxin A, toxin B or toxins A+B

MTT assay for mitochondrial dehydrogenase activity (expressed as O.D. 570 nm) in Myofibroblasts exposed to 100 ng/ml and 1000 ng/ml toxin A, toxin B or toxin A+B for 24 h (A), 48 h (B) and 72 h (C). Data in figures represent mean (±SEM) of 3 experiments performed in triplicate. p values * <0.05, ** <0.01, *** <0.001 when compared with control myofibroblasts.

Comparison of toxin's A, B and A+B was completed after O.D values of toxin treated cells were normalised against control cells and the data presented as a percentage of viable cells. All control (untreated) values were termed 100% viable and the toxin treated cells calculated as a percentage of control cells and subsequently reported as mean percentage viable (±SEM).

Supporting my earlier findings, at 24 h a significant difference was observed when the percentage viable toxin A and toxin B treated myofibroblasts were compared. A significant reduction was seen using 100 ng/ml [(A) 102.60 (± 3.42) vs (B) 84.32 (± 4.32) $p<0.01$] and a highly significant difference at 1000 ng/ml [(A) 100 (±4.03) vs (B) 72.65 (± 1.53) $p<0.0001$]. This significant difference was repeated at 48 h, see Table 6-10. By 72 h, the percentage of viable cells was no longer significantly different in myofibroblasts treated to 100 ng/ml toxin A and toxin B but a highly significant difference was reported to 1000 ng/ml toxin A and toxin B, see Table 6-10.

As would be expected a significant loss in the percentage of viable cells was noted when toxin A treated cells were compared against toxin A+B, (Figure 6-27). At 24 h, a significant difference was reported between 100 ng/ml toxin A and toxin A+B [(A) 102.60 (± 3.42) vs (A+B) 91.20 (± 3.920) $p<0.05$] increasing to [(A) 100.00 (± 4.03) vs 67.38 (± 3.25) $p<0.0001$]. This loss is clearly presented in Figure 6-27 A. A similar difference in toxin A and toxin A+B percentages was seen at 48 h. By 72 h, a significant difference is no longer seen between myofibroblasts exposed to 100 ng/ml toxin A and 100 ng/ml toxin A+B and at 1000 ng/ml, a highly significant was reported at 24 and 48 h but the difference

at 72 h has been reduced with significance at $p<0.05$ [(A) 82.99 (± 4.391) vs (A+B) 66.25 (± 4.58)], see Figure 6-27 C.

6.4.6.1 Comparison of response to toxin B and toxin A+B

At 100 ng/ml, the percentage viable cells in toxin A+B was consistently higher than the percentage of viable cells following exposure to toxin B, see Table 6-10 and by 72 h this difference [(B) 75.76 (±5.83) vs (A+B) 101.10 (±6.17)] had become statistically significant, $p<0.01$, see Figure 6-27 C.

Reviewing the time dependent response, analysis of the percentage of viable cells in toxin exposed myofibroblasts suggests that cells incubated with toxin A were more susceptible between 48 and 72 h to 100 ng/ml and 1000 ng/ml (Figure 6-28 A) [48 h 0.3050 (± 0.00615) vs 72h 0.2536 (± 0.00676) $p<0.0001$; 48h 0.2906 (±0.00594) vs 72 h 0.2436 (±0.00597) $p<0.0001$]. In response to toxin B, a small reduction in mitochondrial dehydrogenase activity was noted between 24 and 48 h to 100 ng/ml, between 48-72 h this reduction became statistically significant [48 h 0.2574 (±0.01392) vs 72 h 0.1649 (± 0.00398) $p<0.05$. In response to 1000 ng/ml a highly significant loss was observed between 24 and 48 h [24 h 0.2404 (± 0.00431) vs 48 h 0.1986 (± 0.00389) $p<0.0001$] and this statistically significant loss was also reported between 48 h and 72 h.

Of particular interest, a highly significant reduction in mitochondrial dehydrogenase in toxin A+B exposed myofibroblasts was observed between 24 h and 48 h to both 100 ng/ml and 1000 ng/ml ($p<0.0001$),

see Figure 6-28 C and this reduction continued through 48 h and 72 h to 100 ng/ml ($p<0.0001$) and 1000 ng/ml ($p<0.0001$).

Table 6-10 Comparison of percentage viable cells in myofibroblasts incubated with C. difficile toxin A, toxin B or toxin A+B

MTT assay for mitochondrial dehydrogenase activity in myofibroblasts exposed to 100 ng/ml and 1000 ng/ml toxin A, toxin B and toxin A+B for 24 h, 48 h and 72 h.. Data in table represent mean (±SEM) of 3 experiments performed in triplicate. Raw O.D. values have been normalised against control (untreated) myofibroblasts and expressed as a percentage of control cells. p values * $p<0.05$ ** $p<0.01$ *** $p<0.001$

24 h

Conc. (ng/ml)	Toxin A	Toxin B	p
100	102.60 ± 3.42	84.32 ± .4.32	0.0043
1000	100.00 ± 4.03	72.65 ± 1.53	<0.0001
Conc. (ng/ml)	**Toxin A**	**Toxin A + B**	**p**
100	102.60 ± 3.42	91.20 ± 3.920	0.0434
1000	100.00 ± 4.03	67.38 ± 3.25	<0.0001
Conc. (ng/ml)	**Toxin B**	**Toxin A + B**	**p**
100	84.32 ± .4.32	91.20 ± 3.920	0.255
1000	72.65 ± 1.53	67.38 ± 3.25	0.162

48 hrs

Conc. (ng/ml)	Toxin A	Toxin B	p
100	94.82 ± 1.69	78.06 ± 4.59	0.0035
1000	90.31 ± 1.49	60.23 ± 1.807	<0.0001
Conc. (ng/ml)	**Toxin A**	**Toxin A + B**	**p**
100	94.82 ± 1.69	89.77 ± 3.84	0.246
1000	90.31 ± 1.49	58.26 ± 3.73	<0.0001
Conc. (ng/ml)	**Toxin B**	**Toxin A + B**	**p**
100	78.06 ± 4.59	89.77 ± 3.84	0.068
1000	60.23 ± 1.807	58.26 ± 3.73	0.641

72 hrs

Conc. (ng/ml)	Toxin A	Toxin B	p
100	86.50 ± 4.91	75.76 ± 5.83	0.178
1000	82.99 ± 4.391	57.31 ± 2.33	<0.0001
Conc. (ng/ml)	**Toxin A**	**Toxin A + B**	**p**
100	86.50 ± 4.91	101.10 ± 6.17	0.083
1000	82.99 ± 4.391	66.25 ± 4.58	0.018
Conc. (ng/ml)	**Toxin B**	**Toxin A + B**	**p**
100	75.76 ± 5.83	101.10 ± 6.17	0.009
1000	57.31 ± 2.33	66.25 ± 4.58	0.101

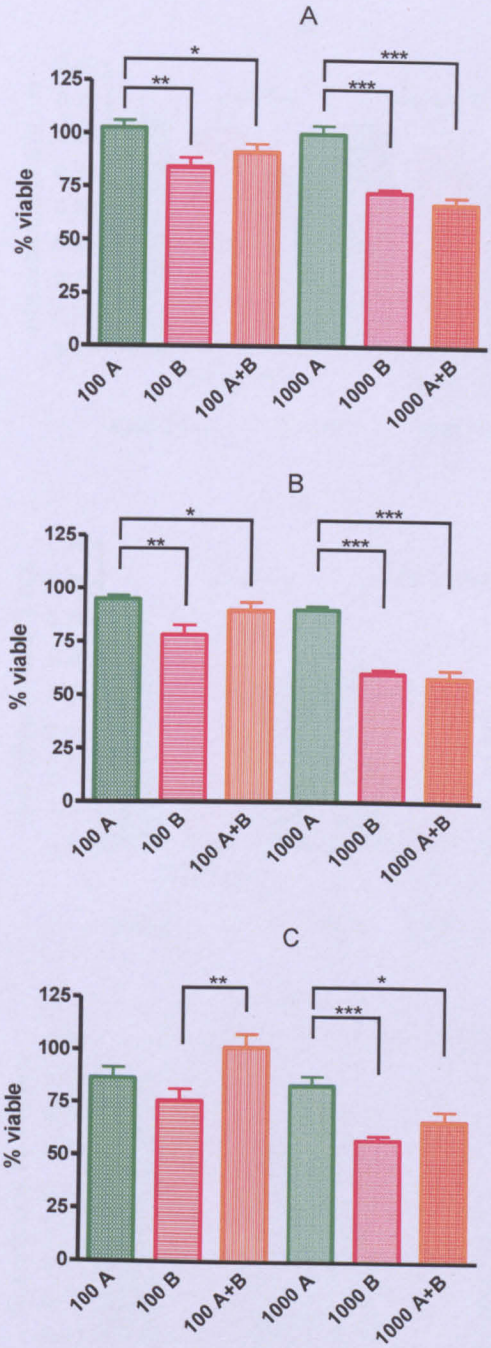

Figure 6-27 Comparison of percentage viable cells in myofibroblasts incubated with C. difficile toxin A, toxin B or toxin A+B

MTT assay for mitochondrial dehydrogenase activity in myofibroblasts exposed to 100 ng/ml and 1000 ng/ml toxin A, toxin B and toxin A+B for 24 h (A), 48 h (B) and 72 h (C). (A) represents data from all time points. Data in figures represent mean (±SEM) of 3 experiments performed in triplicate. Raw O.D. values have been normalised against control (untreated) myofibroblasts and expressed as a percentage of control cells. p values * $p<0.05$ ** $p<0.01$ *** $p<0.001$.

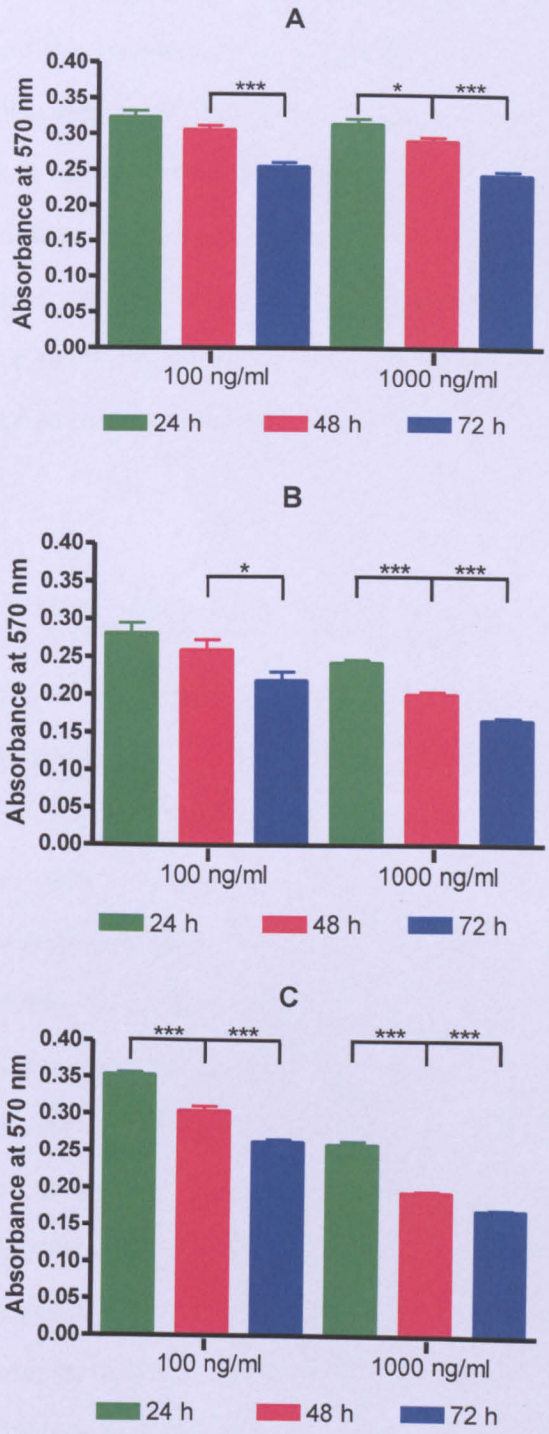

Figure 6-28 Mitochondrial dehydrogenase activity (MDA) in myofibroblasts incubated with toxin A, toxin B or toxin A+B – comparison of duration

MTT assay for mitochondrial dehydrogenase activity (expressed as O.D. 570 nm) in myofibroblasts exposed to 100 ng/ml and 1000 ng/ml of toxin A (A), toxin B (B) and toxin A+B (C). Data in figures represent mean (±SEM) of 3 experiments in triplicate. * $p<0.05$, ** $p<0.01$ and *** $p<0.001$ when period of exposure is compared 24 h – 48 h and 48 h – 72 h.

Investigating the dose response in toxin A, toxin B and toxin A+B exposed myofibroblasts and the increased loss of viability when toxin concentration is increased, this series of experiments suggest that no significant difference in loss is observed in myofibroblasts exposed to 100 ng/ml and 1000 ng/ml toxin A at 24 h through 72 h. In contrast both toxin B and toxin A+B exposed myofibroblasts saw a significant reduction in cell viability when the toxin concentration was increased and this significant reduction in response to dose continued through 72 h.

6.5 Discussion

Initial experiments studied the response of myofibroblasts to *C. difficile* toxin A using intestinal epithelial cells, Caco-2 and HT29 as a benchmark to previously observed responses. Myofibroblasts rounded in a time and dose dependent manner, rounding slower than HT29 and Caco-2 cells in which 50% of the cells were rounded after 1 h; whereas 50% rounding was observed in myofibroblasts after 3 h with cells initially taking a stellate form before rounding. The stellate form is characteristic of the stellate myofibroblast as described by (Powell, Mifflin et al. 1999), however the significance of this form needs further investigation. This stellate form was still seen in some cells after 48 h exposure. Using the MTT assay to investigate cell viability in myofibroblasts, Caco-2 and HT29 cells incubated with toxin A, the response by HT29 and Caco-2 cells was as previously discussed in Chapter 3. A significant reduction in Caco-2 cell viability was observed and HT29 cells appeared resilient to *C. difficile* toxin A. This is in stark contrast to the loss of viability in HT29 cells reported by others, however this may be explained in part by their use of recombinant toxin A (Nottrott, Schoentaube et al. 2007). Benchmarking the myofibroblast response to toxin A, it would appear to be as resilient to toxin A induced

cell death as the intestinal epithelial cell, HT29. Supporting the MTT data, DNA analysis using propidium iodide staining and flow cytometry established normal DNA profiles in cells incubated with 1000 ng/ml toxin A for ≤72h. A ten-fold increase in toxin A concentration to 10000 ng/ml also produced DNA profiles representative of normal viable cells and no difference in the percentage of sub-G1 events was noted when control and toxin treated profiles were compared. It has been reported by others that under- or over-representation of cell cycle phases contribute to the observed response in the host cell (Fiorentini and Thelestam 1991; Nottrott, Schoentaube et al. 2007). Cell cycle analysis compiled using Terry Hoy's CycIhred programme found small differences in the percentages of cells between 8 and 24 hours in toxin treated and control cells but no significant difference was observed at individual time points.

Having observed a similar response in intestinal epithelial cells to *C. difficile* toxins A and B, despite claims that toxin B is significantly more cytotoxic (Chaves-Olarte, Weidmann et al. 1997). I was keen to investigate the response of myofibroblasts to toxin B. Conducting similar experiments to those conducted with toxin A it became apparent that a differential response to *C. difficile* toxins occurred in myofibroblasts. Morphological experiments provided the earliest evidence of a differential response. Cell rounding occurred earlier with 50% rounding being observed at 1 hour following exposure to 1000 ng/ml toxin B and by 24 h the majority of cells appeared fragmented, with signs of surface blebbing and the cells were no longer adherent to ≥100 ng/ml. The observed morphological changes were supported by a series of experiments looking at cell viability. Using the MTT assay, a significant reduction in cellular viability was seen at 24 h to ≥100 ng/ml (100 ng/ml $p<0.05$; 1000 ng/ml

$p<0.01$) and this significant loss continued through to 72 h. DNA analysis of propidium iodide stained cells measured using flow cytometry confirmed a time dependent loss in cell viability with the percentage of events in the sub-G1 region becoming statistically significant at 72 h to 1000 ng/ml toxin B ($p<0.01$). Confirming apoptosis, Hoechst staining of myofibroblasts incubated with 1000 ng/ml toxin B for 24 h displayed chromatin fragmentation and/or condensation. Cell cycle analysis of control and toxin treated myofibroblasts were largely similar with no identifiable differences when compared.

With a differential response to *C. difficile* toxins A and B identified further experiments were conducted to investigate the comparative response of the toxins. Studying the toxins together using the same patient isolates would ensure the response being observed was as a direct result of the toxins and not primary cell variability. To counteract the argument that toxin B is more cytotoxic and therefore a different response is expected a series of experiments were conducted investigating the cytotoxicity of *C. difficile* toxin A and toxin B. The gold standard cell type (Vero cells) was used to ascertain cytotoxicity (Donta, Sullivan et al. 1982) in *C. difficile* toxins and both toxin were subsequently diluted to achieve identical serial dilutions. The diluted toxins were simultaneously applied to confluent Vero cells and myofibroblasts. All cells rounded in a dose and time dependent manner and both toxins induced similar responses in myofibroblasts with largely similar rounding schedules. These same toxin samples were used in the comparative experiments of toxin A and toxin B.

C. difficile toxin A and toxin B was applied to four different myofibroblast isolates, time course changes in cell morphology noted and cell viability

established after 24 h, 48 h, and 48 h using the MTT assay. Confirming our earlier findings where the toxins were studied in isolation of each other, cell viability was not reduced in myofibroblasts exposed to ≤10000 ng/ml toxin A when compared against control (untreated) cells after 72 h.

In contrast and supporting the results outlined in section 6.4.3.2 page 283, a loss in myofibroblast viability was observed as early as 24 h to ≤1000 ng/ml ($p<0.01$) and continued through 72 h. Given the disparity in responses to *C. difficile* toxins and as would be expected comparison of cell viability is significantly different when absorbance values for toxin A and toxin B exposed myofibroblasts are compared. Whilst a time and dose dependent response was noted when morphological changes were reported, if we consider loss of viability only a small reduction was observed in myofibroblasts exposed to 100 ng/ml toxin B and this loss did not reach statistical significance even after 72 h exposure. In addition, if we look at the difference in loss between myofibroblasts incubated with 100 ng/ml and 1000 ng/ml toxin B, a significant difference can be viewed at all time points, however the loss of viability between 1000 ng/ml and 10000 ng/ml is minimal. This may suggest saturation of the myofibroblast with toxin and/or a reduction in the ability to process the toxin. Although toxin internalisation is believed to occur within minutes of exposure (Henriques, Florin et al. 1987), in our experiments some loss was observed at 24 h and continued through 48 h in toxin A and B, however the greatest loss in cell viability was observed between 48 and 72 h in both toxin A and toxin B exposed cells. Whilst statistical significance was not evident in toxin A exposed myofibroblasts when compared against control, some loss was observed and this loss was greatest between 48 and 72 h. This loss

could not be explained by extended culture conditions as only a small non-significant loss was reported in control cells.

To investigate the disparity observed in toxin exposed myofibroblasts, Rho expression in toxin treated myofibroblasts was studied. *Clostridium difficile* toxins target small intracellular proteins (Just, Selzer et al. 1995), and by inactivating these proteins messaging within the cell are disrupted (Jank, Giesemann et al. 2007). The changes to cell morphology observed when myofibroblasts are incubated with *C. difficile* toxins are likely to be due to inactivation of these proteins. Using specific antibodies for non-glucosylated Rac-1 and total RhoA both toxins induced loss of non-glucosylated Rac-1 over a similar time period implying uptake of toxins A and B is similar in myofibroblasts. Analysis of RhoA expression in myofibroblasts using Western blot and specific RhoA antibody remained constant, with no change in total levels of RhoA levels in myofibroblasts exposed to both toxins A or B and may therefore not responsible for the observed differences. However, subsequent experiments investigating the activity of RhoA by G-LISA™ showed a significant reduction in active RhoA when toxin A and toxin B exposed cells were compared with control. This would therefore suggest that the signal being observed using Western blot analysis was in fact inactive (GDP bound) RhoA and challenges the findings of others that inactive RhoA is degraded intracellularly (Dillon, Rubin et al. 1995; Genth, Huelsenbeck et al. 2006). Our intention was to also investigate RhoB expression but despite sourcing mouse brain lysate (positive control) and achieving a good signal, a signal from myofibroblast lysate could not be achieved.

Myofibroblasts consistently responded to toxins A and B by change in morphology to stellate shaped cells. Scanning electron micrographs of control and *C. difficile* toxin-exposed myofibroblasts highlight the changing morphology from a monolayer of 'flat' cells cultured in control medium and the stellate form of toxin A and B exposed cells with numerous processes. In myofibroblasts exposed to either toxin, distinct globular structures are present either close to the cell body or at a distance, associated with a process. These same distinct globular structures are seen in transmission electron micrographs of toxin exposed myofibroblasts.

Reorganisation of the actin cytoskeleton and subsequent cell rounding are early cytopathic responses to *C. difficile* toxins. Myofibroblasts strongly express smooth muscle actin and to further elucidate the differences observed between toxin A and B on intestinal myofibroblasts, immunocytochemical studies investigating alpha smooth muscle actin provided some interesting results. Myofibroblasts in control medium displayed longitudinally arranged alpha-smooth muscle actin - immunoreactive bundles of microfilaments. In myofibroblasts exposed to *C. difficile* toxin A or toxin B for 6 h, the immuno-reactive longitudinally arranged bundles were no longer visible and the cell cytoplasm surrounding the nucleus together with cell processes were immuno-reactive for alpha smooth muscle actin. The main cell bodies and processes of toxin A exposed cells remained strongly immuno-reactive for alpha smooth muscle actin. By contrast, at 48 h toxin B exposed cells displayed variable immuno-reactivity and lacked processes and after 72 h cells were either negative or weakly positive for alpha smooth muscle actin and appeared non-viable.

The consistent expression of alpha smooth muscle actin, combined with the apparent resilience of myofibroblasts to *C. difficile* toxin A and the unique attributes of the intestinal myofibroblast a series of experiments were conducted to see if the cells could recover from pre-exposure to *C. difficile* toxin A. In studies undertaken with myofibroblasts isolated from different donors, morphological recovery of the cells was studied after 3 h pre-exposure to toxin A. While in cultured medium, the myofibroblast morphology gradually reverted to normal. Subsequently, the cells were also able to proliferate after passage. Later studies extending the period of exposure confirmed these finding with intestinal myofibroblasts pre-exposed to *C. difficile* toxin A ≤ 10000 ng/ml for 48 h can recover. This remarkable characteristic of the myofibroblasts may have important implications for mucosal tissue repair and regeneration in patients with colitis due to *C. difficile* infection. Myofibroblasts pre-exposed to *C. difficile* toxin B failed to recover.

Most strains of *C. difficile* produce both toxin A and toxin B and therefore whilst it is important to elicit the response of each toxin, do the toxins work synergistically to exert a greater effect. Conducting a series of experiments investigating the combined effect of toxin A + B, myofibroblasts isolated from three different patients were incubated with either toxin A, toxin B or toxin A+B. Morphological changes were noted and cell viability established at 24 h, 48 h and 72 h. Myofibroblasts incubated with toxin A+B rounded at a similar rate to that observed in cells incubated with either toxin A or toxin B. Supporting my previous finding a significant loss was observed in toxin B exposed myofibroblasts at 24 h, however this loss was observed at a lower concentration, 100 ng/ml ($p<0.01$) and continued through 72 h. In contrast to my earlier finding

(no significant reduction in toxin A exposed myofibroblasts using 10000 ng/ml for 72h), when toxin A exposed myofibroblasts were compared with control (untreated) cells a significant loss in cell viability was observed at 48 h to 1000 ng/ml ($p<0.01$) and a highly significant loss reported at 48 h to 10000 ng/ml toxin A ($p<0.0001$). The differences observed in the myofibroblast mitochondrial dehydrogenase activity in response to toxin A may be explained in part by the inter-individual variability. Myofibroblasts incubated with toxin A+B showed a significant loss of viability at 24 h to 100 ng/ml ($p<0.05$). Of particular interest, whilst a loss continued to be reported at 100 ng/ml at 48 h and 72 h the loss was decreasing with time. It should be considered therefore, that at 100 ng/ml, toxin A protects the myofibroblast against loss of mitochondrial dehydrogenase activity due to toxin B. At the higher concentrations of toxin A+B, cell viability continued to reduce through 72 h. Comparison of viability in toxin A, toxin B and toxin A+B exposed myofibroblast found a significant difference between toxin A and toxin B treated cells as previously reported. As expected, comparing cellular viability in toxin A and toxin A+B exposed myofibroblasts provided similar results, toxin B is a more potent cytotoxin in intestinal myofibroblasts. A significant difference in cell viability was observed when myofibroblasts exposed to 1000 ng/ml of either toxin A or toxin A+B are compared ($p<0.0001$). Supporting my earlier question; myofibroblasts incubated with 100 ng/ml of toxin A+B appeared to reducing their loss of viability over time when compared to the viability of toxin A exposed myofibroblasts, the significant difference between toxin A and toxin A+B observed at 24 and 48 h was not seen at 72 h. Further supporting the potential protective role of toxin A; comparison of cell viability in toxin B and toxin A+B exposed myofibroblasts provides crucial evidence. No significant difference in cell

viability was found when 1000 ng/ml toxin B and toxin A+B exposed myofibroblasts were compared. Of particular interest, a gradual increase in cell viability is observed in toxin A+B exposed myofibroblasts when compared with toxin B exposed myofibroblasts and this increase in cell viability becomes statistically significant by 72 h to 100 ng/ml of toxin A+B.

Investigating the time and dose response of toxins on myofibroblasts, a greater reduction in cell viability is observed to toxin A between 48 and 72 h, with no dose dependent difference. Loss of cell viability in toxin B exposed myofibroblasts was greatest between 48 and 72 h to 100 ng/ml toxin B; at 1000 ng/ml a consistent significant loss in cell viability is observed from 24 through 72h. By contrast, cell viability in cells incubated with toxin A+B also provide a consistent loss in cell viability, however this is observed at 100 ng/ml and 1000 ng/ml. These findings would suggest that toxin A+B does not have a cytotoxic additive effect but the combination may exert a quicker host cell response. A fuller discussion, incorporating key discussion points from this chapter and others can be found at Chapter 7.

CHAPTER 7

7 Discussion

Revisiting the initials aims of this research, my general discussion can be split into three distinct sections; 1) the successful optimization of *C. difficile* toxin B purification to allow – 2) studies investigating the intestinal epithelial response to *C. difficile* toxin A and toxin B; and 3) studies investigating the response of primary colonic myofibroblasts to toxin A, toxin B and toxin A+B.

The protocol for *C. difficile* toxin B has been successfully optimized as outlined in Chapter 4. The purified toxin has been shown to be active and characterization has established a protein concentration ranging 250 µg/ml – 2.0 mg/ml and cytotoxicity (established using Vero cells) as ranging from 10^{-4} to 10^{-94}. The protein can also be stored at 4°C in Tris buffer for a number of weeks before cytotoxicity is reduced. Given the wide range of cytotoxic activity in toxin B samples, groups of experiments were conducted using toxin purified from just one batch and the titre re-checked prior to use. The cytotoxic activity of toxin used in each group of experiments is noted in each chapter.

As discussed in the introduction to Chapter 3, intestinal epithelial cell types, Caco-2 and HT29 were used to investigate the response of epithelial cells to *C. difficile* toxins in the absence of primary cells. Whilst others have investigated the response of different cell types to *C. difficile* toxins, my research used these distinct epithelial types to investigate the comparative response to *C. difficile* toxins and the subsequent investigation of these responses is novel. I

have established a cell specific response to *C. difficile* toxin A and B, where Caco-2 cells are significantly more sensitive to toxin A and toxin B-induced cell death. Investigating the reasons for this dramatic disparity I have shown that by labeling toxin A with a fluorogenic dye no significant difference in toxin internalization is seen when the two cell types are compared. This is supported by a loss of Rac1 (associated with internalization and the subsequent rounding of cells) in both cell types at 4 h and the similar morphological time course of cell rounding in both cell types. Whilst labeling of toxin B was not completed and the uptake not investigated directly, a similar loss of non-glucosylated Rac1 was observed in both cell types to toxin B and cell rounding was largely similar. As commented on in the discussion to Chapters 3 and 5, the dramatic differential response to the *C. difficile* toxins cannot be explained by the internalization and subsequent inactivation of Rac1 by either toxin. Considering another intracellular target of the toxins, expression of RhoA was also investigated in Caco-2 and HT29 cells exposed to toxins A or B. Expression of RhoA in Caco-2 cells exposed to toxins A or B remained constant, however RhoA expression in HT29 cells reduced in a time dependent manner following exposure to *C. difficile* toxins. These findings are in contrast to those of others who have linked the loss of RhoA in response to *C. difficile* toxins with cell death (Huelsenbeck, Dreger et al. 2007). This difference may be explained in part by the use of rat basophilic leukemia cells (RBL). RhoA plays a major role in regulation and localization of stress fibres and the formation of perijunctional rings at the apical side of epithelial cells (Ridley and Hall 1992) and as discussed in Chapter 1 is also linked with cell cycle progression by interacting with a diverse range of effector proteins (Jaffe and Hall 2005). Cell cycle analysis of viable cells following exposure to *C.*

difficile toxins suggests that toxin B exposed Caco-2 cells are failing to pass the M1 checkpoint; similarly a large proportion of toxin A exposed Caco-2 cells appear not be progressing into S phase, this may be explained in part by cells being arrested at the restriction point in G1; the small proportion of cells progressing through to S-phase having already passed the point of no return, 'restriction point' (Blagosklonny and Pardee 2002) prior to toxin exposure. It is therefore possible that toxin A exposed cells are more sensitive in G0/G1, this has been reported by others (Nottrott, Schoentaube et al. 2007). In contrast, a considerable number of HT29 cells appear to undergo cell cycle arrest in G0/G1. RhoA has been specifically linked to G1 progression and mitosis (Jaffe and Hall 2005), inactivation of RhoA has been shown to block G1 progression whilst microinjection of active RhoA restores senescent cells to the cycle (Olson, Ashworth et al. 1995). Comparing these findings with the results of this study, it would be expected that toxin exposed Caco-2 cells would be undergoing cell death in G0/G1 as a result of RhoA inactivation, however RhoA inactivation was not observed. It has also been reported that active Cdc42 (Yasuda, Oceguera-Yanez et al. 2004), another possible target for C. difficile toxins is linked with mitotic arrest and it is therefore possible that toxin B is activating Cdc42 in Caco-2 cells, arresting cells in M phase. Unfortunately Cdc42, as a possible substrate, in Caco-2 cells was not investigated. The disparity observed in the two cells line is therefore not explained by the constant expression of RhoA in Caco-2 and a gradual reduction in RhoA expression in HT29 cells. It has been shown that inactivation of Rac-1 and Cdc42 can induce G1 cell cycle arrest however as with RhoA the mechanism is cell-type specific and the pathways complicated (Coleman, Marshall et al. 2004). Further studies are needed to elucidate the

possible role of RhoA, Cdc42 in C. difficile toxin induced cell death in Caco-2 cells. Later experiments investigating RhoA expression in myofibroblasts exposed to C. difficile toxin A and B used the G-LISA™ to differentiate between total RhoA expression and active RhoA. The G-LISA™ results contrast and enhance those of the western blot with no active RhoA present in toxin exposed myofibroblasts and therefore confirmation of active RhoA in Caco-2 and HT29 suggested with the G-LISA™.

The individual characteristics of these two intestinal epithelial cell lines should not be overlooked when looking for a possible explanation of the differential responses of *Clostridium difficile* toxins. Caco-2 cells are derived from a colorectal adenocarcinoma in a 72 year old male and HT29 cells derived from a colorectal adenocarcinoma in a 44 year old female. Perhaps the most notable difference between the two cell lines is the ability of Caco-2 cells to upon confluence differentiate from colonocyte to an enterocyte phenotype. It is suggested that the timing and degree of transition may cause confusion when interpreting experiments using Caco-2 cells as a model of small intestinal function (Engle, Goetz et al. 1998) and therefore the degree of transition may reflect the absorptive abilities of the cells (Hilgendorf, Spahn-Langguth et al. 2000). In contrast, differentiation of HT29 cells is apparently similar to that observed during embryonic development of the intestine (Le Bivic, Hirn et al. 1988) and whilst *C. difficile* has been isolated in neonates, they remain asymptomatic (Willey and Bartlett 1979). This may explain the resilience observed in HT29 cells. Another possible explanation may be potential expression of P-glycoprotein in Caco-2 cells and not in HT29 cells (Hilgendorf, Spahn-Langguth et al. 2000). This cell membrane associated

protein leads to higher secretion rates and consequently lower permeabilities in the absorptive direction (Faassen, Vogel et al. 2003), however whether this protein plays a role in toxin mediated cell death is still to be investigated. It has been suggested that CYP3A is very weakly expressed in Caco-2 cells, however it has reported by others that levels of CYP3A are not different when the two cells lines are compared (Gervot 1996)

The heightened response of the Caco-2 to toxin B may be explained by the lower seeding density of cells prior to toxin exposure and it is postulated that the near confluent monolayers used in toxin A exposed experiments may have been expressing proteins of the differentiated enterocyte (Stierum, Gaspari et al. 2003). It has been suggested that Caco-2 differentiation results in the formation of dense intercellular junctional complexes presenting a unique paracellular as well as transcellular barrier (Le Ferrec 2001). The absence of this monolayer in toxin B exposed Caco-2 cells would therefore increase basal toxin B receptor availability.

Intestinal myofibroblasts represent a distinct subpopulation of cells located immediately below the single monolayer of epithelial cells. Primary colonic epithelial cells are highly susceptible to *C. difficile* toxin-induced cell death (Riegler, Sedivy et al. 1995; Mahida, Makh et al. 1996). The loss of epithelial cells *in vivo* would be expected to expose myofibroblasts to *C. difficile* toxins. The concentration of toxins A and B used were based upon the maximal concentration of toxin A observed in stool samples analysed previously (Solomon, Webb et al. 2005) and the comparative experiments performed as

part of this study which showed similar cytotoxic activities of toxins on myofibroblasts. By using monolayers of myofibroblasts isolated from normal colonic mucosal samples from different donors, we showed that the cells consistently responded to toxins A and B by a change in morphology to stellate cells. Moreover, scanning electron microscopy showed small globular structures in cells incubated with the toxins, and further studies are required to characterize the nature of these structures. The cell body and processes in toxin-exposed myofibroblasts were strongly immunoreactive for alpha-smooth muscle actin. Although morphological studies and MTT assays suggested that a proportion of colonic myofibroblasts remained viable after 72 h of incubation with toxin B, all cells eventually underwent cell death, even after short (3 h) pre-exposure periods. However, it should also be noted that at low concentrations, the presence of toxin A provided protection against a toxin B-induced loss of viability. Such exposure of myofibroblasts to both toxins is likely to occur in the colonic mucosa *in vivo*.

In contrast to responses to toxin B, a majority of the toxin A-exposed myofibroblasts remained viable, even when exposed to a high (10 µg/ml) concentration of the toxin for up to 72 h. It is worth discussing at this point the obvious discrepancy in absorbance values of myofibroblast experiments, this can be explained in part by the variability of myofibroblast isolates and it may also reflect the use of two different supplies of MTT. Interestingly, after pre-exposure (for 3 h to 48 h) to high concentrations (1 and 10 µg/ml) of toxin A (followed by washing and culture in medium only), the myofibroblast morphology gradually reverted to normal. Subsequently, the cells were also able to proliferate after passage. This remarkable characteristic of the

myofibroblasts may have important implications for mucosal tissue repair and regeneration in patients with colitis due to *C. difficile* infection. Our previous studies showed that following 3 h of pre-exposure to <0.01 μg/ml toxin A, the T84 carcinoma-derived colonic epithelial cell line was able to recover its barrier function during subsequent culture in medium. However, this was not the case if the initial pre-exposure was to >0.01 μg/ml toxin A (Johal, Solomon et al. 2004). Moreover, there was a significant loss of viability in T84 and Caco-2 cell monolayers exposed to >0.1 μg/ml toxin A (unpublished observations in studies performed using the same batch of toxin as that used in the current series of experiments, together with our previous studies (Mahida, Makh et al. 1996)). Thus, primary human colonic myofibroblasts not only are much more resistant to cell death than carcinoma derived epithelial cell lines but also are able to recover after pre-exposure to high concentrations of toxin A. Primary human colonic epithelial cells are more sensitive to toxin A-induced cell death than Caco-2 and T84 carcinoma derived epithelial cell lines (Mahida, Makh et al. 1996). Indeed, our previous studies have shown that among the normal human colonic mucosal cells, epithelial cells and macrophages (and also monocytes) are more sensitive than lymphocytes to toxin A-induced cell death (Mahida, Makh et al. 1996; Mahida, Galvin et al. 1998; Solomon, Webb et al. 2005). Although direct comparisons have not been made, our current studies suggest that colonic myofibroblasts may be more resistant to toxin A-induced cell death than the colonic lamina propria lymphocytes. After exposure to 1 μg/ml toxin A, a large proportion of colonic lamina propria T cells underwent programmed cell death, mainly from 72 h onwards (Mahida, Galvin et al. 1998). In contrast, most of the colonic myofibroblasts incubated with 10 μg/ml toxin A were viable at 72 h. Reasons

for the differences in susceptibility of colonic mucosal cells to toxin A-induced cell death remain to be determined. One possibility is that specific cell types bind and internalize different amounts of toxin A. However, since there is rapid cell rounding and glucosylation of Rac1 (see below), a significant amount of toxin A is likely to be internalized by the myofibroblasts. The persistence of stellate morphology and adherence to the culture dish are other distinct features of toxin A-exposed myofibroblasts compared with epithelial cells. Since similar appearances were not seen with toxin A-exposed NIH 3T3 cells (unpublished observations), the stellate morphology of myofibroblasts could be due to the persistence of alpha-smooth muscle actin. It is likely that the changes in the morphology of myofibroblasts incubated with toxin A or B are due to inactivation (following glucosylation) of the Rho subfamily of GTPases, which are major intracellular targets of the toxins (Barbieri, Riese et al. 2002; Jank, Giesemann et al. 2007). Both toxins induced a loss of the nonglucosylated form of Rac1 in colonic myofibroblasts over similar periods (within 4 h). Together with largely similar rates of cell rounding, these studies imply that the uptake of both toxins is similar in myofibroblasts and that the greater sensitivity to cell death in response to toxin B is unlikely to be mediated via Rac1. Previous studies using rat basophilic leukemia (RBL) cells also suggested that glucosylation/inactivation of Rac1 is responsible for cell rounding (cytopathic effect) but not for cell death (cytotoxicity) (Huelsenbeck, Dreger et al. 2007). Studies of other cell types have shown that inactivation of RhoA is required for cell death (Moorman, Bobak et al. 1996; Bobak, Moorman et al. 1997; Hippenstiel, Schmeck et al. 2002). However, following 4 h of exposure to *C. difficile* toxin A or B, there was a marked reduction in

levels of active, GTP-bound RhoA, implying toxin-induced RhoA inactivation in the colonic myofibroblasts. In contrast, total levels of RhoA did not change in myofibroblasts exposed to either toxin A or B for 24 h. This is in contrast to the case for RBL cells, where high concentrations of toxin B (which led to cell death) induced a loss of RhoA (Huelsenbeck, Dreger et al. 2007). Such a loss may be due to the fact that glucosylated RhoA is degraded more efficiently by the proteasome than the nonmodified form (Dillon, Rubin et al. 1995; Genth, Huelsenbeck et al. 2006), and further studies are required to determine why total levels of RhoA do not change in toxin exposed myofibroblasts. Since there were marked reductions in levels of active, GTP-bound RhoA in response to both toxins, other factors are likely to be involved in the induction of cell death in myofibroblasts cultured with toxin B. In addition to functions in the cytoskeleton and cell adhesion, Rho proteins have been found to regulate a wide range of cellular activities, such as cell polarity, endocytosis, vesicle trafficking, and differentiation (Burridge and Wennerberg 2004). Peptide regulatory factors such as platelet-derived growth factor (PDGF) and epidermal growth factor (EGF) stimulate Rac, leading to Rho activation (Ridley and Hall 1992; Ridley, Paterson et al. 1992). Inactivation of Rac and other members of the Rho subfamily may therefore have a significant impact on the normal functions of colonic myofibroblasts, which include regulation of epithelial barrier function (Beltinger, McKaig et al. 1999; Johal, Solomon et al. 2004) and repair of epithelial wounds (created by loss of injured epithelial cells). For the latter, myofibroblasts have been shown, via their contractile properties, to reduce the size of the wound (Moore, Carlson et al. 1989) and to also enhance restitution (McKaig, Makh et al. 1999), a process by which epithelial cells at the wound edge migrate to cover the mucosal defect. Such

protective responses by the myofibroblasts may explain, at least in part, the focal nature of mucosal inflammation in C. difficile associated colitis. However, once cells are exposed to high concentrations of C. difficile toxins, impairment of myofibroblast functions may lead to severe inflammation, as seen in pseudomembranous colitis. The concentrations of C. difficile toxins used in our studies are likely to be representative of those seen *in vivo*. Thus, we have previously shown that although the median stool concentration of toxin A in patients with C. difficile infection was 4.3 ng/ml, the levels ranged from 0.6 ng/ml to 19 μg/ml (Solomon, Webb et al. 2005).

7.1 Future Work

This research is novel and at the time of writing the response of primary colonic myofibroblasts, a distinct subset of cells located in the lamina propria, to C. difficile toxins had not been reported on. My research provides an opening for future research. My most interesting finding; the recovery of colonic myofibroblasts pre-exposed to toxin A and the protective factor that toxin A appears to exert when toxins A and B are studied together.

Given that we have previously shown that secretion of TGF-beta by myofibroblasts has a protective function, this area should be investigated in more detail. Perhaps myofibroblasts release more TGF-beta in response to toxin A than toxin B and this may explain why the cells recover and also when cells are cultured in toxins A+B a significant difference in cell viability is observed when compared to cells cultured with toxin B alone.

In addition to the work on myofibroblasts, I think further investigation of RhoA expression in epithelial types exposed to toxin A and B may broaden our knowledge of both the pathogenesis of C. difficile disease but also widen our knowledge of the toxins as glucosyltransferases.

Bibliography

Aas, J., C. E. Gessert, et al. (2003). "Recurrent Clostridium difficile colitis: case series involving 18 patients treated with donor stool administered via a nasogastric tube." Clin Infect Dis 36(5): 580-5.

Adams, D. A., M. Riggs, et al. (2007). "Effect of fluoroquinolone treatment on growth of and toxin production by epidemic and non-epidemic Clostridium difficile in the cecal contents of mice." Antimicrob Agents Chemother.

Adamson, P., C. J. Marshall, et al. (1992). "Post-translational modifications of p21rho proteins." J Biol Chem 267(28): 20033-8.

Adegboyega, P. A., R. C. Mifflin, et al. (2002). "Immunohistochemical study of myofibroblasts in normal colonic mucosa, hyperplastic polyps, and adenomatous colorectal polyps." Arch Pathol Lab Med 126(7): 829-36.

al-Barrak, A., J. Embil, et al. (1999). "An outbreak of toxin A negative, toxin B positive Clostridium difficile-associated diarrhea in a Canadian tertiary-care hospital." Can Commun Dis Rep 25(7): 65-9.

al Saif, N. and J. S. Brazier (1996). "The distribution of Clostridium difficile in the environment of South Wales." J Med Microbiol 45(2): 133-7.

Alfa, M. J., A. Kabani, et al. (2000). "Characterization of a toxin A-negative, toxin B-positive strain of Clostridium difficile responsible for a nosocomial outbreak of Clostridium difficile-associated diarrhea." J Clin Microbiol 38(7): 2706-14.

Anand, A. and A. E. Glatt (1993). "Clostridium difficile infection associated with antineoplastic chemotherapy: a review." Clin Infect Dis 17(1): 109-13.

Anon (2001). The Nobel Prize in Physiology or Medicine 2001.

Anumanthan, A., A. Bensussan, et al. (1998). "Cloning of BY55, a novel Ig superfamily member expressed on NK cells, CTL, and intestinal intraepithelial lymphocytes." J Immunol 161(6): 2780-90.

Apodaca, G., M. Bomsel, et al. (1991). "The polymeric immunoglobulin receptor. A model protein to study transcytosis." J Clin Invest 87(6): 1877-82.

Arijs, I., G. De Hertogh, et al. (2009). "Mucosal gene expression of antimicrobial peptides in inflammatory bowel disease before and after first infliximab treatment." PLoS One 4(11): e7984.

Arnon, S. S., D. C. Mills, et al. (1984). "Rapid death of infant rhesus monkeys injected with Clostridium difficile toxins A and B: physiologic and pathologic basis." J Pediatr 104(1): 34-40.

Assoian, R. K. and M. A. Schwartz (2001). "Coordinate signaling by integrins and receptor tyrosine kinases in the regulation of G1 phase cell-cycle progression." Curr Opin Genet Dev 11(1): 48-53.

Bach, S. P., A. G. Renehan, et al. (2000). "Stem cells: the intestinal stem cell as a paradigm." Carcinogenesis 21(3): 469-76.

Banno, Y., T. Kobayashi, et al. (1984). "Biochemical characterisation and biologic actions of two toxins (D-1 and D-2) from Clostridium difficile." Rev Infect Dis 6(Mar-Apr): S11-20.

Barbieri, J. T., M. J. Riese, et al. (2002). "Bacterial toxins that modify the actin cytoskeleton." Annu Rev Cell Dev Biol 18: 315-44.

Barbut, F., V. Lalande, et al. (2002). "Prevalence and genetic characterization of toxin A variant strains of Clostridium difficile among adults and children with diarrhea in France." J Clin Microbiol 40(6): 2079-83.
Barroso, L. A., S. Z. Wang, et al. (1990). "Nucleotide sequence of Clostridium difficile toxin B gene." Nucleic Acids Res 18(13): 4004.
Barth, H., K. Aktories, et al. (2004). "Binary bacterial toxins: biochemistry, biology, and applications of common Clostridium and Bacillus proteins." Microbiol Mol Biol Rev 68(3): 373-402, table of contents.
Barth, H., G. Pfeifer, et al. (2001). "Low pH-induced formation of ion channels by clostridium difficile toxin B in target cells." J Biol Chem 276(14): 10670-6.
Bartlett, J. G. (2002). "Clinical practice. Antibiotic-associated diarrhea." N Engl J Med 346(5): 334-9.
Bartlett, J. G. (2006). "Narrative review: the new epidemic of Clostridium difficile-associated enteric disease." Ann Intern Med 145(10): 758-64.
Bartlett, J. G., T. W. Chang, et al. (1978). "Antibiotic-associated pseudomembranous colitis due to toxin-producing clostridia." N Engl J Med 298(10): 531-4.
Bartlett, J. G., T. W. Chang, et al. (1978). "Antibiotic-induced lethal enterocolitis in hamsters: studies with eleven agents and evidence to support the pathogenic role of toxin-producing Clostridia." Am J Vet Res 39(9): 1525-30.
Bartlett, J. G. and D. N. Gerding (2008). "Clinical recognition and diagnosis of Clostridium difficile infection." Clin Infect Dis 46 Suppl 1: S12-8.
Bartlett, J. G., N. Moon, et al. (1978). "Role of Clostridium difficile in antibiotic-associated pseudomembranous colitis." Gastroenterology 75(5): 778-82.
Bartlett, J. G., A. B. Onderdonk, et al. (1977). "Clindamycin-associated colitis in hamsters: protection with vancomycin." Gastroenterology 73(4 Pt 1): 772-6.
Beagley, K. W., K. Fujihashi, et al. (1993). "The Mycobacterium tuberculosis 71-kDa heat-shock protein induces proliferation and cytokine secretion by murine gut intraepithelial lymphocytes." Eur J Immunol 23(8): 2049-52.
Beagley, K. W., K. Fujihashi, et al. (1995). "Differences in intraepithelial lymphocyte T cell subsets isolated from murine small versus large intestine." J Immunol 154(11): 5611-9.
Beltinger, J., B. C. McKaig, et al. (1999). "Human colonic subepithelial myofibroblasts modulate transepithelial resistance and secretory response." Am J Physiol 277(2 Pt 1): C271-9.
Bennett, G. C., E. Allen, et al. (1984). "Clostridium difficile diarrhoea: a highly infectious organism." Age Ageing 13(6): 363-6.
Bensch, K. W., M. Raida, et al. (1995). "hBD-1: a novel beta-defensin from human plasma." FEBS Lett 368(2): 331-5.
Bernards, A. and J. Settleman (2004). "GAP control: regulating the regulators of small GTPases." Trends Cell Biol 14(7): 377-85.
Bishop, A. L. and A. Hall (2000). "Rho GTPases and their effector proteins." Biochem J 348 Pt 2: 241-55.
Blagosklonny, M. V. and A. B. Pardee (2002). "The restriction point of the cell cycle." Cell Cycle 1(2): 103-10.

Blikslager, A. T. and M. C. Roberts (1997). "Mechanisms of intestinal mucosal repair." J Am Vet Med Assoc 211(11): 1437-41.
Blikslager, A. T., M. C. Roberts, et al. (1997). "Prostaglandins I2 and E2 have a synergistic role in rescuing epithelial barrier function in porcine ileum." J Clin Invest 100(8): 1928-33.
Blot, E., M. C. Escande, et al. (2003). "Outbreak of Clostridium difficile-related diarrhoea in an adult oncology unit: risk factors and microbiological characteristics." J Hosp Infect 53(3): 187-92.
Bobak, D., J. Moorman, et al. (1997). "Inactivation of the small GTPase Rho disrupts cellular attachment and induces adhesion-dependent and adhesion-independent apoptosis." Oncogene 15(18): 2179-89.
Border, W. A. and N. A. Noble (1994). "Transforming growth factor beta in tissue fibrosis." N Engl J Med 331(19): 1286-92.
Borgmann, S., M. Kist, et al. (2008). "Increased number of Clostridium difficile infections and prevalence of Clostridium difficile PCR ribotype 001 in southern Germany." Euro Surveill 13(49).
Borriello, S. P. (1995). "Clostridial disease of the gut." Clin Infect Dis 20 Suppl 2: S242-50.
Borriello, S. P. (1998). "Pathogenesis of Clostridium difficile infection." J Antimicrob Chemother 41 Suppl C: 13-9.
Borriello, S. P., H. A. Davies, et al. (1990). "Virulence factors of Clostridium difficile." Rev Infect Dis 12 Suppl 2: S185-91.
Boursier, L., I. N. Farstad, et al. (2002). "IgVH gene analysis suggests that peritoneal B cells do not contribute to the gut immune system in man." Eur J Immunol 32(9): 2427-36.
Brazier, J. S., S. L. Stubbs, et al. (1999). "Prevalence of toxin A negative/B positive Clostridium difficile strains." J Hosp Infect 42(3): 248-9.
Brito, G. A., J. Fujji, et al. (2002). "Mechanism of Clostridium difficile toxin A-induced apoptosis in T84 cells." J Infect Dis 186(10): 1438-47.
Burckhardt, F., A. Friedrich, et al. (2008). "Clostridium difficile surveillance trends, Saxony, Germany." Emerg Infect Dis 14(4): 691-2.
Burdon, D. W., R. H. George, et al. (1981). "Faecal toxin and severity of antibiotic-associated pseudomembranous colitis." J Clin Pathol 34(5): 548-51.
Burridge, K. and K. Wennerberg (2004). "Rho and Rac take center stage." Cell 116(2): 167-79.
Bury, J. and S. Cross (2003). "Molecular biology in diagnostic histopthalogy - cell cycle." Current Diagnostic Pathology 9(4): 266-275.
Busch, C., F. Hofmann, et al. (2000). "Involvement of a conserved tryptophan residue in the UDP-glucose binding of large clostridial cytotoxin glycosyltransferases." J Biol Chem 275(18): 13228-34.
Busch, C., F. Hofmann, et al. (1998). "A common motif of eukaryotic glycosyltransferases is essential for the enzyme activity of large clostridial cytotoxins." J Biol Chem 273(31): 19566-72.
Calderon, G. M., J. Torres-Lopez, et al. (1998). "Effects of toxin A from Clostridium difficile on mast cell activation and survival." Infect Immun 66(6): 2755-61.
Carlo, E., D. Brown, et al. (2002). "Commensal-associated molecular patterns induce selective toll-like receptor-trafficking from apical membrane to cytoplasmic compartments in polarized intestinal epithelium." Am J Pathol 160(1): 165-73.

Cario, E. and D. K. Podolsky (2000). "Differential alteration in intestinal epithelial cell expression of toll-like receptor 3 (TLR3) and TLR4 in inflammatory bowel disease." Infect Immun 68(12): 7010-7.

Carneiro, B. A., J. Fujii, et al. (2006). "Caspase and bid involvement in Clostridium difficile toxin A-induced apoptosis and modulation of toxin A effects by glutamine and alanyl-glutamine in vivo and in vitro." Infect Immun 74(1): 81-7.

Caron, E. and A. Hall (1998). "Identification of two distinct mechanisms of phagocytosis controlled by different Rho GTPases." Science 282(5394): 1717-21.

Castagliuolo, I., A. C. Keates, et al. (1998). "Clostridium difficile toxin A stimulates macrophage-inflammatory protein-2 production in rat intestinal epithelial cells." J Immunol 160(12): 6039-45.

Castagliuolo, I., C. P. Kelly, et al. (1997). "IL-11 inhibits Clostridium difficile toxin A enterotoxicity in rat ileum." Am J Physiol 273(2 Pt 1): G333-41.

Cepek, K. L., S. K. Shaw, et al. (1994). "Adhesion between epithelial cells and T lymphocytes mediated by E-cadherin and the alpha E beta 7 integrin." Nature 372(6502): 190-3.

CHAI (2006). Investigation of Outbreaks of Clostridium difficile at Stoke Mandeville Hospital, Buckinghamshire Hospitals NHS Trust.

Chang, T. W., S. L. Gorbach, et al. (1978). "Neutralization of Clostridium difficile toxin by Clostridium sordellii antitoxins." Infect Immun 22(2): 418-22.

Chang, T. W., P. S. Lin, et al. (1979). "Ultrastructural changes of cultured human amnion cells by Clostridiu difficile toxin." Infect Immun 23(3): 795-8.

Chaves-Olarte, E., I. Florin, et al. (1996). "UDP-glucose deficiency in a mutant cell line protects against glucosyltransferase toxins from Clostridium difficile and Clostridium sordellii." J Biol Chem 271(12): 6925-32.

Chaves-Olarte, E., P. Low, et al. (1999). "A novel cytotoxin from Clostridium difficile serogroup F is a functional hybrid between two other large clostridial cytotoxins." J Biol Chem 274(16): 11046-52.

Chaves-Olarte, E., M. Weidmann, et al. (1997). "Toxins A and B from Clostridium difficile differ with respect to enzymatic potencies, cellular substrate specificities, and surface binding to cultured cells." J Clin Invest 100(7): 1734-41.

Chernak (2005). Severe Clostridium difficile associated disease in populations previously at low risk - 4 states. M. a. M. W. Report, CDC. 54: 1201-1205.

Cho, J. H. (2008). "The genetics and immunopathogenesis of inflammatory bowel disease." Nat Rev Immunol 8(6): 458-66.

Chong, L. D., A. Traynor-Kaplan, et al. (1994). "The small GTP-binding protein Rho regulates a phosphatidylinositol 4-phosphate 5-kinase in mammalian cells." Cell 79(3): 507-13.

Chott, A., D. Gerdes, et al. (1997). "Intraepithelial lymphocytes in normal human intestine do not express proteins associated with cytolytic function." Am J Pathol 151(2): 435-42.

Ciesla, W. P., Jr. and D. A. Bobak (1998). "Clostridium difficile toxins A and B are cation-dependent UDP-glucose hydrolases with differing catalytic activities." J Biol Chem 273(26): 16021-6.

Clabots, C. R., S. Johnson, et al. (1992). "Acquisition of Clostridium difficile by hospitalized patients: evidence for colonized new admissions as a source of infection." J Infect Dis 166(3): 561-7.
Clark, G. F., H. C. Krivan, et al. (1987). "Toxin A from Clostridium difficile binds to rabbit erythrocyte glycolipids with terminal Gal alpha 1-3Gal beta 1-4GlcNAc sequences." Arch Biochem Biophys 257(1): 217-29.
Clarke, D. J. (2002). "Proteolysis and the cell cycle." Cell Cycle 1(4): 233-4.
Coleman, M. L., C. J. Marshall, et al. (2004). "RAS and RHO GTPases in G1-phase cell-cycle regulation." Nat Rev Mol Cell Biol 5(5): 355-66.
Collins, M. D., P. A. Lawson, et al. (1994). "The phylogeny of the genus Clostridium: proposal of five new genera and eleven new species combinations." Int J Syst Bacteriol 44(4): 812-26.
Cooke, D. L. and S. P. Borriello (1998). "Nonspecific binding of Clostridium difficile toxin A to murine immunoglobulins occurs via the fab component." Infect Immun 66(5): 1981-4.
Corr, S. C., C. C. Gahan, et al. (2008). "M-cells: origin, morphology and role in mucosal immunity and microbial pathogenesis." FEMS Immunol Med Microbiol 52(1): 2-12.
Corthier, G., M. C. Muller, et al. (1991). "Protection against experimental pseudomembranous colitis in gnotobiotic mice by use of monoclonal antibodies against Clostridium difficile toxin A." Infect Immun 59(3): 1192-5.
Craig, S. W. and J. J. Cebra (1971). "Peyer's patches: an enriched source of precursors for IgA-producing immunocytes in the rabbit." J Exp Med 134(1): 188-200.
Czuprynski, C. J., W. J. Johnson, et al. (1983). "Pseudomembranous colitis in Clostridium difficile-monoassociated rats." Infect Immun 39(3): 1368-76.
Dallal, R. M., B. G. Harbrecht, et al. (2002). "Fulminant Clostridium difficile: an underappreciated and increasing cause of death and complications." Ann Surg 235(3): 363-72.
Dansinger, M. L., S. Johnson, et al. (1996). "Protein-losing enteropathy is associated with Clostridium difficile diarrhea but not with asymptomatic colonization: a prospective, case-control study." Clin Infect Dis 22(6): 932-7.
De Andres, S., D. Ferreiro, et al. (2004). "Clostridium difficile colitis associated with valaciclovir." Pharm World Sci 26(1): 8-9.
De Vos P., G. G., Jones D., Krieg N. R., Ludwig W., Rainey F. A., Schleifer K . H., Whitman W. B., Ed. (2009). Bergey's Manual of Systematic Bateriology - The Firmicutes. New York, Springer.
Desmouliere, A., M. Redard, et al. (1995). "Apoptosis mediates the decrease in cellularity during the transition between granulation tissue and scar." Am J Pathol 146(1): 56-66.
Dial, S., J. A. Delaney, et al. (2005). "Use of gastric acid-suppressive agents and the risk of community-acquired Clostridium difficile-associated disease." JAMA 294(23): 2989-95.
Dillon, S. T., E. J. Rubin, et al. (1995). "Involvement of Ras-related Rho proteins in the mechanisms of action of Clostridium difficile toxin A and toxin B." Infect Immun 63(4): 1421-6.

Djuretic, T., P. G. Wall, et al. (1996). "General outbreaks of infectious intestinal disease in England and Wales 1992 to 1994." Commun Dis Rep CDR Rev 6(4): R57-63.
Donta, S. T., N. Sullivan, et al. (1982). "Differential effects of Clostridium difficile toxins on tissue-cultured cells." J Clin Microbiol 15(6): 1157-8.
Dove, C. H., S. Z. Wang, et al. (1990). "Molecular characterization of the Clostridium difficile toxin A gene." Infect Immun 58(2): 480-8.
Drasar, B. S., P. Goddard, et al. (1976). "Clostridia isolated from faeces." J Med Microbiol 9(1): 63-71.
Drudy, D., N. Harnedy, et al. (2007). "Isolation and characterisation of toxin A-negative, toxin B-positive Clostridium difficile in Dublin, Ireland." Clin Microbiol Infect 13(3): 298-304.
Dupuy, B. and A. L. Sonenshein (1998). "Regulated transcription of Clostridium difficile toxin genes." Mol Microbiol 27(1): 107-20.
Ebert, E. C. (1995). "Human intestinal intraepithelial lymphocytes have potent chemotactic activity." Gastroenterology 109(4): 1154-9.
Engle, M. J., G. S. Goetz, et al. (1998). "Caco-2 cells express a combination of colonocyte and enterocyte phenotypes." J Cell Physiol 174(3): 362-9.
Etienne-Manneville, S. and A. Hall (2002). "Rho GTPases in cell biology." Nature 420(6916): 629-35.
Faassen, F., G. Vogel, et al. (2003). "Caco-2 permeability, P-glycoprotein transport ratios and brain penetration of heterocyclic drugs." Int J Pharm 263(1-2): 113-22.
Farstad, I. N., J. Norstein, et al. (1997). "Phenotypes of B and T cells in human intestinal and mesenteric lymph." Gastroenterology 112(1): 163-73.
Fehlbaum, P., M. Rao, et al. (2000). "An essential amino acid induces epithelial beta -defensin expression." Proc Natl Acad Sci U S A 97(23): 12723-8.
Fekety, R. (1997). "Guidelines for the diagnosis and management of Clostridium difficile-associated diarrhea and colitis. American College of Gastroenterology, Practice Parameters Committee." Am J Gastroenterol 92(5): 739-50.
Feltis, B. A., S. M. Wiesner, et al. (2000). "Clostridium difficile toxins A and B can alter epithelial permeability and promote bacterial paracellular migration through HT-29 enterocytes." Shock 14(6): 629-34.
Finne, G. and J. R. Matches (1974). "Low-temperature-growing clostridia from marine sediments." Can J Microbiol 20(12): 1639-45.
Fiocchi, C. (1997). "Intestinal inflammation: a complex interplay of immune and nonimmune cell interactions." Am J Physiol 273(4 Pt 1): G769-75.
Fiorentini, C., A. Fabbri, et al. (1998). "Clostridium difficile toxin B induces apoptosis in intestinal cultured cells." Infect Immun 66(6): 2660-5.
Fiorentini, C., W. Malorni, et al. (1990). "Interaction of Clostridium difficile toxin A with cultured cells: cytoskeletal changes and nuclear polarization." Infect Immun 58(7): 2329-36.
Fiorentini, C. and M. Thelestam (1991). "Clostridium difficile toxin A and its effects on cells." Toxicon 29(6): 543-67.
Florin, I. and M. Thelestam (1983). "Internalization of Clostridium difficile cytotoxin into cultured human lung fibroblasts." Biochim Biophys Acta 763(4): 383-92.

Florin, I. and M. Thelestam (1986). "Lysosomal involvement in cellular intoxication with Clostridium difficile toxin B." Microb Pathog 1(4): 373-85.

Fournier, A. K., L. E. Campbell, et al. (2008). "Rac-dependent cyclin D1 gene expression regulated by cadherin- and integrin-mediated adhesion." J Cell Sci 121(Pt 2): 226-33.

Frey, S. M. and T. D. Wilkins (1992). "Localization of two epitopes recognized by monoclonal antibody PCG-4 on Clostridium difficile toxin A." Infect Immun 60(6): 2488-92.

Frisch, C., R. Gerhard, et al. (2003). "The complete receptor-binding domain of Clostridium difficile toxin A is required for endocytosis." Biochem Biophys Res Commun 300(3): 706-11.

Fritz, G. and B. Kaina (2001). "Ras-related GTPase Rhob represses NF-kappaB signaling." J Biol Chem 276(5): 3115-22.

Fujisawa, K., P. Madaule, et al. (1998). "Different regions of Rho determine Rho-selective binding of different classes of Rho target molecules." J Biol Chem 273(30): 18943-9.

Fukumoto, Y., K. Kaibuchi, et al. (1990). "Molecular cloning and characterization of a novel type of regulatory protein (GDI) for the rho proteins, ras p21-like small GTP-binding proteins." Oncogene 5(9): 1321-8.

Fyderek, K., M. Strus, et al. (2009). "Mucosal bacterial microflora and mucus layer thickness in adolescents with inflammatory bowel disease." World J Gastroenterol 15(42): 5287-94.

Galluzzi, L., S. A. Aaronson, et al. (2009). "Guidelines for the use and interpretation of assays for monitoring cell death in higher eukaryotes." Cell Death Differ 16(8): 1093-107.

Ganz, T. (1999). "Defensins and host defense." Science 286(5439): 420-1.

Garcia, J. R., A. Krause, et al. (2001). "Human beta-defensin 4: a novel inducible peptide with a specific salt-sensitive spectrum of antimicrobial activity." FASEB J 15(10): 1819-21.

Genth, H., J. Huelsenbeck, et al. (2006). "Cellular stability of Rho-GTPases glucosylated by Clostridium difficile toxin B." FEBS Lett 580(14): 3565-9.

George, R. H., J. M. Symonds, et al. (1978). "Identification of Clostridium difficile as a cause of pseudomembranous colitis." Br Med J 1(6114): 695.

Gerding, D. N., C. A. Muto, et al. (2008). "Measures to control and prevent Clostridium difficile infection." Clin Infect Dis 46 Suppl 1: S43-9.

Geric, B., R. J. Carman, et al. (2006). "Binary toxin-producing, large clostridial toxin-negative Clostridium difficile strains are enterotoxic but do not cause disease in hamsters." J Infect Dis 193(8): 1143-50.

Geric, B., M. Rupnik, et al. (2004). "Distribution of Clostridium difficile variant toxinotypes and strains with binary toxin genes among clinical isolates in an American hospital." J Med Microbiol 53(Pt 9): 887-94.

Gervot, L., Carriere, V., Costet, P., Cugnenc, P.H., Berger, A., Beaune, P.H., de Waziers, I. (1996). "CYP3A5 is the major cytochrome P450 3A expressed in human colon and colonic cell lines." Environmental Toxicology and Pharmacology 2: 381-388.

Girardin, S. E., R. Tournebize, et al. (2001). "CARD4/Nod1 mediates NF-kappaB and JNK activation by invasive Shigella flexneri." EMBO Rep 2(8): 736-42.
Glotzer, M. (2004). "Cleavage furrow positioning." J Cell Biol 164(3): 347-51.
Goorhuis, A., D. Bakker, et al. (2008). "Emergence of Clostridium difficile infection due to a new hypervirulent strain, polymerase chain reaction ribotype 078." Clin Infect Dis 47(9): 1162-70.
Gotta, M., M. C. Abraham, et al. (2001). "CDC-42 controls early cell polarity and spindle orientation in C. elegans." Curr Biol 11(7): 482-8.
Gowans, J. L. and E. J. Knight (1964). "The Route of Re-Circulation of Lymphocytes in the Rat." Proc R Soc Lond B Biol Sci 159: 257-82.
Greco, A., J. G. Ho, et al. (2006). "Carbohydrate recognition by Clostridium difficile toxin A." Nat Struct Mol Biol 13(5): 460-1.
Green, A. A., Hughes, W.L. (1955). "Protein solubility on the basis of solubility in aqueous solutions of salts and organic solvents." Methods Enzymol(1): 67-90.
Gulke, I., G. Pfeifer, et al. (2001). "Characterization of the enzymatic component of the ADP-ribosyltransferase toxin CDTa from Clostridium difficile." Infect Immun 69(10): 6004-11.
Guy-Grand, D., C. Griscelli, et al. (1974). "The gut-associated lymphoid system: nature and properties of the large dividing cells." Eur J Immunol 4(6): 435-43.
Guy-Grand, D., C. Griscelli, et al. (1978). "The mouse gut T lymphocyte, a novel type of T cell. Nature, origin, and traffic in mice in normal and graft-versus-host conditions." J Exp Med 148(6): 1661-77.
Hall, I. C. and E. O'Toole (1935). "Intestinal flora in newborn infants with a description of a pathogenic anaerobe, Bacillus dificilis." American Journal of Disease in Childhood(49): 390-402.
Hammond, G. A. and J. L. Johnson (1995). "The toxigenic element of Clostridium difficile strain VPI 10463." Microb Pathog 19(4): 203-13.
Hase, K., L. Eckmann, et al. (2002). "Cell differentiation is a key determinant of cathelicidin LL-37/human cationic antimicrobial protein 18 expression by human colon epithelium." Infect Immun 70(2): 953-63.
He, D., S. J. Hagen, et al. (2000). "Clostridium difficile toxin A causes early damage to mitochondria in cultured cells." Gastroenterology 119(1): 139-50.
He, D., S. Sougioultzis, et al. (2002). "Clostridium difficile toxin A triggers human colonocyte IL-8 release via mitochondrial oxygen radical generation." Gastroenterology 122(4): 1048-57.
Hecht, G., A. Koutsouris, et al. (1992). "Clostridium difficile toxin B disrupts the barrier function of T84 monolayers." Gastroenterology 102(2): 416-23.
Hecht, G., C. Pothoulakis, et al. (1988). "Clostridium difficile toxin A perturbs cytoskeletal structure and tight junction permeability of cultured human intestinal epithelial monolayers." J Clin Invest 82(5): 1516-24.
Henriques, B., I. Florin, et al. (1987). "Cellular internalisation of Clostridium difficile toxin A." Microb Pathog 2(6): 455-63.
Hilgendorf, C., H. Spahn-Langguth, et al. (2000). "Caco-2 versus Caco-2/HT29-MTX co-cultured cell lines: permeabilities via diffusion, inside- and outside-directed carrier-mediated transport." J Pharm Sci 89(1): 63-75.

Hippenstiel, S., B. Schmeck, et al. (2002). "Rho protein inactivation induced apoptosis of cultured human endothelial cells." Am J Physiol Lung Cell Mol Physiol 283(4): L830-8.
Hirschhorn, L. R., Y. Trnka, et al. (1994). "Epidemiology of community-acquired Clostridium difficile-associated diarrhea." J Infect Dis 169(1): 127-33.
Hisamatsu, T., M. Suzuki, et al. (2003). "CARD15/NOD2 functions as an antibacterial factor in human intestinal epithelial cells." Gastroenterology 124(4): 993-1000.
Ho, J. G., A. Greco, et al. (2005). "Crystal structure of receptor-binding C-terminal repeats from Clostridium difficile toxin A." Proc Natl Acad Sci U S A 102(51): 18373-8.
Hofmann, F., C. Busch, et al. (1998). "Chimeric clostridial cytotoxins: identification of the N-terminal region involved in protein substrate recognition." Infect Immun 66(3): 1076-81.
Hofmann, F., C. Busch, et al. (1997). "Localization of the glucosyltransferase activity of Clostridium difficile toxin B to the N-terminal part of the holotoxin." J Biol Chem 272(17): 11074-8.
Hookman, P. and J. S. Barkin (2009). "Clostridium difficile associated infection, diarrhea and colitis." World J Gastroenterol 15(13): 1554-80.
Howard, S. P., A. (1953). "Synthesis of deoxyribonucleic acid in normal and irradiated cells and its relation to chromosome breakage." Heredity(6): 261-273.
HPA (2006). Deaths involving Clostridium difficile: England and Wales 1999-2004. Health Statistics Quarterly 30.
HPA. (2007). "Annual counts and rates of C. difficile." from http://www.hpa.org.uk.
HPA (2008). Identification of Clostridium species. E. a. S. L. Standards Unit. London, HPA: 1-14.
HPA. (2010). "Quarterly Epidemiological Commentaries on MRSA bacteraemia and *C. difficile* infection." December 2010 Retrieved 21/12/2010, 2010, from www.hpa.org.uk.
HPA. (2010). "Summary Points on Clostridium difficile infection." Retrieved 21/12/2010, 2010, from http://www.hpa.org.uk/web/HPAwebFile/HPAweb_C/1278944283388.
Hubert, B., V. G. Loo, et al. (2007). "A portrait of the geographic dissemination of the Clostridium difficile North American pulsed-field type 1 strain and the epidemiology of C. difficile-associated disease in Quebec." Clin Infect Dis 44(2): 238-44.
Huelsenbeck, J., S. Dreger, et al. (2007). "Difference in the cytotoxic effects of toxin B from Clostridium difficile strain VPI 10463 and toxin B from variant Clostridium difficile strain 1470." Infect Immun 75(2): 801-9.
Huelsenbeck, J., S. C. Dreger, et al. (2007). "Upregulation of the immediate early gene product RhoB by exoenzyme C3 from Clostridium limosum and toxin B from Clostridium difficile." Biochemistry 46(16): 4923-31.
Hundsberger, T., V. Braun, et al. (1997). "Transcription analysis of the genes tcdA-E of the pathogenicity locus of Clostridium difficile." Eur J Biochem 244(3): 735-42.
Ihara, K., S. Muraguchi, et al. (1998). "Crystal structure of human RhoA in a dominantly active form complexed with a GTP analogue." J Biol Chem 273(16): 9656-66.

Issa, M., A. Vijayapal, et al. (2007). "Impact of Clostridium difficile on inflammatory bowel disease." Clin Gastroenterol Hepatol 5(3): 345-51.
Jaffe, A. B. and A. Hall (2005). "Rho GTPases: biochemistry and biology." Annu Rev Cell Dev Biol 21: 247-69.
Jank, T., T. Giesemann, et al. (2007). "Rho-glucosylating Clostridium difficile toxins A and B: new insights into structure and function." Glycobiology 17(4): 15R-22.
Jefferson, K. K., M. F. Smith, Jr., et al. (1999). "Roles of intracellular calcium and NF-kappa B in the Clostridium difficile toxin A-induced up-regulation and secretion of IL-8 from human monocytes." J Immunol 163(10): 5183-91.
Jia, H. P., B. C. Schutte, et al. (2001). "Discovery of new human beta-defensins using a genomics-based approach." Gene 263(1-2): 211-8.
Johal, S. S., K. Solomon, et al. (2004). "Differential effects of varying concentrations of clostridium difficile toxin A on epithelial barrier function and expression of cytokines." J Infect Dis 189(11): 2110-9.
Johnson, S., S. A. Kent, et al. (2001). "Fatal pseudomembranous colitis associated with a variant clostridium difficile strain not detected by toxin A immunoassay." Ann Intern Med 135(6): 434-8.
Johnson, S., S. P. Sambol, et al. (2003). "International typing study of toxin A-negative, toxin B-positive Clostridium difficile variants." J Clin Microbiol 41(4): 1543-7.
Johnson, S., M. H. Samore, et al. (1999). "Epidemics of diarrhea caused by a clindamycin-resistant strain of Clostridium difficile in four hospitals." N Engl J Med 341(22): 1645-51.
Joyce, N. C., M. F. Haire, et al. (1987). "Morphologic and biochemical evidence for a contractile cell network within the rat intestinal mucosa." Gastroenterology 92(1): 68-81.
Jump, R. L., M. J. Pultz, et al. (2007). "Vegetative Clostridium difficile survives in room air on moist surfaces and in gastric contents with reduced acidity: a potential mechanism to explain the association between proton pump inhibitors and C. difficile-associated diarrhea?" Antimicrob Agents Chemother 51(8): 2883-7.
Just, I., G. Fritz, et al. (1994). "Clostridium difficile toxin B acts on the GTP-binding protein Rho." J Biol Chem 269(14): 10706-12.
Just, I. and R. Gerhard (2004). "Large clostridial cytotoxins." Rev Physiol Biochem Pharmacol 152: 23-47.
Just, I., J. Selzer, et al. (1995). "The low molecular mass GTP-binding protein Rho is affected by toxin A from Clostridium difficile." J Clin Invest 95(3): 1026-31.
Just, I., J. Selzer, et al. (1995). "Glucosylation of Rho proteins by Clostridium difficile toxin B." Nature 375(6531): 500-3.
Just, I., M. Wilm, et al. (1995). "The enterotoxin from Clostridium difficile (ToxA) monoglucosylates the Rho proteins." J Biol Chem 270(23): 13932-6.
Kamiya, S., P. J. Reed, et al. (1989). "Purification and characterisation of Clostridium difficile toxin A by bovine thyroglobulin affinity chromatography and dissociation in denaturing conditions with or without reduction." J Med Microbiol 30(1): 69-77.

Karlsson, S., L. G. Burman, et al. (1999). "Suppression of toxin production in Clostridium difficile VPI 10463 by amino acids." Microbiology 145 (Pt 7): 1683-93.
Kato, H., N. Kato, et al. (1998). "Identification of toxin A-negative, toxin B-positive Clostridium difficile by PCR." J Clin Microbiol 36(8): 2178-82.
Kawai, T. and S. Akira (2006). "TLR signaling." Cell Death Differ 13(5): 816-25.
Kawamoto, S., K. M. Horton, et al. (1999). "Pseudomembranous Colitis: Spectrum of Imaging Findings with Clinical and Pathologic Correlation1." Radiographics 19(4): 887-897.
Keighley, M. R., D. W. Burdon, et al. (1978). "Randomised controlled trial of vancomycin for pseudomembranous colitis and postoperative diarrhoea." Br Med J 2(6153): 1667-9.
Kelly, C. P., S. Becker, et al. (1994). "Neutrophil recruitment in Clostridium difficile toxin A enteritis in the rabbit." J Clin Invest 93(3): 1257-65.
Kelly, C. P. and J. T. LaMont (1998). "Clostridium difficile infection." Annu Rev Med 49: 375-90.
Kim, H., E. Kokkotou, et al. (2005). "Clostridium difficile toxin A-induced colonocyte apoptosis involves p53-dependent p21(WAF1/CIP1) induction via p38 mitogen-activated protein kinase." Gastroenterology 129(6): 1875-88.
Kirkwood, K. S., N. W. Bunnett, et al. (2001). "Deletion of neutral endopeptidase exacerbates intestinal inflammation induced by Clostridium difficile toxin A." Am J Physiol Gastrointest Liver Physiol 281(2): G544-51.
Klein, E. A., L. E. Campbell, et al. (2008). "Joint requirement for Rac and ERK activities underlies the mid-G1 phase induction of cyclin D1 and S phase entry in both epithelial and mesenchymal cells." J Biol Chem 283(45): 30911-8.
Klein, E. A., Y. Yung, et al. (2007). "Cell adhesion, cellular tension, and cell cycle control." Methods Enzymol 426: 155-75.
Komatsu, M., H. Kato, et al. (2003). "High frequency of antibiotic-associated diarrhea due to toxin A-negative, toxin B-positive Clostridium difficile in a hospital in Japan and risk factors for infection." Eur J Clin Microbiol Infect Dis 22(9): 525-9.
Kovacs, E. J. and L. A. DiPietro (1994). "Fibrogenic cytokines and connective tissue production." FASEB J 8(11): 854-61.
Krivan, H. C., G. F. Clark, et al. (1986). "Cell surface binding site for Clostridium difficile enterotoxin: evidence for a glycoconjugate containing the sequence Gal alpha 1-3Gal beta 1-4GlcNAc." Infect Immun 53(3): 573-81.
Kuehne, S. A., S. T. Cartman, et al. "The role of toxin A and toxin B in Clostridium difficile infection." Nature 467(7316): 711-3.
Kuijper, E. J., F. Barbut, et al. (2008). "Update of Clostridium difficile infection due to PCR ribotype 027 in Europe, 2008." Euro Surveill 13(31).
Kuijper, E. J., B. Coignard, et al. (2006). "Emergence of Clostridium difficile-associated disease in North America and Europe." Clin Microbiol Infect 12 Suppl 6: 2-18.
Kuijper, E. J., J. de Weerdt, et al. (2001). "Nosocomial outbreak of Clostridium difficile-associated diarrhoea due to a clindamycin-resistant enterotoxin A-negative strain." Eur J Clin Microbiol Infect Dis 20(8): 528-34.

Kurtz, C. B., E. P. Cannon, et al. (2001). "GT160-246, a toxin binding polymer for treatment of Clostridium difficile colitis." Antimicrob Agents Chemother 45(8): 2340-7.
Kyne, L., M. Warny, et al. (2001). "Association between antibody response to toxin A and protection against recurrent Clostridium difficile diarrhoea." Lancet 357(9251): 189-93.
Lamontagne, F., A. C. Labbe, et al. (2007). "Impact of emergency colectomy on survival of patients with fulminant Clostridium difficile colitis during an epidemic caused by a hypervirulent strain." Ann Surg 245(2): 267-72.
Larson, H. E., A. B. Price, et al. (1978). "Clostridium difficile and the aetiology of pseudomembranous colitis." Lancet 1(8073): 1063-6.
Lawrence, S. J., L. A. Puzniak, et al. (2007). "Clostridium difficile in the intensive care unit: epidemiology, costs, and colonization pressure." Infect Control Hosp Epidemiol 28(2): 123-30.
Le Bivic, A., M. Hirn, et al. (1988). "HT-29 cells are an in vitro model for the generation of cell polarity in epithelia during embryonic differentiation." Proc Natl Acad Sci U S A 85(1): 136-40.
Le Ferrec, E., Chesne, C., Per, A., Brayden, D., Fabre, G., Gires, P., Guillou, F., Rousset, M., Rubas, W., Scarino, M. (2001). "In vitro model of the intestinal barrier " ATLA 29: 649-668.
Lefrancois, L. (1991). "Phenotypic complexity of intraepithelial lymphocytes of the small intestine." J Immunol 147(6): 1746-51.
Leonard, J., J. K. Marshall, et al. (2007). "Systematic review of the risk of enteric infection in patients taking acid suppression." Am J Gastroenterol 102(9): 2047-56; quiz 2057.
Libby, J. M., B. S. Jortner, et al. (1982). "Effects of the two toxins of Clostridium difficile in antibiotic-associated cecitis in hamsters." Infect Immun 36(2): 822-9.
Lima, A. A., D. M. Lyerly, et al. (1988). "Effects of Clostridium difficile toxins A and B in rabbit small and large intestine in vivo and on cultured cells in vitro." Infect Immun 56(3): 582-8.
Limaye, A. P., D. K. Turgeon, et al. (2000). "Pseudomembranous colitis caused by a toxin A(-) B(+) strain of Clostridium difficile." J Clin Microbiol 38(4): 1696-7.
Liu, A., G. J. Cerniglia, et al. (2001). "RhoB is required to mediate apoptosis in neoplastically transformed cells after DNA damage." Proc Natl Acad Sci U S A 98(11): 6192-7.
Lonnroth, I. and S. Lange (1983). "Toxin A of Clostridium difficile: production, purification and effect in mouse intestine." Acta Pathol Microbiol Immunol Scand [B] 91(6): 395-400.
Loo, V. G., L. Poirier, et al. (2005). "A predominantly clonal multi-institutional outbreak of Clostridium difficile-associated diarrhea with high morbidity and mortality." N Engl J Med 353(23): 2442-9.
Lundqvist, C., S. Melgar, et al. (1996). "Intraepithelial lymphocytes in human gut have lytic potential and a cytokine profile that suggest T helper 1 and cytotoxic functions." J Immunol 157(5): 1926-34.
Lyerly, D. M., K. E. Saum, et al. (1985). "Effects of Clostridium difficile toxins given intragastrically to animals." Infect Immun 47(2): 349-52.
MacDonald, T. T. (2003). "The mucosal immune system." Parasite Immunol 25(5): 235-46.

Madaule, P., M. Eda, et al. (1998). "Role of citron kinase as a target of the small GTPase Rho in cytokinesis." Nature 394(6692): 491-4.
Maegawa, T., T. Karasawa, et al. (2002). "Linkage between toxin production and purine biosynthesis in Clostridium difficile." J Med Microbiol 51(1): 34-41.
Mahida, Y. R., Ed. (2001). Immunological Aspects of Gastronenterology. Immunology and Medicine. Dordrecht, Kluwer Academic Publishers.
Mahida, Y. R., J. Beltinger, et al. (1997). "Adult human colonic subepithelial myofibroblasts express extracellular matrix proteins and cyclooxygenase-1 and -2." Am J Physiol 273(6 Pt 1): G1341-8.
Mahida, Y. R., A. Galvin, et al. (1998). "Effect of Clostridium difficile toxin A on human colonic lamina propria cells: early loss of macrophages followed by T-cell apoptosis." Infect Immun 66(11): 5462-9.
Mahida, Y. R., S. Makh, et al. (1996). "Effect of Clostridium difficile toxin A on human intestinal epithelial cells: induction of interleukin 8 production and apoptosis after cell detachment." Gut 38(3): 337-47.
Maldonado-Contreras, A. L. and B. A. McCormick "Intestinal epithelial cells and their role in innate mucosal immunity." Cell Tissue Res 343(1): 5-12.
Mani, N. and B. Dupuy (2001). "Regulation of toxin synthesis in Clostridium difficile by an alternative RNA polymerase sigma factor." Proc Natl Acad Sci U S A 98(10): 5844-9.
Mani, N., D. Lyras, et al. (2002). "Environmental response and autoregulation of Clostridium difficile TxeR, a sigma factor for toxin gene expression." J Bacteriol 184(21): 5971-8.
Mantyh, C. R., J. E. Maggio, et al. (1996). "Increased substance P receptor expression by blood vessels and lymphoid aggregates in Clostridium difficile-induced pseudomembranous colitis." Dig Dis Sci 41(3): 614-20.
Mantyh, C. R., T. N. Pappas, et al. (1996). "Substance P activation of enteric neurons in response to intraluminal Clostridium difficile toxin A in the rat ileum." Gastroenterology 111(5): 1272-80.
Marshall, C. J. (1993). "Protein prenylation: a mediator of protein-protein interactions." Science 259(5103): 1865-6.
Martinez, R. D. and T. D. Wilkins (1988). "Purification and characterization of Clostridium sordellii hemorrhagic toxin and cross-reactivity with Clostridium difficile toxin A (enterotoxin)." Infect Immun 56(5): 1215-21.
Mastroianni, J. R. and A. J. Ouellette (2009). "Alpha-defensins in enteric innate immunity: functional Paneth cell alpha-defensins in mouse colonic lumen." J Biol Chem 284(41): 27848-56.
Mazanec, M. B., C. L. Coudret, et al. (1995). "Intracellular neutralization of influenza virus by immunoglobulin A anti-hemagglutinin monoclonal antibodies." J Virol 69(2): 1339-43.
McDonald, L. C., G. E. Killgore, et al. (2005). "An epidemic, toxin gene-variant strain of Clostridium difficile." N Engl J Med 353(23): 2433-41.
McFee, R. B. and G. G. Abdelsayed (2009). "Clostridium difficile." Dis Mon 55(7): 439-70.
McKaig, B. C., S. S. Makh, et al. (1999). "Normal human colonic subepithelial myofibroblasts enhance epithelial migration (restitution) via TGF-beta3." Am J Physiol 276(5 Pt 1): G1087-93.
McKay, D. M. and A. W. Baird (1999). "Cytokine regulation of epithelial permeability and ion transport." Gut 44(2): 283-9.

Mead, G. C. and C. S. Impey (1970). "The distribution of clostridia in poultry processing plants." Br Poult Sci 11(3): 407-14.
Meador, J., 3rd and R. K. Tweten (1988). "Purification and characterization of toxin B from Clostridium difficile." Infect Immun 56(7): 1708-14.
Meng, X. Q., S. Kamiya, et al. (1993). "Purification and characterisation of intracellular toxin A of Clostridium difficile." J Med Microbiol 38(1): 69-73.
Meyer, G. K., A. Neetz, et al. (2007). "Clostridium Difficile Toxin a and B Directly Stimulate Human Mast Cells." Infect Immun.
Mims C A, N. A., Stephen J. (2000). Mims' Pathogenesis of Infectious Disease, Academic Press.
Mitchell, M. J., B. E. Laughon, et al. (1987). "Biochemical studies on the effect of Clostridium difficile toxin B on actin in vivo and in vitro." Infect Immun 55(7): 1610-5.
Mizuno, T., K. Kaibuchi, et al. (1991). "A stimulatory GDP/GTP exchange protein for smg p21 is active on the post-translationally processed form of c-Ki-ras p21 and rhoA p21." Proc Natl Acad Sci U S A 88(15): 6442-6.
Monaghan, T., T. Boswell, et al. (2008). "Recent advances in Clostridium difficile-associated disease." Gut 57(6): 850-60.
Montecucco, C. and G. Schiavo (1995). "Structure and function of tetanus and botulinum neurotoxins." Q Rev Biophys 28(4): 423-72.
Moore, R., S. Carlson, et al. (1989). "Villus contraction aids repair of intestinal epithelium after injury." Am J Physiol 257(2 Pt 1): G274-83.
Moorman, J. P., D. A. Bobak, et al. (1996). "Inactivation of the small GTP binding protein Rho induces multinucleate cell formation and apoptosis in murine T lymphoma EL4." J Immunol 156(11): 4146-53.
Morales, V. M., A. Christ, et al. (1999). "Regulation of human intestinal intraepithelial lymphocyte cytolytic function by biliary glycoprotein (CD66a)." J Immunol 163(3): 1363-70.
Mosmann, T. (1983). "Rapid colorimetric assay for cellular growth and survival: application to proliferation and cytotoxicity assays." J Immunol Methods 65(1-2): 55-63.
Mostov, K. E. (1994). "Transepithelial transport of immunoglobulins." Annu Rev Immunol 12: 63-84.
Munoz, P., M. Giannella, et al. (2007). "Clostridium difficile-associated diarrhea in heart transplant recipients: is hypogammaglobulinemia the answer?" J Heart Lung Transplant 26(9): 907-14.
Muto, C. A., M. Pokrywka, et al. (2005). "A large outbreak of Clostridium difficile-associated disease with an unexpected proportion of deaths and colectomies at a teaching hospital following increased fluoroquinolone use." Infect Control Hosp Epidemiol 26(3): 273-80.
Neunlist, M., J. Barouk, et al. (2003). "Toxin B of Clostridium difficile activates human VIP submucosal neurons, in part via an IL-1beta-dependent pathway." Am J Physiol Gastrointest Liver Physiol 285(5): G1049-55.
Neutra, M. R., T. L. Phillips, et al. (1987). "Transport of membrane-bound macromolecules by M cells in follicle-associated epithelium of rabbit Peyer's patch." Cell Tissue Res 247(3): 537-46.
Neutra, M. R., E. Pringault, et al. (1996). "Antigen sampling across epithelial barriers and induction of mucosal immune responses." Annu Rev Immunol 14: 275-300.

Nicoletti, I., G. Migliorati, et al. (1991). "A rapid and simple method for measuring thymocyte apoptosis by propidium iodide staining and flow cytometry." J Immunol Methods 139(2): 271-9.

Nottrott, S., J. Schoentaube, et al. (2007). "Clostridium difficile toxin A-induced apoptosis is p53-independent but depends on glucosylation of Rho GTPases." Apoptosis 12(8): 1443-53.

Nusrat, A., M. Giry, et al. (1995). "Rho protein regulates tight junctions and perijunctional actin organization in polarized epithelia." Proc Natl Acad Sci U S A 92(23): 10629-33.

Nusrat, A., C. von Eichel-Streiber, et al. (2001). "Clostridium difficile toxins disrupt epithelial barrier function by altering membrane microdomain localization of tight junction proteins." Infect Immun 69(3): 1329-36.

Olson, M. F., A. Ashworth, et al. (1995). "An essential role for Rho, Rac, and Cdc42 GTPases in cell cycle progression through G1." Science 269(5228): 1270-2.

Olson, M. F., H. F. Paterson, et al. (1998). "Signals from Ras and Rho GTPases interact to regulate expression of p21Waf1/Cip1." Nature 394(6690): 295-9.

Onderdonk, A. B., B. R. Lowe, et al. (1979). "Effect of environmental stress on Clostridium difficile toxin levels during continuous cultivation." Appl Environ Microbiol 38(4): 637-41.

Ormerod, M. G., A. W. Payne, et al. (1987). "Improved program for the analysis of DNA histograms." Cytometry 8(6): 637-41.

Oswald, E., M. Sugai, et al. (1994). "Cytotoxic necrotizing factor type 2 produced by virulent Escherichia coli modifies the small GTP-binding proteins Rho involved in assembly of actin stress fibers." Proc Natl Acad Sci U S A 91(9): 3814-8.

Ouellette, A. J. and M. E. Selsted (1996). "Paneth cell defensins: endogenous peptide components of intestinal host defense." FASEB J 10(11): 1280-9.

Owen, R. L. and A. L. Jones (1974). "Epithelial cell specialization within human Peyer's patches: an ultrastructural study of intestinal lymphoid follicles." Gastroenterology 66(2): 189-203.

Pardee, A. B. (1974). "A restriction point for control of normal animal cell proliferation." Proc Natl Acad Sci U S A 71(4): 1286-90.

Pauleau, A. L. and P. J. Murray (2003). "Role of nod2 in the response of macrophages to toll-like receptor agonists." Mol Cell Biol 23(21): 7531-9.

Pepin, J., N. Saheb, et al. (2005). "Emergence of fluoroquinolones as the predominant risk factor for Clostridium difficile-associated diarrhea: a cohort study during an epidemic in Quebec." Clin Infect Dis 41(9): 1254-60.

Perelle, S., M. Gibert, et al. (1997). "Production of a complete binary toxin (actin-specific ADP-ribosyltransferase) by Clostridium difficile CD196." Infect Immun 65(4): 1402-7.

Petnicki-Ocwieja, T., T. Hrncir, et al. (2009). "Nod2 is required for the regulation of commensal microbiota in the intestine." Proc Natl Acad Sci U S A 106(37): 15813-8.

Pfeifer, G., J. Schirmer, et al. (2003). "Cellular uptake of Clostridium difficile toxin B. Translocation of the N-terminal catalytic domain into the cytosol of eukaryotic cells." J Biol Chem 278(45): 44535-41.

Pierce, N. F. and J. L. Gowans (1975). "Cellular kinetics of the intestinal immune response to cholera toxoid in rats." J Exp Med 142(6): 1550-63.
Pituch, H., N. van den Braak, et al. (2001). "Clonal dissemination of a toxin-A-negative/toxin-B-positive Clostridium difficile strain from patients with antibiotic-associated diarrhea in Poland." Clin Microbiol Infect 7(8): 442-6.
Pituch, H., A. vavn Belkum, et al. (2003). "Clindamycin-resistant, toxin A-negative, toxin B-positive Clostridium difficile strains cause antibiotic-associated diarrhea among children hospitalized in a hematology unit." Clin Microbiol Infect 9(8): 903-4.
Planche, T., A. Aghaizu, et al. (2008). "Diagnosis of Clostridium difficile infection by toxin detection kits: a systematic review." Lancet Infect Dis 8(12): 777-84.
Podolsky, D. K. (1997). "Healing the epithelium: solving the problem from two sides." J Gastroenterol 32(1): 122-6.
Popoff, M. R., E. J. Rubin, et al. (1988). "Actin-specific ADP-ribosyltransferase produced by a Clostridium difficile strain." Infect Immun 56(9): 2299-306.
Pothoulakis, C., L. M. Barone, et al. (1986). "Purification and properties of Clostridium difficile cytotoxin B." J Biol Chem 261(3): 1316-21.
Pothoulakis, C., I. Castagliuolo, et al. (1994). "CP-96,345, a substance P antagonist, inhibits rat intestinal responses to Clostridium difficile toxin A but not cholera toxin." Proc Natl Acad Sci U S A 91(3): 947-51.
Pothoulakis, C., R. Sullivan, et al. (1988). "Clostridium difficile toxin A stimulates intracellular calcium release and chemotactic response in human granulocytes." J Clin Invest 81(6): 1741-5.
Powell, D. W., R. C. Mifflin, et al. (1999). "Myofibroblasts. I. Paracrine cells important in health and disease." Am J Physiol 277(1 Pt 1): C1-9.
Powell, D. W., R. C. Mifflin, et al. (1999). "Myofibroblasts. II. Intestinal subepithelial myofibroblasts." Am J Physiol 277(2 Pt 1): C183-201.
Prepens, U., I. Just, et al. (1996). "Inhibition of Fc epsilon-RI-mediated activation of rat basophilic leukemia cells by Clostridium difficile toxin B (monoglucosyltransferase)." J Biol Chem 271(13): 7324-9.
Qa'Dan, M., M. Ramsey, et al. (2002). "Clostridium difficile toxin B activates dual caspase-dependent and caspase-independent apoptosis in intoxicated cells." Cell Microbiol 4(7): 425-34.
Qa'Dan, M., L. M. Spyres, et al. (2000). "pH-induced conformational changes in Clostridium difficile toxin B." Infect Immun 68(5): 2470-4.
Qiu, B., C. Pothoulakis, et al. (1999). "Participation of reactive oxygen metabolites in Clostridium difficile toxin A-induced enteritis in rats." Am J Physiol 276(2 Pt 1): G485-90.
Raithel, M., M. Matek, et al. (1995). "Mucosal histamine content and histamine secretion in Crohn's disease, ulcerative colitis and allergic enteropathy." Int Arch Allergy Immunol 108(2): 127-33.
Reinecker, H. C., R. P. MacDermott, et al. (1996). "Intestinal epithelial cells both express and respond to interleukin 15." Gastroenterology 111(6): 1706-13.
Ridley, A. J. (2001). "Rho family proteins: coordinating cell responses." Trends Cell Biol 11(12): 471-7.

Ridley, A. J. and A. Hall (1992). "The small GTP-binding protein rho regulates the assembly of focal adhesions and actin stress fibers in response to growth factors." Cell 70(3): 389-99.
Ridley, A. J., H. F. Paterson, et al. (1992). "The small GTP-binding protein rac regulates growth factor-induced membrane ruffling." Cell 70(3): 401-10.
Riegler, M., R. Sedivy, et al. (1995). "Clostridium difficile toxin B is more potent than toxin A in damaging human colonic epithelium in vitro." J Clin Invest 95(5): 2004-11.
Riegler, M., R. Sedivy, et al. (1997). "Epidermal growth factor attenuates Clostridium difficile toxin A- and B-induced damage of human colonic mucosa." Am J Physiol 273(5 Pt 1): G1014-22.
Roberts, A. I., M. Bilenker, et al. (1997). "Intestinal intraepithelial lymphocytes have a promiscuous interleukin-8 receptor." Gut 40(3): 333-8.
Roberts, A. I., R. E. Brolin, et al. (1999). "Integrin alpha1beta1 (VLA-1) mediates adhesion of activated intraepithelial lymphocytes to collagen." Immunology 97(4): 679-85.
Roberts, A. I., S. C. Nadler, et al. (1997). "Mesenchymal cells stimulate human intestinal intraepithelial lymphocytes." Gastroenterology 113(1): 144-50.
Rocha, M. F., A. M. Soares, et al. (1998). "Intestinal secretory factor released by macrophages stimulated with Clostridium difficile toxin A: role of interleukin 1beta." Infect Immun 66(10): 4910-6.
Rolfe, R. D. and S. M. Finegold (1979). "Purification and characterization of Clostridium difficile toxin." Infect Immun 25(1): 191-201.
Roovers, K. and R. K. Assoian (2003). "Effects of rho kinase and actin stress fibers on sustained extracellular signal-regulated kinase activity and activation of G(1) phase cyclin-dependent kinases." Mol Cell Biol 23(12): 4283-94.
Rouphael, N. G., J. A. O'Donnell, et al. (2008). "Clostridium difficile-associated diarrhea: an emerging threat to pregnant women." Am J Obstet Gynecol 198(6): 635 e1-6.
Roussel, M. F. (1999). "The INK4 family of cell cycle inhibitors in cancer." Oncogene 18(38): 5311-7.
Rupnik, M., V. Avesani, et al. (1998). "A novel toxinotyping scheme and correlation of toxinotypes with serogroups of Clostridium difficile isolates." J Clin Microbiol 36(8): 2240-7.
Rupnik, M., N. Kato, et al. (2003). "New types of toxin A-negative, toxin B-positive strains among Clostridium difficile isolates from Asia." J Clin Microbiol 41(3): 1118-25.
Rupnik, M., S. Pabst, et al. (2005). "Characterization of the cleavage site and function of resulting cleavage fragments after limited proteolysis of Clostridium difficile toxin B (TcdB) by host cells." Microbiology 151(Pt 1): 199-208.
Rupnik, M., A. Widmer, et al. (2008). "Clostridium difficile toxinotype V, ribotype 078, in animals and humans." J Clin Microbiol 46(6): 2146.
Rupnik, M., M. H. Wilcox, et al. (2009). "Clostridium difficile infection: new developments in epidemiology and pathogenesis." Nat Rev Microbiol 7(7): 526-36.

Russell, G. J., C. Nagler-Anderson, et al. (1993). "Cytotoxic potential of intraepithelial lymphocytes (IELs). Presence of TIA-1, the cytolytic granule-associated protein, in human IELs in normal and diseased intestine." Am J Pathol 143(2): 350-4.

Saada, J. I., I. V. Pinchuk, et al. (2006). "Subepithelial myofibroblasts are novel nonprofessional APCs in the human colonic mucosa." J Immunol 177(9): 5968-79.

Salzman, N. H., K. Hung, et al. "Enteric defensins are essential regulators of intestinal microbial ecology." Nat Immunol 11(1): 76-83.

Sambol, S. P., M. M. Merrigan, et al. (2000). "Toxin gene analysis of a variant strain of Clostridium difficile that causes human clinical disease." Infect Immun 68(10): 5480-7.

Sambol, S. P., J. K. Tang, et al. (2001). "Infection of hamsters with epidemiologically important strains of Clostridium difficile." J Infect Dis 183(12): 1760-6.

Sambuy, Y., I. De Angelis, et al. (2005). "The Caco-2 cell line as a model of the intestinal barrier: influence of cell and culture-related factors on Caco-2 cell functional characteristics." Cell Biol Toxicol 21(1): 1-26.

Samra, Z., S. Talmor, et al. (2002). "High prevalence of toxin A-negative toxin B-positive Clostridium difficile in hospitalized patients with gastrointestinal disease." Diagn Microbiol Infect Dis 43(3): 189-92.

Samuel, T., H. O. Weber, et al. (2002). "Linking DNA damage to cell cycle checkpoints." Cell Cycle 1(3): 162-8.

Sanada, I. and S. Nishida (1965). "Isolation of Clostridium Tetani from Soil." J Bacteriol 89: 626-9.

Sauerborn, M., P. Leukel, et al. (1997). "The C-terminal ligand-binding domain of Clostridium difficile toxin A (TcdA) abrogates TcdA-specific binding to cells and prevents mouse lethality." FEMS Microbiol Lett 155(1): 45-54.

Savage, D. C. (1977). "Microbial ecology of the gastrointestinal tract." Annu Rev Microbiol 31: 107-33.

Savidge, T. C., W. H. Pan, et al. (2003). "Clostridium difficile toxin B is an inflammatory enterotoxin in human intestine." Gastroenterology 125(2): 413-20.

Schmidt, A. and A. Hall (2002). "Guanine nucleotide exchange factors for Rho GTPases: turning on the switch." Genes Dev 16(13): 1587-609.

Schmidt, M., U. Rumenapp, et al. (1996). "Inhibition of receptor signaling to phospholipase D by Clostridium difficile toxin B. Role of Rho proteins." J Biol Chem 271(5): 2422-6.

Schroeder, M. S. (2005). "Clostridium difficile--associated diarrhea." Am Fam Physician 71(5): 921-8.

Segner, W. P., C. F. Schmidt, et al. (1971). "Enrichment, isolation, and cultural characteristics of marine strains of Clostridium botulinum type C." Appl Microbiol 22(6): 1017-24.

Seibold, F., B. Seibold-Schmid, et al. (1998). "Regional differences in L-selectin expression in murine intestinal lymphocytes." Gastroenterology 114(5): 965-74.

Sekine, A., M. Fujiwara, et al. (1989). "Asparagine residue in the rho gene product is the modification site for botulinum ADP-ribosyltransferase." J Biol Chem 264(15): 8602-5.

Silen, W. and S. Ito (1985). "Mechanisms for rapid re-epithelialization of the gastric mucosal surface." Annu Rev Physiol 47: 217-29.

Silva, J., Jr., D. H. Batts, et al. (1981). "Treatment of Clostridium difficile colitis and diarrhea with vancomycin." Am J Med 71(5): 815-22.
Simon-Assmann, P., M. Kedinger, et al. (1995). "Extracellular matrix components in intestinal development." Experientia 51(9-10): 883-900.
Smart, C. J., A. Calabrese, et al. (1991). "Expression of the LFA-1 beta 2 integrin (CD11a/CD18) and ICAM-1 (CD54) in normal and coeliac small bowel mucosa." Scand J Immunol 34(3): 299-305.
Smith, J. A., D. L. Cooke, et al. (1997). "Clostridium difficile toxin A binding to human intestinal epithelial cells." J Med Microbiol 46(11): 953-8.
Sneath, P. H. A., N. S. Mair, et al. (1986). Bergey's Manual of Systematics Bacteriology. Baltimore MD, Williams and Wilkins.
Soehn, F., A. Wagenknecht-Wiesner, et al. (1998). "Genetic rearrangements in the pathogenicity locus of Clostridium difficile strain 8864--implications for transcription, expression and enzymatic activity of toxins A and B." Mol Gen Genet 258(3): 222-32.
Soler, P., F. Nogareda, et al. (2008). "Rates of Clostridium difficile infection in patients discharged from Spanish hospitals, 1997-2005." Infect Control Hosp Epidemiol 29(9): 887-9.
Solomon, K., J. Webb, et al. (2005). "Monocytes are highly sensitive to clostridium difficile toxin A-induced apoptotic and nonapoptotic cell death." Infect Immun 73(3): 1625-34.
Sonoda, N., M. Furuse, et al. (1999). "Clostridium perfringens enterotoxin fragment removes specific claudins from tight junction strands: Evidence for direct involvement of claudins in tight junction barrier." J Cell Biol 147(1): 195-204.
Souza, M. H., A. A. Melo-Filho, et al. (1997). "The involvement of macrophage-derived tumour necrosis factor and lipoxygenase products on the neutrophil recruitment induced by Clostridium difficile toxin B." Immunology 91(2): 281-8.
Spencer, J., T. Finn, et al. (1986). "Human Peyer's patches: an immunohistochemical study." Gut 27(4): 405-10.
Sperber, K., L. Silverstein, et al. (1995). "Cytokine secretion induced by superantigens in peripheral blood mononuclear cells, lamina propria lymphocytes, and intraepithelial lymphocytes." Clin Diagn Lab Immunol 2(4): 473-7.
Spyres, L. M., J. Daniel, et al. (2003). "Mutational analysis of the enzymatic domain of Clostridium difficile toxin B reveals novel inhibitors of the wild-type toxin." Infect Immun 71(6): 3294-301.
Spyres, L. M., M. Qa'Dan, et al. (2001). "Cytosolic delivery and characterization of the TcdB glucosylating domain by using a heterologous protein fusion." Infect Immun 69(1): 599-601.
Stabler, R. A., L. F. Dawson, et al. (2008). "Comparative analysis of BI/NAP1/027 hypervirulent strains reveals novel toxin B-encoding gene (tcdB) sequences." J Med Microbiol 57(Pt 6): 771-5.
Stierum, R., M. Gaspari, et al. (2003). "Proteome analysis reveals novel proteins associated with proliferation and differentiation of the colorectal cancer cell line Caco-2." Biochim Biophys Acta 1650(1-2): 73-91.
Stokes, C. R., J. F. Soothill, et al. (1975). "Immune exclusion is a function of IgA." Nature 255(5511): 745-6.

Strong, S. A., T. T. Pizarro, et al. (1998). "Proinflammatory cytokines differentially modulate their own expression in human intestinal mucosal mesenchymal cells." Gastroenterology 114(6): 1244-56.

Stubbe, H., J. Berdoz, et al. (2000). "Polymeric IgA is superior to monomeric IgA and IgG carrying the same variable domain in preventing Clostridium difficile toxin A damaging of T84 monolayers." J Immunol 164(4): 1952-60.

Stubbs, S., M. Rupnik, et al. (2000). "Production of actin-specific ADP-ribosyltransferase (binary toxin) by strains of Clostridium difficile." FEMS Microbiol Lett 186(2): 307-12.

Sullivan, N. M., S. Pellett, et al. (1982). "Purification and characterization of toxins A and B of Clostridium difficile." Infect Immun 35(3): 1032-40.

Svenungsson, B., L. G. Burman, et al. (2003). "Epidemiology and molecular characterization of Clostridium difficile strains from patients with diarrhea: low disease incidence and evidence of limited cross-infection in a Swedish teaching hospital." J Clin Microbiol 41(9): 4031-7.

Synnerstad, I., E. Ekblad, et al. (1998). "Gastric mucosal smooth muscles may explain oscillations in glandular pressure: role of vasoactive intestinal peptide." Gastroenterology 114(2): 284-94.

Takeda, K., T. Kaisho, et al. (2003). "Toll-like receptors." Annu Rev Immunol 21: 335-76.

Tan, K. S., B. Y. Wee, et al. (2001). "Evidence for holin function of tcdE gene in the pathogenicity of Clostridium difficile." J Med Microbiol 50(7): 613-9.

Taylor, N. S. and J. G. Bartlett (1979). "Partial purification and characterization of a cytotoxin from Clostridium difficile." Rev Infect Dis 1(2): 379-85.

Taylor, N. S., G. M. Thorne, et al. (1981). "Comparison of two toxins produced by Clostridium difficile." Infect Immun 34(3): 1036-43.

Teasley, D. G., D. N. Gerding, et al. (1983). "Prospective randomised trial of metronidazole versus vancomycin for Clostridium-difficile-associated diarrhoea and colitis." Lancet 2(8358): 1043-6.

Tedesco, F. J., R. W. Barton, et al. (1974). "Clindamycin-associated colitis. A prospective study." Ann Intern Med 81(4): 429-33.

Thelestam, M. and M. Bronnegard (1980). "Interaction of cytopathogenic toxin from Clostridium difficile with cells in tissue culture." Scand J Infect Dis Suppl(Suppl 22): 16-29.

Tucker, K. D., P. E. Carrig, et al. (1990). "Toxin A of Clostridium difficile is a potent cytotoxin." J Clin Microbiol 28(5): 869-71.

Tucker, K. D. and T. D. Wilkins (1991). "Toxin A of Clostridium difficile binds to the human carbohydrate antigens I, X, and Y." Infect Immun 59(1): 73-8.

von Eichel-Streiber, C., R. Laufenberg-Feldmann, et al. (1990). "Cloning of Clostridium difficile toxin B gene and demonstration of high N-terminal homology between toxin A and B." Med Microbiol Immunol 179(5): 271-9.

von Eichel-Streiber, C., R. Laufenberg-Feldmann, et al. (1992). "Comparative sequence analysis of the Clostridium difficile toxins A and B." Mol Gen Genet 233(1-2): 260-8.

von Eichel-Streiber, C., D. Meyer zu Heringdorf, et al. (1995). "Closing in on the toxic domain through analysis of a variant Clostridium difficile cytotoxin B." Mol Microbiol 17(2): 313-21.
Voth, D. E. and J. D. Ballard (2005). "Clostridium difficile toxins: mechanism of action and role in disease." Clin Microbiol Rev 18(2): 247-63.
Wagenknecht-Wiesner, A., M. Weidmann, et al. (1997). "Delineation of the catalytic domain of Clostridium difficile toxin B-10463 to an enzymatically active N-terminal 467 amino acid fragment." FEMS Microbiol Lett 152(1): 109-16.
Wallace, J. L. and D. N. Granger (1996). "The cellular and molecular basis of gastric mucosal defense." FASEB J 10(7): 731-40.
Ward, S. J., G. Douce, et al. (1999). "Local and systemic neutralizing antibody responses induced by intranasal immunization with the nontoxic binding domain of toxin A from Clostridium difficile." Infect Immun 67(10): 5124-32.
Warnick, T. A., B. A. Methe, et al. (2002). "Clostridium phytofermentans sp. nov., a cellulolytic mesophile from forest soil." Int J Syst Evol Microbiol 52(Pt 4): 1155-60.
Warny, M., J. Pepin, et al. (2005). "Toxin production by an emerging strain of Clostridium difficile associated with outbreaks of severe disease in North America and Europe." Lancet 366(9491): 1079-84.
Watson, J. V., S. H. Chambers, et al. (1987). "A pragmatic approach to the analysis of DNA histograms with a definable G1 peak." Cytometry 8(1): 1-8.
Weber, J. D., W. Hu, et al. (1997). "Ras-stimulated extracellular signal-related kinase 1 and RhoA activities coordinate platelet-derived growth factor-induced G1 progression through the independent regulation of cyclin D1 and p27." J Biol Chem 272(52): 32966-71.
Wedel, N., P. Toselli, et al. (1983). "Ultrastructural effects of Clostridium difficile toxin B on smooth muscle cells and fibroblasts." Exp Cell Res 148(2): 413-22.
Wehkamp, J., N. H. Salzman, et al. (2005). "Reduced Paneth cell alpha-defensins in ileal Crohn's disease." Proc Natl Acad Sci U S A 102(50): 18129-34.
Wei, Y., Y. Zhang, et al. (1997). "Crystal structure of RhoA-GDP and its functional implications." Nat Struct Biol 4(9): 699-703.
Welsh, C. F., K. Roovers, et al. (2001). "Timing of cyclin D1 expression within G1 phase is controlled by Rho." Nat Cell Biol 3(11): 950-7.
Wennerberg, K. and C. J. Der (2004). "Rho-family GTPases: it's not only Rac and Rho (and I like it)." J Cell Sci 117(Pt 8): 1301-12.
Wershil, B. K., I. Castagliuolo, et al. (1998). "Direct evidence of mast cell involvement in Clostridium difficile toxin A-induced enteritis in mice." Gastroenterology 114(5): 956-64.
Wilcox, M. H. and W. N. Fawley (2001). "Virulence of Clostridium difficile toxin A negative strains." J Hosp Infect 48(1): 81.
Willey, S. H. and J. G. Bartlett (1979). "Cultures for Clostridium difficile in stools containing a cytotoxin neutralized by Clostridium sordellii antitoxin." J Clin Microbiol 10(6): 880-4.
Winn, C. W., S. D. Allen, et al. (1997). Koneman's Color Atlas and Textbook of Diagnostic Microbiology, Lippincott Williams and Wilkins.

Wolf, J. L., D. H. Rubin, et al. (1981). "Intestinal M cells: a pathway for entry of reovirus into the host." Science 212(4493): 471-2.
Wren, B. W. (1991). "A family of clostridial and streptococcal ligand-binding proteins with conserved C-terminal repeat sequences." Mol Microbiol 5(4): 797-803.
Wren, B. W., R. R. Russell, et al. (1991). "Antigenic cross-reactivity and functional inhibition by antibodies to Clostridium difficile toxin A, Streptococcus mutans glucan-binding protein, and a synthetic peptide." Infect Immun 59(9): 3151-5.
Yamakawa, K., S. Kamiya, et al. (1994). "Toxin production by Clostridium difficile in a defined medium with limited amino acids." J Med Microbiol 41(5): 319-23.
Yamakawa, K., T. Karasawa, et al. (1996). "Enhancement of Clostridium difficile toxin production in biotin-limited conditions." J Med Microbiol 44(2): 111-4.
Yamamoto, M., K. Fujihashi, et al. (1998). "A mucosal intranet: intestinal epithelial cells down-regulate intraepithelial, but not peripheral, T lymphocytes." J Immunol 160(5): 2188-96.
Yang, C., E. A. Klein, et al. (2008). "Heregulin beta1 promotes breast cancer cell proliferation through Rac/ERK-dependent induction of cyclin D1 and p21Cip1." Biochem J 410(1): 167-75.
Yasuda, S., F. Oceguera-Yanez, et al. (2004). "Cdc42 and mDia3 regulate microtubule attachment to kinetochores." Nature 428(6984): 767-71.
Yearsley, K. A., L. J. Gilby, et al. (2006). "Proton pump inhibitor therapy is a risk factor for Clostridium difficile-associated diarrhoea." Aliment Pharmacol Ther 24(4): 613-9.
Yue, J. and K. M. Mulder (2001). "Transforming growth factor-beta signal transduction in epithelial cells." Pharmacol Ther 91(1): 1-34.
Zerey, M., B. L. Paton, et al. (2007). "The burden of Clostridium difficile in surgical patients in the United States." Surg Infect (Larchmt) 8(6): 557-66.
Zhao, C., I. Wang, et al. (1996). "Widespread expression of beta-defensin hBD-1 in human secretory glands and epithelial cells." FEBS Lett 396(2-3): 319-22.

APPENDIX 1

SOLUTIONS

Vero cell and HT29 cell culture

Dulbecco's Modified Eagle Medium

Supplemented with 10% FCS (Gibco, UK); 100 ng/ml penicillin (Brittania Pharmaceuticals Ltd., Poole, UK); 100 ng/ml streptomycin (Sigma Ltd., Poole, UK); 50 ng/ml gentamycin (Roussel Laboratories, Uxbridge, UK); 200 mM L-glutamine (Sigma Ltd., Poole, UK).

0.25% trypsin

5 mls of 10 x trypsin solution (Gibco, UK), in versine (0.02% EDTA in PBS pH7.2)

Freezing media

5 mls of DMSO (Sigma Ltd., UK) made up to 50 mls with FCS

Caco-2 cell culture

Dulbecco's Modified Eagle Medium

Supplemented with 10% FCS (Gibco, UK); 100 ng/ml penicillin (Brittania Pharmaceuticals Ltd., Poole, UK); 100 ng/ml streptomycin (Sigma Ltd., Poole, UK); 50 ng/ml gentamycin (Roussel Laboratories, Uxbridge, UK); 200 mM L-glutamine (Sigma Ltd., Poole, UK) and 50 µl holotransferrin (Sigma Ltd., Poole, UK).

Trypsin and freezing media as Vero cell.

Myofibroblast isolation and cell culture

Dulbecco's Modified Eagle Medium

Supplemented with 10% FCS (Gibco, UK); 100 ng/ml penicillin (Brittania Pharmaceuticals Ltd., Poole, UK); 100 ng/ml streptomycin (Sigma Ltd., Poole, UK); 50 ng/ml gentamycin (Roussel Laboratories,

Uxbridge, UK); 200 mM L-glutamine (Sigma Ltd., Poole, UK) and 1% non-essential amino acids (Sigma Ltd., Poole, UK).

0.1% trypsin

2 mls of 10 x trypsin solution (Gibco, UK), in versine (0.02% EDTA in PBS pH7.2)

Freezing media as above

Roswell Park Memorial Institute (RPMI 1640)

Supplemented with 10% FCS (Gibco, UK); 100 ng/ml penicillin; 100 µg/ml streptomycin; 50 µg/ml gentamycin (all from Sigma Ltd., Poole, UK).

Hanks Balanced Salt Solution (HBSS) w/o Ca2+ and Mg2+ (x1)

110 ml 10x HBSS w/o Ca2+ and Mg2+ (Sigma Ltd., Poole, UK) to 1 L sterile distilled water. Adjust to pH 7-8 with 1 M sterile NaOH. Add 5 ml Penicillin/Streptomycin (100 µg/ml) and 2.5 ml Gentamycin (50 µg/ml) (Sigma Ltd., Poole, UK)

DTT/HBSS solution (10 mM DTT)

0.077 g Dithiotreitol (DTT) powder (Sigma Ltd., Poole, UK) in 50 ml 1 x HBSS solution. Filter and store at 4°C.

DTT/HBSS solution (1 mM DTT)

5 ml 10 mM DTT solution in 45 ml 1 x HBSS solution. Mix and store at room temperature.

EDTA (100 mM)

1.86 g Ethylenediaminetetracetic acid (EDTA) (Sigma Ltd., Poole, UK) in 50 ml sterile distilled water. Filter and store at 4°C.

EDTA/HBSS solution (10 mM EDTA)

5 ml 100 mM EDTA solution in 45 ml 1 x HBSS solution. Adjust to pH 7-8 with sterile NaOH. Store at 4°C.

EDTA/HBSS solution (1 mM EDTA)

5 ml 10 mM EDTA solution in 45 ml 1 x HBSS solution.

Purification of *C. difficile* toxins

BHI broth (500 mls)

18.5 g BHI powder (Oxoid, UK); 2.5 g Yeast extract (Oxoid, UK); 0.25 g Cysteine hydrochloride (Sigma Ltd., Poole, UK); 0.15 g Sodium formaldehyde sulphoxylate (Fisher Chemicals, UK); 500 mls distilled water.

Solutions for Thyroglobulin column

Acidic buffer (0.1 M glycine, 0.5 M NaCl pH 2.0)

3.75 g glycine (BDH, UK); 14.61 g NaCl (Sigma Ltd., Poole, UK) in 500 mls distilled water, adjusted to pH 2.0 with 1 M HCl. Degas with helium

Basic buffer (0.1 M glycine, 0.5 M NaCl pH 10.0)

3.75 g glycine (BDH, UK); 14.61 g NaCl (Sigma Ltd., Poole, UK) in 500 mls distilled water, adjusted to pH 10.0 with 1 M NaOH. Degas with helium

Tris Buffered Saline (0.15 M NaCl, 0.05 M Tris pH 7.0)

4.38 g NaCl (Sigma Ltd., Poole, UK); 3.0275 Trizma base (Sigma., Poole, UK) in 500 mls distilled water adjusted to pH 7 with 1 M HCl. Degas with helium

Storage solution

0.02 % sodium azide (Sigma Ltd., Poole, UK) in Tris Buffered Saline (as above, 10-20 mls)

Toxin A purification DEAE-FF Sepharose and Mono-Q column solutions

Buffer A (20 mM Tris, pH 7.5)

1.211 g Trizma base (Sigma Ltd., Poole, UK) in 500 mls distilled water, adjusted to pH 7.5 with 1 M HCl. Filter and degas with helium.

Buffer B (20 mM Tris, 1 M NaCl, pH 7.5)

1.211 g Trizma base (Sigma Ltd., Poole, UK); 29.22 g NaCl (Sigma Ltd., Poole, UK) in 500 mls distilled water, adjusted to pH 7.5 with 1 M HCl. Filter and degas with helium.

Dialysis Buffer (20 mM Tris, pH 7)

12.11 g Trizma base (Sigma Ltd., Poole, UK) in 5 L distilled water adjusted to pH 7 with 1 M HCl

Toxin B purification DEAE-FF Sepharose and Mono-Q column solutions

Tris solution for resuspension and dialysis (50 mM Tris, pH 7.4)

6.055 g Trizma base (Sigma Ltd., Poole, UK) per litre of distilled water, adjusted to pH 7.4 using 1 M HCl

Buffer A (50 mM Tris, pH 7.5)

3.0275 g Trizma base (Sigma Ltd., Poole, UK) in 500 mls distilled water, adjusted to pH 7.5 with 1 M HCl. Filter and degas with helium.

Buffer B (50 mM Tris, pH 7.5)

3.0275 g Trizma base (Sigma Ltd., Poole, UK); 29.22 g NaCl (Sigma Ltd., Poole, UK) in 500 mls distilled water, adjusted to pH 7.5 with 1 M HCl. Filter and degas with helium.

Cell viability and cytoxicity assay solutions

MTT (3-(4,5 dimethylthiazol-2,5-diphenyltetrazolium bromide)

Stock solution - dissolve MTT in PBS w/o Ca^{2+} and Mg^{2+} (Sigma Ltd., Poole, UK) to 5 mg/ml. Filter and store at 4°C.

Acid SDS (5% in 0.01 M HCl)

Dissolve 5 g sodium dodecylsulphate (SDS) in 100 ml 0.01 M HCl.

Propidium Iodide staining of DNA – solutions

PBA (Phosphate Buffered Saline with 0.1% Bovine Serum Albumin and sodium azide)

Dissolve 0.1 g Bovine Serum Albumin (Sigma Ltd., Poole, UK) and 0.1 g sodium azide in PBS w/o Ca^{2+} and Mg^{2+} (Sigma Ltd., Poole, UK). Store at 4°C.

Dot Blot solutions

Wash Buffer (100 mM Tris; 150 mM NaCl; 0.1% tween-20 pH 7.5)

6.05 g Trizma base, 4.38 g NaCl and 500 µl tween-20 (all from Sigma Ltd., Poole, UK) in 500 ml distilled water. Adjust to pH 7.5 using 1 M HCl

Blocking Buffer (100 mM Tris; 150 mM NaCl; 0.1% tween-20, 5% skimmed milk powder pH 7.5)

1 g skimmed milk powder (Sigma Ltd., Poole, UK) in 20 ml wash buffer.

Native PAGE solutions

Resolving Buffer 4x (1.5 M Tris, pH 8.8)

91 g Trizma base (Sigma Ltd., Poole, UK) in 500 ml distilled water. Adjust to pH 8.8 using 1 M HCl.

Running Buffer 5x (125 mM Tris, 0.96 M glycine)

7.55 g Trizma base and 36 g glycine (both from Sigma Ltd., Poole, UK) in 500 ml distilled water. Dilute to 1x with distilled water.

Native PAGE Gel

3.35 ml 30% acrylamide/bis acrylamide
5.0 ml 4 x Tris resolving buffer
11.54 ml distilled water
200 µl 10% (w/v) ammonium persulphate
20 µl TEMED

SDS PAGE Gel solution

Resolver 4x Tris-Cl/SDS pH 8.8 (1.5 M Tris with 0.4 % SDS)

91 g Trizma base (Sigma Ltd, Poole, UK) dissolved in 500 ml distilled water adjust to pH 8.8 with 1 M HCl; add 20 ml 10% SDS solution. Store at 4°C

Stacking Buffer 4x Tris-Cl/SDS pH 6.8 (0.5 M Tris with 0.4 % SDS)

6.05 g Trizma base (Sigma Ltd, Poole, UK) dissolved in 100 ml distilled water adjust to pH 6.8 with 1 M HCl; add 4 ml 10 % SDS solution. Store at 4 °C.

Running Buffer 5x Tris-Cl/Glycine/SDS (0.1 M Tris, 0.96 M Glycine with 0.5 % SDS)

15.1 g Trizma base and 72 g Glycine (both from Sigma Ltd, Poole, UK) dissolved in 1 L distilled water. 50 ml 10 % SDS. Store at 4 °C.

7.5 % acrylamide SDS resolving gel (resolving range 36-94 kDa)

3.75 ml 30% acrylamide/bis acrylamide (Sigma Ltd, Poole, UK), 3.75 ml 4x Tris-Cl/SDS (pH 8.8), 7.50 ml distilled water, 50 µl 10 % (w/v) ammonium persulfate and 10 µl TEMED (Sigma Ltd, Poole, UK).

10 % acrylamide SDS resolving gel (resolving range 16-68 kDa)

5.00 ml 30% acrylamide/bis acrylamide (Sigma Ltd, Poole, UK), 3.75 ml 4x Tris-Cl/SDS (pH 8.8), 6.25 ml distilled water, 50 µl 10 % (w/v) ammonium persulfate and 10 µl TEMED (Sigma Ltd, Poole, UK).

Stacking gel

0.65 ml 30% acrylamide/bis acrylamide (Sigma Ltd, Poole, UK), 1.25 ml 4x Tris-Cl/SDS (pH 6.8), 3.05 ml distilled water, 25 µl 10 % (w/v) ammonium persulfate and 5 µl TEMED (Sigma Ltd, Poole, UK).

Western Blot

Transfer Buffer (48 mM Tris; 39 mM Glycine)

Dissolve 3.1 g Trizma base and 14.4 g Glycine in 500 ml distilled water. Add 200 ml methanol and adjust volume to 1 L using distilled water

APPENDIX 2

INFECTION AND IMMUNITY, Apr. 2011, p. 1623–1630 Vol. 79, No. 4
0019-9567/11/$12.00 doi:10.1128/IAI.00686-10

Primary Human Colonic Myofibroblasts Are Resistant to *Clostridium difficile* Toxin A-Induced, but Not Toxin B-Induced, Cell Death[▽]

N. Mullan, K. R. Hughes, and Y. R. Mahida*

Institute of Infection, Immunity and Inflammation, University of Nottingham, Nottingham, United Kingdom

Received 25 June 2010/Returned for modification 21 July 2010/Accepted 29 December 2010

Colonic inflammation in *Clostridium difficile* infection is mediated by released toxins A and B. We investigated responses to *C. difficile* toxins A and B by isolated primary human colonic myofibroblasts, which represent a distinct subpopulation of mucosal cells that are normally located below the intestinal epithelium. Following incubation with either purified toxin A or B, there was a change in myofibroblast morphology to stellate cells with processes that were immunoreactive for alpha-smooth muscle actin. Most of the myofibroblasts remained viable, with persistence of stellate morphology, despite exposure to high concentrations (up to 10 μg/ml) of toxin A for 72 h. In contrast, a majority of the toxin B-exposed myofibroblasts lost their processes prior to cell death over 24 to 72 h. At low concentrations, toxin A provided protection against toxin B-induced cell death. Within 4 h, myofibroblasts exposed to either toxin A or toxin B lost expression of the nonglucosylated form of Rac1, and there was also a loss of the active form of RhoA. Despite preexposure to high concentrations of toxin A for 3 h, colonic myofibroblasts were able to recover their morphology and proliferative capacity during prolonged culture in medium. However, toxin B-preexposed myofibroblasts were not able to recover. In conclusion, primary human colonic mucosal myofibroblasts are resistant to toxin A (but not toxin B)-induced cell death. Responses by colonic myofibroblasts may play an important role in mucosal protection, repair, and regeneration in colitis due to *C. difficile* infection.

Clostridium difficile induces colonic inflammation via two released toxins, A and B, and histologically, the colonic disease is often characterized by focal areas of epithelial ulceration and inflammatory exudates (38, 46). The first host cells that the toxins interact with in the colon are likely to be surface epithelial cells, which normally provide an essential barrier against luminal microorganisms and their products. In intact monolayers of carcinoma-derived intestinal epithelial cell lines *in vitro*, apically applied toxin A induces injury and loss of barrier function (43, 45). Other early responses by intestinal epithelial cells exposed to toxin A include changes in the cytoskeleton (10, 15) and secretion of cytokines, such as transforming growth factor beta (TGF-β) (20) and interleukin-8 (5, 13, 26), before the cells undergo programmed cell death (6, 26). Our previous studies have shown that primary human intestinal epithelial cells, monocytes, and intestinal macrophages are more sensitive than lymphocytes to *C. difficile* toxin A-induced cell death (25, 26, 42).

In the intestinal mucosa, myofibroblasts represent a distinct subpopulation of cells that are located below the intestinal epithelium, separated by a porous basement membrane (37). Intestinal myofibroblasts have morphological and other features of smooth muscle cells and fibroblasts, as illustrated by strong expression of alpha-smooth muscle actin (a characteristic of smooth muscle cells) and vimentin (also expressed by fibroblasts). In addition to controlling the deposition of extracellular matrix (24, 29), intestinal myofibroblasts may regulate epithelial functions, such as electrolyte transport (3), restitution (28), and barrier function (3), and also functions of stem cells (18). In view of their capacity to secrete a number of cytokines and to interact with other cell populations (36), intestinal myofibroblasts are also believed to be key players in inflammatory responses in the intestine (1, 9, 12, 22). They have been shown to provide protection to intestinal epithelial monolayers against loss of barrier function in response to low concentrations of toxin A, via secretion of TGF-β (20). Following injury and loss of toxin-exposed epithelial cells *in vivo*, myofibroblasts, which are capable of migrating onto the surface of the basement membrane (24), would be expected to be exposed to *C. difficile* toxins. However, responses of primary human intestinal myofibroblasts to *C. difficile* toxins remain to be characterized.

A majority of the biological effects of *C. difficile* toxins A and B are believed to be mediated via the ability of their N termini to glucosylate and inactivate Rho GTPases such as RhoA, -B, and C, Rac1-3, RhoG, and Cdc42 (2, 19). Rho GTPases are key regulators of the actin cytoskeleton and influence many cellular processes, such as cell polarity, migration, vesicle trafficking, and cytokinesis (7, 14).

The aims of our studies were to characterize responses of primary human colonic myofibroblasts (isolated from healthy large intestinal mucosal samples) to purified *C. difficile* toxins A and B.

MATERIALS AND METHODS

Purification of toxins A and B. Toxin A was purified as previously described (21). *C. difficile* VPI strain 10463 was cultured anaerobically in brain heart infusion broth (Oxoid, United Kingdom) in dialysis culture flasks. After centrifugation, supernatant samples were loaded onto a bovine thyroglobulin affinity column, and eluted toxin A-containing fractions were then applied to Q Sepharose FF and Mono Q columns (GE Healthcare, Sweden). During the purification

* Corresponding author. Mailing address: Institute of Infection, Immunity and Inflammation, Queen's Medical Centre, Nottingham NG7 2UH, United Kingdom. Phone: 44-115-8231198. Fax: 44-115-8231102. E-mail: yash.mahida@nottingham.ac.uk.

[▽] Published ahead of print on 18 January 2011.

steps, toxin A-containing fractions were identified by dot blot analysis using the anti-toxin A antibody PCG-4 (23).

The purification protocol for toxin B was adapted from previous studies (30, 35, 44). A broth culture of *C. difficile* VPI strain 10463 was centrifuged to remove bacteria from the toxin-containing supernatant. The latter was made 70% saturated by the addition of solid ammonium sulfate. After 1 h, the precipitate was collected by centrifugation and resuspended in 50 mM Tris-HCl buffer (pH 7.4). The process of ammonium sulfate precipitation was repeated to make the solution 50% saturated. Following centrifugation, the pellet was resuspended in 50 mM Tris-HCl buffer (pH 7.4) and then dialyzed for 24 h in 50 mM Tris-HCl buffer (pH 7.4). The dialyzed sample was applied to a DEAE-Sepharose column (GE Healthcare, Sweden) and eluted initially with a linear NaCl gradient in 50 mM Tris-HCl buffer (0.05 to 0.25 M NaCl), followed by 150 ml of 50 mM Tris-HCl buffer (pH 7.4) containing 0.3 M NaCl. Subsequent elution was with a second linear gradient of NaCl (0.3 to 1 M) in 50 mM Tris-HCl buffer (pH 7.4). Toxin B-containing fractions were identified by dot blot analysis using anti-toxin B antibody (Biodesign International), and pooled fractions were dialyzed for 24 h against 10 mM Tris-HCl buffer (pH 8.0) containing 50 mM $CaCl_2$ before application to a Mono Q anion-exchange column (GE Healthcare, Sweden). Purified toxin B was eluted from the Mono Q column by use of a linear NaCl gradient (0 to 1 M) in 10 mM Tris-HCl buffer (pH 8.0) containing 50 mM $CaCl_2$.

Isolation and culture of human colonic myofibroblasts. Fresh, histologically normal colonic mucosal samples (>5 cm from cancer, with tissue surplus to clinical requirements) were obtained (after informed consent) from operation resection specimens. The median age of tissue donors was 69 years (range, 47 to 87 yrs; 6 females and 12 males). Ethical committee approval was provided by the Nottingham Research Ethics Committee (REC Q1020310).

Intestinal myofibroblasts were isolated and established in pure culture as previously described (24). In brief, surface epithelial cells were detached from mucosal samples by three sequential treatments with 1 mmol EDTA, and the tissue samples, denuded of epithelial cells, were cultured (at 37°C and 5% CO_2) in 10% fetal calf serum (FCS)-RPMI (Gibco-Invitrogen, United Kingdom). During culture of mucosal samples devoid of epithelial cells, myofibroblasts migrate out of the subepithelial regions of the lamina propria via basement membrane pores to establish colonies in tissue culture dishes (24). After removal of the tissue samples, the myofibroblasts proliferate to establish monolayers that can be maintained over many passages. Our previous studies have shown that the isolated intestinal myofibroblasts retain their phenotype and functional characteristics over many passages (18, 24, 27).

Isolated colonic myofibroblasts, which expressed alpha-smooth muscle actin and vimentin (but not desmin), were studied at passages 3 to 7 and were maintained in culture in Dulbecco's modified Eagle's medium (Sigma) supplemented with 10% FCS and 1% nonessential amino acids (Gibco-Invitrogen, United Kingdom). Monolayers of the cells were exposed to various concentrations (0 to 10 μg/ml) of purified *C. difficile* toxin A or B for various intervals (3 h to 72 h). In some experiments, morphological recovery of myofibroblasts was studied after preexposure to toxin A or B (at a concentration of 1 μg/ml or 10 μg/ml) for 3 h to 48 h.

Morphological changes to the cells were studied by phase-contrast microscopy (changes assessed in 10 random high-power fields) and scanning electron microscopy. The nuclear morphologies of control and toxin-exposed myofibroblasts were studied by fluorescence microscopy after staining with Hoechst 33342 dye (42). Immunohistochemical studies were undertaken using monoclonal antibodies to alpha-smooth muscle actin, desmin, and vimentin (all from Sigma). Effects on cell viability were investigated using an assay for mitochondrial dehydrogenase activity. Changes to myofibroblast DNA were studied by flow cytometry following propidium iodide staining.

Immunohistochemistry. Control and toxin-exposed myofibroblasts cultured on glass coverslips were fixed in acetone, and immunohistochemical studies were undertaken using a Vectastain ABC peroxidase kit as previously described (24). In brief, the cells were incubated with antibodies to alpha-smooth muscle actin, desmin, and vimentin (all from Sigma) for 30 min, and after being washed, the myofibroblasts were exposed to biotinylated horse anti-mouse antibody, followed by avidin-biotinylated horseradish peroxidase complex. Peroxidase activity was developed with diaminobenzidine, followed by nuclear staining using hematoxylin. Controls included use of buffer instead of primary antibody and an irrelevant primary antibody (anti-cytokeratin).

Assay for mitochondrial dehydrogenase. Metabolism by mitochondrial dehydrogenase of the yellow tetrazolium salt 3-(4,5-dimethylthiazol-2-yl)-2,5-diphenyl tetrazolium bromide (MTT) to the purple formazan reaction product can be quantified spectrophotometrically and can be used as an assay for cell proliferation or cell death (33). MTT assays were undertaken as previously described (26). In brief, cells (40×10^3 applied per well) were grown to confluence in 96-well tissue culture plates (Nunc), and the assays were performed in triplicate. After exposure of cells to toxin A or B (or control medium) for various periods, MTT (Sigma Chemical, St. Louis, MO) was added to each well (to a final concentration of 0.5 mg/ml), and incubation was continued for 4 h. The cells were then incubated overnight in solubilization solution (50% sodium dodecyl sulfate in 0.1 mmol/liter HCl). The spectrophotometric absorbance of the samples was subsequently measured with a microtiter enzyme-linked immunosorbent assay (ELISA) plate reader using a 570-nm filter.

Propidium iodide staining and flow cytometry. Propidium iodide staining was performed as previously described (25, 34). Control and toxin-exposed myofibroblasts were detached using 0.1% (wt/vol) trypsin-0.2% (wt/vol) EDTA. Following centrifugation (400 × *g* for 10 min), the myofibroblasts were fixed and permeabilized with ice-cold 70% ethanol for 60 min. After being washed with phosphate-buffered saline (PBS), the cells were incubated with propidium iodide (100 μg/ml; Sigma) at room temperature in the dark for 15 min. Fluorescence emission of propidium iodide was analyzed with a Beckman Coulter Altra flow cytometer (Beckman Coulter) at 617 nm after excitation with a blue laser at 488 nm. Events that fell within the marked hypodiploid region (apoptotic events) were enumerated by the statistics function of WinMDI V2.8 software, and the results are expressed as percentages of total events.

Western blot analysis. Lysates of control and toxin A- or toxin B-exposed myofibroblasts were separated by SDS-polyacrylamide gel electrophoresis on a 12.5% acrylamide resolving gel (using Bio-Rad Protean II slab gel electrophoresis equipment). After transfer to polyvinylidene difluoride membranes, immunostaining was performed using a Vectastain Elite ABC kit (Vector Laboratories) and antibodies to beta-actin (Abcam Plc, United Kingdom), the nonglucosylated form of Rac1 (11) (clone 102; BD Transduction Laboratories), and RhoA (clone 26C4; Santa Cruz Biotechnology Inc.) (RhoA detection was not affected by glucosylation).

Assessment of changes in RhoA. Changes in levels of the active, GTP-bound form of RhoA in myofibroblasts were studied using an ELISA-based Rho activation assay (RhoA G-LISA activation assay; Cytoskeleton Inc.). Lysates (in buffer containing protease inhibitor) were obtained from monolayers of isolated colonic myofibroblasts that had been exposed for 4 h to control medium (Dulbecco's modified Eagle's medium supplemented with 10% FCS and 1% nonessential amino acids), 1 μg/ml toxin A, or 1 μg/ml toxin B. The lysates were applied to wells coated with Rho-GTP-binding protein. In this assay, active, GTP-bound RhoA in cell lysates binds to the wells, while inactive, GDP-bound Rho is removed during washing steps. The bound active RhoA was detected using a RhoA-specific antibody, followed by a secondary antibody conjugated to horseradish peroxidase. The spectrophotometric absorbance was subsequently measured using a 490-nm filter.

Statistical analysis. Data are expressed as means with standard errors of the means (SEM) and were analyzed by one-way analysis of variance and an unpaired *t* test.

RESULTS

Morphological changes in myofibroblasts exposed to *C. difficile* toxins. Morphological responses to different concentrations (0.1, 1, and 10 μg/ml) of purified toxins A and B were studied by phase-contrast microscopy. Monolayers of isolated intestinal myofibroblasts maintained in control medium spread to occupy a large surface area. In the presence of the highest concentration (10 μg/ml) of either toxin, approximately 50% of cells were rounded (with visible processes) at 2 h, and all cells were rounded at 4 h. When cells were exposed to lower concentrations of the toxins (1 and 0.1 μg/ml), myofibroblast cell rounding occurred a few hours later in toxin A-exposed cells than in those cultured with toxin B.

Myofibroblasts exposed to toxin A changed in morphology from flat cells to those with a stellate appearance. Over 72 h, the cell cytoplasm around the nucleus appeared to decrease further in size, with maintenance of prominent processes. Morphological changes in toxin B-exposed myofibroblasts were initially similar to those in toxin A-exposed cells, but at later time points (48 to 72 h), a majority of the myofibroblasts lost their processes and many appeared nonviable (Fig. 1E and J).

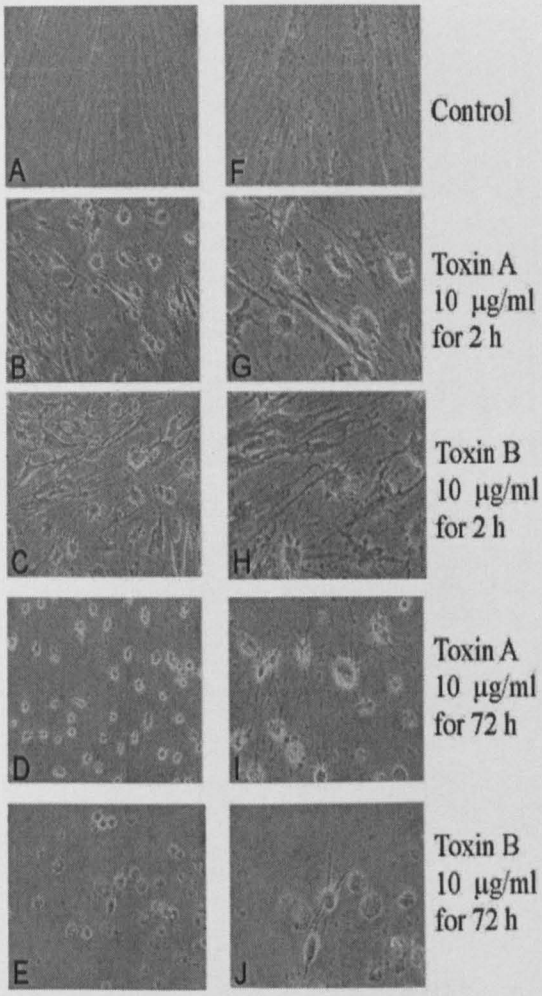

FIG. 1. Images (phase-contrast microscopy) of control and *C. difficile* toxin-exposed myofibroblasts. Monolayers of isolated normal human colonic myofibroblasts were cultured in medium only (A and F) or in the presence of 10 μg/ml toxin A (B, D, G, and I) or toxin B (C, H, E, and J) for 2 h (B, C, G, and H) or 72 h (D, E, I, and J). Low (A to E)- and high (F to J)-power images (similar magnifications were used for panels A to E and for panels F to J) are shown. For cells cultured in medium only (A and F), confluent monolayers of "flat" cells are seen, whereas those exposed to toxin A for 2 h (B and G) or to toxin B for 2 h (C and H) appear stellate, with numerous processes. Myofibroblasts exposed to toxin A for 72 h (D and I) contracted further than those exposed to toxin A for 2 h (B and G). Cells cultured with toxin B for 2 h (C and H) appear morphologically similar to those exposed to toxin A for the same period (B and G). In contrast to myofibroblasts exposed to toxin A for 72 h (D and I), most cells (except two) cultured with toxin B for the same period (E and J) have lost their processes, and many appear nonviable.

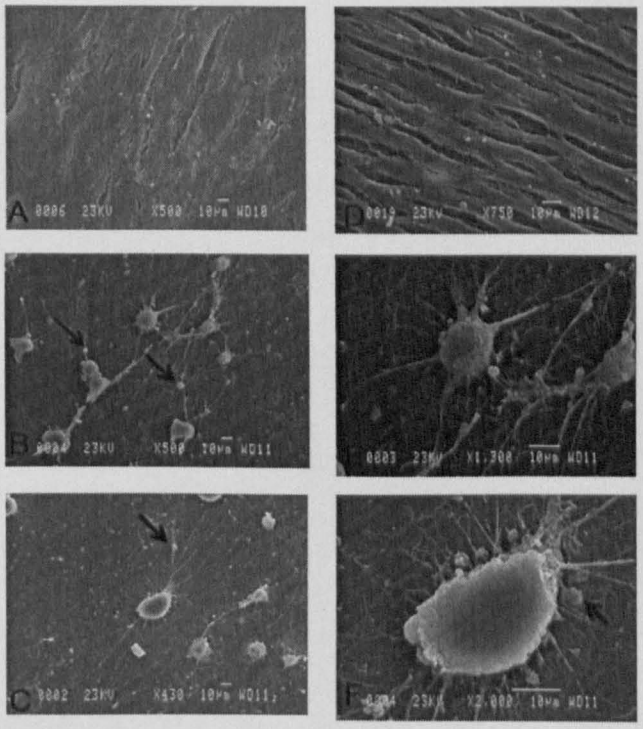

FIG. 2. Scanning electron micrographs of control and *C. difficile* toxin-exposed myofibroblasts. Monolayers of isolated normal human colonic myofibroblasts were cultured in medium only (A and D) or in the presence of 1 μg/ml toxin A (B and E) or toxin B (C and F) for 24 h. Myofibroblasts cultured in medium only (A and D) are seen as confluent monolayers of "flat" cells, whereas those exposed to toxin A (B and E) or toxin B (C and F) appear stellate, with numerous processes. In myofibroblasts exposed to either toxin, distinct globular structures (arrows) are present either close to the cell body or at a distance and are associated with a process. Bars, 10 μm.

However, some toxin B-exposed myofibroblasts remained viable at 72 h, with persistence of processes (Fig. 1J).

Scanning electron microscopy of myofibroblasts exposed to toxin A or toxin B (1 μg/ml) for 24 h showed that in addition to numerous processes of various thicknesses, distinct globular structures were seen either close to the cell body or at a distance and were associated with processes (Fig. 2).

Immunohistochemical studies (at 6 h in response to 1 μg/ml toxin A) showed that the processes in both toxin A- and toxin B-exposed myofibroblasts were strongly immunoreactive for alpha-smooth muscle actin (Fig. 3). At 48 h and 72 h, and as observed by phase-contrast microscopy (see above), a majority of the myofibroblasts exposed to toxin B (1 μg/ml) had lost processes (Fig. 3), but in toxin A-exposed (1 μg/ml toxin) cells, there was persistence of processes that were immunoreactive for alpha-smooth muscle actin. At 72 h, many toxin B-exposed cells appeared to have lost the integrity of their cell membranes, but this did not occur in toxin A-exposed cells.

Recovery following exposure to toxin A. In studies undertaken using myofibroblasts isolated from 8 different donors (cells from 3 to 5 donors were used for each experimental condition), morphological recovery of the cells was studied by phase-contrast microscopy after preexposure to toxin A for 3 h, 24 h, or 48 h. Following 3 h of preexposure to toxin A (cells were incubated with 1 and 10 μg/ml toxin A for 3 h, followed by washing and culture in medium only), the colonic myofibroblasts returned to their normal morphology over 28 to 63 days, with the monolayers becoming fully confluent. Following trypsinization and reculture (passage at a 1:3 split ratio), the 3-h toxin A-preexposed myofibroblasts proliferated to confluence. Following preexposure to 1 μg/ml toxin A for 24 h or 48 h, myofibroblast recovery was slower, but all the cells

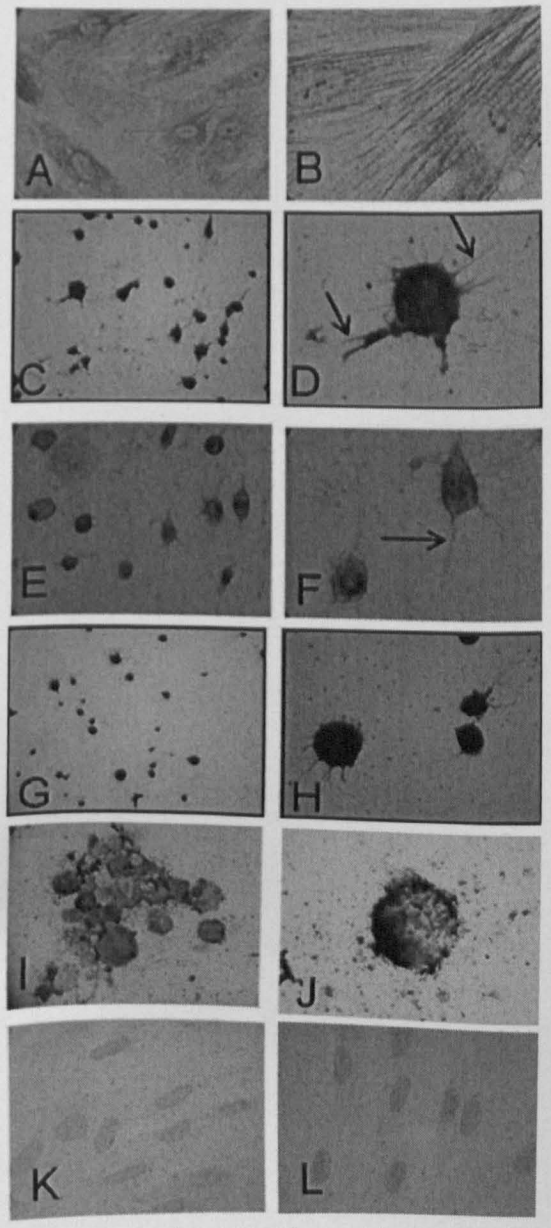

FIG. 3. Alpha-smooth muscle actin expression by control and *C. difficile* toxin-exposed myofibroblasts. Immunocytochemical studies were undertaken with monolayers of isolated normal human colonic myofibroblasts that had been cultured in medium only (A, B, K, and L) or in the presence of 1 μg/ml toxin A for 6 h (C and D) or 72 h (G and H). Myofibroblasts exposed to toxin B (1 μg/ml) for 6 h (E and F) and 72 h (I and J) are also shown. Low-power (A, C, E, G, I, K, and L) and high-power (B, D, F, H, and J) images are shown. Longitudinally arranged, alpha-smooth muscle actin-immunoreactive bundles of microfilament are seen in myofibroblasts cultured in control medium (A and B). In myofibroblasts exposed to *C. difficile* toxin A for 6 h (C and D) or 72 h (G and H) or to toxin B for 6 h (E and F), the cell cytoplasm surrounding the nucleus and the cell processes (arrows) are immunoreactive for alpha-smooth muscle actin. In contrast, cells exposed to toxin B for 72 h (I and J) have lost their processes and show only weak alpha-smooth muscle actin immunoreactivity, and many appear nonviable. Myofibroblasts cultured in medium only were also used as an immunocytochemistry control (K; buffer was used instead of primary antibody) and to show a lack of desmin immunoreactivity (L).

showed normal morphology after culture in medium for 28 days.

In contrast to the case with toxin A, none of the myofibroblast monolayers preexposed (for 3 h, 24 h, or 48 h) to toxin B (at 1 μg/ml) showed any signs of recovery. Thus, after culture in medium for 28 days, no viable myofibroblasts were seen in toxin B-preexposed monolayers.

MTT assays of myofibroblasts exposed to *C. difficile* toxins. MTT assays were undertaken to assess changes in myofibroblast viability in response to toxin A or B. In order to assess the ability of the assay to detect maximal loss of cell viability, monolayers of primary colonic myofibroblasts were cultured in medium for 24 h, in the absence or presence of 0.1% Triton X-100. Compared to the control, there was an 81.3% reduction in the mean absorbance value for the formazan reaction products of myofibroblasts exposed to Triton X-100 (0.353 [0.017] versus 0.066 [0.004]; $P < 0.0001$).

In studies conducted for up to 72 h, mitochondrial dehydrogenase activities of myofibroblasts exposed to 0.1, 1, and 10 μg/ml toxin A did not differ from those of cells cultured in control medium (Fig. 4a). In contrast, myofibroblasts exposed to toxin B (especially those exposed to 1 and 10 μg/ml of the toxin) showed a significant loss of mitochondrial enzyme activity (Fig. 4b). Moreover, the mean (SEM) absorbance values of the formazan reaction products of myofibroblasts exposed to 1 μg/ml and 10 μg/ml toxin B at 24 h (0.391 [0.028] and 0.405 [0.024], respectively), 48 h (0.323 [0.013] and 0.371 [0.021], respectively), and 72 h (0.204 [0.012] and 0.221 [0.007], respectively) were largely similar. This suggests that while the majority of myofibroblasts are susceptible to toxin B (at concentrations of ≥1 μg/ml), a proportion remain viable despite exposure to the highest concentration (10 μg/ml) of toxin B for up to 72 h.

In the presence of toxin A at a concentration of 0.1 μg/ml, myofibroblasts were protected against the effects of toxin B applied at the same concentration (absorbance value for myofibroblasts [expressed as % of value for control cells] after exposure to toxin B only for 72 h, 75.76% [5.83%]; that for cells after exposure to both toxins A and B for 72 h, 101.10% [6.17%]; $P < 0.01$ [$n = 3$]). When toxin B was present at a concentration of 1 μg/ml, absorbance values of myofibroblasts exposed to toxin B alone (for 72 h) were not significantly different from those of cells incubated with both toxins A and B (57.31% [2.33%] versus 66.25% [4.58%]).

DNA fluorescence profiles of myofibroblasts exposed to *C. difficile* toxins. Events in the hypodiploid region of cellular DNA profiles reflect DNA fragmentation due to apoptotic cell death (25, 34). In myofibroblasts (isolated from 3 donors) exposed to 1 μg/ml toxin B, there was a time-dependent increase in the proportion of events in the hypodiploid region (control versus toxin B-exposed cells at 8 h, 1.13% [0.14%] versus 1.29% [0.06%]; at 24 h, 1.44% [0.041%] versus 2.30% [0.24%] [$P < 0.03$]; at 48 h, 1.17% [0.21%] versus 13.38% [3.81%] [$P < 0.04$]; and at 72 h, 0.80% [0.019%] versus 35.15% [1.31%] [$P < 0.0001$]) (Fig. 5a). In contrast, myofibroblasts exposed to 1 μg/ml toxin A showed only small (but statistically significant) increases in hypodiploid events at 48 h (for control versus toxin A-exposed cells, 0.58% [0.16%] versus 2.14% [0.29%]; $P < 0.01$) and 72 h (for control versus toxin A-exposed cells, 0.81% [0.029%] versus 4.22% [0.94%] $P < 0.03$)

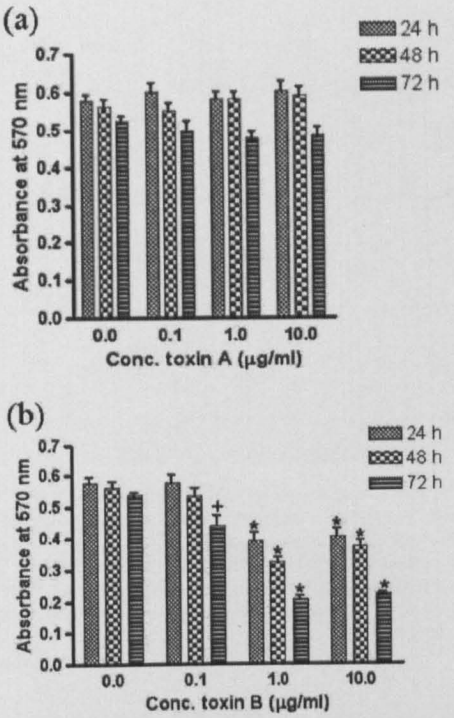

FIG. 4. Mitochondrial dehydrogenase activities of control and *C. difficile* toxin-exposed myofibroblasts. MTT assays were undertaken with monolayers of isolated normal human colonic myofibroblasts that had been cultured in medium only (0 μg/ml toxin) or in the presence of various concentrations (0.1 to 10 μg/ml) of toxin A (a) or toxin B (b) for various intervals (24 to 72 h). Bars in figures represent mean (SEM) absorbance values for 4 different cultures of myofibroblasts (isolated from colonic mucosal cells obtained from 4 donors) in experiments undertaken in triplicate. (a) Responses to toxin A. For each period of culture, there were no significant differences between myofibroblasts incubated with control medium (0 μg/ml toxin A) and those exposed to the three different concentrations of toxin A. (b) Responses to toxin B. Compared to myofibroblasts cultured in control medium (0 μg/ml) for the relevant periods, there were significant reductions in mitochondrial dehydrogenase activity in cells exposed to 0.1 μg/ml toxin B for 72 h and to 1 and 10 μg/ml toxin B for 24 h, 48 h, and 72 h. +, $P < 0.02$; *, $P < 0.0001$.

(Fig. 5b). DNA fluorescence profiles of myofibroblasts exposed to 10 μg/ml toxin A showed that the majority of the cells showed normal DNA profiles (Fig. 5c) that would be expected for viable cells.

Hoechst-stained cells. In myofibroblast monolayers exposed to toxin B, Hoechst staining confirmed significant levels of apoptosis, as demonstrated by nuclear condensation (due to dense chromatin) and nuclear fragmentation (Fig. 6).

Rac1 and RhoA expression in myofibroblasts exposed to *C. difficile* toxins. Western blot analysis using a specific antibody (11) showed loss of the nonglucosylated form of Rac1 from 4 h onwards in myofibroblasts cultured with either toxin A or toxin B (Fig. 7a and b). This implies glucosylation of intracellular Rac1 by both toxins.

In a Western blot analysis conducted over 24 h, levels of expression of RhoA protein (whose detection by the antibody used was not altered by glucosylation) did not change in myofibroblasts exposed to either toxin. However, an ELISA-based Rho activation assay showed marked reductions in levels of active, GTP-bound RhoA in lysates of myofibroblasts exposed to either toxin A or toxin B (Fig. 8).

DISCUSSION

Intestinal myofibroblasts represent a distinct subpopulation of cells located immediately below the single monolayer of epithelial cells. Primary colonic epithelial cells are highly susceptible to *C. difficile* toxin-induced cell death (26, 41). The loss of epithelial cells *in vivo* would be expected to expose myofibroblasts to *C. difficile* toxins. By using monolayers of myofibroblasts isolated from colonic mucosal samples from different donors, we showed that the cells consistently responded to toxins A and B by a change in morphology to stellate cells. Moreover, scanning electron microscopy showed small globular structures in cells incubated with the toxins, and further studies are required to characterize the nature of these structures. The cell body and processes in toxin-exposed myofibroblasts were strongly immunoreactive for alpha-smooth muscle actin. Although morphological studies and MTT assays suggested that a proportion of colonic myofibroblasts remained viable after 72 h of incubation with toxin B, all cells eventually underwent cell death, even after short (3 h) preexposure periods. However, it should also be noted that at low concentrations, the presence of toxin A provided protection against a toxin B-induced loss of viability. Such exposure of myofibroblasts to both toxins is likely to occur in the colonic mucosa *in vivo*.

In contrast to responses to toxin B, a majority of the toxin A-exposed myofibroblasts remained viable, even when exposed to a high (10 μg/ml) concentration of the toxin for up to 72 h. Interestingly, after preexposure (for 3 h to 48 h) to high concentrations (1 and 10 μg/ml) of toxin A (followed by washing and culture in medium only), the myofibroblast morphology gradually reverted to normal. Subsequently, the cells were also able to proliferate after passage. This remarkable characteristic of the myofibroblasts may have important implications for mucosal tissue repair and regeneration in patients with colitis due to *C. difficile* infection. Our previous studies showed that following 3 h of preexposure to <0.01 μg/ml toxin A, the T84 carcinoma-derived colonic epithelial cell line was able to recover its barrier function during subsequent culture in medium. However, this was not the case if the initial preexposure was to ≥0.01 μg/ml toxin A (20). Moreover, there was a significant loss of viability in T84 and Caco-2 cell monolayers exposed to ≥0.1 μg/ml toxin A (unpublished observations in studies performed using the same batch of toxin as that used in the current series of experiments, together with our previous studies [26]). Thus, primary human colonic myofibroblasts not only are much more resistant to cell death than these carcinoma-derived epithelial cell lines but also are able to recover after preexposure to high concentrations of toxin A.

Primary human colonic epithelial cells are more sensitive to toxin A-induced cell death than Caco-2 and T84 carcinoma-derived epithelial cell lines (26). Indeed, our previous studies have shown that among the normal human colonic mucosal cells, epithelial cells and macrophages (and also monocytes) are more sensitive than lymphocytes to toxin A-induced cell death (25, 26, 42). Although direct comparisons have not been

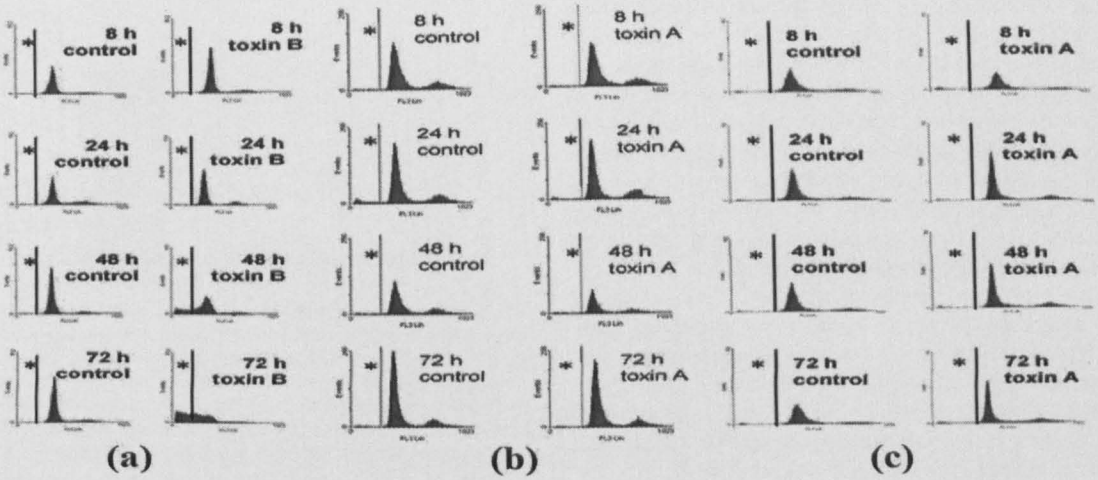

FIG. 5. Representative DNA fluorescence profiles of propidium iodide-labeled preparations of control and *C. difficile* toxin-exposed myofibroblasts. Monolayers of isolated normal human colonic myofibroblasts were cultured in medium only (control) or in the presence of 1 μg/ml toxin B (a), 1 μg/ml toxin A (b), or 10 μg/ml toxin A (c) for various intervals (8 to 72 h). Following permeabilization, detached myofibroblasts were incubated with propidium iodide and DNA fluorescence analyzed by flow cytometry. Events within the hypodiploid region (*) reflect DNA fragmentation due to apoptotic cell death. In contrast to myofibroblasts exposed to 1 μg/ml (b) and 10 μg/ml (c) toxin A, cells cultured with 1 μg/ml toxin B (a) showed a time-dependent increase in events in the hypodiploid (sub-G_1) region.

made, our current studies suggest that colonic myofibroblasts may be more resistant to toxin A-induced cell death than the colonic lamina propria lymphocytes. After exposure to 1 μg/ml toxin A, a large proportion of colonic lamina propria T cells underwent programmed cell death, mainly from 72 h onwards (25). In contrast, most of the colonic myofibroblasts incubated with 10 μg/ml toxin A were viable at 72 h. Reasons for the differences in susceptibility of colonic mucosal cells to toxin A-induced cell death remain to be determined. One possibility is that specific cell types bind and internalize different amounts of toxin A. However, since there is rapid cell rounding and glucosylation of Rac1 (see below), a significant amount of toxin A is likely to be internalized by the myofibroblasts.

The persistence of stellate morphology and adherence to the culture dish are other distinct features of toxin A-exposed myofibroblasts compared with epithelial cells. Since similar appearances were not seen with toxin A-exposed NIH 3T3 cells

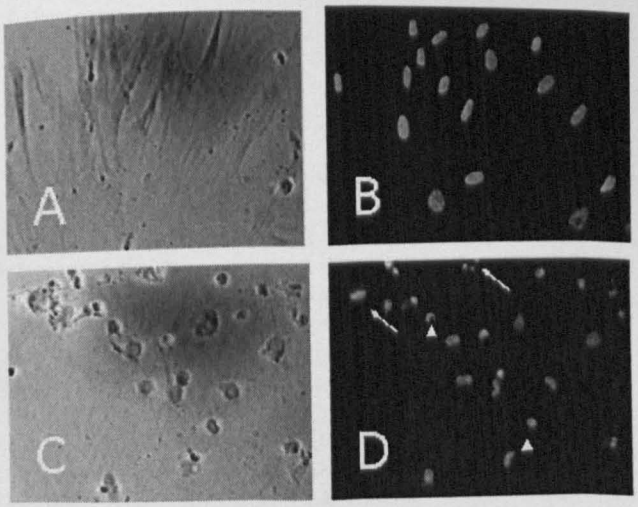

FIG. 6. Hoechst 33342 staining of control (A and B) myofibroblasts and those exposed to toxin B (1 μg/ml) for 72 h (C and D). Phase-contrast (A and C) and fluorescence (B and D) micrographs are shown. (D) Nuclear condensation (arrowhead) and nuclear fragmentation (arrows) are seen in toxin B-exposed cells.

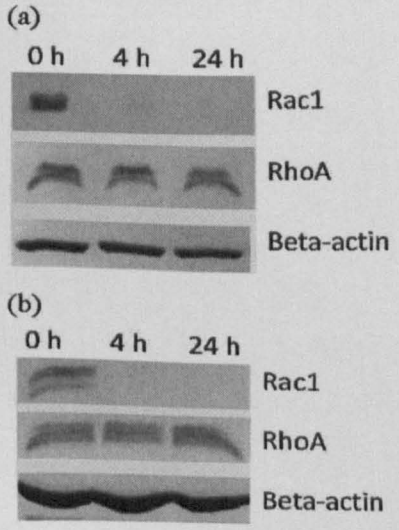

FIG. 7. Expression of Rac1, RhoA, and beta-actin in control and *C. difficile* toxin-exposed myofibroblasts. Lysates were obtained from monolayers of normal human colonic myofibroblasts cultured in medium only (0 h) or in the presence of 1 μg/ml toxin A (a) or 1 μg/ml toxin B (b) for 4 h and 24 h. In contrast to the case for RhoA, loss of the nonglucosylated form of Rac1 was seen in myofibroblasts exposed to toxin A (a) or toxin B (b) for 4 h and 24 h. Equal loading of the lanes is illustrated by beta-actin-immunoreactive bands of similar size. The figures are representative of three experiments using myofibroblasts isolated from colonic mucosal samples from three donors.

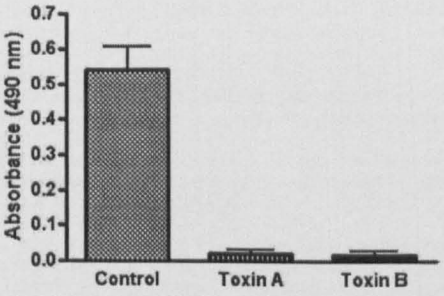

FIG. 8. Levels of active, GTP-bound RhoA in control and *C. difficile* toxin-exposed myofibroblasts. Lysates were obtained from monolayers of normal human colonic myofibroblasts cultured for 4 h in medium only or in the presence of 1 μg/ml toxin A or 1 μg/ml toxin B. GTP-bound RhoA levels were quantified using an ELISA-based assay. Experiments were performed in duplicate, and the bars represent mean (SEM) absorbance values for 3 different cultures of myofibroblasts isolated from colonic mucosal samples obtained from 3 donors. The *P* value was <0.01 for the control versus toxin A or toxin B.

(unpublished observations), the stellate morphology of myofibroblasts could be due to the persistence of alpha-smooth muscle actin. It is likely that the changes in the morphology of myofibroblasts incubated with toxin A or B are due to inactivation (following glucosylation) of the Rho subfamily of GTPases, which are major intracellular targets of the toxins (2, 19). Both toxins induced a loss of the nonglucosylated form of Rac1 in colonic myofibroblasts over similar periods (within 4 h). Together with largely similar rates of cell rounding, these studies imply that the uptake of both toxins is similar in myofibroblasts and that the greater sensitivity to cell death in response to toxin B is unlikely to be mediated via Rac1. Previous studies using rat basophilic leukemia (RBL) cells also suggested that glucosylation/inactivation of Rac1 is responsible for cell rounding (cytopathic effect) but not for cell death (cytotoxicity) (17). Studies of other cell types have shown that inactivation of RhoA is required for cell death (4, 16, 32). However, following 4 h of exposure to *C. difficile* toxin A or B, there was a marked reduction in levels of active, GTP-bound RhoA, implying toxin-induced RhoA inactivation in the colonic myofibroblasts. In contrast, total levels of RhoA did not change in myofibroblasts exposed to either toxin A or B for 24 h. This is in contrast to the case for RBL cells, where high concentrations of toxin B (which led to cell death) induced a loss of RhoA (17). Such a loss may be due to the fact that glucosylated RhoA is degraded more efficiently by the proteasome than the nonmodified form (8, 11), and further studies are required to determine why total levels of RhoA do not change in toxin-exposed myofibroblasts. Since there were marked reductions in levels of active, GTP-bound RhoA in response to both toxins, other factors are likely to be involved in the induction of cell death in myofibroblasts cultured with toxin B.

In addition to functions in the cytoskeleton and cell adhesion, Rho proteins have been found to regulate a wide range of cellular activities, such as cell polarity, endocytosis, vesicle trafficking, and differentiation (7). Peptide regulatory factors such as platelet-derived growth factor (PDGF) and epidermal growth factor (EGF) stimulate Rac, leading to Rho activation (39, 40). Inactivation of Rac and other members of the Rho subfamily may therefore have a significant impact on the normal functions of colonic myofibroblasts, which include regulation of epithelial barrier function (3, 20) and repair of epithelial wounds (created by loss of injured epithelial cells). For the latter, myofibroblasts have been shown, via their contractile properties, to reduce the size of the wound (31) and to also enhance restitution (28), a process by which epithelial cells at the wound edge migrate to cover the mucosal defect. Such protective responses by the myofibroblasts may explain, at least in part, the focal nature of mucosal inflammation in *C. difficile*-associated colitis. However, once cells are exposed to high concentrations of *C. difficile* toxins, impairment of myofibroblast functions may lead to severe inflammation, as seen in pseudomembranous colitis. The concentrations of *C. difficile* toxins used in our studies are likely to be representative of those seen *in vivo*. Thus, we have previously shown that although the median stool concentration of toxin A in patients with *C. difficile* infection was 4.3 ng/ml, the levels ranged from 0.6 ng/ml to 19 μg/ml (42).

ACKNOWLEDGMENTS

This study was supported by the Medical Research Council.
We thank Jacqueline Webb for technical support.

REFERENCES

1. **Bajaj-Elliott, M., E. Breese, R. Poulsom, P. D. Fairclough, and T. T. MacDonald.** 1997. Keratinocyte growth factor in inflammatory bowel disease. Increased mRNA transcripts in ulcerative colitis compared with Crohn's disease in biopsies and isolated mucosal myofibroblasts. Am. J. Pathol. **151:**1469–1476.
2. **Barbieri, J. T., M. J. Riese, and K. Aktories.** 2002. Bacterial toxins that modify the actin cytoskeleton. Annu. Rev. Cell Dev. Biol. **18:**315–344.
3. **Beltinger, J., et al.** 1999. Human colonic subepithelial myofibroblasts modulate transepithelial resistance and secretory response. Am. J. Physiol. **277:** C271–C279.
4. **Bobak, D., J. Moorman, A. Guanzon, L. Gilmer, and C. Hahn.** 1997. Inactivation of the small GTPase Rho disrupts cellular attachment and induces adhesion-dependent and adhesion-independent apoptosis. Oncogene **15:**2179–2189.
5. **Branka, J. E., et al.** 1997. Early functional effects of *Clostridium difficile* toxin A on human colonocytes. Gastroenterology **112:**1887–1894.
6. **Brito, G. A., et al.** 2002. Mechanism of *Clostridium difficile* toxin A-induced apoptosis in T84 cells. J. Infect. Dis. **186:**1438–1447.
7. **Burridge, K., and K. Wennerberg.** 2004. Rho and Rac take center stage. Cell **116:**167–179.
8. **Dillon, S. T., et al.** 1995. Involvement of Ras-related Rho proteins in the mechanisms of action of *Clostridium difficile* toxin A and toxin B. Infect. Immun. **63:**1421–1426.
9. **Di Sabatino, A., et al.** 2009. Transforming growth factor beta signalling and matrix metalloproteinases in the mucosa overlying Crohn's disease strictures. Gut **58:**777–789.
10. **Fiorentini, C., et al.** 1990. Interaction of *Clostridium difficile* toxin A with cultured cells: cytoskeletal changes and nuclear polarization. Infect. Immun. **58:**2329–2336.
11. **Genth, H., et al.** 2006. Cellular stability of Rho-GTPases glucosylated by *Clostridium difficile* toxin B. FEBS Lett. **580:**3565–3569.
12. **Hata, K., et al.** 2002. IL-17 stimulates inflammatory responses via NF-kappaB and MAP kinase pathways in human colonic myofibroblasts. Am. J. Physiol. Gastrointest. Liver Physiol. **282:**G1035–G1044.
13. **He, D., et al.** 2002. *Clostridium difficile* toxin A triggers human colonocyte IL-8 release via mitochondrial oxygen radical generation. Gastroenterology **122:**1048–1057.
14. **Heasman, S. J., and A. J. Ridley.** 2008. Mammalian Rho GTPases: new insights into their functions from in vivo studies. Nat. Rev. Mol. Cell. Biol. **9:**690–701.
15. **Hecht, G., C. Pothoulakis, J. T. LaMont, and J. L. Madara.** 1988. *Clostridium difficile* toxin A perturbs cytoskeletal structure and tight junction permeability of cultured human intestinal epithelial monolayers. J. Clin. Invest. **82:** 1516–1524.
16. **Hippenstiel, S., et al.** 2002. Rho protein inactivation induced apoptosis of cultured human endothelial cells. Am. J. Physiol. Lung Cell. Mol. Physiol. **283:**L830–L838.
17. **Huelsenbeck, J., et al.** 2007. Difference in the cytotoxic effects of toxin B from *Clostridium difficile* strain VPI 10463 and toxin B from variant *Clostridium difficile* strain 1470. Infect. Immun. **75:**801–809.

18. **Hughes, K. R., F. Sablitzky, and Y. R. Mahida.** 2011. Expression profiling of Wnt family of genes in normal and inflammatory bowel disease primary human intestinal myofibroblasts and normal human colonic crypt epithelial cells. Inflamm. Bowel Dis. **17**:213–220.
19. **Jank, T., T. Giesemann, and K. Aktories.** 2007. Rho-glucosylating *Clostridium difficile* toxins A and B: new insights into structure and function. Glycobiology **17**:15R–22R.
20. **Johal, S. S., K. Solomon, S. Dodson, S. P. Borriello, and Y. R. Mahida.** 2004. Differential effects of varying concentrations of *Clostridium difficile* toxin A on epithelial barrier function and expression of cytokines. J. Infect. Dis. **189**:2110–2119.
21. **Kamiya, S., P. J. Reed, and S. P. Borriello.** 1989. Purification and characterisation of *Clostridium difficile* toxin A by bovine thyroglobulin affinity chromatography and dissociation in denaturing conditions with or without reduction. J. Med. Microbiol. **30**:69–77.
22. **Leeb, S. N., et al.** 2003. Reduced migration of fibroblasts in inflammatory bowel disease: role of inflammatory mediators and focal adhesion kinase. Gastroenterology **125**:1341–1354.
23. **Lyerly, D. M., C. J. Phelps, J. Toth, and T. D. Wilkins.** 1986. Characterization of toxins A and B of *Clostridium difficile* with monoclonal antibodies. Infect. Immun. **54**:70–76.
24. **Mahida, Y. R., et al.** 1997. Adult human colonic subepithelial myofibroblasts express extracellular matrix proteins and cyclooxygenase-1 and -2. Am. J. Physiol. **273**:G1341–G1348.
25. **Mahida, Y. R., et al.** 1998. Effect of *Clostridium difficile* toxin A on human colonic lamina propria cells: early loss of macrophages followed by T-cell apoptosis. Infect. Immun. **66**:5462–5469.
26. **Mahida, Y. R., S. Makh, S. Hyde, T. Gray, and S. P. Borriello.** 1996. Effect of *Clostridium difficile* toxin A on human intestinal epithelial cells: induction of interleukin 8 production and apoptosis after cell detachment. Gut **38**:337–347.
27. **McKaig, B. C., K. Hughes, P. J. Tighe, and Y. R. Mahida.** 2002. Differential expression of TGF-beta isoforms by normal and inflammatory bowel disease intestinal myofibroblasts. Am. J. Physiol. Cell Physiol. **282**:C172–C182.
28. **McKaig, B. C., S. S. Makh, C. J. Hawkey, D. K. Podolsky, and Y. R. Mahida.** 1999. Normal human colonic subepithelial myofibroblasts enhance epithelial migration (restitution) via TGF-beta3. Am. J. Physiol. **276**:G1087–G1093.
29. **McKaig, B. C., D. McWilliams, S. A. Watson, and Y. R. Mahida.** 2003. Expression and regulation of tissue inhibitor of metalloproteinase-1 and matrix metalloproteinases by intestinal myofibroblasts in inflammatory bowel disease. Am. J. Pathol. **162**:1355–1360.
30. **Meador, J., III, and R. K. Tweten.** 1988. Purification and characterization of toxin B from *Clostridium difficile*. Infect. Immun. **56**:1708–1714.
31. **Moore, R., S. Carlson, and J. L. Madara.** 1989. Villus contraction aids repair of intestinal epithelium after injury. Am. J. Physiol. **257**:G274–G283.
32. **Moorman, J. P., D. A. Bobak, and C. S. Hahn.** 1996. Inactivation of the small GTP binding protein Rho induces multinucleate cell formation and apoptosis in murine T lymphoma EL4. J. Immunol. **156**:4146–4153.
33. **Mosmann, T.** 1983. Rapid colorimetric assay for cellular growth and survival: application to proliferation and cytotoxicity assays. J. Immunol. Methods **65**:55–63.
34. **Nicoletti, I., G. Migliorati, M. C. Pagliacci, F. Grignani, and C. Riccardi.** 1991. A rapid and simple method for measuring thymocyte apoptosis by propidium iodide staining and flow cytometry. J. Immunol. Methods **139**: 271–279.
35. **Pothoulakis, C., et al.** 1986. Purification and properties of *Clostridium difficile* cytotoxin B. J. Biol. Chem. **261**:1316–1321.
36. **Powell, D. W., et al.** 1999. Myofibroblasts. I. Paracrine cells important in health and disease. Am. J. Physiol. **277**:C1–C9.
37. **Powell, D. W., et al.** 1999. Myofibroblasts. II. Intestinal subepithelial myofibroblasts. Am. J. Physiol. **277**:C183–C201.
38. **Price, A. B., and D. R. Davies.** 1977. Pseudomembranous colitis. J. Clin. Pathol. **30**:1–12.
39. **Ridley, A. J., and A. Hall.** 1992. The small GTP-binding protein Rho regulates the assembly of focal adhesions and actin stress fibers in response to growth factors. Cell **70**:389–399.
40. **Ridley, A. J., H. F. Paterson, C. L. Johnston, D. Diekmann, and A. Hall.** 1992. The small GTP-binding protein Rac regulates growth factor-induced membrane ruffling. Cell **70**:401–410.
41. **Riegler, M., et al.** 1995. *Clostridium difficile* toxin B is more potent than toxin A in damaging human colonic epithelium in vitro. J. Clin. Invest. **95**:2004–2011.
42. **Solomon, K., J. Webb, N. Ali, R. A. Robins, and Y. R. Mahida.** 2005. Monocytes are highly sensitive to *Clostridium difficile* toxin A-induced apoptotic and nonapoptotic cell death. Infect. Immun. **73**:1625–1634.
43. **Stubbe, H., J. Berdoz, J. P. Kraehenbuhl, and B. Corthesy.** 2000. Polymeric IgA is superior to monomeric IgA and IgG carrying the same variable domain in preventing *Clostridium difficile* toxin A damaging of T84 monolayers. J. Immunol. **164**:1952–1960.
44. **Sullivan, N. M., S. Pellett, and T. D. Wilkins.** 1982. Purification and characterization of toxins A and B of *Clostridium difficile*. Infect. Immun. **35**: 1032–1040.
45. **Sutton, P. A., et al.** 2008. Essential role of toxin A in *C. difficile* 027 and reference strain supernatant-mediated disruption of Caco-2 intestinal epithelial barrier function. Clin. Exp. Immunol. **153**:439–447.
46. **Voth, D. E., and J. D. Ballard.** 2005. *Clostridium difficile* toxins: mechanism of action and role in disease. Clin. Microbiol. Rev. **18**:247–263.

Editor: B. A. McCormick

ABBREVIATIONS

ADP	Adenosine diphosphate
AEBSF	4-(2-Aminoethyl) benzenesulfonyl fluoride hydrochloride
AMP	Antimicrobial peptide
AP1	Activating protein 1
aPKC	atypical protein kinase C
ATCC	American Type Culture Collection
BHI	Brain heart infusion broth
Bp	Base pairs
BSA	Bovine serum albumin
C	C-terminal
CDAD	*Clostridium difficile* associated disease
CDI	Clostridium difficile infection
CDK	cyclin dependent kinase
CDKI	cyclin dependent kinase inhibitor
CDT	CD196 ADP-ribsytransferase toxin
CHO (cells)	Chinese hamster ovary (cells)
Cip/Kip	CDK interacting protein / Kinase inhibitory protein
COX (-1 or -2)	Cyclooxygenase (-1 or -2)
CrD	Crohn's Disease
CROPS	Combined repetitive oligopeptides
DE	Downstream effector
DEAE	Diethylaminoethyl
DMEM	Dulbecco's Modified Eagles Medium

DMSO	Dimethylsulphoxide
DNA	Deoxyribonucleic acid
DPX	Distyrene, a plasticizer and xylene mountant
DTT	Dithiothreitol
DXD (motif)	aspartate – any residue – aspartate (motif)
ECM	Extracellular matrix
EGF	Epidermal growth factor
ERK	extracellular signal regulator kinase
FACS	Fluorescence activated cell sorting
F-actin	Filamentous actin
FCS	Foetal calf serum
GAP's	GTPase activating proteins
GDP	Guanine diphosphate
GEF's	Guanine nucleotide exchange factors
G-LISA	G protein linked immuno-sorbent assay
GTP	Guanine triphosphate
GTPase	Small monomeric guanine tri-phospate proteins
HBSS	Hanks Buffered Saline Solution
HMC-1	Human mast cell
HPA	Health Protection Agency
IBD	Irritable bowel syndrome
IEC	Intestinal epithelial cells
IEL	Intraepithelial lymphocyte
IgG	Immunoglobulin G
IL11	Interleukin 11
IL8	Interleukin 8
INK4	Inhibitor of CDK4
Kb	Kilobase

kDa	Kilodaltons
L	Ligand
LP	Lamina propria
Mab	Monoclonal antibody
MAPK	Mitogen-activating protein kinase
MCP	Monocyte chemoattractant protein
MDA	Mitochondrial dehydrogenase activity
MFI	Median fluorescence intensity
MIP-2	Macrophage inflammatory protein 2
MMP	Matrix metalloproteases
Mono-Q	(Mono) - quarternary amine
MTT bromide	3-[4,5-Dimethylthiazol-2-yl]-2,5-diphenyltetrolium
MW	Molecular weight
MWCO	Molecular weight cut-off
N	N terminal
NAD	Nicotinamide adenine dinucleotide
NAP	Nucleasome assembly protein
NEAA	Non essential amino acids
NK-Kβ	nuclear factor kappa beta
NLR	Nod-like receptor
O	Oxygen
OH	Hydroxyl group
PAGE	Poly-acrylamide gel electrophoresis
PaLoc	Pathogenicity Locus
PBA	PBS with 1% bovine serum albumin
PBS	Phosphate buffered saline
PCG-4	Mouse monoclonal antibody to *C. difficile* toxin A

PDGF	Platelet-derived growth factor
PI	Propidium iodide
PMC	Pseudomembranous colitis
PP	Peyer's Patches
PSG	Pencillin, Streptomycin, Gentamycin
PVDF	Polyvinylidene diflouride
R	Receptor
RNA	Ribonucleic acid
RPMI	Roswell Park Memorial Institute
S1	Switch 1
S2	Switch 2
SDS	Sodium dodecyl sulphate
SEM	Standard error of mean
TBS	Tris buffered saline
TcdA	Toxin A
tcdA	Toxin A gene
$TcdA^{488}$	Toxin A labelled with $AlexaFluor^{488}$
TcdB	Toxin B
tcdB	Toxin B gene
TcsL	Clostridium sordellii lethal toxin
TER	Trans-epithelial resistance
TGF-β	Transforming growth factor beta
Thr (35/37)	Threonine at position 35 or 37
TJC	Tight junction complex
TLR	Toll-like receptor
TNFα	Tumor necrotisis factor alpha
UDP	Uridine diphosphate
ZO	Zonular occludin

Y Gamma

e